

Beyond the patch: on landscape-explicit metapopulation dynamics

Présentée le 24 janvier 2020

à la Faculté de l'environnement naturel, architectural et construit
Laboratoire d'écohydrologie
Programme doctoral en génie civil et environnement

pour l'obtention du grade de Docteur ès Sciences

par

Jonathan GIEZENDANNER

Acceptée sur proposition du jury

Prof. R. Bernier-Latmani, présidente du jury
Prof. A. Rinaldo, D. Pasetto, directeurs de thèse
Prof. J. Bascombe, rapporteur
Prof. O. R. Vetaas, rapporteur
Prof. T. I. Battin, rapporteur

1. Ich gehe nicht von einer These, sondern von einer Geschichte aus.
2. Geht man von einer Geschichte aus, muss sie zu Ende gedacht werden.
3. Eine Geschichte ist dann zu Ende gedacht, wenn sie ihre schlimmst mögliche Wendung genommen hat.
4. Die schlimmst mögliche Wendung ist nicht voraussehbar. Sie tritt durch Zufall ein.
5. Die Kunst des Dramatikers besteht darin, in einer Handlung den Zufall möglichst wirksam einzusetzen.
6. Träger einer dramatischen Handlung sind Menschen.
7. Der Zufall in einer dramatischen Handlung besteht darin, wann und wo wer zufällig wem begegnet.
8. Je planmässiger die Menschen vorgehen, desto wirksamer vermag sie der Zufall zu treffen.
9. Planmässig vorgehende Menschen wollen ein bestimmtes Ziel erreichen. Der Zufall trifft sie immer dann am schlimmsten, wenn sie durch ihn das Gegenteil ihres Ziels erreichen: Das, was sie befürchteten, was sie zu vermeiden suchten (z.B. Ödipus) .
10. Eine solche Geschichte ist zwar grotesk, aber nicht absurd (sinnwidrig).
11. Sie ist paradox.
12. Ebenso wenig wie die Logiker können die Dramatiker das Paradoxe vermeiden.
13. Ebenso wenig wie die Logiker können die Physiker das Paradoxe vermeiden.
14. Ein Drama über die Physiker muss paradox sein.
15. Es kann nicht den Inhalt der Physik zum Ziel haben, sondern nur ihre Auswirkungen.
16. Der Inhalt der Physik geht die Physiker an, die Auswirkungen alle Menschen.
17. Was alle angeht, können nur alle lösen.
18. Jeder Versuch eines Einzelnen, für sich zu lösen ,was alle angeht, muss scheitern.
19. Im paradoxen erscheint die Wirklichkeit.
20. Wer dem Paradoxen gegenübersteht, setzt sich der Wirklichkeit aus.
21. Die Dramatik kann den Zuschauer überlisten, sich der Wirklichkeit auszusetzen, aber nicht zwingen, ihr standzuhalten oder sie gar zu überwältigen.

–21 Punkte zu *den Physikern* von Friedrich Dürrenmatt

Acknowledgements

First, and foremost, I would like to thank from the bottom of my hart Andrea Rinaldo, who gave me the opportunity to work in a very interesting field in the past couple of years. Through your incredibly contagious curiosity, thirst for knowledge and enthusiasm you managed to create an incredible environment both on a professional and personal level. Secondly, I would like to thank Damiano Pasetto, my supervisor, but also companion, in this ECOPOTENTIAL adventure, without whom carrying out this thesis would not have been possible. Your jovial personality kept me going throughout this thesis. Next I would like to thank Javier, my amazing office-mate during these four years. Your incredible forward and positive thinking mindset inspired many of my ideas and made it possible to go through these couple of years. A big hank you also to Luca and Pierre, my partners in cycling, which helped me find a healthy balance between work, (beers), and sport. Thank you guys for the amazing cycling trips. Thanks also to Bernard and Flavio, I will never forget the superb ski-touring trips we did along with Pierre and Javier. Thank you Paolo for the Italian lessons. Thanks a lot to all other present and past lab-members, who, through their positivity and joyful being helped create a pleasant working environment: Enrico, Andrea, Chadi, Jean-Marc, Mitra, Ana-Clara, Théo, Anna and Silvia. I would also like to thank all my colleagues at ECOPOTENTIAL, which provided an amazing environment, interesting discussions and opportunities to thrive in.

I also wish to thank my roommates, Sam and Nils, who went through my whole PhD thesis, and provided some welcome distractions at times. Thanks also to all my friends, incredible pillars during these four years and before. Your presence has always been refreshing and joy in my life. A special thank to Tristan, Jonas, Eliott, Pascal, and Anaël for checking in on me in the last hours of the thesis.

At this point I would like to especially thank my parents, Dominique and Thomas, who always gave me their unconditional support in my decisions, which gave me the strength to come this far, and made me, through their ideas the person I am now. A special thanks also to my siblings, Fanny and Ludovic, which inspire me every day with their incredible achievements, and to the other members of my incredible family.

Finally, Colombine, thank you for everything. *T'es la meilleure!*

Lausanne, October 29, 2019

J. G.

Abstract

CLIMATE change threatens biodiversity and species distribution all over the world at unprecedented rates. Human induced changes to landscape structure and habitat are redefining the relation between species and their environment. Understanding, characterizing and modeling the relation between complex landscape features and geographical species presence, the subject of this thesis, have thus gained paramount importance in order to make informed decisions on near- and far-term management strategies for species and landscape protection.

The present thesis pays particular attention to the understanding of how mountain landscapes, described as heterogeneous habitat matrices, govern the presence of a species in space and time. To this end, throughout this thesis a metapopulation model is considered, a spatially-explicit model based on the balance between colonization and extinction events in areas of different suitability. The classical patch-based modelling approach is extended here in various ways in order to incorporate landscape-explicit information about the habitat matrix.

A first theoretical study is performed on geometric, realistic, and real landscapes which highlights how different levels of connectivity, the degree to which different areas of similar habitat are actually linked together in the landscape (say, derived from geomorphic structures, such as valleys and peaks or emerging structures shaped by fluvial erosion and tectonic uplift) impact the dynamic of mountain species under climate change. A second, applied, study investigates how different landscape descriptors derived from Earth Observation data can be used in order to dynamically model the spatial, landscape-explicit, presence of two carabid species (*Pterostichus flavofemoratus* and *Carabus depressus*) in the Gran Paradiso National Park. In a final study, the consistency of the metapopulation model is investigated when considering different resolutions of the landscape matrix, i.e. different levels of coarse-graining. This last part is fundamental to the understanding of how conclusions drawn from local studies can be made general and extrapolated to larger regions.

Overall, this thesis bridges the fields of population and landscape ecology, focusing on modelling metapopulation dynamics in complex landscapes seen as the substrate for ecological interactions. The result from the three studies show that metapopulation ecology can profit from the insights of landscape ecology. The combination of the two fields can be a useful tool

Abstract

in furthering the understanding and monitoring of mountain species.

Key words: Theoretical ecology | Population ecology | Landscape ecology | Metapopulation | Species distribution | Complex landscapes | Mountain | Climate change

Résumé

LE changement climatique menace la biodiversité et la répartition des espèces dans le monde entier à une vitesse sans précédent, causant des changements dans la structure du paysage et de l'habitat qui redéfinissent le lien entre les espèces et leur environnement.

Comprendre, caractériser et modéliser le lien entre les caractéristiques complexes du paysage et la présence géographique des espèces, le sujet de cette thèse, devient d'une importance primordiale afin de prendre des décisions éclairées dans le cadre de la gestion et de la protection à court et long-terme des espèces et du paysage.

L'objectif de la présente thèse se concentre en particulier sur la manière dont les environnements de montagne, décrits comme des matrices d'habitat hétérogènes, régissent la présence d'une espèce dans l'espace et dans le temps. Pour ce faire, un modèle de métapopulation est développé ici. Ce modèle est spatialement explicite et basé sur l'équilibre entre les événements de colonisation et d'extinction de zones adaptées et non-adaptées. L'approche de modélisation classique basée sur des patches est augmentée ici de différentes manières afin d'inclure des informations explicites du paysage sur la matrice d'habitat.

Une première étude théorique est réalisée sur des paysages géométriques, réalistes et réels et souligne la manière dont la connectivité, c'est-à-dire le degré de connection entre les différentes zones d'habitat similaire dans le paysage (dérivé de structures géomorphiques, comme des vallées et des pics ou des structures émergentes formées par l'érosion et le mouvement des plaques tectoniques), influence la dynamique des espèces de montagne sous l'effet du changement climatique. Une deuxième étude, appliquée, examine la manière dont différents descripteurs de paysage, dérivés des données d'observation de la Terre peuvent être utilisés pour modéliser de manière dynamique la présence spatiale et explicite dans le paysage de deux espèces de Carabidés (*Pterostichus flavofemoratus* et *Carabus depressus*) dans le parc national du Grand Paradis. Dans une dernière étude, la cohérence du modèle de métapopulation est investiguée en considérant différentes résolutions de la matrice de paysage, c'est-à-dire différents niveaux de granulation. Cette dernière partie est fondamentale pour comprendre comment les conclusions tirées d'études locales peuvent être généralisées et extrapolées à des régions plus vastes.

Résumé

Dans l'ensemble, cette thèse établit un pont entre les domaines de l'écologie des populations et des paysages, en se concentrant sur la modélisation de la dynamique des métapopulations dans des paysages complexes considérés comme le substrat d'interactions écologiques. Les résultats des trois études montrent que l'écologie des métapopulations peut tirer parti des connaissances de l'écologie du paysage. La combinaison de ces deux domaines peut être un outil utile pour approfondir la compréhension et la surveillance des espèces de montagne.

Mots clés : Écologie théorique | Écologie des populations | Écologie du paysage | Métapopulation | Distribution des espèces | Paysages complexes | Montagne | Changement climatique

Zusammenfassung

KLIMAWANDEL bedroht die Artenvielfalt und die Artenverteilung weltweit in einem bis jetzt beispiellosem Tempo. Die vom Mensch verursachten Veränderungen der Landschaftsstruktur und des Lebensraums definieren das Verhältnis zwischen Arten und deren Umwelt neu. Das Verständnis, die Beschreibung und die Modellierung des Zusammenhangs zwischen komplexen Landschaftseigenschaften und dem geografischen Vorkommen der Arten, das Hauptthema dieser Arbeit, sind daher von höchster Wichtigkeit, um fundierte Entscheidungen über kurz- und langfristige Managementstrategien für den Arten- und Landschaftsschutz treffen zu können.

Die vorliegende Arbeit bemüht sich insbesondere zu verstehen, wie Gebirgslandschaften, die durch heterogene Lebensraummatrizen beschrieben werden, die räumliche und zeitliche Anwesenheit einer Spezies steuern. Diese Arbeit betrachtet zu diesem Zweck ein Metapopulationsmodell, d.h. ein räumlich hoch aufgelöstes Modell das auf dem Gleichgewicht zwischen Besiedlungs- und Aussterbeereignissen in geeigneten und ungeeigneten Gebieten beruht. Die klassische patchbasierete Modellstruktur wird hier auf verschiedene Arten erweitert, um spezifische Informationen über die Landschaftsmatrix zu integrieren.

Um aufzuzeigen wie die unterschiedliche Konnektivität, d.h. das Ausmass der tatsächlichen Verbindung einzelner Gebiete eines Lebensraums (abgeleitet von geomorphen Strukturen wie Tälern und Gipfeln, die durch Flusserosion und tektonischen Auftrieb geprägt sind), sich auf die Dynamik von Gebirgsarten im Klimawandel auswirken, wird eine erste theoretische Studie an geometrischen, realistischen und realen Landschaften durchgeführt. Eine zweite, angewandte Studie untersucht die Verwendung von verschiedenen aus Remotesensingdaten abgeleiteten Landschaftseigenschaften in der dynamischen Modellierung der räumlichen, landschaftsspezifischen Anwesenheit von zwei Carabid-Arten (*Pterostichus flavofemoratus* und *Carabus depressus*) im Gran Paradiso-Nationalpark. In einer abschliessenden Studie wird die Konstanz des Metapopulationsmodells unter unterschiedlichen Auflösungen der Landschaftsmatrix, d. h. unterschiedlicher Grobkörnung untersucht. Dieser letzte Teil ist für das Verständnis der Übertragbarkeit der Schlussfolgerungen aus lokalen Studien auf grössere Regionen von fundamentaler Bedeutung.

Insgesamt schlägt die vorliegende Arbeit eine Brücke zwischen den Bereichen Populations-

Zusammenfassung

und Landschaftsökologie vor und konzentriert sich auf die Modellierung der Metapopulationsdynamik in komplexen Landschaften, die als Substrat für ökologische Interaktion behandelt werden. Das Ergebnis der drei Studien zeigt, dass Metapopulationsökologie von Erkenntnissen der Landschaftsökologie profitieren kann. Die Kombination der beiden Forschungsfelder ist ein nützliches Instrument, um das Verständnis und die Überwachung von Bergarten zu fördern.

Schlüsselwörter: Theoretische Ökologie | Populationsökologie | Landschaftsökologie | Metapopulation | Artenverteilung | Komplexe Landschaften | Berge | Klimawandel

Riassunto

I cambiamenti climatici minacciano la biodiversità e la distribuzione delle specie in tutto il mondo a un ritmo senza precedenti. I cambiamenti indotti dall'uomo nella struttura del paesaggio e nell'habitat stanno ridefinendo il rapporto tra le specie e il loro ambiente. Comprendere, la caratterizzare e modellare la relazione tra le caratteristiche paesaggistiche complesse e la presenza spaziale di specie, oggetto di questa tesi, hanno quindi acquisito un'importanza fondamentale al fine di prendere decisioni informate sulle strategie di conservazione a breve e lungo termine delle specie e del paesaggio.

Questa tesi presta particolare attenzione alla comprensione di come i paesaggi montani, descritti come matrici di habitat eterogenee, governano la presenza di una specie nello spazio e nel tempo. A tal fine, questa tesi sviluppa un modello di metapopolazione, un modello spazialmente esplicito basato sull'equilibrio tra eventi di colonizzazione ed estinzione in aree di diversa idoneità. L'approccio classico alla modellazione basata su patch è esteso qui in vari modi al fine di incorporare informazioni esplicite sulla dell'habitat.

Un primo studio teorico viene condotto su paesaggi geometrici, realistici e reali che evidenziano come diversi livelli di connettività, il grado in cui aree distinte di habitat simile sono effettivamente collegate spazialmente nel paesaggio (derivate da strutture geomorfe, come valli e picchi o strutture emergenti modellate dall'erosione fluviale e dal sollevamento tettonico) influenzano la dinamica delle specie montane in circostanze di cambiamenti climatici. Un secondo studio, applicato, esamina come diversi descrittori del paesaggio derivati da dati satellitari possano essere utilizzati al fine di modellare la dinamica spaziale determinata dal paesaggio della presenza di due specie di carabidi (*Pterostichus flavofemoratus* e *Carabus depressus*) nel Parco Nazionale del Gran Paradiso. In uno studio finale, la coerenza del modello di metapopolazione viene studiata quando si considerano diverse risoluzioni della matrice del paesaggio, vale a dire diversi livelli di granulosità. Quest'ultima parte è fondamentale per la comprensione di come le conclusioni tratte dagli studi locali possano essere rese generali ed estrapolate a regioni più grandi.

Nel complesso, questa tesi collega i campi dell'ecologia delle popolazioni e del paesaggio, concentrandosi sulla modellizzazione delle dinamiche di metapopolazione in paesaggi complessi visti come substrato per le interazioni ecologiche. Il risultato dei tre studi mostra che

Riassunto

l'ecologia delle metapopolazioni può trarre profitto dalle intuizioni dell'ecologia del paesaggio. La combinazione dei due campi può essere uno strumento utile per favorire la comprensione e il monitoraggio delle specie montane.

Parole chiave: Ecologia teorica | Ecologia delle popolazioni | Ecologia del paesaggio | Metapopolazione | Distribuzione delle specie | Paesaggi complessi | Montagna | Cambiamento climatico

Contents

Acknowledgements	i
Abstract (English/Français/Deutsch/Italiano)	iii
List of Figures	xv
List of Tables	xix
Introduction	1
1 A glance at the state-of-the-art of (meta-)population dynamics in complex mountainous landscapes	7
1.1 On the presence of a species in a landscape	7
1.1.1 Niche	8
1.1.2 Environmental availability	9
1.1.3 Regional accessibility and dispersal limitations	9
1.1.4 Population dynamics	10
1.1.5 Temporal induced variations in species presence	11
1.2 On the relation between mountain landscapes and species presence	14
1.2.1 Mountain features and description	14
1.2.2 Elevation gradients in species-richness	16
1.3 Metapopulation - concepts and modeling	20
1.3.1 What is a metapopulation?	20
1.3.2 Beyond the classical metapopulation model	29
1.3.3 Additional considerations	43
2 Metapopulation dynamics of virtual mountain species under climate change	45
2.1 Introduction	46
2.2 Materials and methods	48
2.2.1 A metapopulation framework	48
2.2.2 Fitness	50
2.2.3 Comparable species viability	53
	xi

Contents

2.2.4	Dispersal tradeoffs	55
2.2.5	Modeling climate warming	56
2.2.6	Simulations	56
2.2.7	Landscapes used in the simulation	59
2.3	Results	62
2.3.1	Initial occupancy patterns	62
2.3.2	Climate change effects	62
2.3.3	Extension to real landscapes	65
2.3.4	Effect on species diversity	66
2.4	Discussion	70
2.5	Conclusion	72
3	Earth Observation driven metapopulation dynamics of carabids in a mountain range	75
3.1	Introduction	76
3.2	Materials and methods	78
3.2.1	Raster data acquisition and processing	85
3.2.2	Preliminary data analysis	90
3.2.3	Modeling framework	97
3.3	Results	104
3.3.1	<i>Pterostichus flavofemoratus</i>	105
3.3.2	<i>Carabus depressus</i>	109
3.3.3	Trends in presence and sensitivity to parameters	113
3.4	Discussion	114
3.5	Conclusion	117
4	An exact coarse-graining consistent metapopulation model	119
4.1	Introduction	119
4.2	Materials and methods	122
4.2.1	Metapopulation model	122
4.2.2	Graining problem	123
4.2.3	A metapopulation model consistent with coarse-graining	125
4.2.4	Model comparison	128
4.2.5	Simulations	128
4.3	Results	129
4.3.1	Homogeneous landscape	129
4.3.2	Complex GPNP landscape	131
4.4	Discussion	133
4.5	Conclusion	134
	Conclusions and perspectives	135

A Appendix of chapter 2	141
Bibliography	163
Curriculum Vitae	187

List of Figures

1.1	Example of the impact of niche on a species' presence in the landscape	8
1.2	Example of regional accessibility and dispersal limitation	10
1.3	Example of population dynamics influencing the presence of a species in the landscape	11
1.4	Schematic representation of colonization credit and extinction debt	13
1.5	Relation between elevation and: a) available area; b) species diversity	15
1.6	Schematic example of different approaches to represent a complex landscape in a metapopulation model with corresponding examples from the literature . . .	32
1.7	Loss of information on intra-patch heterogeneity	33
1.8	Example of considering or not the landscape structure in the dispersal kernel .	35
1.9	Subdivision of correlated random fields for the study of SAR	40
1.10	Probability distribution of SAR	40
2.1	Landscapes used in the simulation and overview of the simulation	47
2.2	Approximation of results obtained by Thibaud et al. (2014) with the metapopulation capacity	51
2.3	Addition of aspect in the definition of the fitness	52
2.4	Comparison between the upper bound computed using the Perron-Frobenius theorem (black line), the theoretical value (red line), and the largest eigenvalue with different values of Δx	54
2.5	Example of results when comparable species viability is not considered	55
2.6	Overview of the different states and steps of the simulation	58
2.7	Example of different Optimal channel networks (OCNs)	61
2.8	Outcome of the metapopulation runs given initial optimal elevation z_{opt} , niche width σ and dispersal distance D	63
2.9	Progression of the parameter limits during the simulation	64
2.10	Species occupancy during (2017-2117) and after climate warming (after 2117) relative to the initial median occupancy	65
2.11	α -diversity averaged over 100 runs of the simulation for the OCN	66
2.12	α -diversity averaged over 100 runs of the simulation for the GPNP and Vaud Alpes	67

List of Figures

2.13 Addition of correlated random noise to the elevation field	69
3.1 Overview of the proposed framework as detailed in the methods	77
3.2 Overview of the study site	78
3.3 EO data used in the study to define the species' fitness	84
3.4 Median temperature for the year 2006 in the domain of interest	86
3.5 Example of gap filling	87
3.6 Example of simple composite	87
3.7 Generation of tasseled cap from the composite image	88
3.8 Map of aspect and slope	89
3.9 Map of forest cover for the year 2006 in the domain of interest	90
3.10 Data per plot and year of <i>Pterostichus flavofemoratus</i>	91
3.11 Data per plot and year of <i>Carabus depressus</i>	91
3.12 Pairs plot of EO data	93
3.13 Analysis of explanatory power of EO data	94
3.14 Time series of the dynamic EO data	95
3.15 Relation between <i>Pterostichus flavofemoratus</i> and EO data	96
3.16 Relation between <i>Carabus depressus</i> and EO data	97
3.17 Initial probability of presence	99
3.18 Example of 30 iterations of IF for the species <i>Pterostichus flavofemoratus</i>	101
3.19 Average occupancy of <i>Pterostichus flavofemoratus</i> in time	105
3.20 Relative difference in average occupancy for <i>Pterostichus flavofemoratus</i>	106
3.21 Fitness of <i>Pterostichus flavofemoratus</i> in the GPNP	106
3.22 Relative change in fitness value of <i>Pterostichus flavofemoratus</i> from one year to the other	107
3.23 Median occupancy of <i>Pterostichus flavofemoratus</i> and <i>Carabus depressus</i> in time	108
3.24 Results at plot level for <i>Pterostichus flavofemoratus</i>	108
3.25 Quantiles histogram	109
3.26 Average occupancy of <i>Carabus depressus</i> in time	110
3.27 Relative difference in average occupancy for <i>Carabus depressus</i>	110
3.28 Fitness of <i>Pterostichus flavofemoratus</i> in the GPNP	111
3.29 Relative change in fitness value of <i>Carabus depressus</i> from one year to the other	111
3.30 Results at plot level for <i>Carabus depressus</i>	112
3.31 Sensitivity analysis	113
4.1 Example of coarse-graining a landscape	124
4.2 Loss in information in landscape structure with coarse-graining: example on the GPNP	124
4.3 Behavior of the hypsographic curves with coarse-graining	125

4.4	Close up on coarse-graining	125
4.5	Behavior of the different model formulations under coarse-graining in a flat domain	130
4.6	Behavior of the different model formulations under coarse-graining in a the GPNP domain	132
4.7	Spatial comparison of probability of occupancy in time	133

List of Tables

3.1	Monthly temperature lapse rates for the Alpine region	86
3.2	Tasseled cap coefficients	88
3.3	Calibrated parameter values for the two species of interest	105
4.1	Metapopulation parameters of the species considered in the study	129

Introduction

LITTLE dispute exists regarding the major impacts of climatic changes (possibly human-induced, see e.g. Neukom et al. 2019a; 2019b) and anthropogenic pressure in restructuring species presence in the Anthropocene (Parmesan and Yohe, 2003; Parmesan, 2006; Lenoir and Svenning, 2015; Rumpf et al., 2018). Changing environmental conditions create new pressure for local species, which are facing two survival options: stay or go (Theurillat and Guisan, 2001; Graae et al., 2017), i.e. adapt to the new imposed local conditions, track the displaced suitable conditions, or alternatively go extinct. With the current estimate of the rate of global climate (IPCC, 2013) and habitat (IPBES, 2019) change, and as the rate of warming over the past 50 years (0.13 ± 0.03 °C per decade (IPCC, 2013)) is approximately twice that observed for the previous 50 years, species extinction and loss in biodiversity are at a pivotal point. Endangered species are likely to be challenged by evolving geophysical drivers almost everywhere (IPCC, 2014), a major threat to mountain species owing to their high rate of local endemism (McCain and Colwell, 2007; Elsen and Tingley, 2015). The IPBES report states that natural ecosystems have already declined by 47% of their natural baseline and globally 25% of species are threatened by extinction.

Understanding the relationship between environmental drivers, landscape features, human pressure and species presence has thus become of paramount importance in order to monitor and predict changes in biodiversity and geographical species distribution, as well as making informed decisions on landscape, biodiversity and conservation management (Viterbi et al., 2013; Acevedo et al., 2017). Sustainability science hinges on quantitative response to questions like “*How are ecosystems and the services they provide going to change in the future?*” or “*How do human decisions affect these trajectories?*” (Dietze et al., 2018).

Here, answering this kind of questions is advocated for by refined modelling, a science that requires the ability to forecast ecological processes both on long ecological timescales, like those of climate responses, or near-term (seasonal to decadal) conditions relevant to environmental decision-making. The latter are deemed particularly demanding because they allow for falsifications i.e. comparisons of specific, quantitative predictions to new observational data, one of benchmarks of scientific discovery (Dietze et al., 2018). Thus the opportunity to

iteratively cycle between carrying out theoretical analyses and updating predictions in light of new evidence is of particular importance for ecological research, in that it makes it more relevant to society.

In all such cases, theoretical and applied modeling studies can be instructive (Hanski, 1998, 1999b; Purves et al., 2007; Ovaskainen et al., 2002; Bascompte and Solé, 1996; Fahrig, 2007; Keith et al., 2008; Bertuzzo et al., 2016; Giezendanner et al., 2019). New perspectives towards that end are provided by linking Earth observations (EOs) to *in-situ* ecological data of presence, absence and abundance in order to estimate the geographical distribution of a species in a landscape. This is a topic widely studied by ecologists in the past 30 years (Pasetto et al., 2018). The recent tremendous progress in the acquisition and processing of satellite remote sensing and EO data are providing a large number of high-quality landscape products, which are often freely accessible to the research community. This abundance of data is prompting the integration of landscape-explicit gridded datasets into ecological models, thus improving the numerical description of species distributions (Guisan and Zimmermann, 2000; Pasetto et al., 2018).

These topics have been the focus of the European-funded H2020 project ECO POTENTIAL (2015-2019): '*Improving future ecosystem benefits through Earth observations*'¹. Considering a targeted set of internationally-recognized protected areas in Europe and beyond, ECO POTENTIAL advocated the integration of EO data into the ecological modeling and monitoring in order to gain an extended understanding on current challenges regarding ecosystem protection, and thus improving species monitoring and supporting park stakeholders and managers in the decision making process.

Developed in the context of ECO POTENTIAL, the present thesis pays particular attention to mountain landscapes, chiefly described as complex environmental matrices either obtained by Earth Observation data, digital elevation maps (DEMs) or replicated in a statistically coherent manner via synthetic landscapes matching the statistical features of real landscapes. In mountain domains, understanding the links between the heterogeneous landscape matrix acting as the ecological substrate, and the hosted population dynamics is central (Ricketts, 2001; Urban and Keitt, 2001; With, 2004; Fahrig and Nutton, 2005; Fahrig, 2007; Ovaskainen and Saastamoinen, 2018). In complex topographies, such as mountainous regions shaped by fluvial processes and tectonic uplift (Rodriguez-Iturbe and Rinaldo, 2001) the core of landscape ecology has focused on spatial patterns (Wu and Hobbs, 2002), and therein the need for integration of ecological processes and population dynamics has been convincingly advocated (Wu and Hobbs, 2002; With, 2004; Fahrig and Nutton, 2005; Fahrig, 2007). Studies blending landscape and population ecology still face serious challenges, especially when related to complex topographies (Elsen and Tingley, 2015; Bertuzzo et al., 2016; Graae et al., 2017),

¹ECO POTENTIAL project – <https://ecopotential-project.eu/>

and when confronted with climate change, given that changes in habitat structures appear as dominant drivers (Parmesan and Yohe, 2003; Parmesan, 2006). Indeed, in mountainous landscapes, species movement is strongly defined and limited by geomorphological factors, such as, for example, mountain tops and valleys (Guisan and Theurillat, 2001; Lenoir et al., 2008; Pauchard et al., 2009; Elsen and Tingley, 2015).

The focus of this thesis is thus on the understanding of the spatial metapopulation dynamics of mountain species driven by complex landscape matrices and by changing environmental conditions. Metapopulation biology is concerned with the dynamic consequences of migration among local populations, which determine the conditions for regional persistence of species under the unstable dynamics of local populations (Hanski, 1998). Well established effects of habitat patch area and isolation on migration, colonization and population extinction have now become integrated with classic metapopulation dynamics, leading to models that can be used to predict the movement patterns of individuals, the dynamics of species, and the distributional patterns in multispecies communities in real fragmented landscapes (Hanski, 1998). Within this context, the conceptual thread joining all the various topics covered in this thesis relates to the metapopulation dynamics concept (Hanski and Gilpin, 1991; Hanski, 1998; Hanski and Ovaskainen, 2000). In fact, it is well known that ecologists and conservation biologists have used many measures of landscape structure to predict the population dynamics resulting, say, from habitat loss and fragmentation of ecosystems. Usually, these measures are not directly related to population dynamic theory (Hanski and Ovaskainen, 2000). Concepts derived from metapopulation theory (chief and foremost the concept of metapopulation capacity, introduced to characterize highly fragmented landscapes, but relatively straightforwardly extended to impediments other than fragmentation epitomized by some habitat suitability model) prove of the greatest interest for applications to networks of habitat fragments and of ecological connectivities. Thus, whether on long timescales or near-term, a species is predicted to persist in a landscape if the metapopulation capacity of that landscape is greater than a threshold value determined essentially by the properties of the species, *de facto* conveniently used to rank different landscapes in terms of their capacity to support viable metapopulations. The focus of this thesis is on landscape-explicit ecological modelling in line with the current trends in this area (Rybicki and Hanski, 2013; Dietze et al., 2018; Ovaskainen and Saastamoinen, 2018), whereas the basic aspects of metapopulation persistence in fragmented landscapes had been analyzed with spatially-implicit approaches models like in the seminal Levins model (Levins, 1969). Spatial structure of populations is thus central to population ecology where models suggest a profound influence of spatial locations of individuals, populations and communities on their dynamics (*“the essence of spatial ecology is that the spatial structure of ecological interactions affects populations as much as do average birth and death rates, competition and predation”* (Hanski, 1998). The main driver of the ballistic growth of spatially-explicit ecological models is to be found in their relevance to the

understanding of the consequences of the accelerating destruction of natural habitats – a staple of the Anthropocene.

Each chapter opens with an introduction to the specific topic (and its literature thereof). Usually, technical details beyond the scope of the chapter are confined to boxes meant to highlight specific tools and models in a clearly confined perimeter, to help the reader sail through the material. The thesis is organized as follow:

- Chapter 1 proposes an introduction to landscape and (meta-) population ecology from literature. The chapter first addresses the drivers of species presence, elaborating on different concepts such as the definition of a species' niche, interactions among species and the landscape's habitat, population and species dynamics. A particular attention is then given to known relations between species presence and mountainous landscapes, elaborating on the definition of mountains, their climate, and drivers of species presence along elevation gradients and geographical space. The chapter concludes with an introduction to metapopulation modeling, detailing the origins of the concept of metapopulation and taking the reader through the history of metapopulation modeling, its assumptions and developments.
- Chapter 2 addresses the relation between geomorphology, climate change and metapopulation dynamics. Virtual species defined by specific metapopulation characteristics are considered to be driven by complex elevation fields, proxy of temperature, changing under evolving climatic conditions. The occupancy dynamics of these species are simulated following a landscape-explicit stochastic patch occupancy approach, which helps to identify the relations between landscape structures and descriptors, and fates of mountain species under climate warming. Three different types of landscapes are analyzed, geometric, realistic and real landscapes (Vaud Alpes (CH) and Gran Paradiso National Park (IT)), in order to analyze how different landscape structures dictate the fate of focus species.
- Chapter 3 proposes a modeling framework aimed at describing landscape-explicit metapopulation dynamics in a mountainous landscape by using EO data as model driver. Particular attention is given in integrating the imperfect detection and uncertainty of the *in-situ* data into the modeling process. The proposed framework is demonstrated on a case study designed around *in-situ* data of two carabid species (*Pterostichus flavofemoratus* and *Carabus depressus*). This data was collected in the context of an ongoing large monitoring study conducted in the Gran Paradiso National Park which started in 2006.
- Chapter 4 investigates the behavior and consistency of gridded metapopulation models with coarse-graining. The transient dynamics of different virtual species invading the Gran Paradiso National Park are investigated in order to provide a formulation of the metapopulation model which is consistent with graining. This is important in a context of limited availability of *in-situ* data, where local modeling results could be extrapolated to larger regions, or when computational limitations require to first calibrate the model at coarse resolution and then upscale the result.

A set of conclusions and perspectives then close the thesis. Throughout the thesis, the analysis is based on modelling approaches that explicitly take into account the complex landscape matrix. The mountainous region of the Gran Paradiso National Park, which is one of the protected areas considered in the ECOPOTENTIAL project, is used in each chapter to demonstrate the proposed concepts on a real case study.

1 A glance at the state-of-the-art of (meta-)population dynamics in complex mountainous landscapes

THE focus of this thesis is at the frontier between landscape and population ecology. It is thus important to clearly define the different concepts at the basis of these research fields in order to understand their interactions. Landscape ecology is the study of spatial patterns and their reciprocal influence on ecological processes. Population ecology focuses on the spatial and temporal dynamics of populations of species. Particularly relevant for this work is the impact of spatial heterogeneity on the dynamics of species distributions, which is thus a mix between population and landscape ecology. This chapter is meant to provide overview and context to the different concepts addressed throughout the thesis. The chapter starts with an introduction to the general drivers of species presence. The focus then shifts to the description of the main characteristics and drivers of mountain species, to finally conclude with an overview of metapopulation ecology and modeling relevant to that physical context.

1.1 On the presence of a species in a landscape

Understanding the drivers of geographical presence of a species, or species range, is a long-standing question in ecology (Guisan and Zimmermann, 2000), which is at the core of landscape, population, community and niche ecology. Summarizing from Murphy et al. (1990), Pulliam (2000), Soberón and Peterson (2005) and Guisan et al. (2014), it can be argued that the mechanisms affecting a focus species' range can all be assigned to one of these six categories:

1. The set of abiotic conditions that define the habitat where a species can subsist.
2. The relevant biotic interactions, e.g. competition or mutualism.
3. The availability of this environment in a given domain, extent or landscape.
4. The accessibility of the regions, e.g. dispersal or colonization limitations.
5. Population and metapopulation dynamics, e.g. source-sink dynamics.

6. The natural time, e.g. history of the species in the landscape, including all possible variations in biotic and abiotic factors.

Of course, not any of these factors could drive the species' range on their own, but a complex combination of these mechanisms shapes ecosystems as we observe them. The combination of the two first items are what is commonly referred to as the species' niche.

1.1.1 Niche

The idea of a niche has first been formalized by Hutchinson (1957), where the niche is characterized as a multidimensional hypervolume defined by the environmental conditions. Hutchinson (1957) distinguishes between two niches, the fundamental niche (FN) and the realized niche (RN). The fundamental niche is characterized by the set of climatic conditions, or abiotic factors (e.g. temperature, solar radiation, precipitation, etc.) suitable for a species (Fig. 1.1a). But Hutchinson (1957) further states that there is no direct match between the fundamental niche and the observed geographic distribution of the species, meaning there ought to be other factors influencing the niche. As explained in Pulliam (2000), when Hutchinson wrote his "*Concluding Remarks*", much of the focus of ecologists was on species competition. Hutchinson thus defined the realized niche as the subset of the fundamental niche subject to competition, but was later redefined as: the set of biotic and abiotic environmental conditions characterizing a positive growth rate of the species (c.f. Thuiller et al. (2014)).

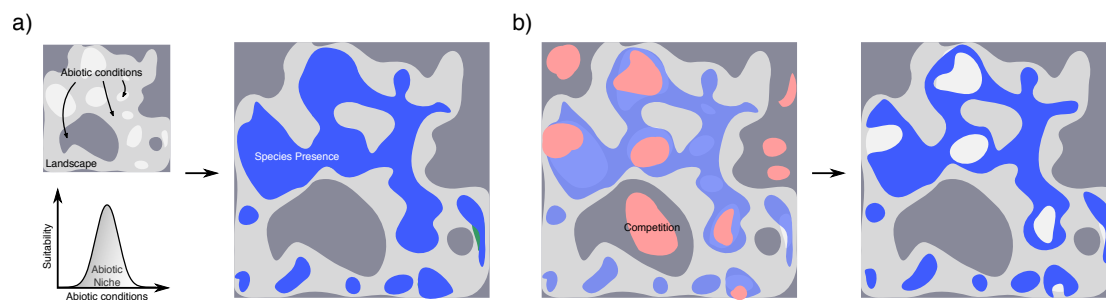


Figure 1.1 – Example of the impact of niche on a species' presence in the landscape. a) Assuming a spatial distribution of abiotic conditions and a certain response of the species to abiotic conditions, if only these factors were determinant would produce the displayed presence of the species (blue); b) Adding biotic interactions in the form of competition (pink), assuming the blue species loses to the orange species, the new blue species presence would be reduced.

Other species thus influence the ability of the focus species to maintain itself in the environment, either by positive (e.g. mutualism, Bascompte (2009); Bascompte and Jordano (2014)) or negative (e.g. competition, Levine et al. (2017)) interactions, or simply by influencing the environment in which they occur (Pulliam, 2000; Soberón and Peterson, 2005). Positive

1.1. On the presence of a species in a landscape

interactions might produce a larger realized than fundamental niche, whereas competition will probably reduce the size of the realized compared to the fundamental niche (Fig. 1.1b).

The combination of the abiotic and biotic factors, i.e. the environmental conditions, meeting physiological requirements of the species to subsist in the landscape, is called the environmental niche (Pearman et al., 2008).

1.1.2 Environmental availability

The availability of the environment, i.e. the presence of suitable habitat or ecosystem in a given region, can largely contribute to the species' presence (Guisan et al., 2014). In a landscape where biotic and abiotic factors needed for the species' survival are absent, the focus species will probably not be found. For instance, for mutualist species, in the absence of one of the two species, the other will not be able to subsist. The same could be said for species requiring warm and humid conditions in dry and cold environments.

This projection of the environmental niche onto the geographic landscape is called the geographical or environmental range (Guisan et al., 2014).

1.1.3 Regional accessibility and dispersal limitations

The accessibility of geographical regions, where movement is not impaired by physical barriers or dispersal limitations, can profoundly shape the presence of a species in the landscape (Soberón and Peterson, 2005). Natural physical barriers such as mountain ranges or valleys (Colwell and Hurtt, 1994; Colwell and Lees, 2000; Bertuzzo et al., 2016) or man-made such as roads or dams (e.g. González-Ferreras et al. (2019)) can impair the possibility of a species to access sub-domains of a landscape. In mountains for instance, a species will have to either go around a hill, climb over a crest, or go down to the valley and back up again in order to access similar conditions (c.f. Fig. 1.2a). This might not be feasible and constrain the species' movement and dispersal capacity.

But barriers do not need to be strictly of solid nature. They may also simply constitute unfavorable terrain, habitat or conditions that species have to cross in order to access favorable regions (c.f. Fig. 1.2b). This phenomenon is commonly referred to as isolation of suitable habitat (With, 2004), with its counterpart being the connectivity, and can drive species presence especially in metapopulations (elaborated later). The best example is maybe in fragmented landscapes, where species will have to move through unfavorable habitat before accessing new favorable regions (e.g. Hanski and Ovaskainen (2000)). For example a species living in different patches of a forest might have to move through open grass to access other patches of this forest. An other example where the limits of suitable habitat are more blurred, relates to temperature.

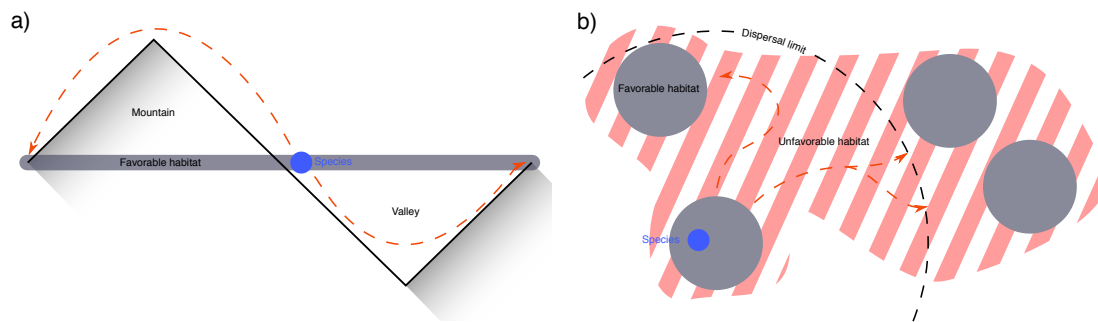


Figure 1.2 – Example of regional accessibility and dispersal limitation. a) A species located in a favorable habitat at mid-elevation has to either go down to the valley and come back up again, or go over the mountain range to access more favorable habitat. The accessibility of favorable habitat is limited; b) A species located in a patch (lower left) has to cross unfavorable habitat to be able to access other favorable habitat patches. Additionally the species is dispersal limited as it can only disperse over certain distance, the patches on the right are thus inaccessible. Note that for simplification, both habitat and dispersal distance are here shown to occur in homogeneous non-habitat terrain (dashed pink/white surface), but could very well be influenced by a more continuously-changing habitat quality.

Specifically, a species might have a certain favorable temperature range, and accessing further suitable habitat might mean going through unfavorable temperature conditions. In cases where this process of moving through inhabitable terrain happens very slowly, e.g. for species with limited dispersal, colonization or migration capacity, this might not be possible. One might even argue that complex heterogeneous landscapes like mountains, although difficult to translate directly into patches, are a good example of fragmented landscape.

Certain parts of the landscape can thus theoretically be favorable to a species, but simply unreachable, and remain unoccupied. These areas are favorable but empty habitats.

1.1.4 Population dynamics

Population dynamics probably represent, next to biotic interactions, the most complex suite of reasons affecting the presence of a species. Source-sink and metapopulation dynamics, as well as population demography can influence the presence of species in both suitable and unsuitable habitats (Fig. 1.3) (Pulliam, 2000). The combination of these factors might result in the presence of species in unsuitable and absence in suitable areas (Moilanen, 2004).

Source-sink dynamics, for instance, describe the movement of individuals from suitable (sources) to unsuitable habitats (sinks). The sources are habitats where the growth rate of the species is positive and large enough to not only support itself, but also permit the emigration of offsprings from these habitats to new habitats, i.e. to occupy unsuitable habitat. This

mechanism permits a species to be present outside of its environmental niche. Sinks are habitats where the species is unable to sustain itself, and resulting in a negative growth rate. Without the incoming offsprings, sink areas would, in time, become unoccupied.

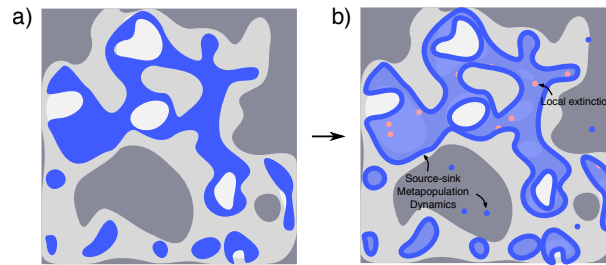


Figure 1.3 – Example of population dynamics influencing the presence of a species in the landscape. Starting from the final spatial configuration (a) described in Fig. 1.1, two effects influence the presence of the species (b): 1) Local extinctions occur through demographic and environmental variability (red dots), creating empty but suitable habitats; 2) Source-sink and metapopulation dynamics permit the presence of the species outside of the suitable habitat (dark blue layer/ dots).

Population demography is important at the local scale, but also influences the colonization capacity at landscape-scale (e.g. with the number of offsprings leaving a patch in order to colonize other patches). Locally, communities can go extinct because of demographic fluctuations, called demographic stochasticity (Hanski and Gilpin, 1991; Ebenhard, 1991). Given that the reproduction rate depends on multiple factors, for example number of individuals, local conditions, etc., a local population can go extinct because of demographic stochasticity. In this case, even though the habitat would be suitable in terms of biotic and abiotic conditions, it would become unoccupied.

Metapopulation dynamics, the subject of this thesis, will be addressed in detail in section 1.3. As an introduction to the subject, the metapopulation combines the two previous mechanisms: colonization, and local extinction. The exchange of individuals between subpopulations permits the species to subsist in the landscape (Hanski and Gilpin, 1991). However, local populations are still subject to demographic and environmental stochasticity, causing possible local extinction. This means that suitable habitat can become temporarily unoccupied, and later recolonized.

1.1.5 Temporal induced variations in species presence

Time is, of course, the dominant factor shaping the patterns of species presence in any given landscape. Time governs the variations in biotic and abiotic factors, demographic stochasticity and environmental variability, change in species phenology through evolutionary processes which changes the species niche and the history of the species, population dynamics, etc.

One can distinguish between two major drivers of changes in species presence in time: changes in the environment, i.e. in biotic and abiotic conditions reflecting the species presence, demography and population dynamics, and changes in the species itself, i.e. evolutionary capacity of the species.

Over larger time periods, a species can genetically evolve to be better suited to its environment (Soberón and Peterson, 2005; Pearman et al., 2008). When this happens, the niche of the species, i.e. the biotic and abiotic conditions favorable for a certain species, will change. Over short periods of time, niche conservations can be assumed, but Pearman et al. (2008) have shown that niche shifts can sometimes happen over long periods of time. As niche conservatism is considered throughout this thesis, the subject of evolutionary capacity of the species is not further addressed, but remains nonetheless an important topic.

The variations in the environment can occur over short or long time spans, and in spatially-correlated or uncorrelated manners (Pulliam, 2000). Over short periods of time, one commonly talks about environmental stochasticity. This stochasticity can be spatially-correlated, e.g. the temperature variation over a day, which changes synchronously over the landscape, or uncorrelated, which can generate local stochasticity, e.g. demographic stochasticity. Variations happening over longer periods of time, are usually referred as trends in species distribution instead of stochasticity. This could be, for instance, due to long-term effects such as climate change. Stochasticity more generally refers to short-term fluctuations around a mean, whereas trends refer to long-term changes in the species presence, distribution and range.

The history of the species inhabiting the landscape shapes, through all effects mentioned until now, the presence of a focal species in the landscape (Soberón and Peterson, 2005) (Lande (1987): the “*general life history pattern*”). How long a species has been present in a certain landscape will inevitably determine the time the species had to colonize the space, whether the species is at equilibrium with the environment (Moilanen, 2000) or still holds extinction debts (Tilman et al., 1994) and/or colonization credits (Jackson and Sax, 2010; Rumpf et al., 2019).

The concept of equilibrium, species lag, extinction debt and colonization credit In time, a species will always be dynamic in its distribution in the landscape, but at certain times, a species can reach a pseudo-equilibrium, which assumes that the species fluctuates around a spatial distribution in balance with the factors driving its distribution. This does not mean that the presence of the species will not continue to change. Seasonal fluctuations in environmental conditions or demographic stochasticity will still influence the presence, but without generating significant trends or large fluctuations around a mean presence (Moilanen, 2000; Thomas and Hanski, 2004).

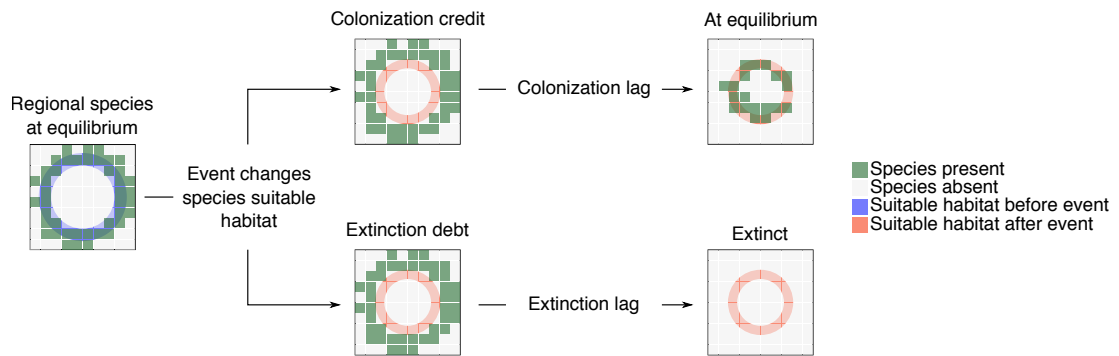


Figure 1.4 – Schematic representation of colonization credit and extinction debt. The species is at equilibrium in the landscape around a certain suitable habitat. When a major event changes the species’ suitable habitat, the species is not at equilibrium anymore, and lags behind the changes in the landscape, at which point it can either reach a new equilibrium, or go extinct. If the species’ new equilibrium is extinction, the species is considered to have an extinction debt. On the other hand, if the species has colonization potential of suitable habitat, and it can reach that habitat, the species is said to have a colonization credit.

When major changes occur in the environment or the variables driving the species, in the form of habitat destruction, climate change, or any other change in the drivers of species distribution, the species will be perturbed and considered not to be at equilibrium anymore. At this point, the system described by the species distribution will converge towards a new equilibrium, which can either be a new distribution of the species, or its extinction (Fig. 1.4). During the lapse of time at which the species is not at pseudo-equilibrium, the species is considered to lag behind the changes. If the species lags behind its inevitable extinction, it is called extinction lag (Jackson and Sax, 2010), and the species is considered to have an extinction debt (Tilman et al., 1994). The extinction debt thus characterizes the late extinction of species due to past events. On the other hand, the species can as well lag behind a new equilibrium distribution without the species’ eventual extinction. In this case, the species can either increase or decrease its presence, depending on whether or not the imposed changes favor the species’ characteristics. In the case that changes generate new, suitable areas for a species, the duration for which the species lags behind the new equilibrium is called colonization lag, and the species is considered to have a colonization credit (Rumpf et al., 2018). The colonization credit thus characterizes a late change in geographic species presence due to past events.

These lags can not only drive a species towards a new distribution, but can also generate new interaction types (Alexander et al., 2016). If two competing species lagging behind their suitable habitat do not migrate synchronously, one species might catch up to the other and create new, previously unobserved, competition. This is for instance the case with an upward

range shift of alpine species under climate warming. In a two species scenario, even when both species theoretically covet different areas, if the lower species catches up to the higher species because it is tracking its habitat towards higher altitudes, and the higher species lags behind its own habitat, competition between the species occurs (Pauchard et al., 2009; Alexander et al., 2016).

These process of lagging behind equilibrium conditions are one of the biggest challenges in species modeling. The observed distribution generated from field campaigns might not depict a correct picture of the species' health, with certain observed species already on their way to eventual extinction. When assessing the impacts of climate change for instance, the short-term changes in species distribution and diversity might not reflect the long-term consequences, which are hardly predictable.

1.2 On the relation between mountain landscapes and species presence

The fractal nature of mountains (Mandelbrot, 1983; Palmer, 1992; Rinaldo et al., 1998; Rodriguez-Iturbe and Rinaldo, 2001) defines them as a paradigm of spatially heterogeneous landscapes. The combination of elevation, steepness and aspect influences the physical conditions of the landscape. For example, wind is strongly conditioned by landscape topography, and aspect and steepness directly control the hours of sunshine per day. Elevation is closely tied to atmospheric pressure, temperature and clear-sky turbidity (Körner, 2007). Mountain tops and valleys form physical barriers (Colwell et al., 1994, 2000), inhibiting species movements due to reduced landscape connectivity (Bertuzzo et al., 2016). The interplay of these effects thus forms highly diverse conditions in space, a heterogeneous landscape, which influences the dynamics of species.

1.2.1 Mountain features and description

Mountain topography As famously said by Mandelbrot (1983), mountain landscapes are, at least at a regional level, not cones (see e.g. Elsen and Tingley (2015); Bertuzzo et al. (2016)). In terrains formed by the interplay of channeled and unchanneled areas, fluvial erosion shapes the terrain, creating a fractal landscape (Mandelbrot, 1983; Rodriguez-Iturbe and Rinaldo, 2001). Elsen and Tingley (2015) investigated 182 mountain ranges, and have been able to classify them into different categories of shapes. Due to the specific topography of mountains, the hypsographic curves¹ corresponding to the mountain chain frequently do not show a cone, since at the base or at the top, the mountain chain might not be as winding than at

¹The hypsographic curve is defined as the area distribution at the various elevations.

1.2. On the relation between mountain landscapes and species presence

mid elevation. At mid elevation, mainly due to river shaping and the self-affine nature of mountain landscapes (Rodriguez-Iturbe and Rinaldo, 2001), along an isoline, one often has to travel a greater distance in the attempt of completing a loop around the mountain. This can seem counterintuitive, as the total area available above a certain height decreases (Körner, 2000, 2007; Lomolino, 2001), but the frequency of area available at a certain elevation (the hypsographic curve) more than often follows a hump shape, especially at local, or regional scale (Bertuzzo et al., 2016). In self-affine landscapes, at the same elevation, one may be wither at a peak or at a trough because of the nature of the landscape. Linear slopes simply do not exist in nature unless for limited regions (Bertuzzo et al., 2016). Elsen and Tingley (2015) have identified four shapes for mountain ranges (see Fig. 1.5a)): a diamond shape (e.g. the Rocky Mountains), a pyramid shape (e.g. the Alps, which is the closest to a cone, but still displays a hump at lower-mid elevation), an inverse pyramid shape (e.g. the Kulun Mountains) and an hourglass shape (e.g. the Himalayas). Note that the shape of the hypsographic curve always depends on the considered extent. This distribution of available land mass at certain elevations is expected to influence the dynamics of species in mountains.

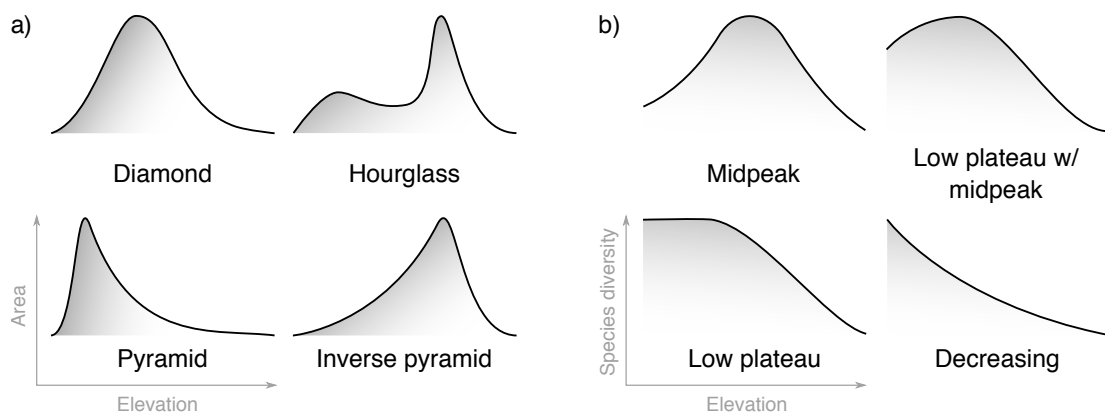


Figure 1.5 – Relation between elevation and: a) available area; b) species diversity. a) The four different types of hypsographic curves (relation between area and elevation) that can be found when analyzing mountain ranges (redrawn freely from Elsen and Tingley (2015)). b) The four different shapes of species diversity gradients along elevation observed in nature (redrawn freely from McCain and Grytnes (2010)).

Environmental factors Körner (2007) explains that the physical properties observed in mountain landscapes can be separated in two categories: those tied to elevation, and those which are not. Physical properties tied to elevation include atmospheric pressure, temperature and radiation (Körner, 2007), as well as area, cloud cover and soil quality (McCain and Grytnes, 2010). Atmospheric pressure, reducing with altitude, influences animal respiration and gas exchanges for plants, in turn influencing animal dynamics. Like pressure, temperature de-

creases with altitude (McCain and Grytnes, 2010) almost linearly (around 4 to 8°C per 1000m.), but different species might be affected in different ways (Körner, 2007). For instance, trees might be subject to temperatures close to the actual air-temperature whereas close to ground vegetation might be exposed to soil surface temperature, and thus more resistance to differences in air-temperature. Variations in temperature are thus not perceived in the same way by different organisms. Körner (2007) further states that it is not the annual mean temperature that should be considered in a biologically meaningful framework, but the one which has a physiological effect, the temperature during the growing season. Clear-sky altitudinal radiation increases with altitude (McCain and Grytnes, 2010), but solar radiation in general has no global altitudinal trend, because clouds strongly influence the amount of radiation, which tends to increase with altitude. Physical properties not generally related to elevation include precipitation, wind velocity, and seasonality (Körner, 2007). Precipitation for instance, has no “*general altitudinal trend, and gradients can go in any direction*”. Certain mountains display a prevalent precipitation gradient with altitude (McCain and Grytnes, 2010), but a multitude of factors such as the slope or proximity to a large water body might strongly influence local precipitation conditions. Tropical mountains seem to have the strongest precipitation at mid-elevation (McCain and Grytnes, 2010).

1.2.2 Elevation gradients in species-richness

Species-richness is well known to vary with elevation, but in subtle manners (Kessler, 2000; Brown, 2001; Lomolino, 2001; Grytnes and Vetaas, 2002; Vetaas and Grytnes, 2002; McCain and Grytnes, 2010; Kessler et al., 2011; Lee et al., 2012; Viterbi et al., 2013; Bertuzzo et al., 2016). Species-richness gradients due to elevation can be separated in four categories (McCain and Grytnes, 2010)(Fig. 1.5b)): i) Decreasing; ii) Low elevation plateau; iii) Low elevation plateau with mid-peak; iv) Mid-peak. Which one of these patterns a given species follows highly depends on their suitability and different response to environmental conditions and external forcing. Mid-elevation peaks in species-richness have received increased support in the recent literature (Kessler, 2000; Brown, 2001; Vetaas and Grytnes, 2002; Kessler et al., 2011; Lee et al., 2012; Viterbi et al., 2013), where species-richness has long been believed to monotonically decrease with altitude (Stevens, 1992; Rahbek and Museum, 1995; Lomolino, 2001). McCain and Grytnes (2010) further state that three effects can artificially influence species-richness patterns: scale, sampling and disturbance. Typically, a mountain range, if taken as a whole, will display a different pattern of species-richness than if each mountain is considered separately. Similarly if sampling is not done uniformly over the whole domain, biases in species-richness patterns might occur because of that. Anthropogenic pressure, i.e. disturbance due to humans, usually stronger in lower elevations (e.g. lowland deforestation), might influence the gradient, creating a hump-shaped species-richness pattern instead of a

1.2. On the relation between mountain landscapes and species presence

decreasing one. Different theories exist as of why these patterns arise, which can be separated in four categories (Lomolino, 2001; McCain and Grytnes, 2010): climate, space, evolutionary history and biotic and abiotic process. There are over 120 different theories on how species-richness varies with elevation (Vetaas, 2015), only a few, related to climate and space are addressed here.

Climate and environmental factors Climate limits the number and type of individuals which can survive in a certain area (McCain and Grytnes, 2010). This is mainly due to physiological traits of the species, which respond more or less well to temperature, rainfall, or other environmental conditions.

Environmental conditions: Environmental conditions such as temperature and precipitation are drivers of species metabolism, it is thus important to quantify their impact. Mild climatic conditions at mid domain (high humidity, moderate temperature) might allow the coexistence of different taxa which would have other altitudes as center of distribution (high or low), and therefore creating an overlap in the middle (Becker et al., 2007). Air temperature decreases with increasing elevation (lapse rate) (McCain and Grytnes, 2010), and so a positive relation between temperature and species-richness (decreasing species-richness with decreasing temperature) has been observed in large-scale studies. One theory to explain this relation is the metabolic theory of ecology (MTE) which relates species metabolisms to temperature, but this theory predicts a negative relationship. Additionally, a positive relationship between temperature and species-richness only explains decreasing patterns, not hump-shaped or low elevation plateaus. Temperature is therefore usually not the sole driver of species-richness. Precipitation appears to have a positive slope with species-richness, but precipitation does not vary linearly with elevation, and it is difficult to show a clear elevation to precipitation effect on species-richness, but rather an additional effect on spatial heterogeneity (McCain and Grytnes, 2010).

Energy: The energy available in the landscape is also thought to drive species-richness. One theory proposes energy to be limited by trophic cascade (Hawkins et al., 2003; Davies et al., 2007), where availability of water and solar radiation limits plant growth, plant primary production limits herbivore growth, which in turn limits predators. This theory, based on energy flows rather than energy available per unit area, is called the productivity hypothesis (Hawkins et al., 2003). Another theory is based on ambient energy inputs (Hawkins et al., 2003; Davies et al., 2007), which can be in the form of temperature, solar radiation and others. For instance, high elevations might be unsuitable for certain species, because ambient energy in the form of temperature declines during winter, and in other places sunlight during summer season might be too low. O'Brien (2006) proposes that energy in the form of change in water states drives species diversity. Life forms only exist in relation with the existence of liquid

water, which therefore would drive species-richness, and the change from this liquid state to other phases. Vetaas (2015) further states that energy alone in the form of sun with lack of water does not provide a suitable enough environment, as shown by energy-rich deserts. Hawkins et al. (2003) as well use water to predict species-richness in the tropics, and concludes that the key component should be a water-energy variable.

Space and geometric constraints Space has a strong impact on how species can survive in a certain landscape. Relations such as available area, boundary conditions or landscape connections influence the way species are distributed in space.

Area: There exists an overall belief that available area has a notable effect on species-richness (Hanski et al., 2013). This effect is called the species-area relationship (SAR). SAR is based on the assumption that with smaller suitable available area, a smaller number of individuals will survive (extinction rates will increase), and the overall number of species will therefore be lower. Rahbek (1997), Sanders (2002), McCain (2007) and Romdal and Grytnes (2007) among others study this relationship in mountain ecosystems. As described in McCain (2007) and McCain and Grytnes (2010), most studies assume a monotonically decreasing available area with elevation, which therefore would not explain the mid-elevation peak in species-richness, only a decreasing species-richness. But Elsen and Tingley (2015) show that only 32% of mountains around the globe display a monotonically decreasing area to elevation relation, with the other 68% displaying mid-elevation peaks or trough, and even an increase in some cases. Romdal and Grytnes (2007) provide some evidence of species diversity being explained by hump-shaped area to elevation relations, but concludes that decreasing trends explain the richness better. McCain (2007) refutes the observed mid-domain effect to be explained by available area, but rather to be a source of error, or an explanation of the observed variance. Sanders (2002) on the other hand suggest that the area might in part explain the mid-domain peak.

Spatial constraints and boundaries – mid-domain effect: Stevens (1992) extends the Rapoport's latitudinal rule to altitude. The rule states that species diversity declines with altitude (originally decreases the further away one moves from the equator) because of an increase in altitudinal range of species in higher elevations. Species with smaller ranges would therefore only be found in lower elevations, and be mostly maintained by migration. Sanders (2002), Vetaas and Grytnes (2002) and Rahbek (1997) among others refute this theory, since mid-elevation peaks arise from range overlaps. Colwell et al. (1994, 2000, 2004) show that boundaries, such as mountain tops and valleys can have a strong effect on species-richness, causing a mid-elevation peak in diversity. The idea is that species with varying niche size will eventually overlap in the middle, creating a hump-shaped pattern. This is called the mid-domain effect. Species with large or moderate niche size are less likely to be found close

1.2. On the relation between mountain landscapes and species presence

to the boundary, but rather close to the middle of the domain. As species with smaller niche sizes can be found in the whole domain, the different ranges overlap in the middle. In Colwell and Lees (2000) this is shown as a triangular location on domain to range size relation (maximum in the middle), where species with a mid-point close to a boundary have a small niche width, bounded by the border. This attempt to explain the mid-domain effect does not try to mimic reality (Colwell et al., 2004), but is a baseline to understand the mechanism and the effect of the boundaries and geometric constraints on the species-richness. Grytnes and Vetaas (2002) attempt to separate this boundary effect from a linear relation to elevation and interpolation when incomplete sampling is done. They conclude that while the combination of the three effects can explain the observed patterns in species-richness, the hump shape is mainly explained by the domain borders. Lee et al. (2012) as well investigate an observed hump-shaped species diversity pattern in South Korea, and conclude that the mid-domain effect, along with climatic factors is a good explanation for certain species, notably woody plants and large-ranged species. The mid-domain effect is therefore an interesting way of modeling observed effects, but there is no evidence that the model could be used as a predictor (McCain and Grytnes, 2010).

Fractals: There exist several ways to describe distinctively scaling structures, mainly depending on the nature of the scaling - self-similar (same pattern at different scale, isotropic scaling) or self-affine (anisotropic scaling) fractal systems (Rodriguez-Iturbe and Rinaldo, 2001). Attention has to be dedicated to a proper characterizations of the roughness of the landscape, possibly described by a suitable fractal dimension. Palmer (1992) works with different self-similar fractal dimensions to assess how the complexity of the landscape influences the species diversity. Note that real self-similar landscapes can not be, and are merely used as imaginary case-studies (Palmer, 1992). The results show that there is an increasing number of species per sites with increasing fractal dimension (decreasing spatial dependence), which might be an indication on how the complexity or heterogeneity of the landscape influences species-richness. However, such results need to be re-examined on the basis of a more precise definition of the proper fractal dimension (Rodriguez-Iturbe and Rinaldo, 2001).

Connectivity: Bertuzzo et al. (2016) show that using connectivity maps derived from elevation data, the mid-domain hump-shaped species-richness could be explained. In this paper, three different aspects are identified to affect species-richness: “*i) finiteness of the landscape elevation range; ii) frequency distribution of areal extent at different elevation; iii) differential elevation connectivity*”. The first aspect of the finiteness of elevation range refers to the mid-domain effect (Colwell and Lees, 2000), which is a geometric constraint explained above. The second aspect refers to the SAR, also covered above, but taken from a perspective where the concept of fractal dimension of mountains (Rodriguez-Iturbe and Rinaldo, 2001), as well as the hump shape in area distribution addressed by Elsen and Tingley (2015) is taken into

account. The third effect addressed is the elevation connectivity. Same-elevation areas are seen as facilitators of movement, so called ecological corridors (Graves et al., 2014; Bertuzzo et al., 2015), which affect how individuals move in space. Areas where surroundings are of similar properties (here elevation) and better connected to other areas of the same type, in the sense that the species does not need to move through unfavorable areas to get there, tend to display a higher species-richness. In Bertuzzo et al. (2016) this connectivity to other areas is called the landscape elevational connectivity (LEC, see also Salles et al. (2019); Salles and Rey (2019)), and is a function of the closeness of each pixel in the landscape. The closeness is computed as the average distance from a pixel at a given elevation to all other pixels in the landscape when moving along a least cost path, or in simpler terms, how well the pixel is connected to the rest of the landscape. Interestingly, this measure depicts rather well the per elevation average α -diversity measured in the landscape.

Topography and spatial heterogeneity: Räsänen et al. (2016), Davies et al. (2007) and Richerson and Lum (1980) use topographic features, mainly elevation ranges, but also slope and aspect (Räsänen et al., 2016), in an attempt of modeling the species-richness observed in mountain landscapes. They employ topographic features against other predictors (such as energy, habitat diversity, normalized difference vegetation index (NDVI), temperature, etc.) within descriptive statistical models (for instance a generalized linear model GLM), which allows them to understand which variables best describe the observed species-richness. It appears that, interestingly, topography is in most cases one of the dominant descriptive variable. Räsänen et al. (2016) note that topography highly directs human actions, which could be one of the causes of topography explaining landscape patterns in species-richness. In most of these cases though, topography explains the spatial heterogeneity of the observed species-richness, rather than the elevation gradient itself.

The spatial variability in species-richness is strongly affected by the heterogeneity of the presented effects, and their entanglement contributes to the presence of a focus species in mountain landscapes (Dufour et al., 2006).

1.3 Metapopulation - concepts and modeling

1.3.1 What is a metapopulation?

A metapopulation is commonly described as a population of populations of a single species (Hanski and Gilpin, 1991), i.e. a population comprised of multiple subpopulations, called local populations inhabiting the same landscape, but in distinct geographical locations (Lande, 1987). The metapopulation concept is an abstraction of the concept of population, where an ensemble of interacting individuals is considered to a higher level, and where interacting

subpopulations are considered (Hanski and Gilpin, 1991).

The term is first introduced by Levins (1969) who is interested in understanding why certain areas, although evidently suitable for a focus species, are at times not inhabited (Lande, 1987; Ovaskainen and Saastamoinen, 2018). Levins postulates that a patch, an aggregation of suitable area, would experience high population turnover, with local extinction and re-establishment of the population from surrounding occupied patches. The patches are thus only empty because the local extinction rate exceeds the colonization rate, and remain so while waiting to be repopulated by offsprings from surrounding subpopulations (Lande, 1987).

Spatially-implicit metapopulation model Levins designed a model which permits to compute the fraction of the landscape which is occupied by the metapopulation ($p(t)$) at time t (Levins, 1969):

$$\frac{dp(t)}{dt} = cp(t)(1 - p(t)) - ep(t) \quad (1.1)$$

where e and c are the extinction and colonization rates respectively. The proportion of empty patches is controlled by the extinction and colonization rates (Lande, 1987).

Intrinsic to the metapopulation theory, is that the metapopulation as a whole maintains itself in the landscape by relying on the exchanges between local subpopulations and would otherwise go extinct (Hanski and Gilpin, 1991). The interplay between the colonization and extinction rates controls the equilibrium of the system. Local death and reproduction rates are not explicitly modeled, but rather assumed to influence the global colonization and extinction rates, the two processes which define the persistence of the species in the landscape. This equation assumes two stationary points, namely the absence from the landscape ($p = 0$), and the steady state $p^* = 1 - \frac{e}{c}$. The latter sets the condition on species survival to $c/e > 1$ (Gyllenberg et al. (1997), Hanski (1997)); Colonization (and migration) of individuals to unoccupied patches ensures that the species (the metapopulation) survives, even if going extinct locally. As explained in Hanski (1999a), this model assumes an infinite number of habitat patches, and that neither distance nor connection between patches has an effect. This assumption, albeit restricting movement in space, is a good approximation of the mean-field theory (Hanski, 1999a), stating that all patches are equally connected to all other patches.

Levins' model assumes that when a species goes extinct, the population can not appear again. MacArthur and Wilson (1967) around the same time introduce the concept of island biogeography. In this model, islands connected to each other will have a turnover, and a species will always be able to restart on an island. The probability p of the species re-occupying an island when absent from the island is therefore not zero:

$$\frac{dp}{dt} = m(1 - p) - ep \quad (1.2)$$

where m is the immigration constant. This is called the rescue effect. This concept has further been investigated, and the idea of an infinite pool of species existing on the mainland and colonizing the islands has emerged (Gilpin and Hanski, 1991)

$$\frac{dp}{dt} = (c_m + cP)(1 - P) - eP \quad (1.3)$$

where c_m represents the colonization rate from the mainland. These two concepts are important, because they assume that individuals can enter into the system from outside and influence the dynamics of the local species.

Levins ideas have since then been challenged, but the core idea of balance between colonization and extinction processes has remained a strong pillar of metapopulation ecology.

Spatially-explicit metapopulation model Hanski in particular (Hanski and Gilpin, 1991) is intrigued by the idea of abstraction of dynamics of a focus species at different scales: the local scale, defined by patches where most of the individuals interact; and the landscape-scale, where populations interact. Rather than focusing on the survival of a single individual, Hanski tries to understand what drives a focus species as a whole to persist in a given landscape. He rapidly understands the limitations of Levins approach (Gyllenberg et al., 1997; Hanski and Gyllenberg, 1997; Hanski and Ovaskainen, 2003): the patches are all of equal habitat quality and equally well connected to each other, with unlimited dispersal (mean-field theory). This does not fit with his main concern: how does habitat fragmentation and habitat loss affect the persistence of the species (Hanski and Gilpin, 1991).

Inspired by MacArthur and Wilson's idea of island biogeography, Hanski (1994) proposes that fragments of suitable area in the landscape constitute patches connected by dispersal, with each patch able to rescue other patches (implicit integration of the rescue effect), effectively reducing the probability of local extinction. The governing variables of this spatially-explicit metapopulation model are patch area and isolation. These two variables are affecting the movement of individuals, the extinction of local populations, and the establishment of new populations at empty sites (Hanski, 1998). Patch area is meant as a proxy for population size and habitat quality, hence influencing the number of offsprings and the probability of a local population to go extinct (Ovaskainen and Saastamoinen, 2018). The chance of some individuals in the population performing well even within a bad-performing population is higher with larger population size. This also prevents the population to go extinct because of environmental stochasticity. With decreasing patch area, the probability of local extinction increases, and with decreasing isolation (or increasing connectivity), the chance of colonization increases (Fleishman et al., 2002). With more favorable area available, the population will become larger, and the local extinction risk decreases. In turn, with larger population

size, the number of colonizing (and migrating) individuals from the patch increases. Indeed, individuals are assumed to emigrate from the patch whenever their departure increases the overall fitness of the population in the patch, through, for example, inbreeding avoidance, sibling competition, high patch density, low density and escaping imminent extinction (Hanski, 1999a). The colonization towards a patch is therefore proportional to the size of the connected patches. The isolation of each patch, and hence the connectivity between patches, is modeled by spatially locating the individual patches, and thus the distance between them, which in turn dictates the dispersal capacity.

Hanski proposes the following model: the probability of patch i , denoted p_i , being occupied is given as (Hanski and Gyllenberg, 1997):

$$\frac{dp(t)_i}{dt} = C_i(t) [1 - p(t)_i] - E_i p(t)_i \quad (1.4)$$

where the extinction rate E_i is area-dependent and the colonization rate C_i area and distance dependent (Hanski and Ovaskainen, 2003):

$$E_i = e / A_i \quad (1.5)$$

$$C_i(t) = c \sum_{j \neq i} \exp[-d_{ij}/D] p_j(t) A_j \quad (1.6)$$

where A_i is the area of patch i , d_{ij} is the distance between patch i and j and D is the dispersal distance. The value $S_i = \sum_{j \neq i} \exp[-d_{ij}/D] A_j$ is defined as the connectivity of patch i to the rest of the landscape, which controls how offsprings disperse to other patches by an exponential dispersal kernel. Note that here the colonization depends on surrounding occupied patches, whereas the extinction only on the focus patch area.

As mentioned before, this model was primarily developed to understand the consequences of one of the main threat to most species (Saari et al., 1998; Hanski, 2001; Ovaskainen et al., 2002; Ovaskainen and Hanski, 2003): landscape fragmentation, habitat loss and destruction caused by humans (Hanski, 1998; Albert et al., 2013), which have deep effects for biodiversity, survival and persistence of a focus species (Bascompte and Solé, 1998).

Habitat loss changes the spatial arrangement and the fragmentation of the remaining habitat and increases the isolation of the remaining patches (Ewers and Didham, 2006). The fragmented patches introduce new habitat boundaries, increasing edge effects (loss of biodiversity at the edge of the patch) and restructure the relations between patches at the landscape level. Fragmentation and destruction of habitat generate perturbations throughout the whole network of connected patches, and have cascading impacts (Gilaranz et al., 2017), the extent of which is often only measurable later, when the metapopulation reaches its new equilibrium, or goes extinct (extinction debt).

Metapopulation capacity of fragmented landscapes In order to assess the persistence of a metapopulation in a landscape, Hanski and Ovaskainen (2000; 2001; 2002) proposed the concept of metapopulation capacity, meant to quantify the capacity and the necessary conditions of a species to survive in a fragmented landscape, taking into account the spatial composition and the area of the patches hosting the species. By computing the Jacobian of the system (see Box 1.1 for the derivation):

$$\mathbf{J} = c\mathbf{M} - e\mathbf{I}, \quad (1.7a)$$

$$\mathbf{M} = \begin{cases} \exp(-d_{ij}/D)A_iA_j & \text{for } i \neq j \\ 0 & \text{for } i = j \end{cases}, \quad (1.7b)$$

one can set the condition for persistence of the species in the landscape (having $p_i^* > 0$) to:

$$\max(\lambda(\mathbf{J})) > 0 \quad (1.8a)$$

$$\rightarrow \max(\lambda(\mathbf{M})) = \lambda_M > e/c \quad (1.8b)$$

where λ_M is the leading eigenvalue of the matrix \mathbf{M} defined above. By ensuring the leading eigenvalue of the Jacobian to be greater than zero, the state of species extinction ($\mathbf{p}_0 = p_i = 0 \forall i$) is unstable, and any perturbation of the system leads to the alternate state ($p_i^* > 0$), ensuring species survival in the given patch network (see e.g. Bertuzzo et al. (2015)). The weighted average steady state over all patches is expressed as:

$$\mathbf{p}_\lambda^* = 1 - \frac{e/c}{\lambda_M}. \quad (1.9)$$

Note that this is not an exact result but an approximation of the appropriately weighted average of the equilibrium occupancy probability value. This implies that, when the conditions for persistence are satisfied, the higher the metapopulation capacity, the higher the expected occupancy of the population.

One additional quantity of interest related to metapopulation capacity is the relative contribution of the individual patches:

$$\lambda_i \equiv x_i^2 \lambda_M \quad (1.10)$$

where x_i is the i^{th} element of the leading eigenvector, with the values of x_i^2 scaled to sum up to unity. This allows to estimate potential weak links in the landscape, and measure heterogeneous landscape suitability for a species.

The concept of metapopulation capacity has been instrumental in understanding whether a species, represented by its set of parameters, is meant to exist in a given landscape or not. It has for instance been used in different applications regarding the specie-area relationship

(SAR (Hanski et al., 2013), see box 1.3 for a case study of an application of the metapopulation capacity applied to SAR, as used in Zaoli et al. (2019)).

Box 1.1 – Derivation of the metapopulation capacity The concept of metapopulation capacity is a fundamental mathematical tool to study the extinction or persistence of a species according to a metapopulation model, as presented by Hanski and Ovaskainen (2000) and Ovaskainen and Hanski (2001). A detailed derivation of the metapopulation capacity formula is presented here, expanding and clarifying the steps followed by Ovaskainen and Hanski (2001).

Consider the metapopulation model on n patches described in equation 1.4-1.6:

$$\frac{dp_i}{dt} = C_i(1 - p_i) - E_i p_i, \quad (1.11a)$$

$$= c \sum_{i \neq j} \mathcal{K}_{i,j} A_j p_j (1 - p_i) - \frac{e}{A_i} p_i, \quad (1.11b)$$

with p_i the probability of occupancy in patch i ($i = 1, \dots, n$), A_i the area of patch i , e and c the extinction and colonization rates, and $\mathcal{K}_{i,j}$ the function describing the dispersal between patches i and j . Let \mathbf{p} be the solution vector, $\mathbf{p} = (p_1, \dots, p_n)'$.

The stability of the system is discussed around a stationary solution $\tilde{\mathbf{p}}$, i.e. solutions that satisfy $\frac{d\tilde{\mathbf{p}}(t)}{dt} = 0$ (each component of $\tilde{\mathbf{p}}$ is constant in time). This is the case, for example of the null solution, $\tilde{\mathbf{p}}_i = 0$ ($i = 1, \dots, n$), representing the extinction of the species in all patches. A stationary solution $\tilde{\mathbf{p}}$ is stable if, starting from a small perturbation of the system around $\tilde{\mathbf{p}}$, the system converges to $\tilde{\mathbf{p}}$. A necessary condition for the stability of a stationary solution is that all the eigenvalues of the Jacobian matrix of the system evaluated in the stationary point, i.e. $\mathbf{J}(\tilde{\mathbf{p}})$, have negative real part.

In this case, the elements of the Jacobian of the system read:

$$\mathbf{J}_{ij}(\mathbf{p}) = \begin{cases} c A_j \mathcal{K}_{ij} (1 - p_i) & \text{for } i \neq j \\ -c \sum_{i \neq j} \mathcal{K}_{i,j} A_j p_j - \frac{e}{A_i} & \text{for } j = i \end{cases}. \quad (1.12)$$

Evaluating the Jacobian in the stationary null solution $\tilde{p}_i = 0$ provides:

$$\mathbf{J}_{ij}(0) = \begin{cases} c A_j \mathcal{K}_{ij} & \text{for } i \neq j \\ -e / A_i & \text{for } i = j \end{cases}. \quad (1.13)$$

Let $\lambda_i^{\mathbf{J}}$ ($i = 1, \dots, n$) be the eigenvalues of $\mathbf{J}(0)$. Then, $\tilde{\mathbf{p}} = 0$ is stable if

$$\Re(\lambda_i^{\mathbf{J}}) < 0 \quad \text{for all } i = 1, \dots, n \quad (1.14)$$

and unstable if there is at least one eigenvalue of $\mathbf{J}(0)$ with real part greater than zero.

There are some difficulties in the numerical computation of the eigenvalues of matrix $\mathbf{J}(0)$ due to the following facts:

- $\mathbf{J}(0)$ is non-symmetric
- $\mathbf{J}(0)$ is ill-conditioned when the patches' areas vary of several order of magnitude among patches.

These conditions imply a very slow convergence of the numerical algorithms for the eigenvalues computation. To overcome these difficulties, it can be noted that $\mathbf{J}(0)$ is factorized as follows:

$$\mathbf{J}(0) = \mathbf{D}\mathbf{S}, \quad (1.15)$$

where \mathbf{D} is the diagonal matrix with terms $\mathbf{D}_{ii} = \frac{1}{A_i}$ and \mathbf{S} is the following symmetric matrix:

$$\mathbf{S}_{ij} = \begin{cases} cA_iA_j\mathcal{K}_{ij} & \text{for } i \neq j \\ -e & \text{for } i = j \end{cases}. \quad (1.16)$$

Since \mathbf{S} is symmetric, its eigenvalues are real numbers. In the following the eigenvalues of \mathbf{S} are termed as $\lambda_i^{\mathbf{S}}$, with $\lambda_1^{\mathbf{S}} \geq \lambda_2^{\mathbf{S}} \geq \dots \geq \lambda_n^{\mathbf{S}}$. Due to the relation between $\mathbf{J}(0)$ and \mathbf{S} (equation 1.15), it is possible to demonstrate that also the eigenvalues of $\mathbf{J}(0)$ are real and their sign is the same of the eigenvalues of \mathbf{S} .

In fact, matrix \mathbf{S} is congruent to matrix $\mathbf{S}' = \mathbf{D}^{-\frac{1}{2}}\mathbf{S}\mathbf{D}^{-\frac{1}{2},T}$, they thus have the same number of positive, negative and zero eigenvalues, and all eigenvalues are real numbers (this is consequence of Sylvester's law). Moreover, \mathbf{S}' is similar to $\mathbf{J}(0)$, meaning that they have the same eigenvalues:

$$\mathbf{D}^{\frac{1}{2}}\mathbf{S}'\mathbf{D}^{\frac{1}{2}} = \mathbf{D}\mathbf{S} = \mathbf{J}(0).$$

As a consequence of this, if the largest eigenvalue of \mathbf{S} is positive, i.e. $\lambda_1^{\mathbf{S}} > 0$, then also the largest eigenvalue of \mathbf{J} is positive, $\lambda_1^{\mathbf{J}} > 0$, implying that the condition of stability is not satisfied.

The main advantage of this step is that the eigenvalues of \mathbf{S} can be obtained from those of a matrix \mathbf{M} , which does not depend upon e and c :

$$\mathbf{M} = \frac{1}{c}(\mathbf{S} + e\mathbf{I}_n) \quad (1.17)$$

where \mathbf{I}_n is the identity matrix (diagonal matrix, with 1 along the diagonal). The elements of \mathbf{M} read:

$$\mathbf{M}_{ij} = \begin{cases} A_iA_jK_{ij} & \text{for } i \neq j \\ 0 & \text{for } i = j \end{cases}. \quad (1.18)$$

\mathbf{M} and \mathbf{S} have the same eigenvectors. In fact, let \mathbf{v}_i be an eigenvector of \mathbf{M} , and $\lambda_i^{\mathbf{M}}$ its

associated eigenvalues. by definition:

$$\mathbf{M}\mathbf{v}_i = \lambda_i^{\mathbf{M}}\mathbf{v}_i \quad (1.19)$$

$$\frac{1}{c}(\mathbf{S} + e\mathbf{I}_n)\mathbf{v}_i = \lambda_i^{\mathbf{M}}\mathbf{v}_i \quad (1.20)$$

$$\mathbf{S}\mathbf{v}_i = (c\lambda_i^{\mathbf{M}} - e)\mathbf{v}_i \quad (1.21)$$

and then $\lambda_i^{\mathbf{S}} = c\lambda_i^{\mathbf{M}} - e$ is an eigenvalue of \mathbf{S} .

The stability condition of the null solution translates in the following condition on the eigenvalues of \mathbf{M} :

$$\lambda_1^{\mathbf{S}} < 0 \implies c\lambda_1^{\mathbf{M}} - e < 0 \implies \lambda_1^{\mathbf{M}} < \frac{e}{c} \quad (1.22a)$$

i.e., the largest eigenvalue of \mathbf{M} must be smaller than $\frac{e}{c}$. Note that, in this way, eigenvalues of the matrix are computed independently from the extinction and colonization rates of the species. Moreover, \mathbf{M} is symmetric and has a condition number much lower than $\mathbf{J}(0)$, thus the largest eigenvalue can be computed with a reduced computational effort. It is interesting to note that, matrix \mathbf{S} is strictly related to the dynamical system arising from a basic modification of equation 1.11:

$$\frac{1}{A_i} \frac{dp_i}{dt} = c \sum_{j \neq i} \mathcal{K}_{i,j} A_j p_j (1 - p_i) - e/A_i p_i, \quad (1.23a)$$

$$\implies \frac{dp_i}{dt} = c A_i \sum_{j \neq i} \mathcal{K}_{i,j} A_j p_j (1 - p_i) - \cancel{A_i} \cancel{\mathcal{K}_{i,i}} e p_i. \quad (1.23b)$$

In this new system, the extinction rate is independent of the size of the patch. The colonization rate is dependent on the product of source and target patch areas, thus implicitly using the quality of both patches in the colonization process. It is easy to show that the Jacobian matrix of this system, evaluated in the null stationary solution, corresponds to matrix \mathbf{S} . Thus, this system and the original metapopulation model have the same condition for the extinction of the species. However, equation 1.23 implies that in the second system the speed of the colonization processes is dependent on the source patch and the extinction independent of the patch itself, implying that the transient phase among these systems might be drastically different even if starting from the same initial configuration.

Introducing temporal environmental stochasticity The deterministic model expressed in equation 1.4 was initially expressed as a discrete-time stochastic patch occupancy model, called incidence function model (IFM, Hanski (1994)). Here, rather than simulating the

probability of occupancy, the model simulates the states of occupancy of each patch, either occupied or empty. The model is defined as a discrete time Markov-Chain. The patches have a probability to change from occupied ($w = 1$) to empty ($w = 0$) and vice versa at each time step Δt (Hanski, 1994; Tilman and Kareiva, 1997; Hanski, 1998):

$$P(w_i(t) = 1 \rightarrow w_i(t + \Delta t) = 0) = E_i = \min \left[\frac{e}{A_i^x}, 1 \right], \quad (1.24a)$$

$$P(w_i(t) = 0 \rightarrow w_i(t + \Delta t) = 1) = C_i = \frac{S_i^2}{S_i^2 + y^2}, \quad (1.24b)$$

$$S_i = c \sum_{j \neq i} \exp[-d_{ij}/D] A_j p_j \quad (1.24c)$$

where the parameters x and y control the shape of the probability function.

An alternate version of this spatially-explicit stochastic patch occupancy model (SPOM) is expressed as (Moilanen, 2004; Ovaskainen and Hanski, 2004):

$$P(w_i(t) = 1 \rightarrow w_i(t + \Delta t) = 0) = E_i = 1 - \exp(-e/A_i), \quad (1.25a)$$

$$P(w_i(t) = 0 \rightarrow w_i(t + \Delta t) = 1) = C_i = 1 - \exp(-S_i). \quad (1.25b)$$

At each step, the change of state is drawn at random to simulate patch-independent stochasticity.

The integration of random stochasticity in the extinction and colonization processes reduces the ability of a metapopulation to persist (Lande, 1987; van Nouhuys, 2016), implicitly simulating variations in population demography close to extinction, or variation in environmental conditions (Hanski and Gilpin, 1991; Ovaskainen and Saastamoinen, 2018) such as resource availability or weather (Ebenhard, 1991), although environmental stochasticity might be correlated in space. These two models assume patch-independent stochasticity, but environmental fluctuations usually induce regional stochasticity (Hanski and Gilpin, 1991; Moilanen, 1999), which can influence the dynamic of multiple subpopulations simultaneously (Hanski, 1998). For instance spatially-correlated weather conditions or diseases can generate large-scale spatial synchrony in population dynamics (Hanski, 1998; Ovaskainen and Hanski, 2003; Moilanen, 2004). To simulate these landscape-wide phenomenon, Moilanen (2004) multiplies the area of each patch by a common random number at each step, generating synchronous fluctuations in patch area.

Other studies have incorporated weather conditions derived from satellite data or local weather stations (Purves et al., 2007; García-Valdés et al., 2013; Giezendanner et al., 2019) effectively implementing realistic stochasticity (see below).

Rescue effect Although the rescue effect (decreasing extinction rate with increasing immigration (Gyllenberg and Hanski, 1997)) is to some extent implicitly included in equation 1.24, cells can still become unoccupied and not rescued in the same step, as only one state transition is allowed per step. To mediate this effect, the rescue effect can be explicitly modeled to decrease the local extinction rate, as proposed in Hanski (1994):

$$E'_i = (1 - C_i) E_i = (1 - C_i) \cdot \min \left[\frac{e}{A_i^x}, 1 \right]. \quad (1.26)$$

This means that each cell can be rescued by incoming migrating individuals before the cell becomes extinct. Given that this effect depends on dispersal, the extinction rate becomes spatially dependent on the surrounding contributing cells.

1.3.2 Beyond the classical metapopulation model

Hanski has laid the ground for the definition of spatially-explicit metapopulation theory, and his focus on habitat loss and landscape fragmentation has brought multiple answers and perspectives to landscape management and conservation applications.

In recent years multiple variations of this initial patch-area isolation approach have been proposed to address certain shortcomings, or to explicitly model certain mechanisms implicitly incorporated before. They concern (in a non exhaustive list): patch quality, intra- and inter-patch heterogeneity (i.e. landscape-explicit modeling, including landscape-driven dispersal), species interactions (abiotic factors), structured metapopulations (i.e. local population demography) and genetics (and evolutionary processes). Given the large body of literature surrounding the concept of metapopulation, only certain topics, relevant to the focus of the thesis, are addressed here. Species interactions, population demography, as well as genetic and evolutionary processes are therefore not considered.

Patch definition Defining the limits of a patch so that the area can be quantified can be challenging. For species where a clear biome characterizes its presence (e.g. forests (Opdam, 1991) or ponds (Fortuna et al., 2006)), this can be relatively well done, but in a different context where complex abiotic and biotic interactions coupled with edge effects drive a species' niche, patch limits can be blurred and characterizing its area difficult.

Defining patches can be done in different ways. One possibility comes from expert knowledge on species habitat and characteristics, usually done with distinct features in mind (Fig. 1.6).

Another way is to aggregate suitable habitat from a lattice together to form patches (Urban and Keitt, 2001). Such a method is proposed in Akçakaya et al. (1995) (refined in Akçakaya

(2000) and Anderson et al. (2009)), where a habitat suitability model (HSM, see box 1.2) is used to characterize the suitability of each lattice element for a focus species, and subsequently apply a threshold to the suitability value (Fig. 1.6).

Box 1.2 – Habitat suitability and species distribution models Species distribution models (SDMs, see, e.g., Guisan and Thuiller (2005); Araújo and Guisan (2006); Guisan et al. (2017)) focus on computing the landscape-explicit spatial probability of presence of a species based on the realized niche. This occurs by relying primarily on the habitat suitability (HS, (Kearney and Porter, 2009)), that is, the suitability given the habitat's biotic and abiotic factors, which is believed to drive the probability of presence of a species at equilibrium (Busby, 1988; Booth et al., 2014). This approach implies that the presence of a species in the landscape reflects its niche, and other processes like dispersal, colonization or migration do not have major effects (Thuiller et al., 2014). In SDMs, most processes are implicitly incorporated in the habitat suitability, and hence in the species' niche (Guisan and Zimmermann, 2000).

The suitability of the species is commonly inferred by reproducing in-situ data of species presence from statistical models using raster-like EO data (satellite images, remote sensing, etc.).

SDMs provide an accurate static picture of the species distribution in the landscape at a certain time (Stanton et al., 2012). However, processes such as (meta-) population dynamics are rarely explicitly modeled, and with them the transient times between two different spatial species distributions.

The cells displaying a value above the threshold are then grouped into aggregated patches. Once the patches are defined in this first modeling step, together with their area and spatial distances, it is possible to set up a classical metapopulation model for the species of interest (note that a demographically structured metapopulation model is used in Akçakaya (2000), not the classical one).

The problem with such an approach is that mechanisms such as dispersal and colonization are intrinsically considered within the species distribution model, and as such only patches where the species has been observed are considered as suitable. But Hanski's metapopulation model relies on the turnover between colonization and extinction, and the fact that suitable habitats can be empty is at the very root of the metapopulation process. The patches defined by the SDMs thus provide a biased view of the actual patch network which the species can profit from. Nevertheless, this approach is still interesting for certain applications, given the complexity of defining the area of the different patches.

Patch quality In the classical metapopulation approach, the defining feature of the patch is its area. But Hanski himself (Hanski, 2001) has stated that area is suggested as a surrogate for expected population size, and that any factor could modify the “*virtual*” area of the patch, in order to reflect the more realistic contribution of the patch to the dynamics of the focus species.

The “*quality*” of a patch represents the suitability of the focus patch for the given species, and may thus vary between species for a same patch, and of course between patches for a same species. Habitat quality is one of the key drivers of local species dynamics (Moilanen and Hanski, 1998; Ovaskainen and Hanski, 2003), as it defines how suited a species is in a certain habitat. Species forced to evolve in unfavorable habitat will rapidly decline in number of individuals if they can not reach new habitats more suited for them. On the other hand, species profiting from well suited habitats will increase in numbers and eventually spread offsprings which will colonize other parts of the landscape. The quality of a habitat can be defined as combination of variables describing the landscape (e.g. land use, occupying species, environmental and climatic conditions among others). Different species do not have the same response to different type and degree of underlying quality and different environmental parameters will be used to describe the optimal conditions for each species. Purves et al. (2007) for instance show that environmental heterogeneity is a fundamental attribute that influences richness and distribution of species in a landscape, and Fleishman et al. (2002) show that area could effectively be replaced by the patch quality without loss of explanatory power when modeling occupancy and turnover in patches via environmental variables such as food resources, topography, vegetation and others. Frey et al. (2012) goes as far as saying that failing to include quality in the patch definition can “*mask relative importance of local scale features*” and completely change the modeled distribution of the species at landscape-scale.

An example of implementing altered patch quality is given by Moilanen and Hanski (1998) who found the standard approach too restrictive and introduced two modifiers, one which affects the area of the patch (quality modifier), and a second factor affecting the emigration from the patch (isolation modifier). Equation 1.24c is modified as follows (Moilanen and Hanski, 1998):

$$M_i = V_i \sum_{j \neq i} p_j V_j \exp(-d_{ij}/D) U_j A_j \quad (1.27)$$

where U_j is the quality modifier defining how the area changes with changing environmental conditions, and V_j is the patch isolation modifier, which changes the way offsprings leave the patch and reach new patches. In the case where only one environmental factor affects U and

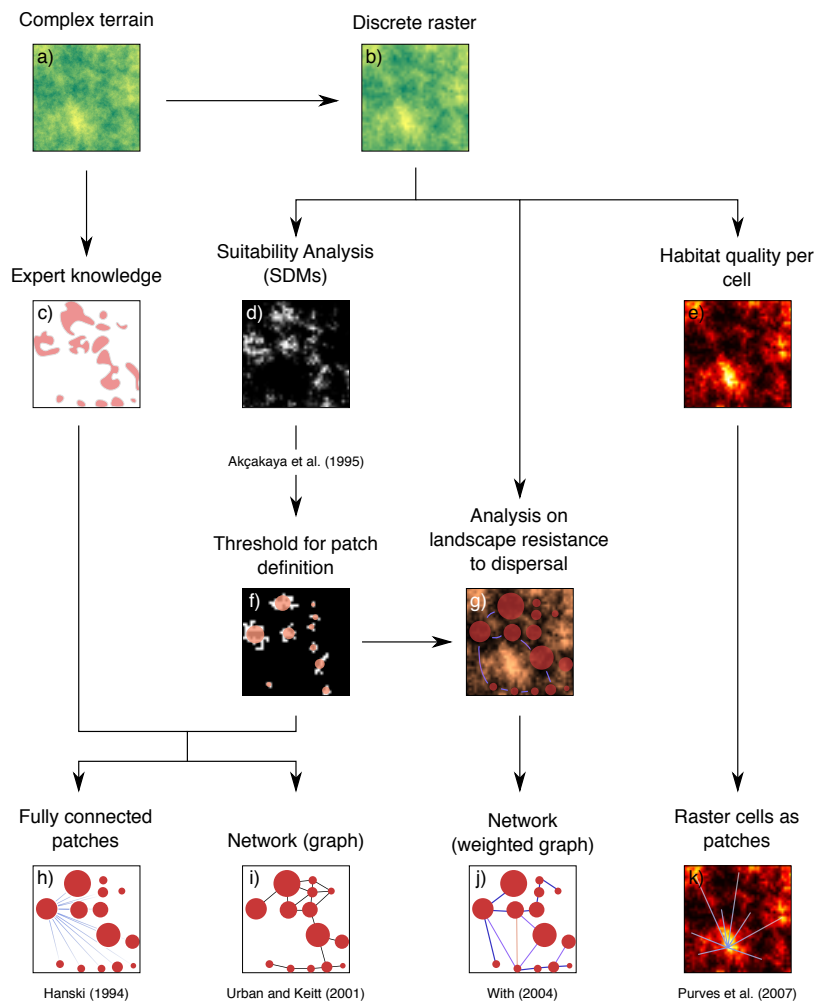


Figure 1.6 – Schematic example of different approaches to represent a complex landscape in a metapopulation model with corresponding examples from the literature.

Starting from a complex terrain with continuous characteristics (a), one possibility is to define suitable patches from expert knowledge inferred from landscape features such as forest patches or ponds (c). A second possibility is to rely on discretizing this continuous landscape by sampling the values in a grid, as done for example with rasters (b). From this raster, one can perform a suitability analysis (d), which can be used to define the patch limits (f). Both approaches (c and f), permit to construct a spatially-explicit network of patches where the area of the patch, along with other variables, define the node size. The nodes can either be fully connected to other nodes via a dispersal kernel (h), or arranged in a graph with specific connections (i). The graph can become weighted (j), if the landscape resistance to dispersal (inter-patch quality) is considered (g). From the discrete raster (b), one other possibility is to consider each cell as patch of equal area, and to assign a quality to each cell (e). The different cells are then connected by dispersal (k). Note that in the approach proposed by Purves et al. (2007), at fine enough grain size, the intra-patch heterogeneity is explicit. Also note that the methods are by no means exclusively used in the proposed literature, but merely show examples of the different approaches.

V they are modeled as a polynomial of degree three (Moilanen and Hanski, 1998):

$$U_i = ag_i^3 + bg_i^2 + cg_i + d \quad (1.28a)$$

$$V_i = ah_i^3 + bh_i^2 + ch_i + d \quad (1.28b)$$

where g_i , respectively v_i are the environmental factor themselves. U and V are thus the fitness of the given species to the environmental driver of interest. The extinction probability is defined as $E'_i = (1 - C_i) E_i$, and thus also includes the effect of the modifiers, as well as the rescue mentioned above. In this model, patch quality does not affect the diffusion kernel, but rather the behavior of the offsprings.

Intra-patch heterogeneity In reality, the landscape within a patch is never characterized by a homogenous feature (Fig. 1.7), and this intra-patch variations can influence the local extinction and dynamics of the species (Gyllenberg and Hanski, 1997). Additionally, ignoring the geometry of the patch might lead to the assumption that all areas of a patch are equally accessible, which might rarely be the case. It has been shown that the structure of the habitat

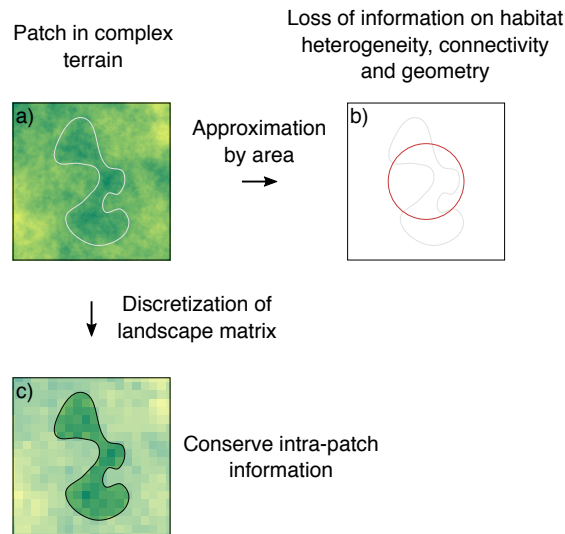


Figure 1.7 – Loss of information on intra-patch heterogeneity. The interior of a patch and its immediate surrounding are of heterogeneous quality (a). When approximating the patch by its area and assuming homogenous quality (b), losses in information on habitat heterogeneity, connectivity inside the patch as well as geometry which influence population at the edge are implicitly modeled. The regular discretization of the continuous space and the application of population models on these discrete cells can be an option to explicitly model intra-patch heterogeneity (c).

changes towards the edge of the patch and that species-richness is negatively correlated with the distance from the fragment's interior (the so-called edge effect, Ewers and Didham (2006)). This can be, for instance, due to random colonization from the patch interior towards the

patch edge (Lande, 1987). The populations inhabiting these edges are therefore the most sensitive to alterations in the landscape structure and to environmental change (Anderson et al., 2009).

These effects are, to a certain extent, implicitly taken into account in the extinction rate, but explicitly modeling the landscape can be of interest (see below), especially if intra-patch movements and edge effects are known to influence the focus species.

Connectivity, dispersal, and inter-patch heterogeneity “*Connectivity refers to the ability of organisms to access habitat, which affects colonization rates, and thus [...] persistence on the landscape*” (Harrison and Taylor, 1997). Connectivity is thus a crucial environmental quality to be considered while studying species dynamics. As mentioned before, Hanski (1999b) defined connectivity using patches, where isolation, or alternatively, the Euclidean distance from one given patch to all others is considered the main driver of connectivity between patches. The patches are assumed to be scattered over a landscape of unfavorable, non-habitable, terrain (Hanski, 1999b). This idea, similar to islands surrounded by an inhospitable ocean, has been challenged (Ricketts, 2001). Of importance is indeed the distance between patches, but also what lies in-between (Wiens, 1997), as patches close together, but with absolutely uncrossable areas, will not be connected in patch-networks, and this has to be taken into consideration when modeling the patch connectivity. In Muneeppeerakul et al. (2008), for example, river networks are defined as ecological corridors supporting movement of communities in the landscape. In Bertuzzo et al. (2016) same-elevation areas are used to define pathways in the landscape. Even the essence of islands being surrounded by homogenous non-habitat area has been challenged, because ocean currents have been shown to modify the effective distance between two islands (Ricketts, 2001). This concept of considering the inter-patch heterogeneity into the connectivity has been dubbed the “*effective isolation*” or “*effective connectivity*”, or “*landscape resistance*” to dispersal and colonization (Ricketts, 2001; McVinish and Pollett, 2013; Graves et al., 2014).

To counter this notion of uniformly non-habitat surrounding habitat patches, Moilanen and Hanski (1998), who also introduced the modifiers to the patch quality, proposed a method which directly affects the diffusion kernel:

$$M_i = \sum_{j \neq i} p_j \exp \left(- \sum_h d_{hij} / D_h \right) A_j \quad (1.29)$$

where h describes the given landscape. Essentially, in this approach, the quality of the patches is assumed to influence the migration distance D as well as the distance between patches. Less appropriate environment between patches will “increase” the distance between them, whereas well suited areas will “shorten” the inter-patch distance.

Graves et al. (2014) investigate the use of landscape features to modify the shape of the dispersal kernel. Instead of using the Euclidean distance between origin and settlement location, they use a least-cost approach which relies on the Dijkstra algorithm. The Dijkstra algorithm finds the path of least resistance (or in case of elevation, of smallest distance, i.e. smallest cost) in a landscape, which is not necessarily the Euclidean distance, as a path going around an unfavorable area might be more efficient (Fig. 1.8). The distance used is then the one of the least cost path, and the rest of the kernel definition stays the same. Graves et al. (2014) find that dispersal kernels modified by the cost have a better predictive power than standard dispersal kernel based on Euclidean distance.

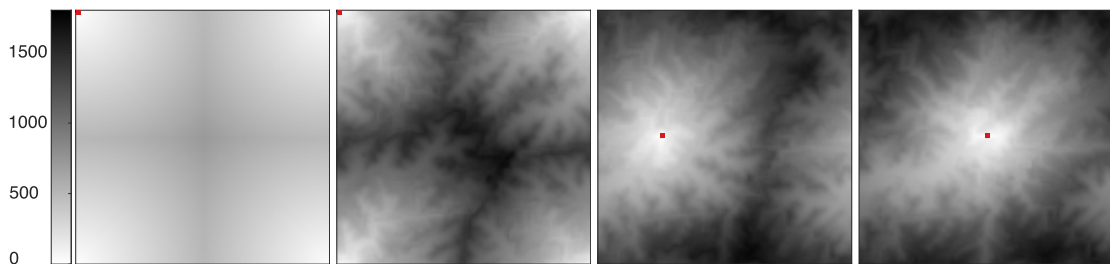


Figure 1.8 – Example of considering or not the landscape structure in the dispersal kernel.

Example of distance from the reference pixel (red) to all other pixels in a virtual landscape. The first image shows the Euclidean distance between pixels, while the following images show the distance between points when computed using the shortest path between cells (Dijkstra algorithm) which takes into consideration the topography of the landscape. All distances assume periodicity at the boundary of the landscape.

Different studies have proposed to extend the idea of graph-like connected patches (Fortuna et al., 2006; Gilarranz and Bascompte, 2012; Gilarranz et al., 2017) by using weighted graphs to describe the habitat patches and the links between them (Urban and Keitt, 2001; With, 2004; Albert et al., 2013), where the links between patches depend on the habitat matrix, with the suitability of the habitat influencing the weight of the link (Fig. 1.6). The higher the weight, the easier the focus species can move from one patch to the other. This approach basically assumes that the patches are linked by habitat corridors facilitating the dispersal between them (Hanski and Gilpin, 1991). One possibility to compute the weights is to follow Graves et al. (2014), where the distance between patches are considered as the path of least resistance and computed via the Dijkstra algorithm.

Landscape-explicit metapopulations The combination of inter-and intra-patch heterogeneity means that the whole landscape is modeled explicitly. Combining population ecology with an explicit description of the landscape matrix has been advocated by many authors in the literature (Wu and Hobbs, 2002; With, 2004; Fahrig and Nutton, 2005; Fahrig, 2007). Hanski and Gilpin (1991) already praised the similarities between population and landscape ecology

(Turner, 1989, 2005), predicting that the two field would eventually merge. Hanski (2001) recognized that the patch-based approach had its limitations, given that, as mentioned above, certain landscape can not be summarized to patches, but need a continuous description (With, 2004). In such cases, he mentioned the possibility to discretize the landscape as commonly done with raster data (Urban and Keitt, 2001) (Fig. 1.6), in the same fashion than done with cellular automata (see Bascompte and Solé (1996) and Keymer et al. (1998) for examples of metapopulation models using cellular automata). This would mean that the landscape matrix is explicitly modeled (Ricketts, 2001; Ewers and Didham, 2006; Ovaskainen and Saastamoinen, 2018), incorporating the complex landscape mosaic into metapopulations (Wiens, 1997; With, 2004). An additional effect is that, when modeling the whole landscape, areas considered as non-favorable could still be occupied by a focus species from source-sink mechanisms (With, 2004), and accommodate species which need more than one habitat type (Fahrig and Nuttle, 2005).

Purves et al. (2007) propose to decompose the landscape into gridded cells, and treat each cell of the landscape as an individual patch (Fig. 1.6). The original cellular automata model assumes interdependence of cells, where only the nearest neighbor of each cell contributes to the survival of the cell via dispersal. By taking a cellular landscape (a grid), the area is assumed to be unitary (also in Rybicki and Hanski (2013); García-Valdés et al. (2013); Bertuzzo et al. (2015); Giezdanner et al. (2019)), which makes it disappear from equation 1.6, but is replaced by the quality of the cell. Each cell is given a quality, and each the species is assumed to have a certain suitability, or fitness, to the given quality which is computed from environmental factors following a sigmoid function (Purves et al., 2007; García-Valdés et al., 2013):

$$f_i = \frac{1}{1 + e^{-f_i(P, T, i)}} \quad (1.30)$$

where f_i is a function (either constant, linear or non-linear) of the environmental conditions (P and T) in patch i with different coefficients for extinction and colonization.

In Rybicki and Hanski (2013), the habitat is proposed to be modeled by an arbitrary value of quality q :

$$f_i = \exp\left(-\frac{(q_i - \phi)^2}{2\gamma^2}\right) \quad (1.31)$$

with q the quality, or habitat type, ϕ the phenotype of the species (or which habitat type is most suitable for the species), and γ the niche width. The phenotype and niche width change for each species.

These alternatives allows to model the variation in suitability of a species to the underlying landscape quality continuously, which is interesting, as certain species will have more or less favorable terrain. If and when the terrain quality can be continuously modeled, this allows to

create continuous habitat suitability maps for different species, thus explicitly modeling the complex landscape suitability. In this way, the effect of habitat stochasticity on the presence of metapopulation species in the landscape can be investigated (c.f. box 1.3).

Box 1.3 – On the probabilistic nature of the species-area relation *The section “Effect of habitat stochasticity in a metapopulation dynamics model” has been written as a contribution to the paper “On the probabilistic nature of the species-area relation” (Zaoli, Giometto, Giezendanner, Maritan and Rinaldo, 2019) which focused understanding the distributions of species-area relationship in different models with different types of stochasticity. The contributed part focused on habitat stochasticity using the metapopulation capacity (Hanski and Ovaskainen, 2000).*

Context (Zaoli et al. (2019)) Although natural ecosystems are often characterized by striking diversity of form and function, deep regularities emerge almost inevitably across scales of space, time and organizational complexity (Levin, 1992; Harte et al., 2009; Rybicki and Hanski, 2013). Such regularities are subsumed by macroecological ‘laws’ that describe statistical patterns in species’ number, abundances and sizes (Brown, 1995; Brown et al., 2004; Marquet et al., 2005; Banavar et al., 2007; Southwood et al., 2006; Zaoli et al., 2017). Each of these patterns might be affected by alterations of ecosystem features, like systematic effects of global environmental change (Thomas et al., 2004), spatial heterogeneities (Borile et al., 2013), regional habitat modifications (Ney-Nifle and Mangel, 2000; Hanski et al., 2013; Hanski, 2016), reduced speciation (Rosenzweig, 1995), spatial scaling of trophic interactions (Levin, 1992; Rybicki and Hanski, 2013) or modifications of the matrix available to ecological interactions, especially if affecting its topolog (Fagan, 2002; Benda and et al., 2004; Muneeppeerakul et al., 2008; Bertuzzo et al., 2011). Scaling theory offers a powerful tool to make way for coherent, unified descriptions of these patterns (Marquet et al., 2005; Marquet, 2017), highlighting linkages and constraints among them (Southwood et al., 2006; Banavar et al., 2007; Zaoli et al., 2017). Arguably, the most important example of ecological ‘law’ is the Species–Area Relationship (SAR). The SAR quantifies the observation that species-richness S tends to increase with increasing sampling area A , in a relationship firmly placed at the origins of quantitative ecology (Arrhenius, 1921; Gleason, 1922; MacArthur and Wilson, 1967). More precisely, the standard formulation of the SAR states that the number of species S inhabiting an ecosystem increases as a power of its area, A , such that $S = cA^z$, where c is a constant and $z \leq 1$ is the SAR’s scaling exponent.

The interest in SARs has been broad from all of ecology, in particular for their implied predictive use to forecast the effects of large-scale environmental or climatic change on biodiversity (Thomas and Hanski, 2004), in particular as a consequence of habitat loss or

fragmentation (Durrett and Levin, 1996; Hanski et al., 2013; Rybicki and Hanski, 2013; Borile et al., 2013). In fact, within a deterministic power-law framework, the fraction of species surviving a habitat reduction from area A to area A_{new} would simply be equal to $(A_{new}/A)^z$. Note that, to the end of such predictions, only the scaling exponent z matters (and not the proportionality constant), explaining the interest in its value (see e.g. Whitmore and Sayer (1992); May et al. (1995); Brooks and Balmford (1995); Pimm and Askins (1995); Hanski and Gyllenberg (1997); Ney-Nifle and Mangel (2000); Brooks (2002); Kadmon and Allouche (2007)). Against this background, assessing the nature of SARs and the reliability of their predictions is particularly important and an issue of longstanding interest to community ecology, biogeography, and macroecology (MacArthur and Wilson, 1967; Rosenzweig, 1995; Blackburn and Gaston, 2003; Lomolino, 2000; Hanski et al., 2013).

An important factor has been overlooked both in the modeling and in the interpretation of SARs: the fluctuations of the number of species S that the ‘law’ is meant to address. Deterministic approaches, in fact, only address the average biodiversity, neglecting any fluctuations due to the intrinsic stochasticity of the processes taking place in an ecosystem and the external sources of variability. In models of ecosystem dynamics, the number of species S in stationary conditions results from the balance of competing stochastic processes, which according to neutral theory are speciation, immigration and drift. Therefore, the number of species S , as well as other variables describing the state of the ecosystem, should be seen as stochastic variables and thus subject to fluctuations. If one were able to capture its evolution in time within one single ecosystem, or compare it in exact replicas of the same ecosystem with the same area, S would assume different values according to its stationary distribution $p(S, t \rightarrow \infty) = p(S)$.

Effect of habitat stochasticity in a metapopulation dynamics model In a given ecosystem, the availability of different niches might change in time, affecting the number of species surviving in it and therefore creating additional variability. It might also differ between ecosystems of the same size. A spatially-explicit metapopulation model was studied, a well-established tool to study biodiversity patterns in a spatially heterogeneous environment (Hanski and Ovaskainen, 2000; Rybicki and Hanski, 2013; Grilli et al., 2015) (see also Bertuzzo et al. (2015) for a study of the metapopulation capacity applied to fluvial landscapes) which allows assessing the role of habitat stochasticity in the variability of S . The metapopulation model is based on the interplay between extinction and colonization dynamics. Each species has a probability p_i to be present (with one or more individuals) in a site i of the landscape, which is a $L \times L$ lattice. Species do not interact, thus they have independent dynamics. Let E_i be the rate at which a species becomes extinct in patch i and C_i the rate at which the patch is colonized. The probability of

occupancy p_i of patch i is then governed by

$$\frac{dp_i}{dt} = C_i(1 - p_i) - E_i p_i. \quad (1.32)$$

Each patch is characterized by a habitat type, determined by the value of a parameter h , $0 \leq h \leq 1$. A species is characterized by 5 parameters: the colonization rate c , the extinction rate e , the phenotype ϕ , the niche width γ and the average dispersal distance $1/\alpha$. For a focal species, the fitness in a patch i with habitat parameter h_i is $q = \exp[-(h_i - \phi)^2/(2\gamma^2)]$. The fitness, which is larger when ϕ is similar to h_i , determines how well the species will perform in that patch, i.e. the probability that it will become extinct, the extinction rate being defined as $E_i = e/q_i$. In turn, the colonization rate, given by $C_i = c/(2\pi) \sum_{j \neq i} \alpha^2 e^{-d_{ij}\alpha} q_j p_j$, governs the interactions between the different patches. The parameters needed to generate these virtual species are extracted at random from a uniform distribution in a suitable interval. The values of h characterizing the landscape are also extracted at random, but with a fixed spatial correlation (see below for details) and are constant in time. It was shown (Hanski and Ovaskainen, 2000) that the condition under which equation 1.32 has an equilibrium solution different from $p_i = 0 \forall i$ is

$$\lambda_M > e/c, \quad (1.33)$$

where λ_M is the metapopulation capacity, i.e. the leading eigenvalue of an appropriate matrix, which depends on the landscape and on the species phenotype Φ , niche width γ and dispersal range $1/\alpha$. It is therefore said that a species is persistent in the landscape if it satisfies the condition in equation 1.33.

To study the variability in the number of species persisting in a landscape of a given size in the presence of habitat stochasticity, a pool of $S_0 = 500$ species was considered, evaluated how many satisfied the condition in equation 1.33 and repeated the evaluation in a set of 1000 different random landscapes at fixed spatial correlation with the same pool of species. Spatially-correlated random landscapes were generated with two alternative methods (Fig. 1.9). The first is the one used in Rybicki and Hanski (2013), while the second uses the HYDRO_GEN algorithm (Bellin and Rubin, 1996) for the generation of correlated random fields, which has the advantage of allowing us to set a prescribed correlation. The landscape areas $A = 25^2, 50^2, 100^2, 200^2$ were considered. Initially 1000 landscapes of size 200^2 were generated, then the 1000 smaller landscapes were obtained as subsets. Species parameter ranges were taken as follow: $c \in [0.25, 2]$, $e \in [0.025, 0.4]$, $\phi \in [0.1, 0.9]$, $\gamma \in [0.1, 0.5]$, $\alpha \in [0.07, 1]$. To increase the species pool without increasing the computational time (mainly dependent on the λ_M computation), for each of the 500 sets of ϕ , γ and λ 15 additional values of c and e were extracted, effectively enlarging the species pool to $S_0 = 8000$.

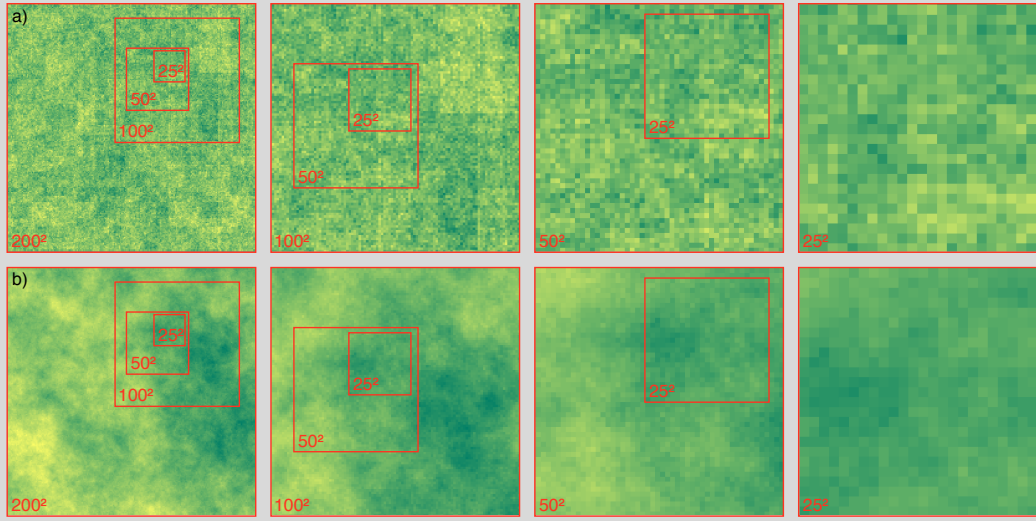


Figure 1.9 – Subdivision of correlated random fields for the study of SAR. Example of one of the 1000 landscapes of area $A = 200^2$ and subdomains generated according to Rybicki and Hanski (2013) (a) and with the HYDROGEN algorithm (Bellin and Rubin, 1996) (b). The different sub domains, of sizes $A = 25^2, 50^2, 100^2$ are selected at random within the initial domain.

In this model the number of persisting species is not determined by the equilibrium of the competing stochastic processes of speciation and extinction, but by the diversity of habitat types present in the landscape. A larger landscape tends to have more habitat diversity, therefore more species (on average) are able to persist in it.

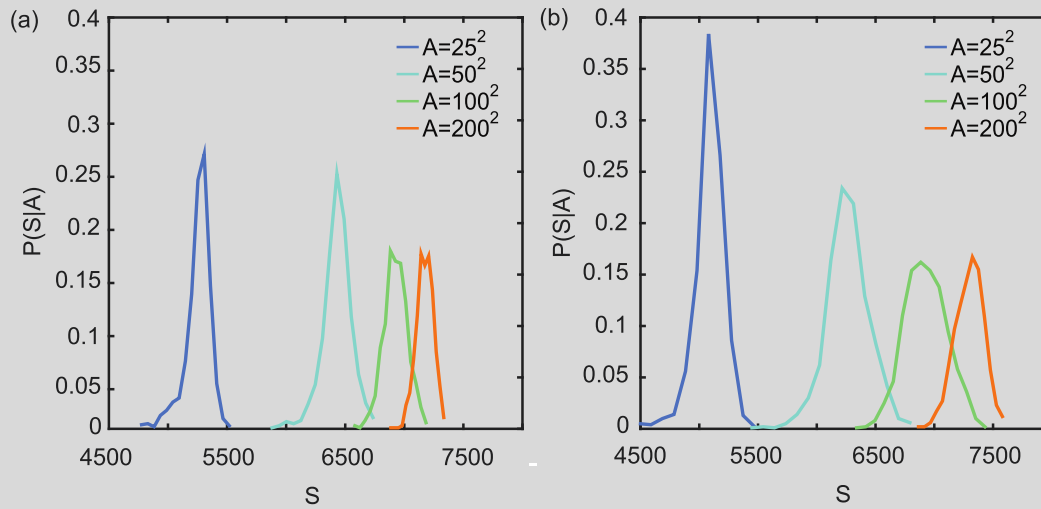


Figure 1.10 – Probability distribution of SAR. $p(S|A)$ for the metapopulation model with landscapes generated according to Rybicki and Hanski (2013) (a) and with the HYDROGEN algorithm (Bellin and Rubin, 1996) (b) (Fig. 1.9). Colors, from blue to orange, refer to landscape sizes $A = 25^2, 50^2, 100^2, 200^2$.

The $p(S|A)$ resulting from the metapopulation model with the two different methods

of landscape generation are shown in Figs. 1.10 (a) and (b). The variance decreases with the mean with a pattern that is not described by a power-law, and therefore an estimation of β is not possible. However, relative fluctuations decrease with the average much faster than in all other considered models, at least as $1/\langle S \rangle$. Note that by using the condition in equation (1.33) to count the number of surviving species, the average is effectively taken over the stochasticity of the dynamics in each individual landscape. Therefore the observed variability is only that due to the habitat stochasticity. It can therefore be concluded that the variability generated by habitat stochasticity at fixed spatial correlation is negligible with respect to the one possibly caused by community dynamics, at least within the assumptions of this model.

Landscape-explicit dispersal In Purves et al. (2007), García-Valdés et al. (2013) and Rybicki and Hanski (2013), all cells are connected via a dispersal kernel, as presented in equation 1.6, but with certain modifications presented here. Rybicki and Hanski (2013) propose to modify the dispersal such that the volume is unitary:

$$\mathcal{K} = \exp(-d/D) / (2\pi D^2). \quad (1.34)$$

In doing so, Rybicki and Hanski (2013) avoid that species with high dispersal distance also benefit from a strong local colonization pressure. With the normalization of the dispersal kernel, species with small dispersal distance have a higher chance of colonization at small distances than species with high dispersal values, but a smaller chance of dispersing far from the origin, whereas species with large dispersal distance have a higher chance to disperse at long distances, but a rather low probability to disperse locally.

Box 1.4 – Computing landscape-explicit dispersal efficiently In the presented landscape-explicit approaches, dispersal connects all cells between them via a dispersal kernel. When computing the colonization (equation 1.25), a convolution between the dispersal kernel and the fitness-driven occupancy is performed:

$$S = \mathcal{K} * W, \quad (1.35)$$

$$W_i = w_i \cdot f_i, \quad (1.36)$$

where $*$ is the convolution operator, W the matrix of occupied cells w_i and their respective fitnesses f_i . Theoretically, a different dispersal kernel could be used for each pixel, to account for landscape resistance to dispersal via, e.g. the Dijkstra algorithm (Graves et al., 2014; Bertuzzo et al., 2016), but the convolution can be very slow to compute, especially

if a fine discretization of the landscape is to be considered.

The 2D-Fourier transform is a useful mathematical tool to speed up the computation of the convolution (Rybicki and Hanski, 2013):

$$\mathcal{K} * W = \mathcal{F}^{-1} [\mathcal{F}(\mathcal{K}) \cdot \mathcal{F}(W)], \quad (1.37)$$

where \mathcal{F} is the Fourier transform operator. To compute the Fourier transform, the fast Fourier transform algorithm is used, which is significantly faster than a standard convolution. The drawback is that for this method the dispersal kernel has to be the same for all pixels, which means that landscape resistance can not be accounted for when using the Fourier transform.

On the other hand, Purves et al. (2007) propose to normalize local dispersal by the number of possible sites where dispersal can occur:

$$\frac{\exp[-d_{ij}/D]}{\sum_{i \in H} \exp[-d_{ij}/D]} \quad (1.38)$$

where H represents the set of possible dispersal sites. This normalisation is basically a numerical approximation to the analytical normalisation, as the sum of dispersal volume is equal to 1.

Purves et al. (2007) additionally assume an offspring rain (Keymer et al., 1998; Gotelli, 1991; García-Valdés et al., 2013), where each site can equally contribute regardless of distance, which is in line with the mean-field model (Hanski, 1999a). For each site they define the equal probability of dispersal to be $\frac{1}{|H|}$, with $|H|$ being the number of receiving sites, so to affect the whole domain uniformly.

Dispersal can be affected by external features which limits and constrains the flow of offsprings in a given direction, and is then called directed dispersal. External effects include direction of offsprings flight (Purves et al., 2007), presence of forest (García-Valdés et al., 2013), or connectivity of specific habitat structures such as river networks, which influence fish dynamics (Muneepeerakul et al., 2008; Carrara et al., 2012; Mari et al., 2014). In Purves et al. (2007), H is then modified to only contain suitable patches instead of all patches. In Muneepeerakul et al. (2008), the distance between patches is defined as the path in the river network, which accounts for the direction of the stream, i.e. it is more costly to swim upstream than downstream.

1.3.3 Additional considerations

Metapopulation models have evolved in multiple directions (e.g. Ovaskainen and Saastamoinen (2018)), explicitly modeling increasingly complex phenomenon (Akçakaya et al., 1995). As well summarized in Hanski and Gilpin (1991) and Guisan and Zimmermann (2000) (based on Levins (1966)), models can not simultaneously satisfy generality, realism and precision, of which two have to be chosen.

Two possible layers of complexity Two complexification of the metapopulation models, adding elements of realism are briefly presented, with little detail given the focus of this thesis on generality and precision.

Interactions with other species: Several studies have included species interactions in metapopulation dynamics (Nee and May, 1992; Hanski, 1998; Bascompte and Solé, 1998), which have later on become known as metacommunity models (Hanski and Gilpin, 1991; Leibold and Miller, 2004), and have displayed interesting effects of habitat distribution on competition (e.g. habitat destruction might favor inferior competing species (Nee and May, 1992)). It has also been demonstrated that certain predator prey dynamics rely on metapopulation dynamics to persist in a landscape (Bascompte and Solé, 1998; van Nouhuys, 2016).

The stochastic patch occupancy model used throughout this thesis makes the assumption of little to no species interactions, implicitly included in the model stochasticity, or path synchronous abiotic influence which modify the colonization force of all patches in the same way. This assumption is of course a simplification of real processes and of the actual complex interactions observed in the field.

Structured metapopulations, demography: Demography has been addressed by several studies (Ebenhard, 1991; Akçakaya et al., 1995; Akçakaya, 2000; Anderson et al., 2009; Sutherland et al., 2014), in the form of structured local populations. A common approach consists of hierarchical models which propose to model the metapopulation at different levels: local structured populations generating offsprings, and a landscape level metapopulation model influenced by the local structure of the subpopulations (Akçakaya et al., 1995). Establishment of a new population in a previously empty patch is also believed to influence the extinction of the local population (Ebenhard, 1991). Initially, the probability of extinction is higher, and once the population is settled, the probability is reduced, as offsprings are generated and a stable population structure arises.

The number of parameters involved in structured metapopulation models requires a careful consideration on the availability of a sufficient amount of age-structured data for the focus species (Ebenhard, 1991). Those models are thus hard to integrate in future projections

(Sutherland et al., 2014). Structured metapopulations are not considered in this thesis.

2 Metapopulation dynamics of virtual mountain species under climate change

THE present chapter¹ addresses the prediction of the fate of mountain species in a time-frame where climate change is assumed to unfold, where climatic and geomorphic factors but also endogenous species characteristics are jointly expected to control species distributions. A significant step towards the establishment of reliable scenarios, of obvious relevance to science and society, would single out reliably landscape effects, given their constraining role and relative ease of theoretical manipulation. Here, population dynamics is addressed in ecosystems where the substrates for ecological interactions are mountain landscapes subject to predictable warming scenarios for air temperature within ecological timescales (no evolutionary response of the focus species is considered in response to warmer conditions). A minimalist model of metapopulation dynamics based on virtual species (i.e. a suitable assemblage of focus species) is used where dispersal processes interact with the spatial structure of the landscape. Climate warming is subsumed by an upward shift of species habitat altering the metapopulation capacity of the landscape and hence species viability. The landscape structure appears to be a powerful determinant of species survival, owing to the specific role of the predictably evolving connectivity of the various habitats. Range shifts and lags in tracking suitable habitat experienced by virtual species under warming conditions are singled out in different landscapes. The range of parameters is identified for which these virtual species (characterized by comparable viability thus restricting their possible fitnesses and niche widths) prove unable to cope with environmental change. The statistics of the proportion of species bound to survive is identified for each landscape, providing the temporal evolution of species range shifts and the related expected occupation patterns. A baseline dynamic model for predicting species fates in evolving habitats is thus provided.

¹The content of this chapter has been adapted from Giezdanner et al. (2019): Giezdanner, J., Bertuzzo, E., Pasetto, D., Guisan, A. and Rinaldo, A. (2019). A minimalist model of extinction and range dynamics of virtual mountain species driven by warming temperatures. *PLoS ONE*, 14:1-19. (<https://doi.org/10.1371/journal.pone.0213775>)

2.1 Introduction

By taking into account upward shifts of suitable species habitats (Seebens et al., 2018), effects of climate warming would be reflected in the increase/decrease of suitable occupied sites along elevation gradients (Vetaas and Grytnes, 2002; Dullinger et al., 2012) and the resulting displacements of species (Theurillat and Guisan, 2001; Lenoir and Svenning, 2015). Field evidence on changes in species lower and upper range limits, optima, and abundances (Rumpf et al., 2018) may thus be examined for specific landscapes. Whereas environmental drivers affecting species ranges are various and competing, at progressively larger spatial scales, air temperature, tightly linked to elevation, emerges as a key player (MacArthur, 1972; Brown, 1995). General frameworks in the literature frequently consider many other drivers. Some of them change predictably with elevation (for instance, anthropogenic pressure and, to a lesser extent, precipitation (Körner, 2007; Nogues-Bravo et al., 2008)), while others are not elevation-dependent (such as moisture, clear-sky turbidity and cloudiness, sunshine exposure and aspect, wind strength and exposed lithology to name a few without specific taxa in mind (Körner, 2007; McCain and Grytnes, 2010)). However, theoretical analyses aimed specifically at geomorphic factors are essential to inch towards the prediction of spatial biota responses (Lenoir et al., 2008; Marquet et al., 2014; Elsen and Tingley, 2015).

The structure of the environmental matrix is known to affect biodiversity patterns (Wiens, 1997; Economo and Keitt, 2008; Muneeppeerakul et al., 2008; Economo and Keitt, 2010; Bertuzzo et al., 2011; Carrara et al., 2012). Mountain landscapes provide a complex matrix, often shaped chiefly by fluvial erosion and geologic uplift (Rodriguez-Iturbe and Rinaldo, 2001), resulting in the majority of their surface to lie at intermediate elevations (Bertuzzo et al., 2016). Owing to the ubiquitous self-affine nature of their topographies (Rodriguez-Iturbe and Rinaldo, 2001), in such landscapes one may find peaks or troughs at the same elevation, resulting in different degrees of isolation and connectivity (Colwell and Lees, 2000). Warming temperatures would prompt species to experience alterations of the spatial configuration of their habitat, as well as an alteration of the microclimatic heterogeneity (Graae et al., 2017), because of the change in the area available at the elevation yielding optimal fitness, and hence of the proximity of areas with similar ecological characteristics (connectivity) and the dispersal ability (Jacob et al., 2018), crucial determinants of species persistence (Harrison and Taylor, 1997; Bertuzzo et al., 2016; Rumpf et al., 2018). This also implies that deriving species distribution patterns from linear elevational gradients, for simplistic geometric shapes with same relief, is ecologically useful mostly as a null model against which to compare patterns derived from real landscapes (Elsen and Tingley, 2015; Bertuzzo et al., 2016).

Here, a metapopulation modelling framework (Hanski, 1998) is used, generalized by the incorporation of a specific fitness function (section 2.2.2) describing how suitable the local

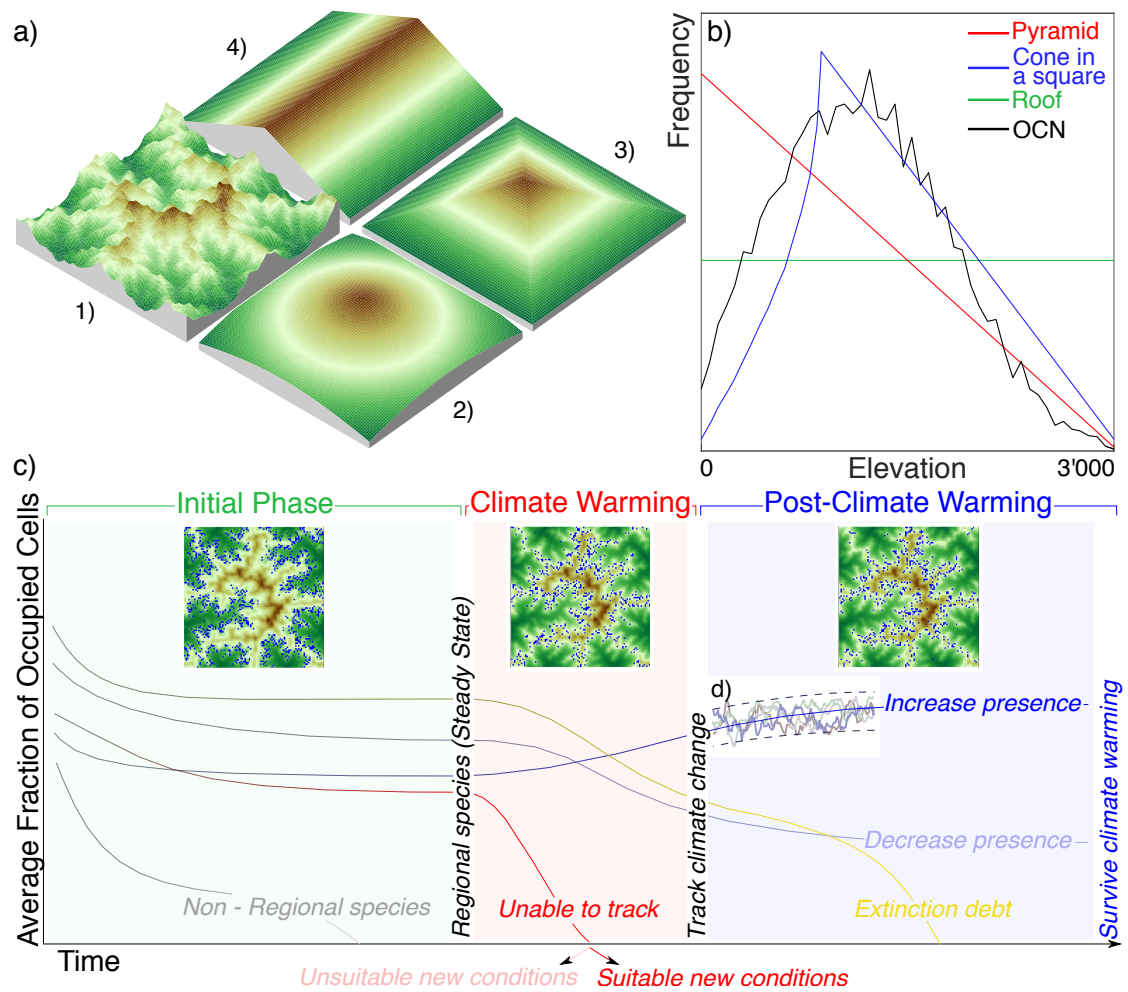


Figure 2.1 – Landscapes used in the simulation and overview of the simulation. (a) The four synthetic landscapes used in the simulations meant to single out geomorphic effects: 1) a virtual realistic landscape based on the Optimal channel network model (OCN, see Appendix S2), 2) a cone-in-a-square, 3) a pyramid and 4) a roof. (b) Hypsographic curves, defined as the area distribution at the various elevations. (c) A sketch of the three phases of the experiment: an initial phase (green) to select regional species; a climate warming phase (red) characterized by an upward shift in species optimal elevations, which discriminates between species able and unable to track climate warming; and post-climate warming phase (blue) exploring if the surviving species are suited to the new conditions, or experience extinction debt. The smooth lines depicted in the figure are meant as schematic representations of possible pathways of ensemble averages of several realizations (d) for a given species.

landscape features are for a virtual species to thrive in (i.e. the quality of a cell (Purves et al., 2007; Rybicki and Hanski, 2013)), similarly to what is done in habitat suitability models (HSMs) involving virtual species (Thibaud et al., 2014; Fernandes et al., 2018b,a). For the main purpose

of this chapter, which is to highlight the impact of different topographies on species occupancy and survival to climate warming, the minimalist assumption is made that fitness depends only on elevation. While one should be careful in using terminology like habitat when the models only consider elevation as an environmental layer, the choice is justified by a twofold argument: on the one hand, ecological detail are kept to a minimum to be capable of sorting out true landscape effects; on the other hand, extensions of this framework to include other environmental covariates, as typically done in HSMs (Guisan et al., 2017) and other dynamical ecological models (Pasetto et al., 2018), is straightforward (see box 2.2 for an example directly incorporating additional landscape attributes, as well as chapter 3), although outside the main scope of this paper. Landscapes are thus fully characterized by their elevation structure that defines the local species fitnesses and the processes governing species occupancy. By contrasting the occupancy results for a selection of landscapes, the influence of the elevational structure is studied.

The regional persistence of the virtual species studied here stems from balancing colonization and extinction processes (Graae et al., 2017) driven by local suitability specific to each landscape for an exactly identified range of species parameter values. In order to consistently investigate the geomorphological influence of different landscapes, these virtual species are characterized by comparable viability (i.e. the same metapopulation capacity (Hanski and Ovaskainen, 2000)) in unbiased conditions, thus restricting their possible fitnesses and niche widths to specific parameter values. These virtual species have either large niche breadth but low fitness everywhere, or the opposite.

The overarching goal of this study is to systematically investigate how topography interplays with species parameters to concert their survival as a result of given climatic warmings (Fig. 2.1). Owing to its deliberate simplicity and minimal parameter use, the metapopulation model is used extensively in this chapter to explore the spatial occupancy of the various species. Even with such simple structure, enough degrees of freedom exist to produce realistic occupancy results.

2.2 Materials and methods

2.2.1 A metapopulation framework

A spatially-explicit stochastic patch occupancy model (SPOM (Moilanen, 2004; Purves et al., 2007; Rybicki and Hanski, 2013)), similar to what was described in chapter 1 in the context of the introduction to the metapopulation model, is employed to simulate the distribution of a virtual species in a landscape. SPOM is here applied in a manner similar to that proposed in Purves et al. (2007) and Rybicki and Hanski (2013), which considers each cell of a raster (here a

digital elevation model (DEM)) as individual patches. The equations relative to this approach are elaborated in section 1.3.2 and recalled here in box 2.1.

Box 2.1 – SPOM - reminder Building on a grid with N cells, SPOM computes a possible distribution of occupied cells at every simulation time t by considering extinction and colonization processes, whose rates depend on the species properties and on the landscape features. A binary state variable $w_i(t)$ is set to 1 when the cell i is occupied and 0 when empty ($i = 1, \dots, N$). Starting from a given initial distribution of occupied cells, at each time step, the model allows unoccupied cells to be colonized by surrounding occupied cells with probability $P_{C,i}(t + \Delta t) = P[w_i(t + \Delta t) = 1 | w_i(t) = 0]$. Then, the cell becomes occupied at time $t + \Delta t$ depending on a random sample from a Bernoulli distribution with parameter $P_{C,i}(t)$. Similarly, species in occupied cells can go extinct with probability $P_{E,i}(t + \Delta t) = P[w_i(t + \Delta t) = 0 | w_i(t) = 1]$. SPOM works as a Markov chain, where, for each cell, the probabilities of colonization and extinction events are modelled with the following exponential distributions (and the probabilities of these events not happening as their respective complements):

$$P_{C,i}(t + \Delta t) = P[w_i(t + \Delta t) = 1 | w_i(t) = 0] = 1 - \exp(-C_i(t) \cdot \Delta t), \quad (2.1a)$$

$$P_{E,i}(t + \Delta t) = P[w_i(t + \Delta t) = 0 | w_i(t) = 1] = 1 - \exp(-E_i \cdot \Delta t), \quad (2.1b)$$

where Δt is the simulation time step and E_i and $C_i(t)$ are the extinction and colonization rates (with dimension $1/t$) for cell i at time t . Note that $C_i(t)$ is time-dependent because it depends on the current distribution of the species. The colonization and extinction mechanisms are directly related to a fitness function, f_i (described in the next section), which measures the suitability of the features of patch i for the species. The local extinction rate on a cell i is inversely proportional to the fitness, i.e., $E_i = e/f_i$, where e is the extinction constant. The colonization rate of an unoccupied cell is driven by the sum of the contributions from surrounding occupied cells and is defined by a two-dimensional exponential kernel multiplied by the fitness associated with the source cells, i.e. the connectivity to the different cells as defined by metapopulation theory (Hanski, 1998, 1999a; Ovaskainen and Hanski, 2001; Gu et al., 2002; Moilanen, 2004):

$$C_i(t) = c \sum_{j \neq i} p_j(t) \frac{\exp(-d_{ij}/D)}{2\pi D^2} f_j, \quad (2.2)$$

where d_{ij} is the distance between cells i and j , D the dispersal distance and c the colonization constant. Notice that connectivity is solely based on Euclidean distance and does not depend on the suitability of the path between cells.

2.2.2 Fitness

An important issue is concerned with the fair comparison among species in this context. The species suitability is represented at cell i with elevation z_i by the following fitness function f_i (Bertuzzo et al., 2016):

$$f_i = f_{\max} \exp \left(-\frac{(z_i - z_{\text{opt}})^2}{2\sigma^2} \right), \quad (2.3)$$

where: z_{opt} describes the elevation where the species shows its maximal fitness; σ is the niche width, which sets how fast fitness decreases departing from z_{opt} ; and f_{\max} is the maximum value of the fitness of the chosen pool of species. Once these species-specific parameters assigned, the heterogeneity of the landscape matrix dictates the spatial distribution of fitness. It is reasonable to assume that the details of the shape of the fitness function do not have overwhelming importance. The assumption is thus made that two main traits (the elevation where maximum fitness is achieved, and the niche width σ that characterizes the degree of specialization of the focus species) suffice in characterizing the main attributes relevant to metapopulation dynamics Giezendanner et al. (2019).

In the ensuing simulations, fitness is assumed to depend strictly on elevation. In another context, where geomorphic effects are not the main subject of inquiry, such a condition could be relaxed by considering other environmental covariates (see box 2.2), making fitness more realistically dependent on habitat suitability (see e.g. (Guisan et al., 2017)).

Box 2.2 – Generalisation of the fitness model, a comparison The fitness presented here, strictly dependent on elevation, can be relaxed to make fitness landscapes more realistic and capable of contrasting real data, e.g. including climatic and topographic predictors like degree-days above 3°, suitable moisture indices, daily average global potential short-wave radiation per month or annual average number of frost days during the growing season for plants (Thibaud et al., 2014). Fitness f_i may easily be made dependent also on elevation-independent factors. It is then possible to derive the contribution of the i -th pixel (λ_i) to the metapopulation capacity λ_M of the landscape by computing the eigenvector x_i corresponding to the maximum eigenvalue of m_{ij} and by projecting x_i to yield (Hanski and Ovaskainen, 2000) $\lambda_i = x_i^2 \lambda_M$. The probability of occurrence of actual species in real landscapes could therefore be mapped by the proposed fitness function.

Comparative studies Thibaud et al. (2014) have measured the relative effect of factors affecting species distribution model predictions and mapped the probability of occupancy in the Vaud Alpes for different species. They employed a statistical framework using spatial autocorrelation with respect to five climatic and topographic predictors. Using the method described earlier as a proof of concept, their results can be qualitatively

approximated (Fig. 2.2).

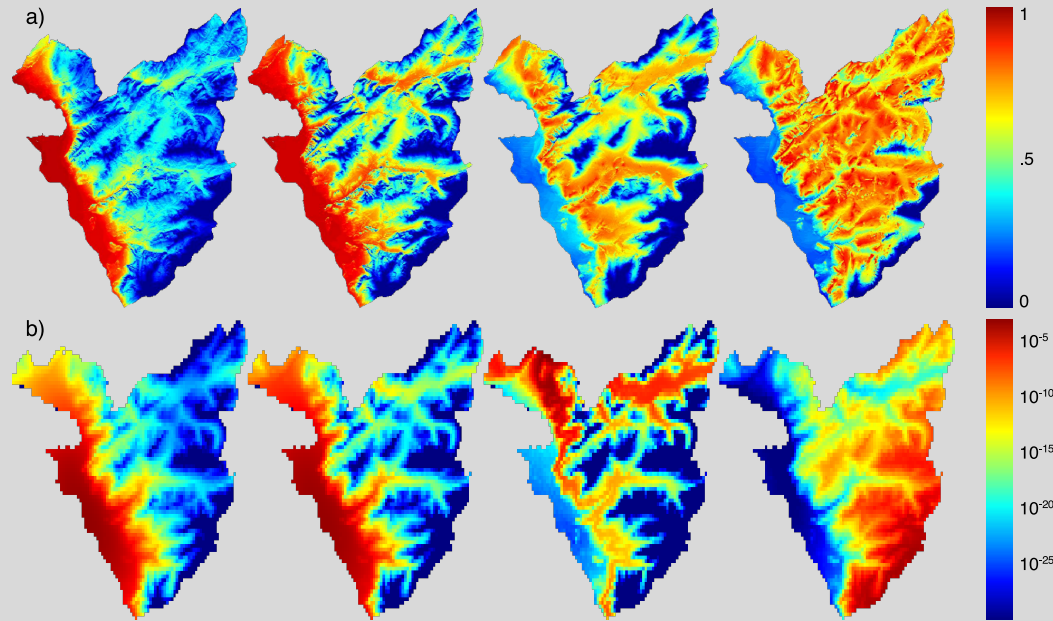


Figure 2.2 – Approximation of results obtained by Thibaud et al. (2014) with the metapopulation capacity. Four of the species computed by Thibaud et al. (2014) (a) and the visual approximation obtained with the landscape capacity method (log-value) (b). The parameters found to best suit the original images are as follow ($\sigma - D - z_{\text{opt}}$): (300 - 2.3 - 0), (240 - 4.2 - 0), (115 - 2.9 - 666), (297 - 4.2 - 2000)

While no serious attempt at calibrating parameters has been made here, the general patterns observed in Thibaud et al. (2014) seem to be relatively well reproduced by the eigenvector projection method when cherrypicking the right parameter set.

The above result is worth future investigations, as demonstrated by the following exercise. In fact, the strength of the metapopulation capacity approach, modified to embed heterogeneous local fitnesses, is that f_i can be suitably made a function of any relevant factor of choice. For instance, following *ex post* the suggestion of Thibaud et al. (2014), one could take into account factors derived from any GIS technique or database like e.g.: degree-days above $+3^\circ\text{C}$, a moisture index between June and August, daily average potential short-wave radiation per month, annual average number of frost days during the growing season and an index of topographic position. Here, as a proof of concept, aspect is additionally considered to define the metapopulation fitness. Specifically, the fitness is modified in the following way:

$$f_i = \sqrt{\frac{1}{\sigma}} \exp\left(-\frac{(z_i - z_{\text{opt}})^2}{2\sigma^2}\right) \cdot \phi(\alpha) \quad (2.4)$$

where α is the aspect, and $\phi(\alpha)$ a function of the aspect, chosen here in this way:

$$\phi(\alpha) = a + \frac{\sin(\alpha + b) + 1}{2} \cdot (1 - a) \quad (2.5)$$

where a defines the minimum modifier value, and b the angle with maximal fitness.

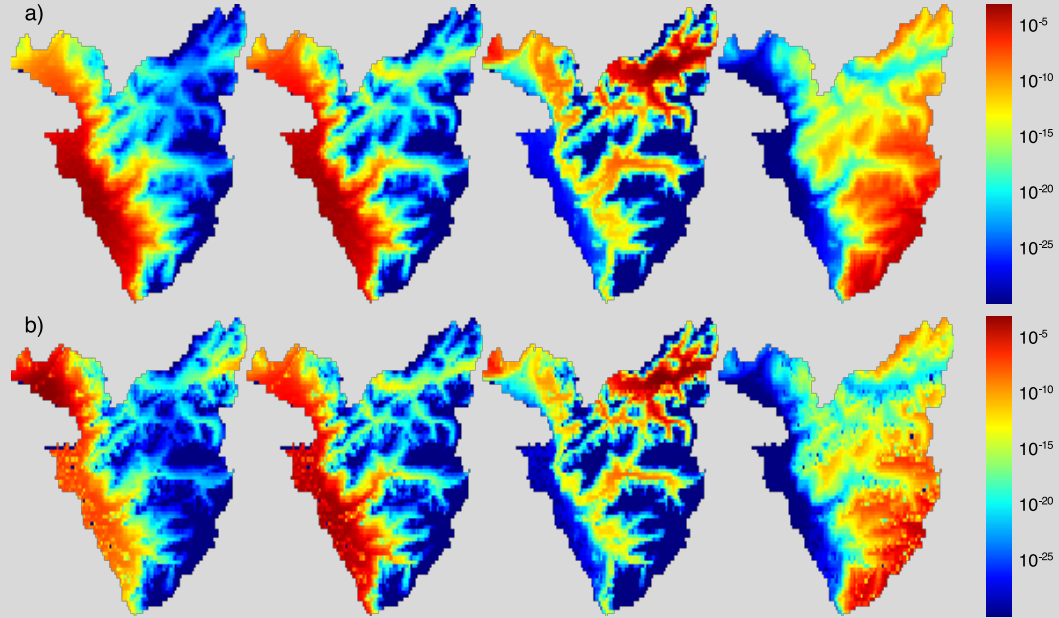


Figure 2.3 – Addition of aspect in the definition of the fitness. The same four virtual species as in Fig. 2.2, but with the aspect modifier included (equation 2.5) a): $a = 0.5$, b): $a = 0$, with parameter b set to 0 in both cases. Note that in (a) the impact of aspect on the overall fitness (equation 2.4) is weaker than in (b).

Fig. 2.3 shows the same four species as shown before, but with the additional aspect modifier, with the max fitness being fixed when south-facing and a constrained minimal modifier a of 0.5 and 0.0, meaning that aspect has a greater impact on the second species. The northern and southern valleys are more easily distinguished by the projection of the eigenvector, but overall it seems that the elevation already explains most of the observed patterns, leading to the suggestion that beyond a certain scale, only the elevation field remains the key determinant, as noted earlier (Pradervand et al., 2014). It can thus be concluded that the present method can be made compatible with the procedure of Thibaud et al. (2014) while retaining the predictive character implicit in the metapopulation model. For the goals of the present paper, centered as it is on a predictive framework to discuss how climate change might impact biodiversity in mountain environments, suffice here to note that the landscape matrix approach allows a novel perspective, akin to scenarios of temperature rise objectively treated.

A number of approaches have used similar fitness functions (e.g. Rybicki and Hanski (2013);

Bertuzzo et al. (2016); Papaïx et al. (2013)). For example, in studies of adaptation dynamics of spatially heterogeneous metapopulations, individuals have been assumed to be classified with respect to their phenotypes. Phenotypes are characterized by the value, or the strategy, x_i of a continuous trait x (Papaïx et al., 2013), where each habitat encountered in each patch determines the probability of survival of the phenotype, typically via equation 2.3. Therein, differences between optimal traits (analog to z_{opt}) for the different habitats generate tradeoffs and selective maladaptations.

2.2.3 Comparable species viability

The overarching goal of this paper is to highlight the effects of geomorphology on species survival in the context of a minimalist metapopulation model. In order to single out these effects, a framework is designed where, for selected combinations of f_{max} and σ (equation 2.3), the considered species all display a comparable viability (i.e. metapopulation capacity *sensu* Hanski (Hanski and Ovaskainen, 2000), see box 1.1). This is done in a geomorphologically unbiased environment, i.e. a landscape which does not favor selected species under mean-field assumptions (infinite dispersal, Giezdanner et al. (2019)). This ensures that a hypersurface in parameter space is postulated that contains only species with comparable viability, such that differences in species fate computed in various landscapes are directly related to different geomorphologies.

Such geomorphologically unbiased environment is here defined moving from a 1D-landscape with a constant slope and infinite length where the metapopulation capacity is influenced by neither niche width nor optimal elevation. Within these assumptions, the landscape is centered on the optimal elevation (i.e., $z(x=0) = z_{opt}$) and consider a finite domain of size $[-L, L]$, with L large enough. The spatial discretization of the domain consists of $N+1$ elements, $x_0 = -L, \dots, x_{N/2} = 0, \dots, x_N = L$, with the distance between two points defined as Δx ($\Delta x = 1$ in this paper) and corresponding elevations $z_i(x_i) = x_i$ for $i = 0, \dots, N$.

Consider the matrix \mathbf{M} containing information about the landscape and the quality of the patches, and the associated largest eigenvalue, i.e. metapopulation capacity, λ_M , defining the theoretical threshold of the extinction to colonization ratio above which the population has no chance of survival (i.e., a species persists in the domain if and only if $\lambda_M > e/c$, see box 1.1 for the derivation). In the context of a geomorphologically unbiased landscape, and considering the mean-field approach, the elements of \mathbf{M} are $m_{ij} = f_i f_j$ if $i \neq j$ and $m_{ij} = 0$ if $i = j$. The values of the largest eigenvalue cannot be computed analytically. However, the Perron-Frobenius theorem provides an upper bound to the largest eigenvalue. Such upper bound is given as the maximum of the sums of the absolute value in a single row (or column) of the matrix. Considering the definition of \mathbf{M} , the maximum of the row sum is obtained for

the row corresponding to $z = z_{\text{opt}}$, i.e. $i = N/2$:

$$\lambda_M(f) \leq \sum_{j=0}^N f(z_{\text{opt}}) f(z_j) \Delta x, \quad (2.6)$$

where f is the fitness function for a given species described in equation 2.3. Letting L go to ∞ and reducing the size of the single elements to zero, the series in equation 2.6 converges to the following integral:

$$\begin{aligned} & \int_{-\infty}^{\infty} f(z_{\text{opt}}) f(z(x)) dx, \\ &= (f_{\text{max}})^2 \int_{-\infty}^{\infty} \exp\left(-\frac{(z(x) - z_{\text{opt}})^2}{2\sigma^2}\right) dx, \\ &= (f_{\text{max}})^2 \sigma \sqrt{2\pi}, \end{aligned} \quad (2.7)$$

which, in order to constrain the largest eigenvalue of \mathbf{M} to the same value for all niche widths, yields:

$$f_{\text{max}} = \frac{1}{\sqrt{\sigma}}, \quad \forall \sigma. \quad (2.8)$$

By incorporating this result in equation 2.3, an ensemble of species is obtained having the same metapopulation capacity (i.e., same probability of surviving) in this theoretical domain. Thus, comparing virtual species having the proposed fitness function permits to understand the real structural effects of the landscapes once confronted to the complex landscape matrix, given initially unbiased species in the sense of survival ability.

Numerical proof of concept As the demonstration ensures consistency among the upper bound of the metapopulation capacity of different species, it is interesting to numerically verify the actual metapopulation capacity values in a similar conceptual landscape.

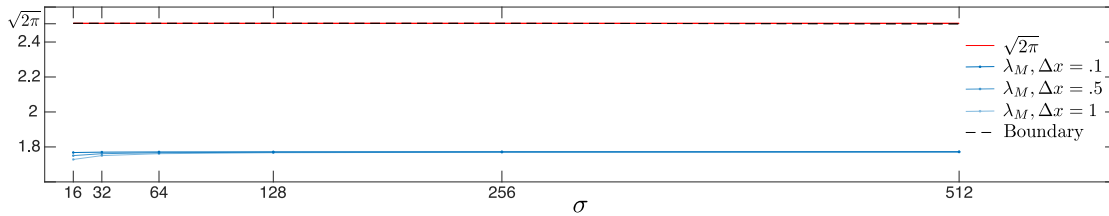


Figure 2.4 – Comparison between the upper bound computed using the Perron-Frobenius theorem (black line), the theoretical value (red line), and the largest eigenvalue with different values of Δx

Fig. 2.4 shows the numerical results obtained computing the metapopulation capacity and

its upper bound for different species ($\sigma = 16, 32, 64, 128, 256$, and 512) in a domain of size $L = 1500$ and different discretization refinements, $\Delta x = 0.1, 0.5, 1.0$. Numerically, at decreasing values of Δx the metapopulation capacity λ_M values associated with different species tend to the same constant, while the numerical upper bound proves a good estimate of the theoretical value $\sqrt{2\pi}$. With decreasing distance between the elements, the metapopulation capacity λ_{\max} values associated to different species tend to the same constant, while the numerical upper bound is a good estimation of the theoretical value $\sqrt{2\pi}$.

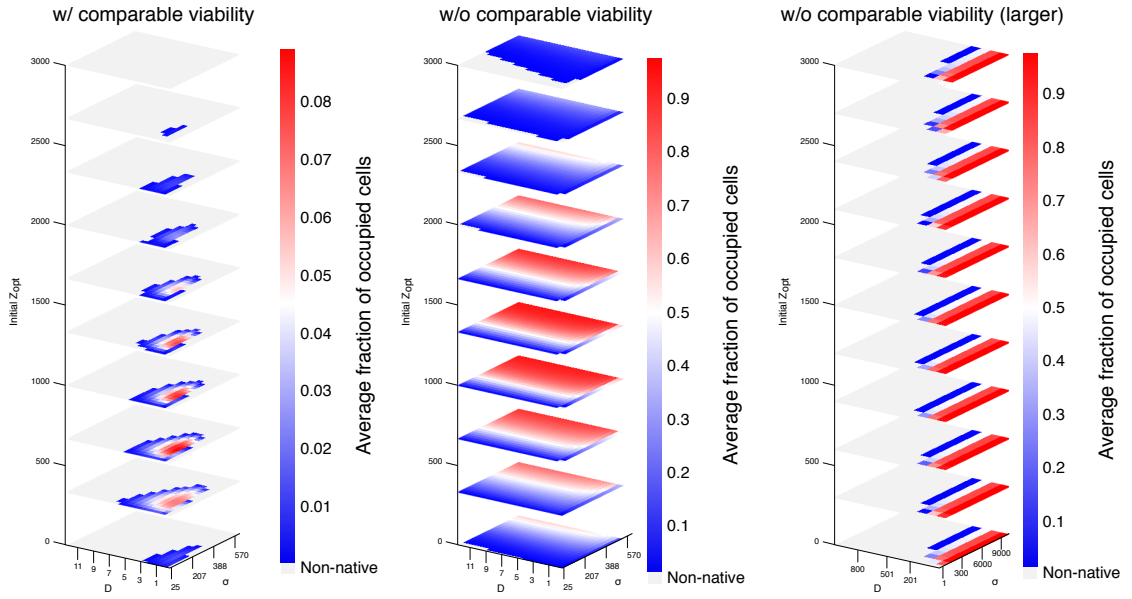


Figure 2.5 – Example of results when comparable species viability is not considered. Comparison between the fraction of occupied cells for different species in the OCN landscape with comparable species viability (left panel) or without (central and right panels). The central and right panels show that w/o comparable viability, with increasing values of niche width, the fraction of occupied space tends towards one, as all space is suited for these species when the niche becomes large enough.

Fig. 2.5 shows how the parameter space gets clouded by super species able to survive everywhere when not considering comparable species viability, rendering any effort to display geomorphic effects meaningless.

2.2.4 Dispersal tradeoffs

As an additional normalization step to ensure species inter-comparability, the exponential dispersal function \mathcal{K} between two patches with distance d is designed such that the kernel respects a unitary volume for all species with different dispersal parameters D (Rybacki and

Hanski, 2013):

$$\mathcal{K} = \exp(-d/D) / (2\pi D^2) \quad (2.9)$$

Proof:

$$\int \int_{\mathbb{R}^2} \frac{\exp(-\sqrt{x^2 + y^2}/D)}{2\pi D^2} dx dy \quad (2.10a)$$

$$\stackrel{\text{polar}}{\Rightarrow} \int_0^{2\pi} \int_0^\infty d\mathcal{K} d\theta = 1 \quad \forall D \quad (2.10b)$$

This ensures that two species with different dispersal coefficients have the same dispersal volume (Rybicki and Hanski, 2013).

2.2.5 Modeling climate warming

To simulate climate warming impacts, the optimal elevation of each species is gradually shifted upwards. The IPCC reports different possible long-term greenhouse gas concentration trajectories, representative concentration pathways (IPCC, 2014). The worst-case scenario, RCP 8.5, predicts an increase in temperature in the range of $\Delta T = 4^\circ\text{C}$ over the next century (Δt_c). This scenario is chosen in order to enhance as much as possible, yet not unrealistically, the impact of climate warming on the metapopulation model. The optimal elevation of each species is changed uniformly in the landscape: assuming a typical average global environmental lapse rate for air temperature of $\gamma_w = 1/150^\circ\text{C}/\text{m}$ (Barry and Chorley, 2009), the optimal elevation thus changes at a speed of $\Delta z / \Delta t = \Delta T / (\gamma_w \cdot \Delta t_c) = (4 \cdot 150) / 100 = 6 \text{ m/year}$, leading to a new optimal elevation $z_{opt}(t + \Delta t) = z_{opt}(t) + \left(\frac{\Delta T}{\gamma_w \Delta t_c}\right) \Delta t$ after each time step.

While the choice of lapse rate is justified based on rates of environmental change, empirical evidence suggests that many species, mostly plants (Bertrand et al., 2011) and birds (Devictor et al., 2012), shift in elevation at slower paces than those assumed here for the drivers (Alexander et al., 2016). Note that lags can differ greatly in intensity for different altitudes (Bertrand et al., 2011). Lags are obtained here by simulation and depend on the transient states given the imposed warming.

As anticipated above, this is deemed a minimalist model to predict the above effects, yet – as will appear in the following – capable to showcase highly nontrivial results.

2.2.6 Simulations

A pool of 4000 virtual species is generated with the parameter range for dispersal distances, niche widths and optimal elevations assumed such that they cover the scope of the regional species parameter, determined by running the first step of the simulation several times be-

forehand ($z_{\text{opt}} \in [0, 3000]$, $\sigma \in [25, 600]$ and $D \in [0.1, 12]$) for fixed values of $e = 0.02$ and $c = 15 \text{ years}^{-1}$. From this pool, a subset of virtual species, starting from a fully occupied landscape (i.e. each cell is occupied by the species, initial condition), persist in the landscape after a simulation is carried out until stationarity under constant climatic condition (Fig. 2.6, step 1). Species belonging to this regional pool serve as initial condition for the evaluation of the effects of warming scenarios. Owing to the stochastic nature of SPOM, the persistence of a species is evaluated by repeating the simulation 100 times for each set of parameters (i.e., species) and landscape. Species that are still present in the landscape at the end of at least half of the 100 random runs are considered as regional species (Fig. 2.6, Step 1).

In order to obtain 100 occupancy configurations for each of these species, runs leading to species disappearing from the landscape during step 1 are replaced by randomly selecting an equilibrium configuration from the remaining ones.

Starting from the occupancy of species obtained in step 1, climate warming is applied (step 2) as an upward shift of the niche for approximately 100 years.

Step 2 identifies species unable to track climate warming, i.e. thus initial species that go extinct during climate warming. Climatic conditions are then frozen and the experiment continues until the extinction debt has been paid off (step 3) which identifies the species unable to cope with the new temperatures (i.e. species affected by extinction debt (Tilman et al., 1994)).

The last two steps (steps 4-5) consist in understanding whether the species which went extinct during the climate warming phase would be able to survive given their new optimal elevation (extinct suited), or if they would have gone extinct anyway due to loss of suitable habitat (extinct unsuited). In step 4, species are allowed once again to fully occupy the landscape, but their optimal elevations are shifted to the value after climate warming. The simulation is then run until reaching a steady state (step 5), permitting to find the species surviving in the new conditions, and by comparison with state 2b, identifying the fate extinct suited/unsuited.

This method underpins observations of species transient states, and therefore singles out specific fates. Such fates can be the disappearance of species suitable to post-climate warming conditions due to their inability to track favorable conditions, or species survival for some time after climate warming, only to go extinct later. Note that the induced understanding of transient effects distinguishes metapopulation studies from habitat suitability and species distribution models (SDMs) (Guisan and Thuiller, 2005; Guisan et al., 2017). Note also that dynamical models implemented on top of SDMs (Kéry et al., 2013) exist, which capture the transient states and take advantage of the powerful SDMs tools.

The coefficients of extinction e and colonization c have been chosen such that all the possible species fates are observed in the simulations. Other choice would have been possible because,

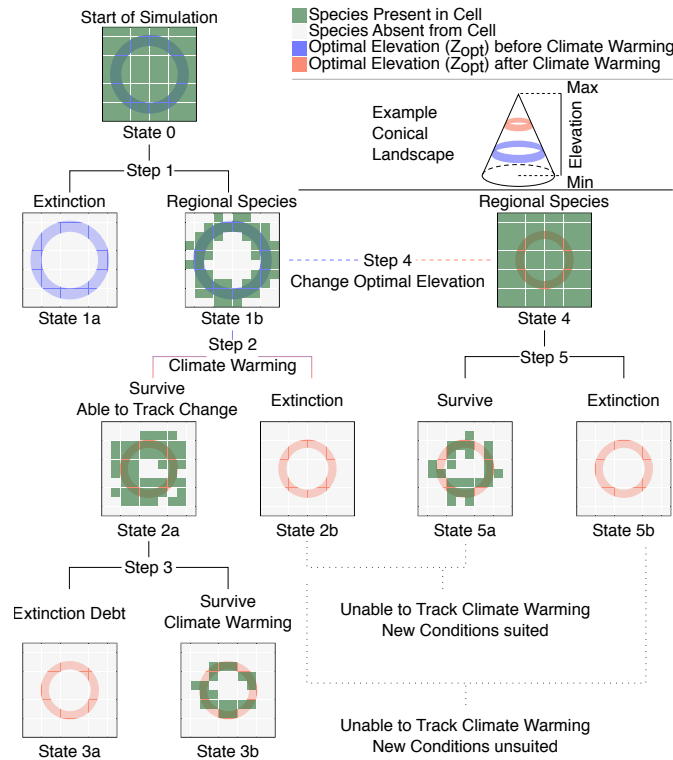


Figure 2.6 – Overview of the different states and steps of the simulation. For simplicity the landscape is displayed as a cone. 100 random solution of the SPOM model are generated for all different combinations of parameters and landscapes. In Step 1 of each run, SPOM reaches an equilibrium occupancy starting from full occupancy (State 0). Species belonging to the regional pool, i.e. surviving Step 1, are utilized (State 1b) and climate warming is applied (Step 2) leading to survival (State 2a) or extinction (State 2b). Extinction debt is evaluated by computing the equilibrium condition for the species surviving to climate warming (Step 3). Additionally, new simulations are started (Steps 4-5) by computing their equilibrium occupancy starting from full occupancy and considering the optimal elevation after climate warming. This step identifies species unable to track climate warming but which would have been able to survive the new conditions (extinct suited), and species which went extinct with climate warming and for which these conditions would not have been suited anyway (loss of suitable habitat, extinct unsuited).

as long as the ratio between the coefficients stays constant, the outcome of the simulation remains the same (for small enough values of dt (Hanski and Ovaskainen, 2000)). Other coefficient values would have generate a different pool of regional species, but the landscape occupancy would have been preserved (c.f. Fig. 2.8 in the results section).

2.2.7 Landscapes used in the simulation

Three different types of landscapes are considered: synthetic (roof, cone-in-a-square and pyramid, Fig. 2.1), realistic synthetic (Optimal channel networkks (OCNs), box 2.3, Fig. 2.7) and real (the Gran Paradiso National Park - GPNP, Italy and the Vaud Alpes, Switzerland, Fig. 2.10). OCNs, synthetic landscapes with periodic boundary conditions previously used for ecological applications in the context of climate warming (Carraro et al., 2018), are obtained by a metaheuristic approach by looking for a local minimum of total energy dissipation by iterating over different configurations of drainage directions corresponding to different topographic slopes (Rodriguez-Iturbe and Rinaldo, 2001; Banavar et al., 2001; Rinaldo et al., 2014; Balister et al., 2018) (Box 2.3).

Box 2.3 – Building statistically identical replicas of mountain topographies: Optimal channel networkks (OCNs) Are considered here, without loss of generality (Rodriguez-Iturbe and Rinaldo, 2001; Rinaldo et al., 2014), landscapes formed by square lattices with side L with $N = L \times L$ pixels (nodes). Each node has a link to one of its eight nearest neighbors forming a spanning tree with a single root – the outlet. To each pixel i of the tree, total contributing area A_i (the number of upstream pixels connected to i through flow directions) is expressed in pixel units as

$$A_i = \sum_j W_{ji} A_j + 1, \quad (2.11)$$

where W_{ji} is the arbitrary element of the connectivity matrix \mathbf{W} (i.e. $W_{ji} = 1$ if $j \rightarrow i$ and 0 otherwise), and 1 represents the unit area of the pixel that discretizes the surface. A_i provides a proxy of the flow at point i , i.e. accumulated flow Q_i , as the sum of the injections over all connected sites upstream of site i (included) $Q_i = \sum_j W_{ji} Q_j + r_i$ (where r_i is the distributed injection). In the case of uniform injection r_i for landscape-forming events, one has $Q_i \propto A_i$, a commonly accepted hydrologic assumption. The tree configuration is uniquely determined by the set of total contributing areas $s = (A_1, A_2, \dots, A_N)^T$ at any of the N sites making up the landscape. From equation 2.11 one has $s = (\mathbf{I} - \mathbf{W}^T)^{-1} (\mathbf{I}$ being the identity matrix). A necessary condition for the existence of s is that the matrix at right-hand side can be inverted. In turn, this corresponds to specific spectral properties of the connectivity matrix \mathbf{W} implying uniqueness of the paths from any site to the outlet i.e. s must be a tree (Rinaldo et al., 1992).

OCNs are spanning trees minimizing a functional describing total energy dissipation $H(s)$ of the aggregate's configuration s . At a local level, say, along the i -th link of the network, energy dissipation is $H_i \propto Q_i \Delta z_i$, which makes use of suitable landscape-forming discharges ($Q_i \sim A_i$) and of the drop in elevation along a drainage direction. Theory and

field evidence indicate $\Delta z_i \sim A_i^{\gamma-1}$ with $\gamma = 0.5$ (Rodriguez-Iturbe and Rinaldo, 2001). Spanning, loopless network configurations characterized by minimum energy dissipation are thus obtained by selecting the configuration s that minimizes the functional (Rodriguez-Iturbe et al., 1992a,b; Rinaldo et al., 1992):

$$H_\gamma(s) = \sum_{i=1}^N H_i \propto \sum_{i=1}^N A_i^\gamma. \quad (2.12)$$

In the selection process one needs to choose consistently tree-like configurations. This, in turn, is exactly admissible because every tree is a local minimum of total energy expenditure (Banavar et al., 2000) whenever one has $\gamma < 1$ directly from the physics of the problem recapitulated by a deterministic slope-area relation (Banavar et al., 2001; Rinaldo et al., 2014).

A simulated annealing strategy is adopted to find OCNs (Rinaldo et al., 1992). The algorithm starts from an initial network configuration chosen to span the whole $L \times L$ landscape towards an imposed outlet, chosen at a single or multiple sites (Rodriguez-Iturbe and Rinaldo, 2001). Every network configuration is completely described by the connectivity matrix \mathbf{W} . At every iteration of the optimization process, one pixel is drawn at random and its link is rewired to a different nearest neighbor, provided that no loops are formed. This change affects the matrix' elements W_{ij} and, in turn, the values of the aggregated areas A_i . The change in configuration $s \rightarrow s'$ is always accepted if total energy dissipation is decreased (i.e. $H_\gamma(s') < H_\gamma(s)$). Perturbations to higher values may be accepted, however, with a probability that depends on a parameter T , termed 'temperature' owing to the thermodynamic annealing analog. On following a schedule of decreasing values of T , the network resulting from a perturbation is accepted according to the Metropolis rule, i.e., if

$$\exp\left(-\frac{H_\gamma(s') - H_\gamma(s)}{T}\right) < R \quad (2.13)$$

where R is a random number drawn from a uniform distribution in the interval $(0, 1)$. In this manner, when the temperature is initially high, unfavorable changes are likely to be accepted thus making the algorithm capable of jumping out of structures conditioned by the initial condition. As the temperature is reduced, changes are only accepted if they lower total energy dissipation and thus the optimum configuration gets refined and 'frozen' around a dynamically accessible minimum.

The exact linkage of OCNs with the stationary solutions of the general landscape evolution equation (Banavar et al., 2001) allows us to treat OCNs as replicable planar constructs that reproduce statistically identical sets of drainage directions corresponding to stationary states of a landscape evolution equation where fluvial erosion and geologic uplift are

balanced.

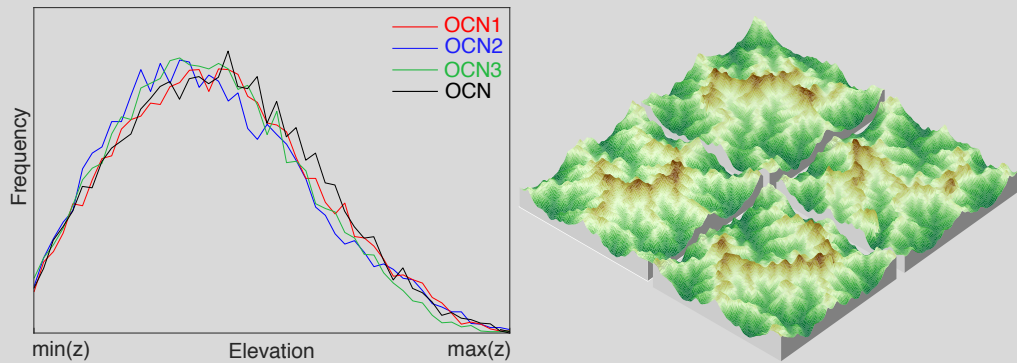


Figure 2.7 – Example of different Optimal channel networks (OCNs). Hypsographic curves and elevation fields of the four OCNs employed in the experiment, the one on the left being referred to in the main text.

From OCNs to mountain topographies A 3D landscape topography is associated to a planar OCN via the following procedure. Recall that a slope-area law is implied in the value of γ i.e. at site i , the upstream drop in elevation at the i -th site (Rodriguez-Iturbe and Rinaldo, 2001) is $\Delta z_i = \mathcal{C} A_i^{-1/2}$ (where \mathcal{C} is a constant determining ultimately the overall relief of the synthetic topography, and A_i is the total contributing area at i). Moving from an outlet, whose elevation is set to 0, one follows the connectivity to attribute the elevation of the j nodes connected to it. Owing to the exact tree-like features (there exist a unique path from any site j to the outlet because loops are excluded (Banavar et al., 2001) if $\gamma < 1$. Field observations and theoretical results suggest values $\gamma \approx 1/2$) such that a topography is uniquely associated with any OCN. It should be noted that the validity of the slope-area law is restricted to the channeled portion of the landscape where fluvial erosion and uplift are the dominating, balanced landscape-forming processes (Rodriguez-Iturbe and Rinaldo, 2001). Suffice here to say that this is tantamount to assume that the scale of the landscape must then be much larger than the (inverse of) the drainage density of the river basin (Rodriguez-Iturbe and Rinaldo, 2001). Should one be interested in reproducing a proper mountain range, one could selectively choose the value of C . For the scopes of the present work, it is deemed that a constant value of \mathcal{C} is an appropriate choice together with the assumption that the drainage density is contained within the pixel size. In the present theoretical experiments the constant is regulated such that the relief is confined to a standard relief of 3000 m, i.e. elevation ranges from 0 to 3000 m to produce a physically meaningful context. The result of this process can be seen in Fig. 2.7.

The DEM of the real landscapes (GPNP and Vaud) are extracted from the online earth explorer

tool, courtesy of the NASA EOSDIS Land Processes Distributed Active Archive Center (LP DAAC), USGS/Earth Resources Observation and Science (EROS) Center, Sioux Falls, South Dakota (<https://earthexplorer.usgs.gov/>). The results are computed on the administrative limits of GPNP and Vaud Ales (red lines in Fig. 2.10), while the simulations are performed over a square with a buffer around the area to avoid border effects. The elevation fields are rescaled such that the relief would match to the synthetic landscapes (0-3000 meters).

These different landscape shapes are designed to probe boundary and structural geomorphic effects. For instance, the typical hump-shaped distribution of hypsographic curves (defined as the area distribution at the various elevations) found in nature (Elsen and Tingley, 2015; Bertuzzo et al., 2016) (GPNP, Vaud Alpes) can be constructed in unrealistic geometries (Fig. 2.1b, cone in a square) and realistic synthetic landscapes (OCN). The comparison among the different occupancies provided by the metapopulation model for a virtual species on these different landscapes highlights the influences of the spatial complexity of the topography on the habitat connectivity and fragmentation (e.g. comparing cone and OCN) and the possible impact of boundary problems (e.g. comparing OCN and real landscapes). Geometric landscapes are further used to understand how relief boundaries interact with niche width (comparing pyramid and roof), and how connectivity changes with constant hypsographic curves, as in the case of the roof. Comparative studies on real topographies and OCN landscapes are employed to highlight the influence of steep slopes characteristic of real landscapes, which are not present in OCNs where fluvial erosion is the dominant factor.

2.3 Results

2.3.1 Initial occupancy patterns

It is analyzed how landscape features control the persistence of species with specific parameter values. In all landscapes, and for all the optimal elevations characterizing the different species, only a subset of the considered species persisted after the initial phase with constant climatic conditions (regional species, color-coded in Fig. 2.8). The various landscape shapes have differing presence patterns even if endowed with similar elevation distributions, like the OCNs and the cone in a square (Figs. 2.1, 2.9). The OCNs showed a limited region of parameter constituting the regional pool of species, suggesting an important effect of spatial aggregation of suitable habitat/landscape fragmentation (Fig. 2.8).

2.3.2 Climate change effects

In all considered landscapes, a subset of the parameters leads to the extinction of the species after climate change (Figs. 2.8 (red) and 2.9 (dashed line)). Results show that extinction debt

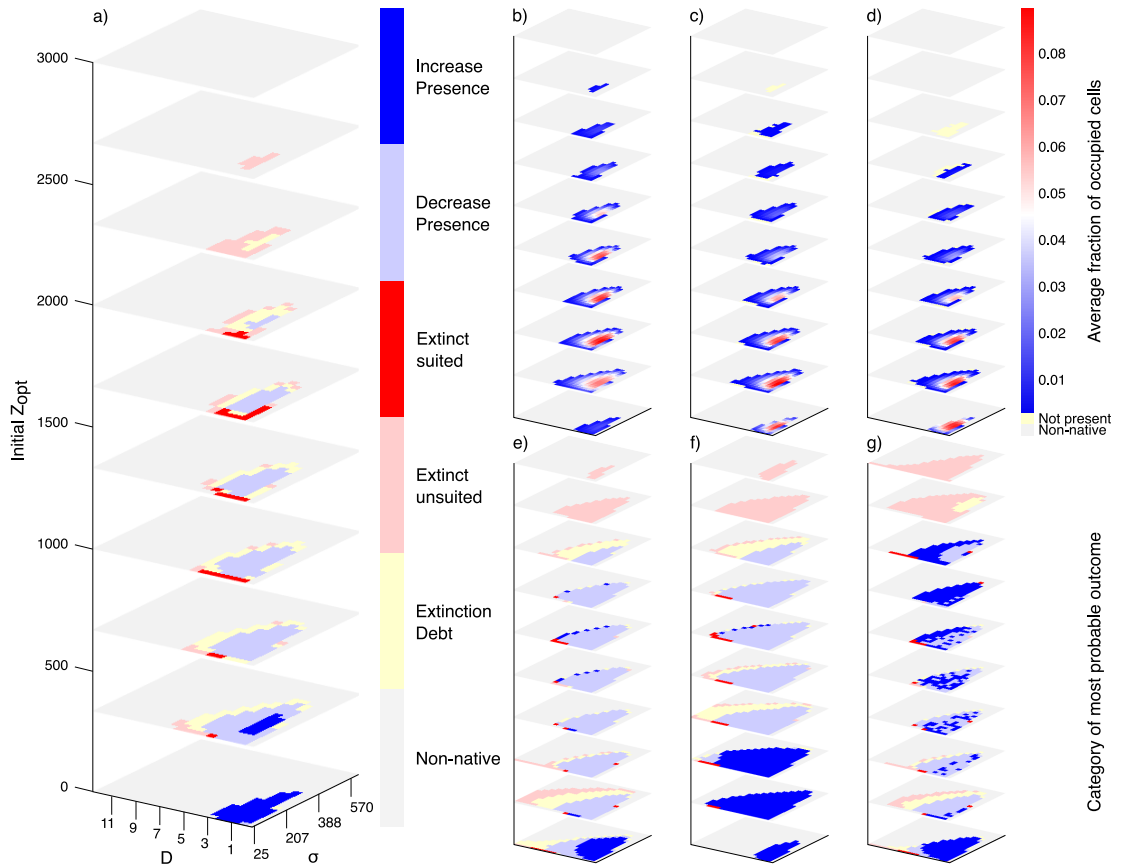


Figure 2.8 – Outcome of the metapopulation runs given initial optimal elevation z_{opt} , niche width σ and dispersal distance D . Colors represent the fate of the virtual species (same color-code as in Fig. 2.1 with detailed explanation of the fates in Fig. 2.6), which is determined by the most probable outcome after 100 random model runs. Results are presented for the following landscapes: (a) OCN; (e) pyramid; (f) cone in a square; and (f) roof-like landscape. (b-d): intermediate simulation results (average fraction of occupied cells over 100 experimental runs) for the OCN initially (b), after climate change (c) and in steady state after climate change (d), which led to the classification in a. The range of parameters shown has been chosen to contain the areas where significant change is detected. See Appendix A for the complete set of results.

is frequent for large niche widths and dispersal distances (Figs. 2.8 (yellow) and 2.9 (dotted line)). Part of the regional pool of species having an initial optimal elevation facing a rising hypsographic curve, that is, an increase of area of suitable habitat resulting from the upslope shift, i.e. when z_{opt} is located below the position of the peak (species in dark blue in Fig. 2.8a,c) experienced an increase in their occupancy and range, whereas species ending up around peaks in the landscape after climate change, or when z_{opt} is located above the peak in the hypsometric curve, were unequivocally affected by a strong occupancy reduction and range reduction (all colors except dark blue in Fig. 2.8a,c for $z_{\text{opt}} > (500/1000)$ m). Thus, for a

hump-shaped hypsographic curve, where the majority of land lies at intermediate elevations (OCNs, cones, real landscapes), the fate of a species depends on the relative position of the peak elevation compared to its initial z_{opt} .

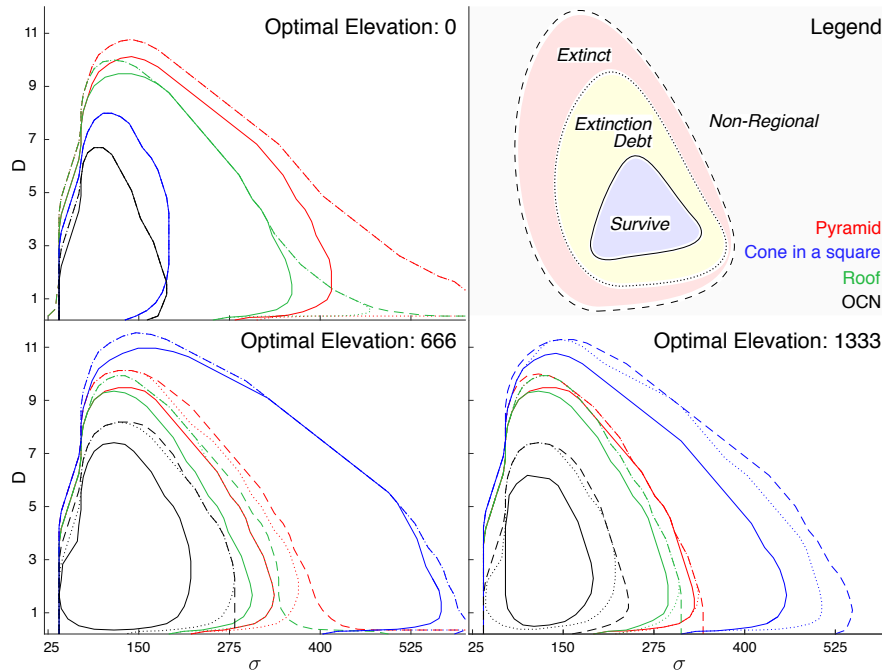


Figure 2.9 – Progression of the parameter limits during the simulation. Parameter limits (niche width σ , dispersal D) of the initial pool of regional virtual species (dashed), species present after climate change (dotted) and species present at steady state after climate change (line). The figures show species with initial optimal elevations (z_{opt}) of 0, 666 and 1333 m.

Extinction due to inability to track change has many causes. Species unsuited to new conditions are found where suitable habitat shrinks or disappears (loss of suitable habitat). Interestingly, however, in real landscapes and OCN replicas, species with small niche width are confronted with this likely outcome even if they gain habitat area or connectivity (Hanski, 1998) with climate change. Species unable to track, but that would have been capable of surviving under altered conditions, i.e., lagging behind the rate of climate change (Bertrand et al., 2011; Alexander et al., 2016) (extinct suited, Fig. 2.8, dark red), were found only for a small number of parameter sets, mostly for species with small niche width and relatively large dispersal values, and almost exclusively on species with optimal elevations situated in the decreasing part of the hypsographic curves. Species surviving climate warming (Fig. 2.8, blue, Fig. 2.9, straight line) were found to adjust their occupancy compared to their initial states. Species with a decreasing presence (Fig. 2.8, light blue) were found when suitable area and/or proximity/connectivity decreased or when their niche ranges exceeded the maximum elevations. This pattern was commonplace for the pyramid where area monotonically decreases

with elevation (Fig. 2.1b).

2.3.3 Extension to real landscapes

Real landscapes are analyzed using DEMs for GPNP and Vaud Alps (Fig. 2.10). It was looked at how the geographic range of a pool of regional species shifts in response to climate warming. Fig. 2.10 shows the temporal changes in the percentage of occupied area by a species compared

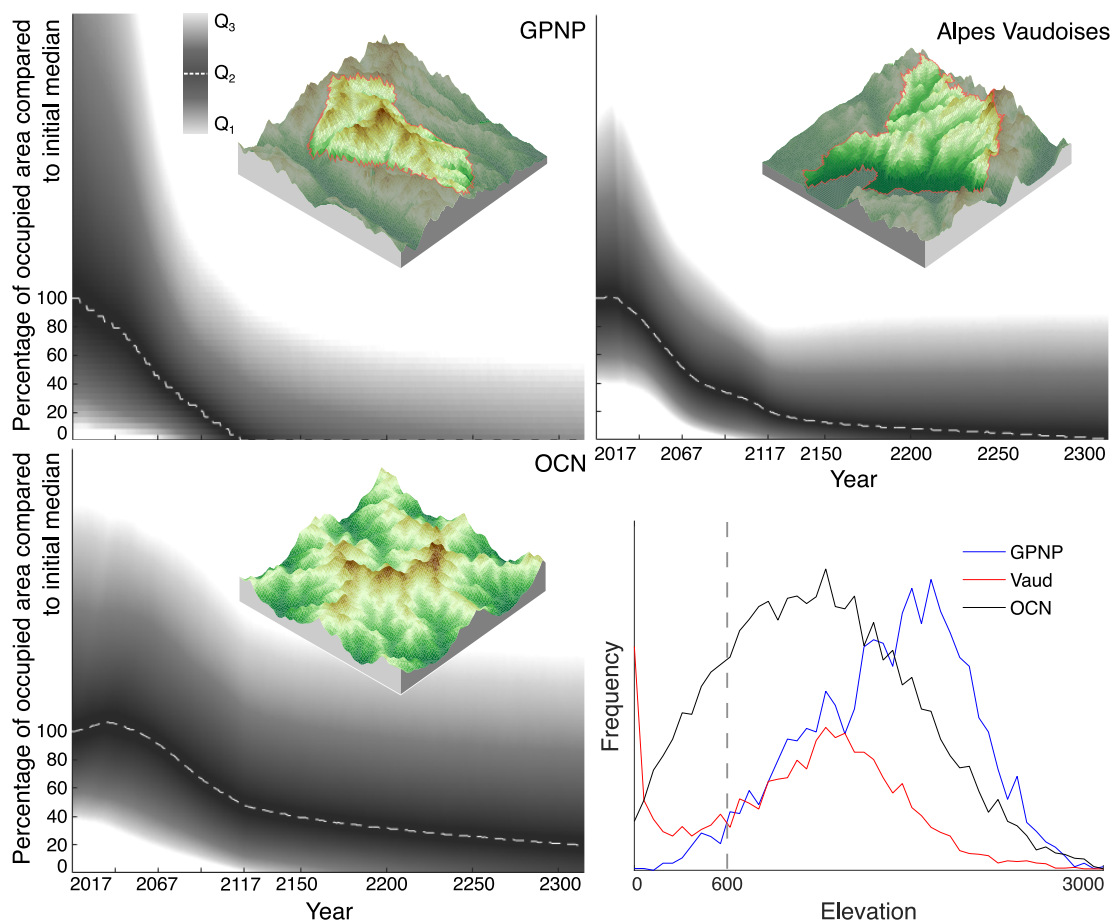


Figure 2.10 – Species occupancy during (2017-2117) and after climate warming (after 2117) relative to the initial median occupancy. The dashed line represents the median percentage of occupied area by regional virtual species that decreases during and after climate warming. The red lines in the DEMs represent the limits where area was considered. The bottom right panel shows the elevation frequency plot (hypsographic curves) of the three landscapes. The dashed line in the elevation frequency plot represents the parts that can be lost due to climate change, which represents 3.42 % of the surface for Gran Paradiso, 21.89 % for the Vaud Alps, and 18.13 % for the OCN.

to the initial median occupation. Are not considered in this analysis species that can immigrate

from outside the system (e.g., from lower elevations) but focus only on the fates of regional species. As expected, occupancy decreased during climate warming. Interestingly, a long period is required to stabilize the occupancy after the imposed change. Species occupancy continued to decrease after the climate stabilized, and the median occupancy tended to zero in GPNP and Vaud Alpes. Owing to its geomorphological attributes, the GPNP region, which has the majority of land close to the maximum elevation, suffered the most from the loss in occupancy.

2.3.4 Effect on species diversity

Figs. 2.11 and 2.12 (see Appendix A for a complete set of results for all landscapes) show the α -diversity (i.e. the number of species, among the selected pool of regional species, that

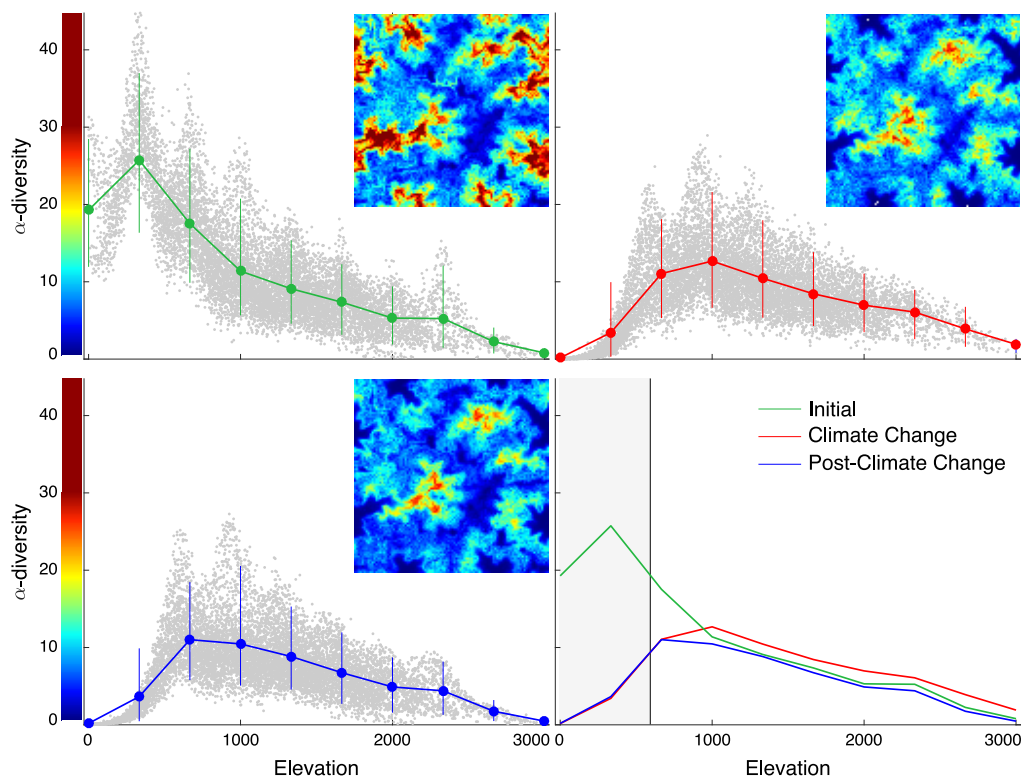


Figure 2.11 – α -diversity averaged over 100 runs of the simulation for the OCN. The maps and the scatter plots show the values in the landscape at the initial situation, after climate change and at steady state after climate change. The last plot shows a comparison between the three phases. The grayed-out zone represents the difference in elevation caused by climate change, from the lowest elevation in the area, incidentally defining the part of the study area where caution should be taken in any interpretation, as no new species can colonize from lower elevations outside the area.

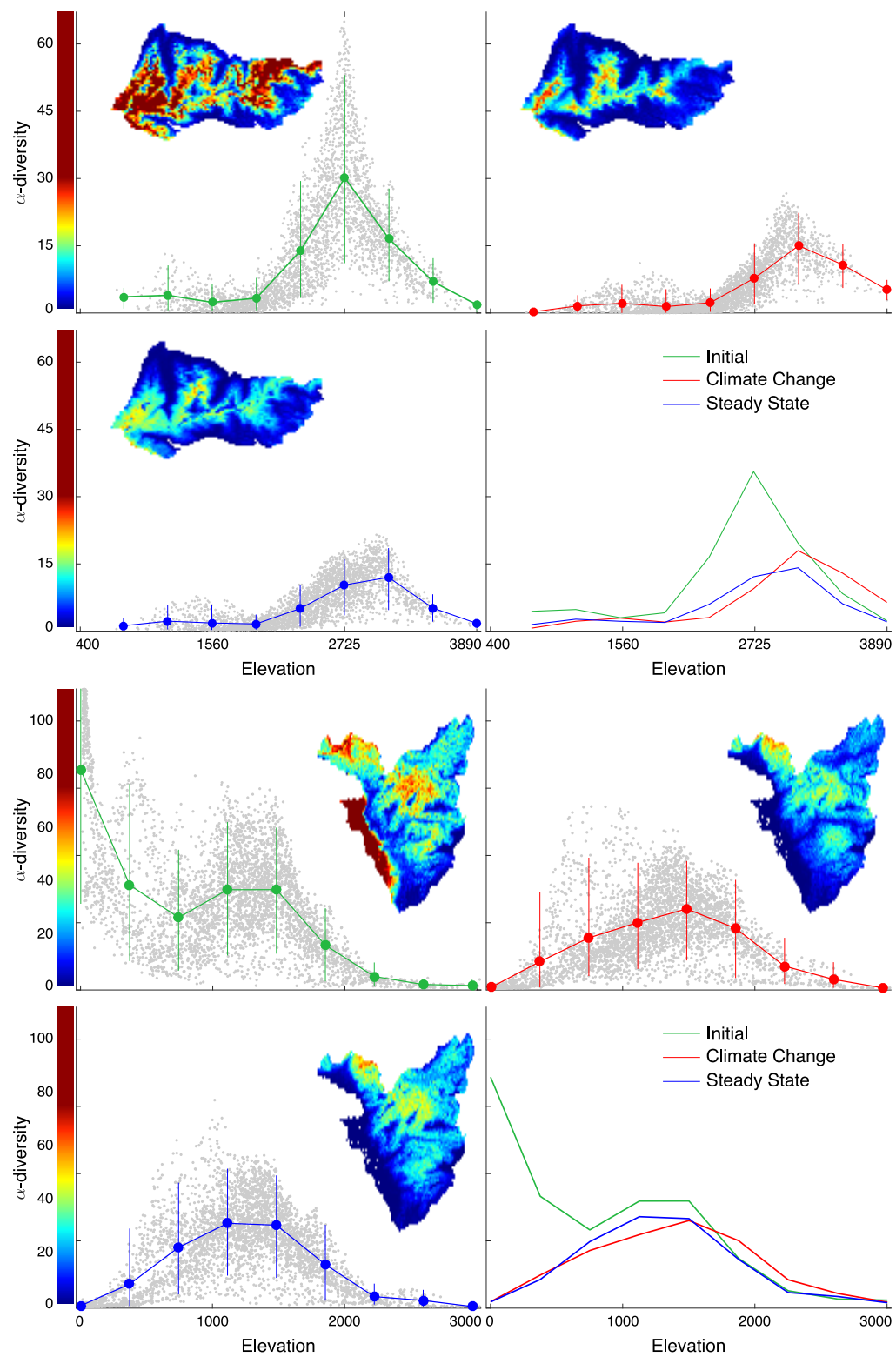


Figure 2.12 – α -diversity averaged over 100 runs of the simulation for the GPNP and Vaud Alpes. Same as Fig. 2.11 (α -diversity) but for GPNP (top) and Vaud Alpes (bottom)

simultaneously occupy a patch (note that no interactions are considered here)) in the OCN, GPNP and Vaud alpes respectively for the different phases of the experiment, i.e. initially, after climate change and at steady state after climate change, computed from a discrete choice of values of σ , D and z_{opt} .

Under climate change, the peak of α -diversity is naturally shifted towards the mid-domain as species start moving upwards, and no other possibly invading species are considered (the species pool is not changing). The scatter plots show how the average α -diversity at mid-elevation tends to increase compared to the initial situation, only to later stabilize and end up at a lower level than the initial value.

Species lagging in adapting their distribution to the actual optimal range imposed by climate change overlap with species catching up from below, creating an artificial temporal elevated value of α -diversity, which is then lowered by the species moving towards their respective ranges at steady state, and other species going extinct in the process.

Different currencies exist (correlative, mechanistic, and trait-based) to assess species' climate change vulnerability (Pacifi et al., 2015). For example, α - and β -diversities are often viewed as suitable measures to assess the change occurring at a certain location (Whittaker, 1972; Anderson et al., 2011). In this context, Fig. 2.11 suggests that such indicators have to be handled with caution.

In fact, at high elevations, unaffected by the species pool, climate change seems to show an increase in α -diversity compared to the initial value. This temporary increase is generated by a lag of species presence in the process of adapting to their new habitat, which might be interpreted as an early warning.

Box 2.4 – Singeling out geomorphic effects in the results

In order to understand if the observed result effectively stem from the landscape's geomorphic features, one can perturb the elevation field by incorporating correlated noise in the landscape matrix.

Random fields are generated using HYDRO_GEN (Bellin and Rubin, 1996) (Fig. 2.13, the same tool used in box 1.3), with the integral scale between 1 and 50 pixels (half of the field size), and variance of coefficient of variation between 0.1 and 1. The mean remains at 1 for all randomly generated fields. For each species, a random field is generated, and the fitness modified:

$$f'_i = X_i \cdot f_i \cdot \frac{\sum_j f_j}{\sum_j f_j \cdot X_j} \quad (2.14)$$

such that the sum of the fitness over the landscape is preserved. X_i represents here the value of the random field at pixel i .

Fig. 2.13 shows the difference between fates of species before, and after the addition of noise to the elevation field, for the OCN, Vaud Alpes and GPNP landscapes.

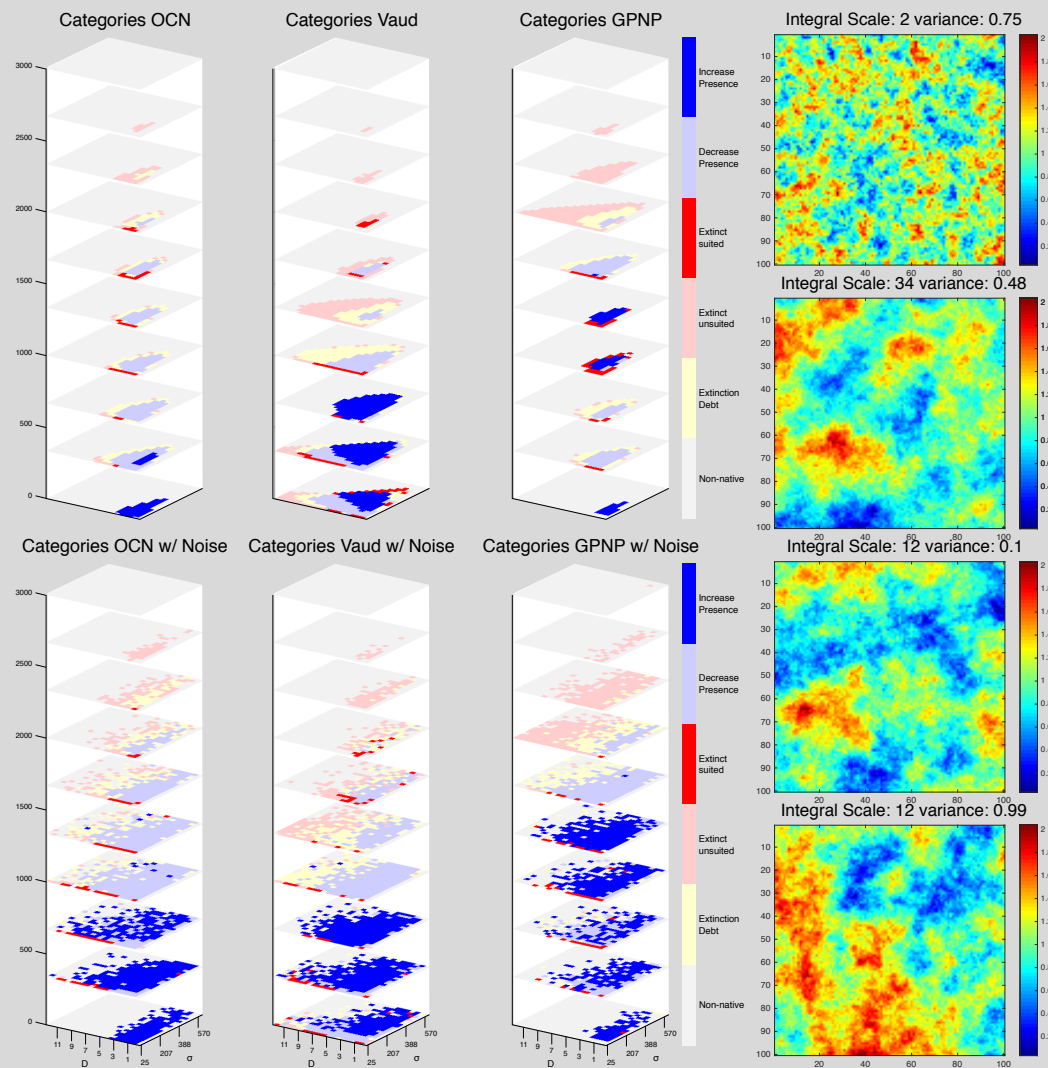


Figure 2.13 – Addition of correlated random noise to the elevation field. Comparison of two sets of results: between using only elevation as fitness and adding noise while conserving the total fitness over the landscape for the OCN, Vaud Alpes and GPNP. The noise fields (sample on the right) were generated using HYDRO_GEN Bellin and Rubin (1996), with integral scale and variance randomly selected for each species. Note that this correlated random field generator is the same one as used in box 1.3.

The added noise field renders the impact of the complex mountainous structure null, and thus the effect of the niche width, while at the same time highlighting the effect of dispersal, with a clear gradient of ‘surviving’ to ‘extinction debt’ to ‘extinction’ when going from small to large niche width in the upper parts of optimal elevation. This

means that in this new landscape, where the elevation structure almost disappears, the main driver of species presence is the dispersal, given that the fitness of the species is dominated by the noise field.

These results thus suggest that the observations made in this chapter on niche width and optimal elevation are indeed to be related to the geomorphic effects and the landscape structure.

2.4 Discussion

Given the chosen parameter set, three intertwined factors govern the fate of the species at any site in a landscape: the initial occupancy distribution, the distance at each site from areas sharing similar fitness, and the available area around the optimal elevation, the main niche factor. Taken separately, the effects do not suffice in predicting the fate of a species under climate warming. For example, the hypsographic curve alone does not subsume all processes governing species presence. Even in the simple, unrealistic geometric landscapes designed to distinguish geomorphic effects (c.f. box 2.4), the entanglement of those processes generates unforeseen outcomes (Figs. 2.8, 2.9). For instance, species endowed with their niche partially outside the landscape elevation range before climate warming, may actually exploit increased geographic range projection even if the specific hypsographic curve is steadily decreasing (Figs. 2.1b, 2.7, 2.10). Occupancy thus reflects a complex balance between area availability, connectivity and realized niche (see also (Guisan et al., 2017) for an analogous effect captured by habitat suitability models). One may note that connectivity does not refer to dispersal alone. In fact, it typically incorporates some measures of land cover, land use, or landscape 'permeability' and is considered more a feature of the landscape rather than simply of the species ecology (like the dispersal distance) (Elsen and Tingley, 2015).

The results suggest that equally viable species endowed with very large niche widths σ successfully track climate warming but often do not survive afterwards. In fact, under the imposed constraint on species parameters, such species have a relatively low fitness everywhere, which only allows survival if enough surface is colonized. Strong colonization is thus required to grant species survival relative to large dispersal distances. Otherwise, colonization will not compensate the low fitness and most of such areas - even if large - will slowly become unsuitable, leading to extinction debts. This particularly affects strong dispersers, whereas weak dispersers are more subject to landscape fragmentation because they rely on close-by areas to persist. Species with smaller niche and higher fitness are less affected by extinction debts, but may go extinct before the end of the imposed temperature rise, i.e., they might either track climate warming, and thus thrive given the new conditions, or go extinct during the process despite being suitable to the new conditions because of their isolation and the lag in tracking

the new conditions. For such species, the local conditions are of utmost importance, because the fitness in a single patch suffices to make them survive without help from surrounding occupied cells (reduced available area), which causes them to be particularly sensitive to changes in available, close-by suitable habitats, and fragmentation (lack of short distance escape opportunities (Bertrand et al., 2011)). Such species are highly sensitive to microclimatic heterogeneity (Graae et al., 2017).

Realistic landscape heterogeneities are found to strongly impact species survival (Fig. 2.9). The domain of parameters describing surviving species proves much smaller than that obtained for simple geometries. The defining role of connectivity is confirmed by noting that OCNs and the cone-in-a-square construct exhibit a rather similar hypsographic curve (Fig. 2.1b) but rather different species fates (Fig. 2.8). Local effects, such as mid-elevation plateaus or isolated peaks, influence the spatial projection of the niche, the geographical range and the proximity of similar areas (as in (Engler et al., 2009)), thus locally reducing the fitness of the species. If a landscape has a self-affine structure like many mountain ranges (Rodriguez-Iturbe and Rinaldo, 2001), highly fragmented connectivity is generated whereby species with larger niches but lower fitness struggle to subsist due to the weaker mutual rescue effect of occupied cells owing to meta-population processes of patch colonization-extinction. The differences between real and model landscape results are explained by the fact that OCNs imply large drainage densities (small ratios of the total river length to the catchment area normalized by the landscape characteristic size) and thus flatter slopes than in the real mountain landscapes studied here.

Certain assumptions of the minimalist model may be relaxed. They concern:

- the lack of incorporation of actual habitat suitabilities, here subsumed by the model equation 2.3 chosen to strengthen the signals due to landscape effects. Although generalizable, such assumptions prevent a detailed ecological study of the species surviving the range shift beyond broad-brush statistics of their survival – however useful;
- the choice of characterizing climate warming as uniform and driven only by air temperature. Such assumption may be relaxed by using suitable climate and weather generators of various origins. This, however, would come at the risk of clouding the geomorphic effects highlighted in this work;
- the lack of heterogeneity of range shifts at the landscape-scale (Lenoir et al., 2010; Tingley et al., 2012), here modeled by a simple upslope shift;
- the parameter choices describing local fitnesses, which is related to the constraints placed to maximal fitness (f_{\max}) to approximately conserve metapopulation capacity (Methods). This assumption reduces the number of species analyzed and yields a comparison in that similar viability of the species is assumed. Such assumption, like for instance the introduction of super-species with large width and high fitness that would

colonize any landscape at every elevation, could be introduced for specific studies at no change in the procedure (see Appendix S1 for an example of a simulation with such a species);

- the neglect of invasions of species from lower elevations, unrepresented here. While standing by this choice in view of the scopes of this paper, it has to be noted that neglecting them prevents a specific ecological study of how generalist or specialist species fare under the same circumstances in a given landscape. To that end, forthcoming metapopulation studies will be based on field evidence, possibly using generalized fitnesses that include all relevant covariates. Box 2.2 gives more details about the effects of the factors currently neglected in the mainstream discussion, and about technicalities on possible generalizations.

Moreover, long-term evolution of populations can lead to local adaptation to environmental conditions (see e.g. (Papaix et al., 2013) for a dynamic study based on spatially heterogeneous metapopulations). However, as noted in the introduction to this chapter, in the minimalist model pursued herein ecological timescales are assumed to be much smaller than evolutionary ones. Phenotypic evolution of spatial metapopulations could instead be a possible development of the present approach, where heterogeneities might be provided by habitat suitability models (Guisan and Thuiller, 2005) tailored to mountain ecosystems.

It can nonetheless be suggested, from the bulk of the extensive calculations described in this chapter, that strong influences are waged by broad geomorphic features of a landscape not only for biodiversity in equilibrium with the current climate (Elsen and Tingley, 2015; Bertuzzo et al., 2016), but also for the long-term impact of climate warming on species survival. This is likely to be true in general, but especially so locally for heterogeneous landscapes. The extinction debt (Tilman et al., 1994; Dullinger et al., 2012; Steinbauer et al., 2018), which is hardly measurable as an ongoing process, is found to be a dominant feature in species dynamics according to this modeling approach for any realistic landscape. This feature would make it difficult (if not impossible) to predict changes before they actually happen without models. Especially alarming seems the suggestion that the effects of warming would not be limited to phasing, but would rather be also characterized by the disappearance of large amounts of occupied areas long time after the actual change in the driver. The timescales of the ecological response triggered by the imposed geographic range shift, in fact, are suggested to be much longer than that of the phasing itself, as extinction debts may be operating even centuries later.

2.5 Conclusion

The main conclusions of this chapter can be summarized as follows.

Computational studies on the effects of climate warming prove essential to sort out genuine landscape effects on metapopulation range dynamics and spatial occupation of species under climate warming, not simply in terms of stationary states but also of transients defining the range of possible extinction timescales. Geomorphic effects on species survival can be sorted out because a climate warming scenario was applied to a regional pool of species previously filtered for the initial temperature regime under the discriminating (and defining) requirement of equal ecological viability (i.e. same metapopulation capacity). This results in a specific constraint on the virtual species' fitnesses sensitive to the geomorphic effects sought after.

Minimalist models of the type explored here underpin quantitative studies of how extinction debts unfold. This is due to their computational ease that allows extensive search in the space of species parameters.

Future work will exploit the proposed framework to include other dimensions of habitat suitability in generalized fitness models. This may be done by correlating fitness to a number of environmental covariates (e.g., precipitation, soil type, aspect (box 2.2), resources, land-use, etc.) rather than simply to elevation, or allowing metapopulation capacity to vary, i.e., incorporating species with both small/large niche breadth/fitness.

3 Earth Observation driven metapopulation dynamics of carabids in a mountain range

THE present chapter¹ addresses the near-term predictions of spatial distributions of species, essential for assessing the risk to biodiversity within changing ecosystems. Earth observations integrated by field surveys provide key grounds for improving modeling of landscape-wide biodiversity scenarios. To that end, a methodology is developed here, applied to a relevant case study, suited to merge earth/field observations with spatially-explicit stochastic metapopulation models to study the near-term ecological dynamics of target species in complex terrains. The framework, discussed in detail in this chapter, incorporates the use of species distribution models for a reasoned estimation of the initial presence of the target species, and accounts for imperfect detection from the field surveys. It also uses a metapopulation fitness function derived from earth observation data subsuming the ecological niche of the target species. This framework is applied to contrast abundances of two species of carabids (*Pterostichus flavofemoratus*, *Carabus depressus*) observed in the context of a large ecological monitoring program carried out within the Gran Paradiso National Park (GPNP, Italy). Results suggest that the proposed framework may indeed exploit the hallmarks of spatially-explicit ecological approaches and of remote Earth observations. The model reproduces well the observed *in-situ* data. Moreover, it projects in the near-term the two species' presence both in space and time, highlighting the features of the metapopulation dynamics of colonization and extinction, and their expected trends within verifiable timeframes.

¹The content of this chapter has been adapted and submitted to a peer reviewed journal as follow: Giezendanner, J., Pasetto, D., Perez-Saez, J., Cerrato, C., Viterbi, R., Terzagio, S., Palazzi, E. and Rinaldo, A. (submitted 2019). Earth and field observations underpin metapopulation dynamics in complex landscapes: case study on Carabids.

3.1 Introduction

The main drivers of the geographic distribution of a species are (Pulliam, 2000; Soberón and Peterson, 2005): i) the set of abiotic factors characterizing its fundamental niche (Hutchinson, 1957); ii) the interactions with other individuals (biotic interactions and demography) (Keith et al., 2008; Economo and Keitt, 2008; Akçakaya, 2000); and iii) the accessibility of geographical regions where species movement is not impaired (e.g. mountain tops, valleys or man-made dams and roads (Colwell and Hurr, 1994; Economo and Keitt, 2010; Bertuzzo et al., 2016; González-Ferreras et al., 2019)). The combination of the fundamental niche with the species interactions defines the realized niche (Soberón and Peterson, 2005) i.e. the fraction of the fundamental niche which shows a positive population growth rate despite competition (Pearman et al., 2008). Species distribution models (SDMs) (Guisan and Thuiller, 2005) concern the modeling of the landscape-explicit probability of presence of a species based on the realized niche. This occurs by relying primarily on the habitat suitability (Kearney and Porter, 2009) given its biotic and abiotic factors. Habitat suitability drives the probability of presence of a species at equilibrium (Busby, 1988; Booth et al., 2014), implying that the presence of a species in the landscape reflects its niche while other processes, like dispersal, colonization or migration, do not have major effects (Thuiller et al., 2014). In species distribution models, most processes are implicitly incorporated into the habitat suitability, and hence into the species' niche (Guisan and Zimmermann, 2000). Physical barriers, sources-sinks, population and metapopulation dynamics are thus not modeled explicitly (Thuiller et al., 2014), although models have been developed to integrate certain features of the relevant dynamics with SDMs (Akçakaya, 2000; Keith et al., 2008; Kéry et al., 2013; Gavish et al., 2017).

Here, the focus explicitly set on the linkage of attributes of the landscape matrix with stochastic metapopulation dynamics (Fahrig, 2007; Purves et al., 2007; Rybicki and Hanski, 2013; García-Valdés et al., 2013; Giezenlander et al., 2019) where the landscape is subdivided into cells, as commonplace when EO rasters are used. Each cell constitutes a patch *sensu* Hanski, from which a focus species can colonize other empty patches or go extinct. This allows us to characterize precisely the abiotic conditions within each cell based on EO data, and derive a species' fitness, or the local habitat suitability. Once the niche of species is estimated, the metapopulation model can, in time, reflect the unfolding colonization of geographical regions, and account explicitly for physical barriers that prevent it. Moreover, a method estimating this niche by calibrating the parameters driving processes relevant to metapopulations has to account for the gaps in data in space and time as well as the imperfect detection of species (MacKenzie et al., 2003; Ovaskainen and Saastamoinen, 2018). The method proposed here merges the use of SDMs (Guisan et al., 2017) with the demands of stochastic metapopulation models (Hanski (1998, 1999a,b), see Fig. 3.1 for an overview of the general scheme). EO data are employed to characterize habitat suitability in space and time by reproducing observed spatial

and temporal presences of the *in-situ* data for the focus species. As SDMs prove particularly apt at depicting a species' static probability of presence, a reasoned generalized linear model (GLM) is used to estimate the initial presence in the landscape. A stochastic metapopulation framework (spatially-explicit patch occupancy model (SPOM, used e.g. by Moilanen (2004); Purves et al. (2007); Rybicki and Hanski (2013); García-Valdés et al. (2013); Giezendanner et al. (2019)) is employed to dynamically model the presence of the focus species in time (Bertuzzo et al., 2016; Guisan et al., 2017). A suitably modified metapopulation fitness is defined based on

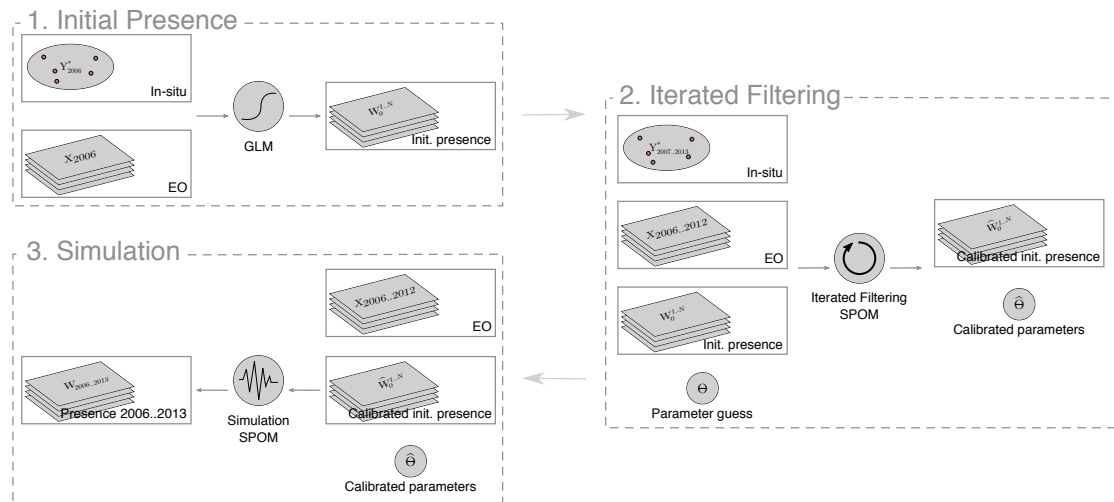


Figure 3.1 – Overview of the proposed framework as detailed in the methods. 1) The species' initial spatial occupancy is estimated by a generalized linear model (GLM) based on earth observation data (EO) and calibrated with in-situ data of the first sampled year (2006 in this case); 2) The metapopulation model (SPOM) parameters and the initial presence are calibrated by iterated filtering (IF), with the EO data of each year used for the species' fitness, and the in-situ data for the likelihood. 3) The calibrated initial presence and parameters are used to run the metapopulation model as a simulation in order to predict the focus species' presence in the landscape.

the core concept of GLMs, which is calibrated by using an iterated filtering scheme (IF, Ionides et al. (2015)), a technique particularly powerful when applied to partially observed Markov processes. An application to a case study then showcases the capabilities of the framework by replicating the observed spatial and temporal dynamics of two species of carabids viewed as significant biodiversity indicators – an outcome of a large field observations program in the Gran Paradiso National Park in the Italian Alps.

3.2 Materials and methods

The proposed method aims at linking the power of SDMs with the advantages of a dynamical metapopulation model (see Fig. 3.1 for an overview of the framework). EO data are used to characterize the suitability of a habitat for a given species in space and time in order to reproduce the observed spatial and temporal presence of the in-situ data. As SDMs are particularly good at modeling the probability of species in space for a given time, a generalized linear model (GLM) is used to estimate the initial guess of the presence of a species in the landscape, which is then further calibrated. As in the previous chapter, a metapopulation framework called spatially-explicit patch occupancy model (SPOM, Moilanen (2004); Purves et al. (2007); Rybicki and Hanski (2013); Giezdanner et al. (2019)) is then used to dynamically model the presence of the species in time. A modified metapopulation fitness based on the same core concept as GLMs is proposed, which is then calibrated using an iterated filtering scheme (Ionides et al., 2015), a technique particularly powerful when used to calibrate partially observed Markov processes.

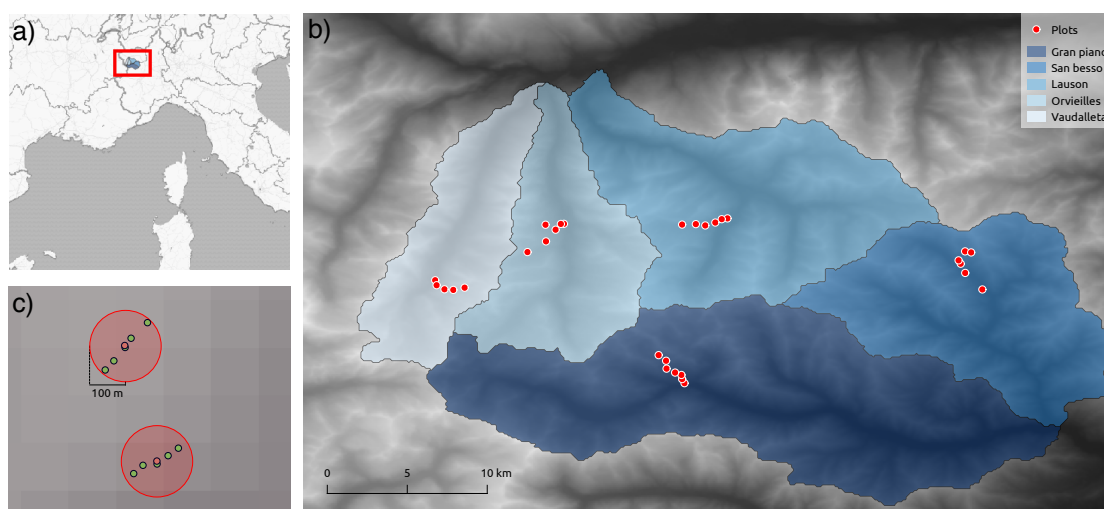


Figure 3.2 – Overview of the study site. a) Location of the Gran Paradiso National Park (GPNP), b) overview of the GPNP's five valleys with the location of the plots in the valleys, c) example of traps aggregated in a 100 meter radius forming two plots. The two plots are separated by 200 meters in elevation.

The developed framework is demonstrated on data originating from a large ecological monitoring program called “*Biodiversity Monitoring Project*” performed in the Gran Paradiso National Park (GPNP), a protected area located in the Italian Alps (Fig. 3.2a). In this study, data on invertebrates (Coleoptera Carabidae, Coleoptera Staphylinidae, Araneae, Hymenoptera Formicidae, Orthoptera, Lepidoptera Rhopalocera) and birds (Aves) have been routinely gathered since 2006 to gain an extended understanding on elevation-driven biodiversity patterns (Viterbi et al., 2013). The data have been gathered in the park's five valleys (Gran Piano, San

Besso, Lauson, Orvieilles, Vaudaletaz, Fig. 3.2b), in a 2 years sampling, 4 years break scheme, i.e. the processed data is available in 2006, 2007, 2012, 2013. The project monitors species presence and abundance by considering a series of circular plots (5 to 7 in each valley) of a radius of 100 m. These plots are separated by 200 m in elevation along a transect of the valley (Fig. 3.2c).

The focus is here on carabids, one of the taxon collected. Carabids, or Ground Beetles, are a family of terrestrial arthropods (*Carabidae* taxon) composed of more than 40'000 species worldwide (Thiele, 1977; den Boer, 1990; Kotze et al., 2011).

Box 3.1 – Study reasons and interests Carabids have been, and continue to be, widely studied, and continue to be, for two principal reasons. 1) In agriculture they are often seen as useful in pest controls (Kromp, 1999; Rainio and Niemelä, 2003). Natural enemies of pests, they are cost effective, sustainable and ecological. 2) They serve as good bioindicators (Lövei and Sunderland, 1996; Niemelä, 2001; Rainio and Niemelä, 2003; Jopp and Reuter, 2005; Kotze et al., 2011). Due to their sensitivity to change in environmental conditions, carabids are used as bioindicators of environmental, ecological or biodiversity status, which rely on species presence, number of individuals, and diversity (number of species) (Rainio and Niemelä, 2003). They are commonly seen as sentinels of environmental pollution, soil-nutrient status, habitat classification for nature protection, habitat quality, change, and alteration, and used to assess the state of communities of other species. Certain reservations on their use as bioindicators remain because of their seasonal variation and because standard sampling methods often favor capture of active and/or generalist species (activity-dependent densities) (Niemelä, 2001; Rainio and Niemelä, 2003).

Carabids are one of the best studied taxon in entomology (Kotze et al., 2011), in part because of their use as bioindicators and in agriculture (see box 3.1), and have significantly advanced the understanding of conservation biology and landscape and population ecology (see box 3.2).

Box 3.2 – Models Mathematical models considered in the literature to describe carabid populations are various, but they can basically be divided into two categories: statistical models which aim at predicting the presence or the abundance of a certain species, and dynamical models which aim at reproducing the observed processes. Statistical models include index based models (e.g. mean individual biomass) (Skłodowski, 2009), scaling laws (Gudowska et al., 2017), linear regressions (Kleinwächter and Rickfelder, 2007) and habitat suitability models (or species distribution models) (Schröder, 2008). Dynamical models range from individual based models (Jopp and Reuter, 2005) to patch occupancy

models (Akçakaya, 2000), over probabilistic and spatially-implicit dynamical models (Griffith and Brown, 1992), networks (Jordán et al., 2007) and demographic (Rushton et al., 1996; Benjamin et al., 2008; Pichancourt et al., 2006), or their suitable combinations thereof, often called hierarchical models. These models can be either spatially-implicit or explicit and static or dynamic in time.

The most frequently used models are the demographic models, coupled with landscape models (Jopp and Reuter, 2005; Reuter et al., 2005; Pichancourt et al., 2006; Benjamin et al., 2008). These models explicitly consider the age structure of populations of carabids (according to the life cycle, see below) and their internal dynamics (Rushton et al., 1996), and use a landscape model to link them together through, for instance dispersal (Jopp and Reuter, 2005). The top-level landscape model can in some cases be a classical metapopulation model (Akçakaya, 2000) with typical patch dynamics.

During the four years of sampling, ninety different species of carabids have been identified, in various frequencies of occurrence and plots. Two species are focused on here, which display different occurrence dynamics: *Pterostichus flavofemoratus*, relatively stable in terms of occurrences and *Carabus depressus* with more fluctuations. The analysis the two species' in-situ data is presented below.

Box 3.3 – Life cycle Carabids have four development stages (Wachmann et al., 1995): egg, larvae, pupa and finally adult beetle. Depending on the speed of larval development, carabids can hibernate as larvae or adults (Kotze et al., 2011), with reproduction occurring in spring or early summer (Wachmann et al., 1995; Lövei and Sunderland, 1996; Kotze et al., 2011). They usually develop from egg to adult in less than a year, but for certain species this can last up to four years (Lövei and Sunderland, 1996). After reproduction, they then normally perish, but certain species can last longer (Lövei and Sunderland, 1996; Wachmann et al., 1995). The activity period in the year for mountain carabids is usually of 3-4 months, distributed from spring to fall depending on the species (Kotze et al., 2011). The reproduction rate is strongly affected by temperature and external factors such as food availability. Depending on carabid species, females lay a dozen eggs if they guard them, and up to a couple of hundreds if they do not guard them.

The aim is to model the inter-annual dynamics of the carabids, not the seasonal one. This choice for the temporal resolution of the model output is justified by three reasons: first, carabids have a life cycle which spans over a year (see box 3.3), and most changes in density are observed between years. Second, the main drivers of the model are EO data, and obtaining accurate EO data multiple times a year is challenging due to cloud covering and possible sensor failures. Third, the carabids are here collected by pitfall trapping. Pitfall trapping

produces an estimate of the activity-density of individuals in a region, and is largely accepted as a good estimate of density fluctuations between years, but not within a single year (see box 3.4). The data is thus aggregated by plots and years, focusing on presence rather than density, and as such reduce the uncertainty associated with categorizing each individual.

Box 3.4 – Pitfall trapping, data gathering and sampling For gathering data on carabids, pitfall trapping has been one of the most commonly used field method, both for their ease to use and cost effectiveness (Rainio and Niemelä, 2003; Tenan et al., 2016). In literature, pitfall trapping has been criticized at times, because it poses certain issues regarding: the scattered distribution of traps versus the heterogenous spatial distribution of a species, as well as the passivity of the trap versus the activity of the species. Traps usually fail to capture small and scattered species (Tenan et al., 2016), which influence the sampling and the interpretation of the results. Additionally, spatially and temporally scattered sampling fails to capture many species (Woodcock, 2007). Traps depend on individuals to make their way toward them, and so the sampling is heavily biased by the relative activity of a species, coupled with its actual abundance (Thiele, 1977; Parkinson and Marshall, 1998; Rainio and Niemelä, 2003; Woodcock, 2007; Tenan et al., 2016). Even species with high abundance might not be sampled accurately if mostly inactive (Woodcock, 2007). Generally, pitfall trapping seems to over-represent generalist species compared to specialized species. It has therefore been argued that instead of talking about abundance resulting from pitfall traps, one should call them “activity-abundance” (Thiele, 1977; Woodcock, 2007), or “activity-density” (Parkinson and Marshall, 1998). Nevertheless, pitfall trapping can be very instructive. Year-long data can be used to accurately estimate yearly density, and between year fluctuations are well captured (Newell, 1986; Lövei and Sunderland, 1996; Woodcock, 2007). Data from spatially-scattered sub-populations can be assembled to gain an overview of the metapopulation structure in the landscape (Niemelä, 2001).

For each year and plot, the number of times a certain species is found is counted (k) along the number of times the plot was sampled (n), which corresponds to the number of times each trap in a plot was visited in a given year. This provides a good estimate of the reliability with which a species has been identified and captured in a given plot, assuming that the species have the same activity during the sampling period (see section 3.2.2.1 for an overview of the in-situ data).

The carabids have been confirmed as a taxon following metapopulation dynamics (Lövei and Sunderland, 1996; Kotze et al., 2011), which frames them as good candidates for this study (see box 3.5). Additionally, it has been shown that environmental drivers such as temperature, humidity or height of the herbaceous layer drive these species. EO data capturing these

landscape features are therefore good candidates to model their niche.

Box 3.5 – Population dynamics and ecology

Metapopulation dynamics Most carabid species function as metapopulations (Lövei and Sunderland, 1996; Kotze et al., 2011), operating at two scales (Burel et al., 2004), the local scale composed of subpopulations, driven by habitat quality, and the landscape or large-scale, at which exchanges between subpopulations occur (Tenan et al., 2016; Matern et al., 2008), maintaining declining, isolated subpopulations through dispersal and colonization processes, and even colonize new favorable habitats. Without these landscape-wide metapopulation processes, certain species of carabids would go extinct (den Boer, 1990; Jordán et al., 2007). At the landscape-scale, fragmentation and connectivity play a major role in the survival of a species as metapopulation.

Local scale - habitat quality and ecology At the local scale, biotic and abiotic factors influence habitat quality and carabids abundance (Wachmann et al., 1995). Carabids can be divided into three groups of tolerance to habitat quality (Rainio and Niemelä, 2003; Eversham et al., 1996): geographically wide-ranged species present in the whole landscape (ubiquitous), species adapting to a wide range of habitats (eurytopic), and species that prove sensitive to a particular habitat quality (stenotopic). Different factors influencing habitat quality are mentioned in the literature: temperature (Thiele, 1977; Newell, 1986; Lövei and Sunderland, 1996; Rainio and Niemelä, 2003; Gobbi et al., 2007; Kotze et al., 2011; Viterbi et al., 2013); humidity (Newell, 1986; Lövei and Sunderland, 1996; Rainio and Niemelä, 2003; Kotze et al., 2011); light (Newell, 1986); presence of vegetation (Rainio and Niemelä, 2003; Viterbi et al., 2013); food conditions (Lövei and Sunderland, 1996; Rainio and Niemelä, 2003); presence of competitors (Lövei and Sunderland, 1996; Rainio and Niemelä, 2003). Among these factors, temperature emerges as a the key factor, along with humidity and presence of vegetation (and height of the herbaceous layer), and to a lesser extent, light. Activity, in the sense of mobility, seems to be most influenced by rainfall, temperature and seasonality (Parkinson and Marshall, 1998; Gobbi et al., 2007; Kotze et al., 2011).

Landscape-scale - fragmentation and connectivity At the landscape-scale, or large-scale, there seems to be a general agreement that fragmentation, the “*partitioning of a continuous habitat into many small remnants*” (Niemelä, 2001), and landscape connectivity strongly influence the presence of carabids (Petit and Burel, 1998; Parkinson and Marshall, 1998; Thiele, 1977; Niemelä, 2001; Rainio and Niemelä, 2003; Burel et al., 2004; Jopp and Reuter, 2005; Jordán et al., 2007; Matern et al., 2008; Tenan et al., 2016), as well as the maintenance of populations and subpopulations in heterogenous landscapes, although some argue that fragmentation does not seem to have an effect on carabids diversity (see e.g. (Davies and Margules, 1998)), and limited to no effect on certain species

(e.g. (Niemelä, 2001)). Fragmentation, connectivity and habitat availability operate at the landscape level (Burel et al., 2004). Subpopulations further away from sources of colonizers may struggle to maintain their population (Petit and Burel, 1998), such that the distribution of individuals in the landscape directly reflects the history (although lagged, i.e. extinction debt, adaptation lag (Petit and Burel, 1998; Jordán et al., 2007)), and the current state of the network (connectivity to suitable habitat) (Thiele, 1977; Petit and Burel, 1998; Rainio and Niemelä, 2003). Species organized as metapopulations, i.e. composed of subpopulations, and connected by dispersal, seem to have a better chance of maintaining their species in the landscape (Niemelä, 2001). These species, of course, take advantage of the landscape connectivity.

Landscape-scale - dispersal In the literature, carabid dispersal, defined as the “*undirected movement away from the habitat of origin*”, emerges as the key-component for maintenance of a population on the landscape level (Newell, 1986; den Boer, 1990; Lövei and Sunderland, 1996; Thomas et al., 1997; Niemelä, 2001; Jopp and Reuter, 2005; Matern et al., 2008). Without dispersal, the survival of these species would not be possible. The exchange of individuals, even doomed to go extinct in unsuitable habitat, is the main mechanism of the persistence of a metapopulation type of species in a landscape. Dispersal has two primary functions: to re-populate habitat with low presence, and to colonize empty habitats. The two mechanisms jointly ensure that a turnover of extinction and recolonization exists which guarantees the survival of the species in a heterogeneous landscape (Newell, 1986; den Boer, 1990). For carabids, dispersal is not only a mean to escape unsuitable habitat, as individuals are also observed to explore areas away from suitable habitat, even entering sites endowed with unfavorable conditions. In certain species, females even carry eggs on their back while dispersing (Lövei and Sunderland, 1996). The dispersal mechanism, driven by connectivity (den Boer, 1990; Thomas et al., 1997; Niemelä, 2001; Matern et al., 2008), is what maintains the population.

Dispersal occurs in two different types of movements: directed and undirected (or random) walk (Newell, 1986; Lövei and Sunderland, 1996). Directed walk occurs when an individual finds itself in the middle of unfavorable habitat, moving in a straight line as a strategy to move away as fast as possible from the unsuitable conditions until favorable habitat is found, where undirected walk is then again undergone. Undirected walk is mainly performed to find food in favorable habitat. Much greater distances are covered in directed walk. Carabids are believed to be able to cross long distances. Field studies report average movements between 2.5 and 10 meters per day (Thomas et al., 1997), while others go as far as up to 50 meters per day depending on species and individuals (Newell, 1986), mostly driven by hunger which drives higher mobility (directed walk).

The raster EO data (Fig. 3.3) have been selected based on the carabid ecology described in the

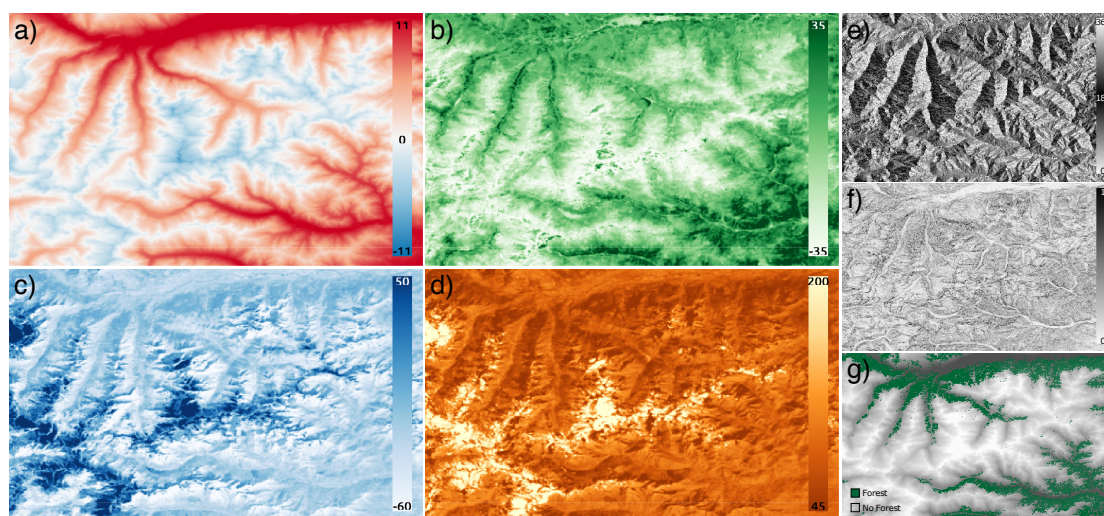


Figure 3.3 – EO data used in the study to define the species' fitness. Dynamic data with one map per year (2006 shown): a) Temperature; b) Greenness; c) Wetness; d) Brightness. Static data: e) Aspect; f) Slope; g) Forest presence. The resolution of all rasters is of 180 meters.

literature (see box 3.5) to best describe the carabids' niche, i.e. a multidimensional function describing the suitability of the habitat (Hutchinson, 1957; Pearman et al., 2008; Kearney and Porter, 2009; Thuiller et al., 2014). Carabids being sensitive to temperature (Kotze et al., 2011), this is the first environmental descriptor to be considered, with complementary topographic data (slope and aspect) which describe the local terrain characteristics. Additionally, carabids are influenced by humidity, light and the presence of vegetation (Kotze et al., 2011; Viterbi et al., 2013). In order to quantify these three factors, the tasseled cap indices are considered (Kauth and Thomas, 1976), which are a series of transformations (linear combinations) of the Landsat bands designed to best quantify the degree of greenness, wetness and brightness present in each pixel. Greenness is linked to the amount of vegetation present, wetness to humidity and brightness to solar radiation. Finally, forest presence has been mentioned multiple times as an important descriptor of carabid presence (Lövei and Sunderland, 1996; Kotze et al., 2011) and is therefore included in the list of explanatory variables.

This study highlights two challenges. First, in-situ data on carabids presence and abundance refers only to a small number of pixels within the modeling landscape. The species presence in the other cells has to be extrapolated through the model, adequately calibrated on the available in-situ data. Second, the sampling records are not continuous, with a four years gap between them. The calibration scheme has to account for this temporal gap, during which stochastic randomness can arise. The iterated filtering scheme (section 3.2.3.3) is designed to handle these constraints.

The methods are organized as follow: i) the acquisition and processing of raster EO data used as drivers of the metapopulation model are presented; ii) a preliminary data analysis is performed around the relation between in-situ and EO data; iii) the modeling framework is presented, describing the main steps followed to set up and calibrate the metapopulation model.

3.2.1 Raster data acquisition and processing

EO data derived from Landsat have an original resolution of 30 m, while those derived from the digital elevation model have a resolution of 90 m. These raster data have been upscaled to 180 meters resolution in order to match the dimension of the plots used for the in-situ observations. Data of each raster have been linearly scaled between -1 and 1 by selecting the minimum and maximum value over the considered period of time (2006-2013). This operation facilitates the interpretation of the parameters and improves the calibration process. This section provides more details about the data acquisition, source and, where needed, processing.

Temperature data

The temperature dataset originates from the E-OBS gridded dataset (Cornes et al., 2018), which has been downscaled to a 90 meter resolution using stochastic downscaling (D'Onofrio et al., 2014).

The temperature data originates from the E-OBS gridded dataset, a European land-only daily gridded dataset for precipitation and minimum, maximum, and mean surface air temperature at 25 km resolution starting in 1950 and regularly updated. The dataset builds on daily observations at more than 2,000-point locations available through the European Climate Assessment and Data set portal (ECA&D², Haylock et al. (2008)).

In mountain areas, meteo-climatic features show strong spatial variability over short distances, especially along elevational gradients. Reconstructing reliable elevation gradients of the important variables based on observations is challenging because weather stations are often sparse and do not offer adequate/homogeneous coverage. In particular, high elevations are often under-sampled or not monitored at all (Dodson and Marks, 1997).

The rate at which air cools with elevation may vary in the range between $-9.8^{\circ}\text{C} / \text{km}$ (i.e., the dry-air adiabatic lapse rate) for unsaturated air and $-4^{\circ}\text{C} / \text{km}$ (i.e., the saturated adiabatic lapse rate, Dodson and Marks (1997)) for saturated air. When air is saturated, the cooling rate for a rising air parcel is lower due to the release of latent heat by the condensation process.

²<http://eca.knmi.nl/>

Average temperature lapse rates show strong variability in relation to the climatic zone, as well as to the season. The highest values are reached in summer, over tropical deserts; the strongest negative rates are reached in winter over Siberia, Canada, and polar regions (Barry, 2008).

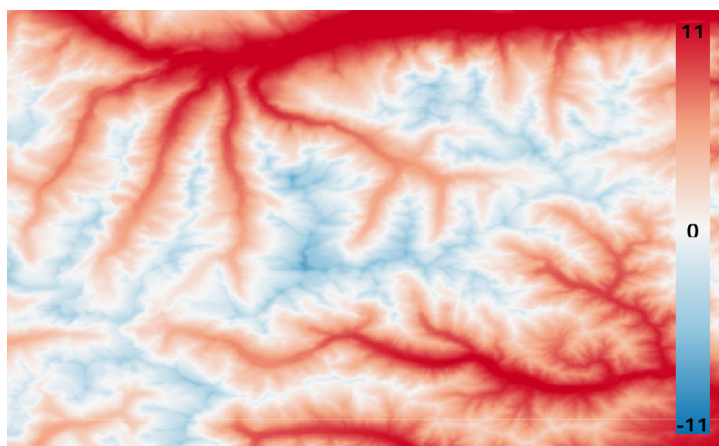


Figure 3.4 – Median temperature for the year 2006 in the domain of interest.

In order to reproduce the small-scale patterns of temperature, the E-OBS large-scale (25 km) fields is corrected for the elevation mismatch between their original smooth orography and the elevation in a fine-resolution (90 m) digital elevation model (DEM) by applying a simple correction based on the air temperature lapse rate. The correction has been applied on a monthly basis, employing monthly air temperature lapse rates observed in the Alpine region (Rolland (2003), see Table 3.1). The temperature downscaling software has been published here: <https://github.com/jhardenberg/RainFARM.jl>.

Table 3.1 – Monthly temperature lapse rates for the Alpine region. In [$^{\circ}\text{C (1000m)}^{-1}$] (based on Rolland (2003))

Month	Jan	Feb	Mar	Apr	May	Jun	Jul	Aug	Sep	Oct	Nov	Dec
Lapse Rate	4.5	5	5.8	6.2	6.5	6.5	6.5	6.5	6	5.5	5	4.5

For the purpose of this study, the median temperature over the study period (April to October) is then computed for each pixel thus obtaining one temperature map per year for from 2006 to 2012 (see Fig. 3.4 for an example of median temperature for the year 2006).

Tasseled Cap Indices

The aim of the EO data is to accurately represent the mean conditions on the ground during the sampling period, from April to October. For each tasseled cap product and for each study year, a composite image is created covering the region of interest and the time period.

The tasseled cap map is derived from Landsat 7 images, the only high-resolution satellite covering the whole study period from 2006 to 2013 (Pasetto et al., 2018). Only images covering the entire study region were considered, which results in 5 - 9 images per year. Landsat 7 has one major flaw, in that the Scan Line Corrector (SLC) failed on May 31 2003. All the satellite images taken after this period therefore contain gaps which need to be filled or compensated.

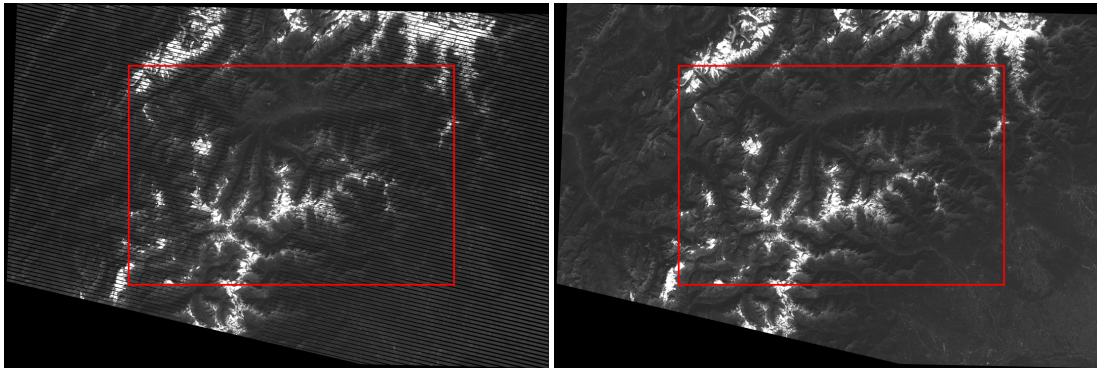


Figure 3.5 – Example of gap filling. Left: original Landsat 7 image acquired on October 10 2006, with gaps left from SLC failure. Right: same image after gap filling.

The goal is to generate one composite image per year. The composite image requires a distribution of values of each pixel in time, which requires one to fill the gaps for the years when gaps are found by computing the focal median in a given neighborhood for each missing pixels. This method is applied to all images covering the region of interest in the period (see Fig. 3.5 for an example of gap filling using this technique). Once the time-series of images

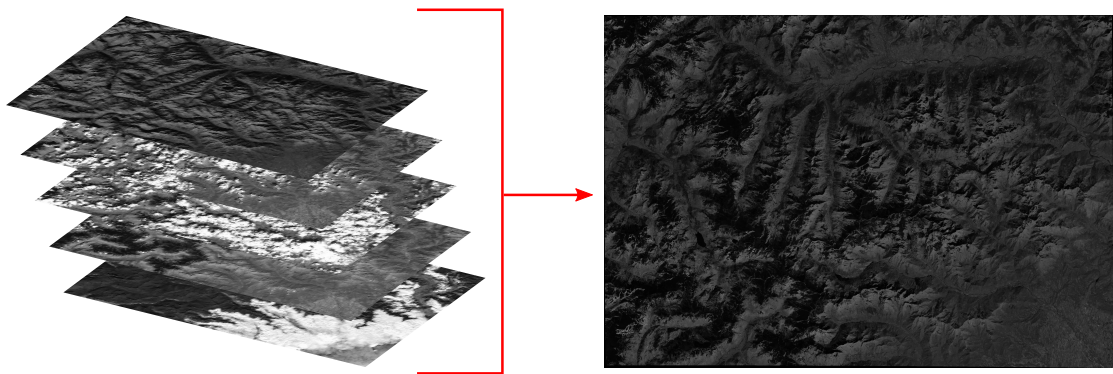


Figure 3.6 – Example of simple composite. From a series of images, the algorithm composes a median image taking into account the cloud score. The example shows the 'red' bands of a series of images of 2006 on the left, and the resulting composite 'red' band on the right.

is gap-filled, a composite image which accounts for cloud cover is created through Google

Earth Engine's simple-composite algorithm³. This algorithm computes a cloud score for each pixel, which is then used as weight when combining the images (the higher the cloud score, the less important the contribution of that pixel). The resulting image contains the weighted median value of the time series for each pixel and each band (see Fig. 3.6).

Finally, the three tasseled cap transformations are computed from the composite image.

Table 3.2 – Tasseled cap coefficients. Coefficients for the linear combination of bands for computing the different tasseled cap indexes (based on Huang et al. (2002)).

Index	Red	Green	Blue	NIR	SWIR1	SWIR2
Brightness	0.3561	0.3972	0.3904	0.6966	0.2286	0.1596
Greenness	-0.3344	-0.3544	-0.4556	0.6966	-0.0242	-0.2630
Wetness	0.2626	0.2141	0.0926	0.0656	-0.7629	-0.5388

The three indexes, brightness, greenness and wetness, are derived from a linear combination of the bands (table 3.2) contained in the Landsat 7 composite images (see Fig. 3.7).

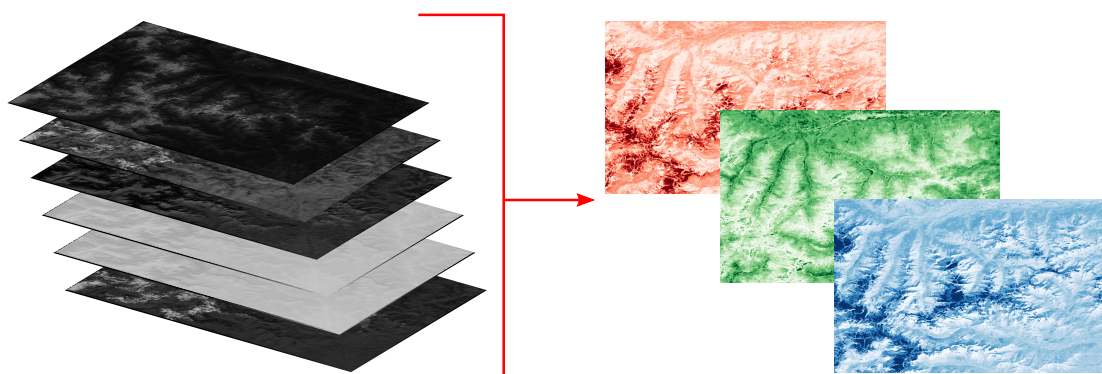


Figure 3.7 – Generation of tasseled cap from the composite image. Example of creation of the three tasseled cap products, brightness, greenness and wetness (right) from the bands of the composite image (left). The example shows the composite image of 2006.

This same process is applied for each year in order to obtain one image describing the median conditions in each pixel for each year.

Topographic data

All topographic data are generated from a digital elevation model (DEM) of 90 m resolution of the GPNP region. The DEM is extracted from the online Earth explorer tool, courtesy of the NASA EOSDIS Land Processes Distributed Active Archive Center (LP DAAC),

³<https://developers.google.com/earth-engine/landsat#simple-composite>

USGS/Earth Resources Observation and Science (EROS) Center, Sioux Falls, South Dakota (<https://Earthexplorer.usgs.gov/>). The DEM is used to generate slope and aspect, which is in turn divided in northness and eastness.

The slope is given as the largest difference in elevation from one cell to the eight neighbors. The slope is obtained for each pixel as⁴:

$$\text{slope} = \arctan \sqrt{\left(\frac{dz}{dx}\right)^2 + \left(\frac{dz}{dy}\right)^2} \quad (3.1)$$

with $\frac{dz}{dx}$ and $\frac{dz}{dy}$ the gradients to the neighboring pixels in the direction of x (the columns of the raster) and y (the rows of the raster) computed with the moving windows:

$$\frac{dz}{dx} : \frac{1}{8} \begin{bmatrix} -1 & 0 & 1 \\ -2 & 0 & 2 \\ -1 & 0 & 1 \end{bmatrix}, \frac{dz}{dy} : \frac{1}{8} \begin{bmatrix} -1 & -2 & -1 \\ 0 & 0 & 0 \\ 1 & 2 & 1 \end{bmatrix} \quad (3.2)$$

with the factors of the matrix multiplying the elevation values in the neighboring cells to obtain the difference gradient.

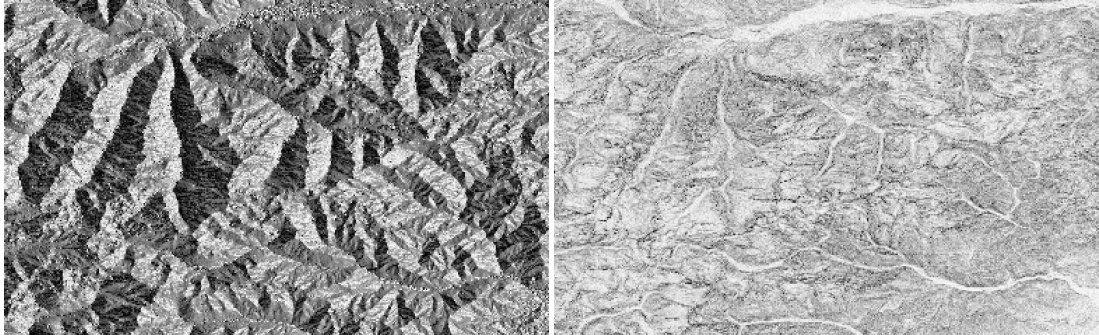


Figure 3.8 – Map of aspect and slope. Derived from the digital elevation model.

Aspect is defined as the cardinal direction of the maximum slope from one cell to its neighbors. Similarly to the slope, the aspect is obtained by using a moving window computing a gradient on its neighbors. The angle of the steepest slope is then computed from these informations⁵:

$$\text{aspect} = \arctan2\left(\frac{dz}{dy}, -\frac{dz}{dx}\right) \quad (3.3)$$

Aspect is then translated in eastness and northness, which are computed by applying the cosine and the sine respectively. This transformation ensures continues values bounded

⁴<http://webhelp.esri.com/arcgisdesktop/9.2/index.cfm?TopicName=How%20Slope%20works>

⁵<http://webhelp.esri.com/arcgisdesktop/9.2/index.cfm?TopicName=How%20Aspect%20works>

between -1 and 1.

Forest Cover

The forest cover in each pixel is here assigned to the final product estimated by the European Commission for the year 2006: <https://forest.jrc.ec.europa.eu/en/past-activities/forest-mapping/>. The classification proposes to fuse data from different sources (Land Cover Data from CORINE, EO data from MODIS) in order to produce maps of forest presence (Kempenneers et al., 2011).

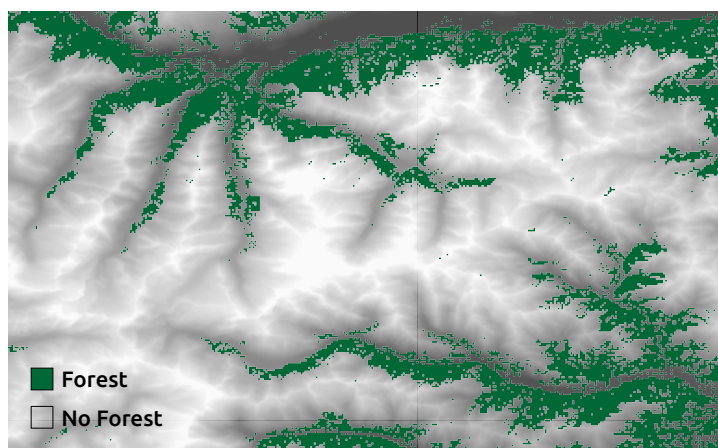


Figure 3.9 – Map of forest cover for the year 2006 in the domain of interest.

The product is only available for the year 2006, it is thus here assumed that the forest cover does not drastically change in the considered time span (8 years) and chosen resolution (180 meters).

3.2.2 Preliminary data analysis

Common data analysis operations have been performed in order to gain a basic understanding on the relations between the in-situ data and the environmental drivers, and about the dynamics of the species themselves.

3.2.2.1 In-Situ data

One of the first tasks is to understand the dynamics of the observed species in space and time. In order to do so, the number of times the species of interest are observed is plotted, respectively the ratio between the number of times observed and the number of times sampled in each plot per year (see Figs. 3.10 and 3.11). *Pterostichus flavofemoratus* was selected in order

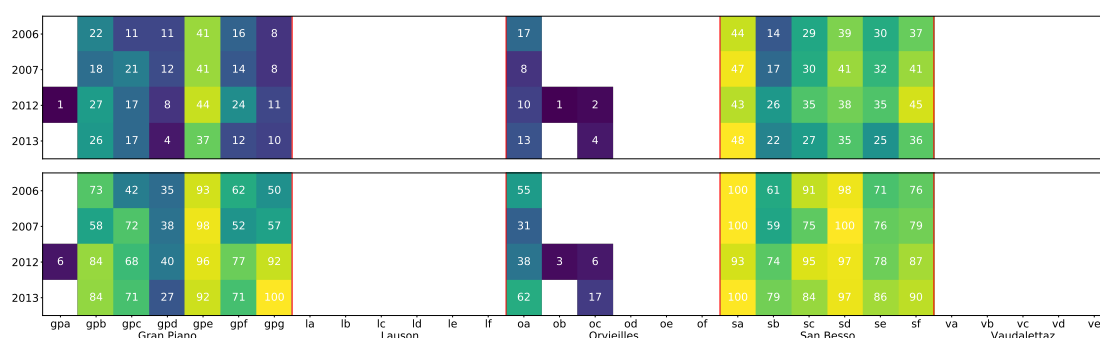


Figure 3.10 – Data per plot and year of *Pterostichus flavofemoratus*. Number of times *Pterostichus flavofemoratus* was observed (top) and ratio of number of times observed vs number of times sampled (in %)(bottom) in each plot and year. In each valley the plots are ordered from lowest to highest elevation. The blank pixels indicate that the species was not found in this plot/year.

to confront the modeling framework to a dynamically stable species. Fig. 3.10 shows how, albeit not present everywhere, the plots where the species is observed are relatively constant and consistent in presence over time. In the San Besso and Gran Piano valleys, the species is consistently present in all plots and years, with a gradient in presence to be observed in both valleys. In Orvieilles the species is present in the lowest plot and almost always absent in the other plots.

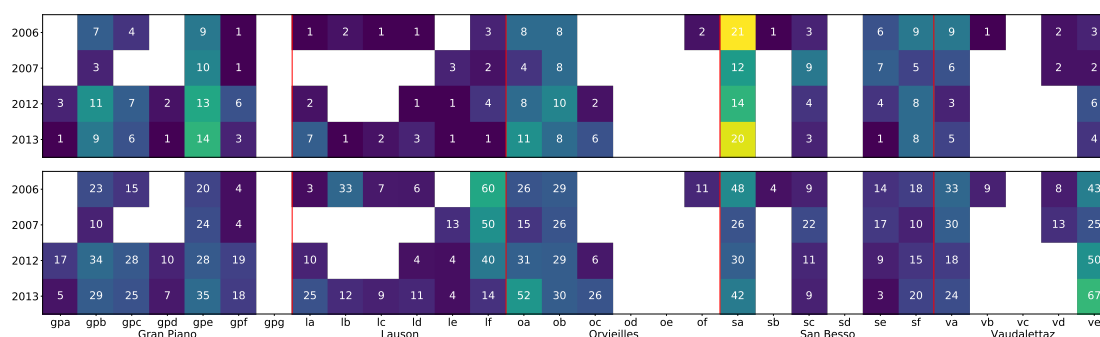


Figure 3.11 – Data per plot and year of *Carabus depressus*. Number of times *Carabus depressus* was observed (top) and ratio of number of times observed vs number of times sampled (in %)(bottom) in each plot and year. In each valley the plots are ordered from lowest to highest elevation. The blank pixels indicate that the species was not found in this plot/year.

If *Pterostichus flavofemoratus* was selected for its stability, *Carabus depressus* was selected because of its variations in time. The species is present in all valleys at times, appearing and disappearing between years. In Lauson for instance, the species has been observed in 2006, disappeared from most plots in 2007, slowly reappeared in 2012 to finally return in 2013. Additionally, the number of times the species was observed per year is constantly lower than

Pterostichus flavofemoratus. In the case of *Pterostichus flavofemoratus*, the number of times the species was observed is fairly high, and this permits a stronger reliance on the species' actual presence or absence. This is not the case for *Carabus depressus*, where the species was on average observed less than half of the times in each plot. This, of course, does not necessarily have anything to do with the accuracy of the sampling, since, as mentioned before, pitfall trapping measures activity-density.

3.2.2.2 EO data

In this modeling work EO data are fundamental to characterize the species habitat and its possible changes during the years of simulation.

Considering that the model is calibrated on the sampled data, it is first interesting to understand whether these plots are representative of the environmental conditions in the modeling regions, i.e. the GPNP. Fig. 3.12 shows the distribution of each variable and the relation between them, for each pixel value in the GPNP (in blue), and at the sampling points (in orange). The histograms in the diagonal show the orange and blue density plots seem to overlap in most cases, which implies that the data at the sampling points are a good representation of the whole park. In isolated cases, for instance for temperature when paired with most of the variables, the values recorded at the plots are not covering the whole range of values at the GPNP. This is especially evident when temperature is considered in relation with the tasseled cap indexes, where for lower temperatures the sampled values do not seem to be as well represented. A reasonable explanation for this fact is that lower temperatures are mostly found at higher elevations, where the sampling was not performed as few species survive above a certain altitude, especially in areas with year-long snow covers or on glaciers. In terms of correlations, the chosen variables seem to be independent of each other. Even in cases with relatively strong correlation (for example greenness vs temperature), the spread around the trend is very large suggesting that the combination of variables can have more explanatory power than the variable on its own. The relation between brightness and wetness depicts a particular behavior, having a positive correlation when considering the whole GPNP, but a negative one when only selecting the data in the sampled plots. To a lesser extent the inverse can be observed between greenness and brightness. By looking at the density plots of these variables, one might speculate that these behaviors are artifacts induced by outliers, as in the density plots most data seem to follow the same trend. The pairs plot indicates that all chosen variables are needed and that none could be discarded.

The relevance of each variable is further tested by performing a principal component analysis (PCA). PCA is technique widely adopted to understand the degree of correlation in a given data set (Janžekovič and Novak, 2012). PCA performs an transformation of the data matrix (i.e.

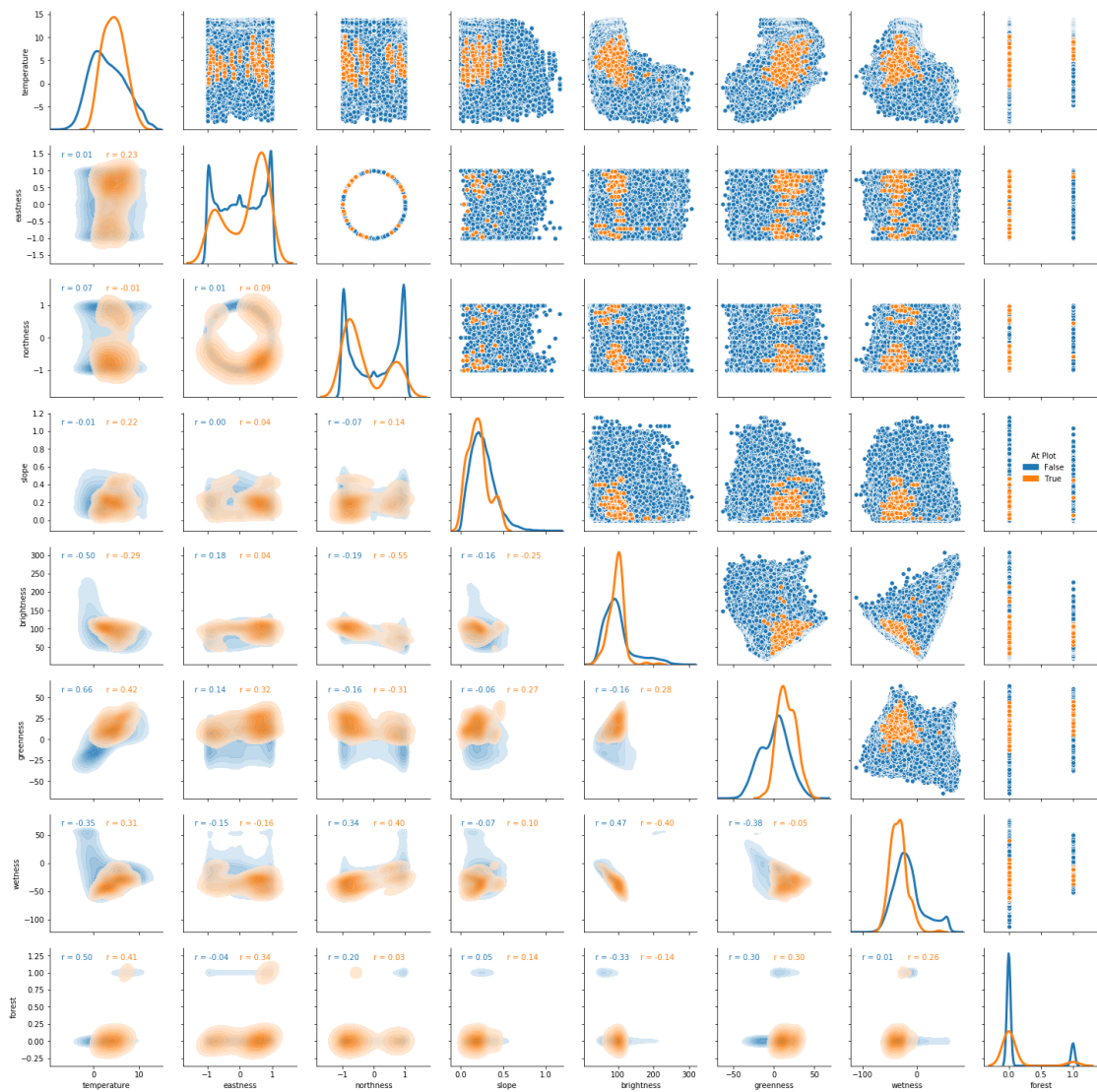


Figure 3.12 – Pairs plot of EO data. In the sampling plots (in orange), and in the whole GPNP (in blue). The diagonal shows the distribution of the variable. The upper grid shows the scatter plot of each variable plotted against all others. This permits to display the combined distribution of the variables, one pair at a time. The lower grid shows the density plots derived from the scatter plots, along the computed correlation coefficient. Note that there are two correlation coefficients, one for the data at the plot positions, and one in the whole GPNP.

here the EO data) into an orthogonal uncorrelated data set (Zuur et al., 2007; Janžekovič and Novak, 2012). The technique projects the data onto a base of orthogonal axes called principal components. The eigenvalues associated with each axis, or the fraction of the eigenvalue compared to the sum of all eigenvalues, determine the proportion of variance of the data explained by each axis. A large eigenvalue can be interpreted as a large correlation between

the data in the original data set. Apart from analyzing eigenvalues, the result of a PCA are usually interpreted by projecting the original data set onto the two first axes of the PCA (see Fig. 3.13). The original vectors corresponding to the original data set are then displayed in direction and magnitude relative to the degree to which they contribute to each axis, which permits to identify unnecessary covariates.

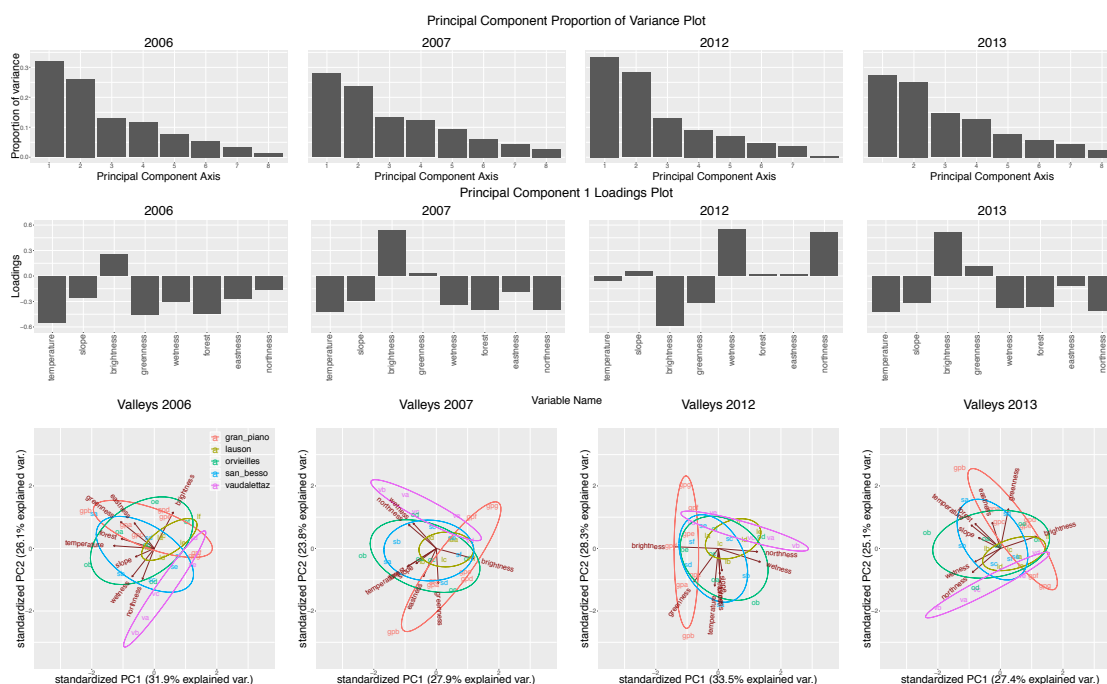


Figure 3.13 – Analysis of explanatory power of EO data. Proportion of variance explained by each principal component for each sampled year (top). Loadings plot showing the contribution of each variable to the first principal component for each sampled year (middle). Projection of the EO data on the two first principal component, and grouping of the data by valley (bottom).

Fig. 3.13 shows the outcome of one PCA per sampling year for the data in the sampling locations. In each year, the proportion of variance does not exceed 35%, indicating that the various EO axes can not be projected on a single strong component. In 2006 and 2012, the two first components seem to explain most of the data variance compared to the other years, but even in this case most axes are needed. This means that each variable is needed in order to accurately depict the environmental conditions in each plot, and no variable can be removed. The composition of the principal component (loadings plot) shows that most variables contribute roughly equally, with variations in time: for example in 2012 where tasseled cap data and northness explain most of the first component's variance.

From the projection of the variables on the two first axes (third line), a clear difference can be seen regarding the composition of the different valleys. Especially Gran Piano and Vaudalettaz

seem to differentiate themselves, with the others closer together. In all years, the variable axes are well distributed and rarely overlapping, which again confirms the importance of keeping all variables to characterize the habitat.

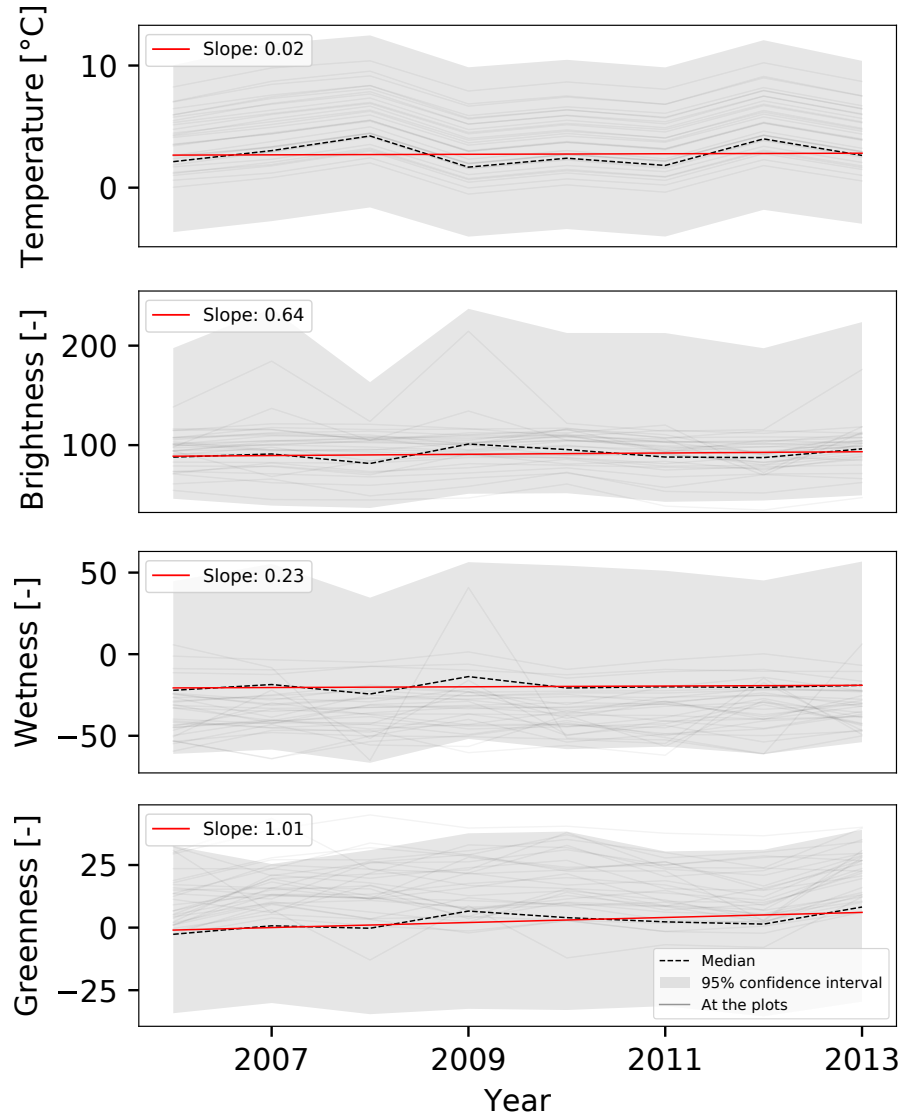


Figure 3.14 – Time series of the dynamic EO data. Median and 95% confidence interval of the time-varying variables, as well as the slope of the linear regression over the 8 years. The light grey lines show the the path for the variables at the plot locations.

Another important information is the trend and distribution of the variables in time. Over the GPNP domain the trends for the time-varying variables (temperature, wetness, brightness and greenness, Fig. 3.14) appear relatively stable. With a slope of 1.01, greenness is the variable with the strongest increasing trend, followed by brightness with 0.64. The trajectories of the plots (in grey in Fig. 3.14) show that temperature homogeneously follows the median, with most of the lines above the median. These homogeneous lines can be explained by the nature

of the temperature data, stemming from a downscaled model relying on elevation. The plot lines for the other variables are more heterogeneous. Wetness and brightness in the plots lie below the median, and greenness above. All of them follow the trend set by the slope of the distribution, meaning the trends observed in the plots are representative of the trends observed in the landscape.

3.2.2.3 Combined in-situ and EO data analysis

To model the two species of interest, the relation between the presence of the species in the landscape and the descriptors, here the EO data, has to be understood. Figs. 3.15 and 3.16 show the same PCA as in Fig. 3.13, but grouping the plots recording species presence (blue) or absence (orange) *Pterostichus flavofemoratus* and *Carabus depressus*, respectively. The PCA in

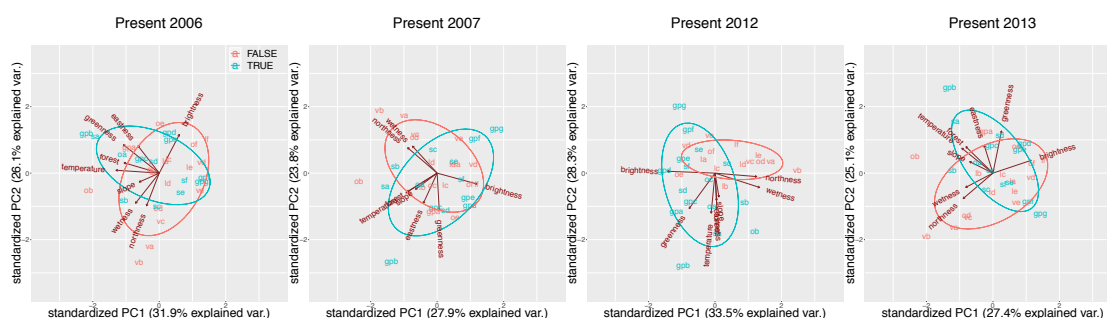


Figure 3.15 – Relation between *Pterostichus flavofemoratus* and EO data. Projection of the EO data on the two first principal component, and grouping of the data by presence/absence of the species *Pterostichus flavofemoratus*.

Fig. 3.15 shows that the covariates can not entirely differentiate the plots with presence from the plots with absence, which was to be expected as two first axes only explain around 60% of the variance each year. Still, certain plots are not overlapping, especially in 2012. For these plots, the prediction of presence or absence might be easier solely based on fitting the EO data to the in-situ data.

The PCA in Fig. 3.16 shows a relatively strong overlapping of the presence and absence group. Given the relatively similar EO conditions for present and absent plots, spatial dynamics have to be considered in order to explain the spatial distribution of the species, solely relying on EO is not enough.

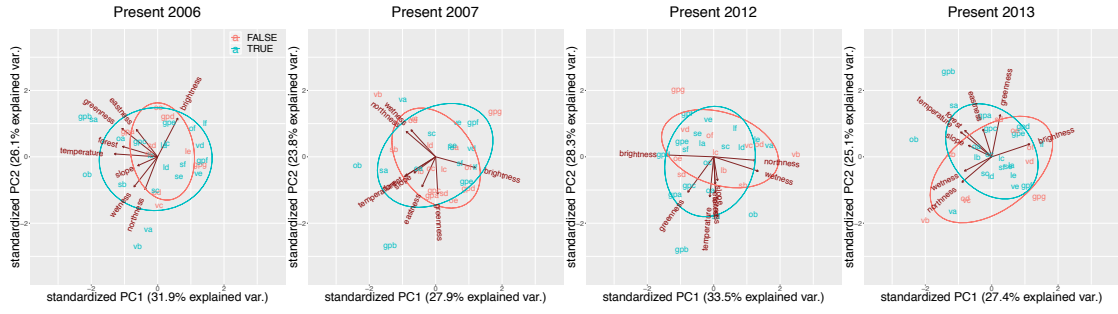


Figure 3.16 – Relation between *Carabus depressus* and EO data. Projection of the EO data on the two first principal component, and grouping of the data by presence/absence of the species *Carabus depressus*.

3.2.3 Modeling framework

3.2.3.1 Metapopulation Model

Building on the results of the previous chapter, a spatially-explicit patch occupancy model is employed to simulate the presence of the species in the landscape (c.f. box 3.6 as a reminder).

Box 3.6 – SPOM - reminder As detailed earlier in box 2.1, in this box the basic features of the stochastic metapopulation model are recalled.

SPOM is a Markov chain, where, for each cell i and simulation time t , the probabilities of colonization and extinction events are computed from the current presence $W_i(t)$:

$$\begin{aligned} P_{C,i}(t + \Delta t) &= P[W_i(t + \Delta t) = 1 | W_i(t) = 0] \\ &= 1 - \exp(-C_i(t) \cdot \Delta t), \end{aligned} \quad (3.4)$$

$$\begin{aligned} P_{E,i}(t + \Delta t) &= P[W_i(t + \Delta t) = 0 | W_i(t) = 1] \\ &= 1 - \exp(-E_i(t) \cdot \Delta t), \end{aligned} \quad (3.5)$$

where Δt is the simulation time step and $E_i(t)$ and $C_i(t)$ are the extinction and colonization rates (with dimension T^{-1}) for cell i at time t . The colonization and extinction mechanisms are directly related to a fitness function, $f_i(t)$ (see below), which measures the suitability of patch i for the species. The local extinction rate on a cell i is inversely proportional to the fitness, i.e., $E_i(t) = e/f_i(t)$, where e is the extinction constant. The colonization rate of an unoccupied cell is driven by the sum of the contributions from surrounding occupied cells:

$$C_i(t) = c \sum_{j \neq i} W_j(t) \frac{\exp(-d_{ij}/D)}{2\pi D^2} f_j(t), \quad (3.6)$$

where d_{ij} is the distance between cells i and j , D the dispersal distance and c the colonization constant.

Although the core of the model remains the same, certain changes are made to it as elaborated below, notably regarding the definition of the species' fitness.

Fitness The species suitability at cell i and time t is represented by the following fitness function $f_i(t)$ inspired by the non-linear functions adopted in GLMs (Purves et al., 2007; García-Valdés et al., 2013):

$$f_i(t) = \frac{1}{1 + \exp\left(-\alpha_0 - \sum_j \beta_j x_i^j(t)\right)} \in (0, 1), \quad (3.7)$$

where $x_i^j(t)$ is the value of the EO cofactor j at position i and time t , α_0 the intercept and β_j the parameter associated with the EO cofactor j .

3.2.3.2 Initial Distribution Estimation

Given the discrete nature of spatial sampling, the carabid's initial (2006) distribution in the GPNP needs to be estimated, for which a SDM is used. SDMs are a range of statistical models used to assess the probability of presence of a focus species in a landscape given in-situ data, and often, EO-data (Guisan and Zimmermann, 2000; Guisan and Thuiller, 2005).

Here, a subtype of SDM, a Generalized Linear Model (GLM) is used (Yee, 2013; Guisan et al., 2017). A GLM attempts to model the presence and absence data by linearly combining explanatory variables (Fox, 2015):

$$\eta_i = \alpha'_0 + \sum_j \beta'_j x_i^j. \quad (3.8)$$

where α'_0 and β'_j are the GLM's parameters. A logit link function is then used to link the linear predictor (η_i) to the probability of presence (μ_i) assuming a binomial distribution (Fox, 2015):

$$g(\mu_i) = \eta_i, \quad (3.9a)$$

$$\mu_i = g^{-1}(\eta_i) = \frac{1}{1 + \exp(-\eta_i)}. \quad (3.9b)$$

The species presence is estimated based on the 2006 sampled vs observed carabids data and the EO data. The sampled and observed data describe the number of times a species was sampled in a plot, versus the number of times it was actually found in the given plot, and

permits to use a binomial distribution for the calibration of the probability of presence:

$$P(k_i|n_i, \mu_i) = \binom{n_i}{k_i} \mu_i^{k_i} (1 - \mu_i)^{n_i - k_i}, \quad (3.10)$$

where μ is the probability of the species predicted by the GLM, k the number of times the species was observed in the plot in n times the plot was sampled, and $n - k$ the number of times the plot was found empty. The values of α'_0 and β'_j are calibrated by maximum likelihood estimation (Yee, 2013; Fox, 2015).

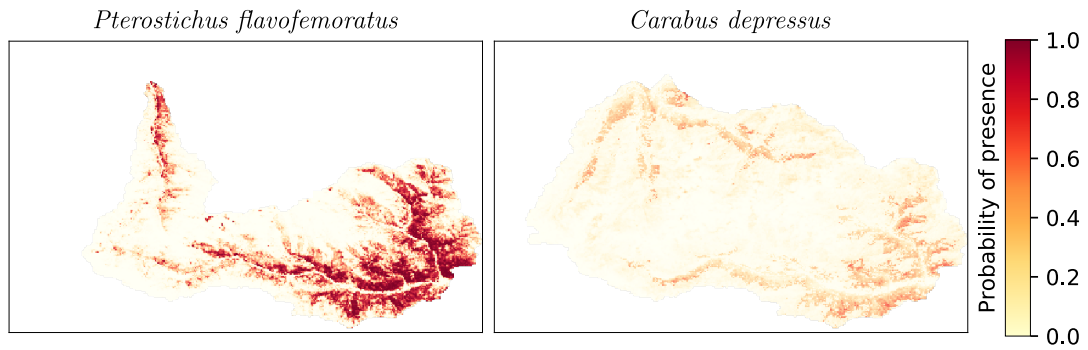


Figure 3.17 – Initial probability of presence. Estimated by a species distribution model for two species of interest *Pterostichus flavofemoratus* and *Carabus depressus*.

The hypothesis is made here that the absence of a species from a valley is explained by the species not having colonized that valley rather than by the differences in niche definition, given the similar EO data in the different sampling sites (see section 3.2.2.3, PCA). The pixels in the valleys where no individuals were observed for the species during the whole year are thus set to have probability zero. Once the GLM calibrated, the output probability of presence is used (Fig. 3.17). Random initial occupation landscapes are generated by sampling the produced probability of presence. These initial occupancy maps are then further refined through the iterated filtering algorithm (see below) and spin-up period, as it is important to ensure that the initial presence is relaxed around the quasi-equilibrium imposed by the metapopulation parameters (Moilanen, 1999).

Spin-up period Starting from a certain spatial configuration, a dynamic model such as SPOM is almost always far from equilibrium, and needs to be relaxed to reach a quasi-equilibrium. In SPOM, this is the case while more extinction than colonization events occur, or vice-versa (Moilanen, 2004). From this initial configuration, it is possible to tend to a pseudo-steady state, a situation where the occupancy oscillates around a stable state (Moilanen, 1999). This phase, which requires to run a certain number of Markov steps (equation 3.4), is called the spin-up

period. The model is simply run without changing the parameters nor the cofactors until the simulations stabilize. This can take a certain time depending on the parameter values, especially the values of c and e . When keeping the ratio between c and e constant, the larger their values, the shorter the spin-up period. While small values of c and e will require long spin-up periods, large values will tend faster to this equilibrium.

Note that incorporating this spin-up period in the model is, given that the calibration is made against dynamic EO-data, not equivalent to making the equilibrium assumption (Moilanen, 2004), but merely a necessary step in order to ascertain that the observed trends don't stem from a modeling bias, but rather from the simulation stochasticity and changes in explanatory variables.

Here, starting from an initial distribution, the spin-up is run at each iteration of the calibration in order to make sure the model oscillates around the quasi-equilibrium state.

3.2.3.3 Iterated filtering algorithm

The iterated filtering (IF) algorithm has been proposed as a way to calibrate partially observed Markov processes (POMP, Ionides et al. (2015)) using a frequentist approach based on maximum likelihood estimation. Here, algorithm IF2 is used based on Ionides et al. (2015). IF2 proposes to search for the maximum likelihood by spawning a given number of particles which all perform the Markov process multiple times (called iterations, Fig. 3.18). Each particle is associated with certain values for each parameter. Before each step of the Markov process, the parameters are perturbed, and then the step performed. After the step, if in-situ data is available, a new set of particles is drawn by randomly sampling from the pool of particles based on a weighted distribution proportional to the likelihood, meaning one particle can be selected multiple times if it outperforms the other particles, or by randomness (Arulampalam et al., 2002). A measurement model then links the model states to the observations (see below). The process then goes on by perturbing the parameters and running the Markov step.

The perturbation of the parameters is done by sampling from a gaussian distribution around the values of the parameters (transformation of the sampling space can be performed for only positive parameters (log), bounded parameters (logistic), etc.) and with a standard deviation which decreases in time to ensure the convergence of the parameters. The convergence of IF2 to the MLE has been proven in Ionides et al. (2015).

IF2 applied to SPOM IF2 is here sought to be applied to SPOM. A likelihood function is proposed which takes advantage of the in-situ data structure, capitalizing on the yearly sampled vs observed data. A binomial function is used with a probability depending on the model

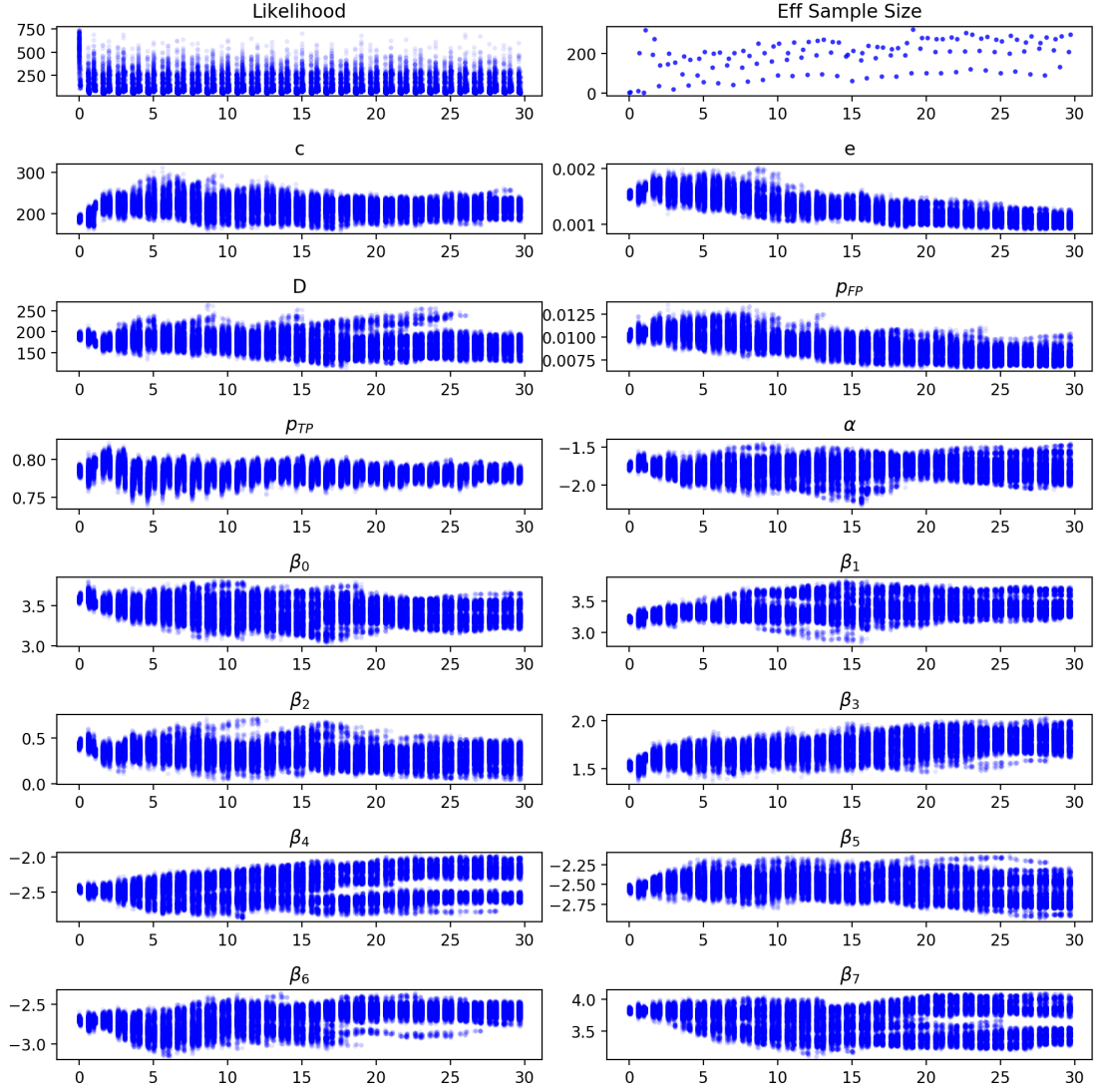


Figure 3.18 – Example of 30 iterations of IF for the species *Pterostichus flavofemoratus*.

This example shows the algorithm after three IF layers. The graph on the top left shows the negative log-likelihood, and on the top right the effective sample size which measures the relative importance of each particle. The effective sample size is computed as (Arulampalam et al., 2002) $\hat{N}_{\text{eff}}^{\text{ens}} = \frac{1}{\sum_{i=1}^{N^{\text{ens}}} (\omega_i^2)}$, with N^{ens} the number of particles, and ω_i the weight of particle i computed from the likelihoods. To ensure a correct calibration process, it is of advantage to have large effective sample size values, which ensures no particle depletion, a phenomenon where all but a few particles have very small weights and are discarded at each filtering. The remaining plots display the values of the parameters at each step and iteration.

prediction and integrating imperfect detection:

$$\mathcal{L}(\theta)(t) = \prod_i \begin{cases} B(n_i(t), k_i(t), p_{FP}) & \text{if } w_i(t) = 0 \\ B(n_i(t), k_i(t), p_{TP}) & \text{if } w_i(t) = 1 \end{cases} \quad (3.11a)$$

$$= \prod_i (1 - w_i(t)) B(n_i(t), k_i(t), p_{FP}) + w_i(t) B(n_i(t), k_i(t), p_{TP}) \quad (3.11b)$$

with θ the parameters of the model, $B(n_i(t), k_i(t), p_{FP})$ the binomial distribution as described above at time t , $w_i(t)$ the state of the model at time t and in pixel i and p_{FP}, p_{TP} the species miss-identification (probability of false positive) and the detection probabilities (probability of true positive) respectively. Note that $1 - p_{FP}$ corresponds to p_{TN} , the probability of true negative, hence the probability of correctly measuring the absence of the species, and $1 - p_{TP}$ corresponds to p_{FN} , the probability of missing the species in the sampling. The likelihood is computed in each pixel where in-situ data is available (one pixel per plot). The two probabilities described here are considered as two parameters calibrated along the other parameters of the model.

As mentioned above, each particle corresponds to a set of parameter values and model states in each pixel. The initial parameter values are drawn by means of latin hypercube sampling (LHS, McKay et al. (1977)). LHS is a technique designed to randomly sample from a multi-dimensional distribution, but which, unlike the uniform random sampling, takes into consideration the previously sampled values. This technique improves the sampling efficiency of the solution space. For each initial value drawn via LHS, the calibration is performed.

The initial occupancy of the landscape after the spin-up period is here added to the particle definition. At the beginning of each iteration, for each particle the spin-up is run with the initial presence contained in each particle, and the final state is conserved for the next iteration. Since the parameters change at each step and iteration, it is important to re-run the spin-up at the beginning of the iteration to ensure the pseudo-equilibrium. Since the parameters change slowly over the calibration process, the final state of the previous iteration is already close to the new equilibrium imposed by the sampled parameters. This state is therefore used as initial occupancy for the new parameters and spin-up, which final state then becomes the new initial presence for the particle. To summarize, each particle contains: parameter values $\Theta(D, c, e, \alpha_0, \beta_j)$ and an initial presence W_0 .

For each species, a broad calibration process is first performed which takes into account the length of the spin-up period. Since the spin-up period is dependent on the scale of c and e , and as the scale of these two parameters influences the speed of the process after the spin-up, the different species require different spin-up length. The optimal spin-up period is chosen based on the likelihood and the effective sample size which measures the relative importance of each particle. The effective sample size is computed as (Arulampalam et al., 2002) $\hat{N}_{\text{eff}}^{\text{ens}} = \frac{1}{\sum_{i=1}^{N^{\text{ens}}} (\omega_i^2)}$, with N^{ens} the number of particles, and ω_i the weight of particle i computed from the likelihoods. Small values of effective sample size indicate that one particle is absorbing all others, and the parameter space is not efficiently sampled. Only spin-up periods yielding an acceptable effective sample size are considered.

Once the spin-up length determined, a first LHS is performed on a broad range for each

parameter value. The fitness parameters are sampled in the interval $[-4, 4]$, D in $[50, 500]$, c in $[100, 500]$ and e in $[10^{-3}, 10^{-2}]$ (or for c and e a factor of these values depending on the spin-up period). A second LHS is then performed around the parameter values with the best likelihood values from the previous sampling. The final calibrated values are the values generated from IF with the best likelihood.

The calibration process is summarized here:

- 1 The initial spatial distribution of the species in the landscape is determined:
 - a. The initial probability of presence is computed via GLM based on in-situ and EO data from 2006.
 - b. For each of the N^{ens} particles of the IF a presence-absence map is drawn from the probability map ($w_0^{1..N}$).
- 2 The first phase is designed to determine the spin up period:
 - a. A number of initial parameter guesses are drawn via LHS (θ_0), including different spin up periods and scales of c and e .
 - b. For each LHS guess, IF2 is performed.
 - c. The process with the best likelihood and effective sample size is selected, and determines the spin up period for the species.
- 3 The second phase is designed to narrow the range of the parameters:
 - a. Keeping the scale of c and e fixed and fixing the length of the spin up period, a number of new parameter guesses are drawn from LHS with the initial broad range of parameters.
 - b. For each guess, IF2 is performed.
 - c. The guess with the best likelihood is kept.
- 4 The last phase is designed to select the optimal values of the parameters around the already narrowed parameters:
 - a. A final LHS drawing is performed around the values of the best performing guess.
 - b. For each guess, IF2 is performed.
 - c. The final parameter set is taken from the maximum likelihood over all guesses.

The IF2 algorithm applied to SPOM reads as follow (adapted from Ionides et al. (2015)):

Inputs:

- Number of iterations M
- Number of iterations without propagation M'
- Number of particles N^{ens}
- Initial spatial species presence for each particle $w_0^1, \dots, w_0^{N^{\text{ens}}}$
- LHS parameter guess θ_0
- In-situ data $Y_{2006,2007,2012,2013}^*$, with Y^* containing the observations k and n for the year.
- EO data $X_{2006...2012}^j$

For $m = 0$ to M :

Propagate parameters with the density function h and perturbation sequence σ_m :

$\Theta_{1..N^{\text{ens}}} \sim h_{1..N^{\text{ens}}}(\theta | \Theta_{1..N}; \sigma_m)$

```

Compute fitness function (equation 3.7)
Perform the spin up with EO data  $X_{2006}^j$  to produce presence  $w_{2006}^1, \dots, w_{2006}^{N^{ens}}$ 
Set new initial presence:  $w_0^j = w_{2006}^j, j = 1, \dots, N^{ens}$ 
Compute likelihood based on in-situ data of 2006:  $\mathcal{L}^j(\theta^j | Y_{2006}^*, w_t^j), j = 1, \dots, N^{ens}$  (see
equation 3.11)
Filter particles based on weight of each particle:  $w_j = \frac{\mathcal{L}^j}{\sum_n^{N^{ens}} \mathcal{L}^n}$  (see algorithm 2 in Arulampalam et al. (2002))
For  $y = 2006$  to 2012:
    Propagate parameters:  $\Theta_j \sim h_j(\theta | \Theta_j; \sigma_m), j = 1, \dots, N^{ens}$ 
    Compute fitness function
    Perform Markov step with EO data of year  $y$   $X_y^j$  to produce presence  $w_{y+1}^j$  (see section
    3.2.3.1)
    If  $(y+1)$  is in in-situ:
        Compute likelihood based on in-situ data of  $(y+1)$ :  $\mathcal{L}^j(\theta^j | Y_{2006}^*, w_t^j)$ 
        Filter particles based on weights
    end if
end for
end for
Select best parameter set based on maximum likelihood, set parameters in all particles to the
best particle.
For  $m = 0$  to  $M'$ :
    Perform the same operations but without parameter propagation, compute average likelihood
    over the iterations.
end for
Outputs: - Calibrated parameters
           - Calibrated initial presence
           - Associated average likelihood
    
```

With the calibrated parameters and initial occupancy, the model is then run without filtering and parameter propagation in order to generate the species distribution. This simulation is run with 480 independent repetitions to obtain occupancy distributions for each pixel.

3.3 Results

The results presented here show the output of the model for the two species of interest, the *Pterostichus flavofemoratus* and *Carabus depressus*, simulated with the calibrated parameters (see table 3.3), result of the latin hypercube sampling and layers of the filtering algorithm (see section 3.2.3.3). The spin up periods for *Pterostichus flavofemoratus* and *Carabus depressus* have been set 400 and 120 steps, respectively. The uneven durations are due to the differences between the calibrated colonization and extinction rates of the two species resulting in different ecological timescales.

Table 3.3 – Calibrated parameter values for the two species of interest. The first row consists in the parameters meant for the relation between the measures and the model, and the main parameters of the metapopulation model. The second and third row shows the parameters generating the fitness function. The second row shows the base fitness value (α_0) and the parameters multiplying a time-varying covariate, and the third row shows the parameters for the static explanatory variables.

	p_{TP}	p_{FP}	c	e	D
<i>Pterostichus flavofemoratus</i>	79%	1%	187.62	$1.53 \cdot 10^{-3}$	189.91
<i>Carabus depressus</i>	63%	1%	733.06	$1.205 \cdot 10^{-2}$	173.00
	α_0	$\beta_{\text{Temperature}}$	β_{Wetness}	$\beta_{\text{Brightness}}$	$\beta_{\text{Greenness}}$
	2.06	3.57	3.21	0.42	1.54
	3.36	-0.52	-0.28	0.80	-3.61
	β_{Eastness}	$\beta_{\text{Northness}}$	β_{Slope}	β_{Forest}	
	-2.44	-2.54	-2.68	-3.82	
	-2.68	-3.99	1.43	0.08	

3.3.1 *Pterostichus flavofemoratus*

Figs. 3.19 shows the simulated average occupancy of *Pterostichus flavofemoratus* in the landscape for each year, computed from 480 repetitions. To better appreciate the temporal changes, the relative difference in average occupancy in each cell computed as the difference between two consecutive years relative to the year before is highlighted in Fig. 3.20.

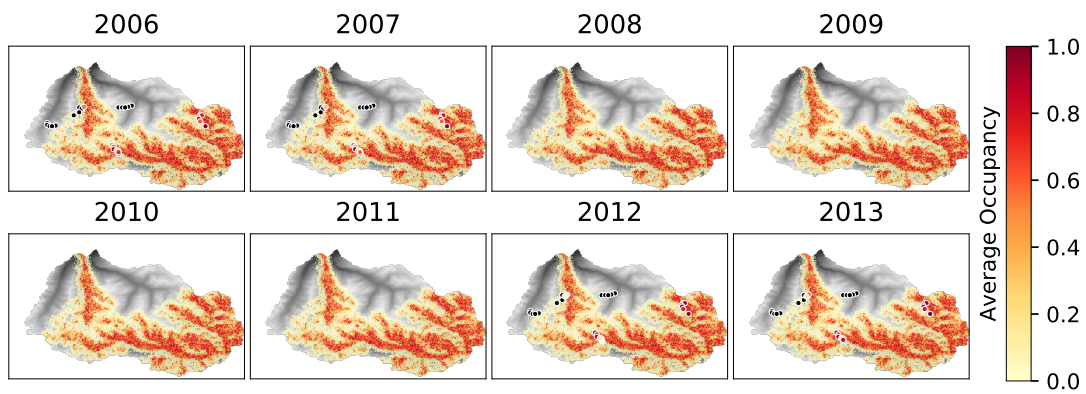


Figure 3.19 – Average occupancy of *Pterostichus flavofemoratus* in time. Output of the filtering algorithm for the calibrated parameters: average occupancy of *Pterostichus flavofemoratus* in time. For the sampling years (2006, 2007, 2012 and 2013) the ratio of number of times a species was observed vs the number of times it was sampled is displayed at the sampling location with a bullet colored using the displayed color scheme.

The modeled average occupancy of *Pterostichus flavofemoratus* (Fig. 3.19) well match the in-situ observed ratio at most of the plots. This fact suggests that the calibration process identified a parameter combination that results in an appropriate fitness function and metapopulation dynamics.

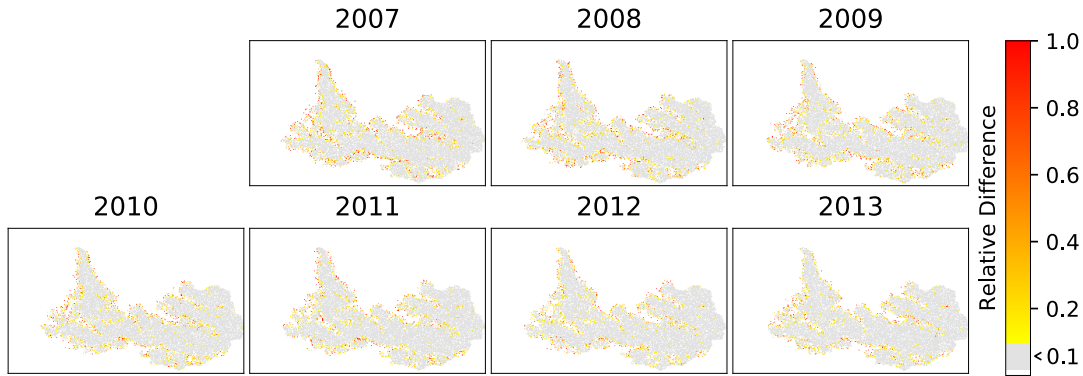


Figure 3.20 – Relative difference in average occupancy for *Pterostichus flavofemoratus*.

The relative difference is computed from one year to the other as $|\hat{x}_y - \hat{x}_{y-1}| / \hat{x}_{y-1}$ which highlights large changes compared to the initial value. The color scale is shown in white where no change occur, grey where less than 10% of difference is observed, and a linear gradient capped at 100% for values above.

The occupancy in the landscape of *Pterostichus flavofemoratus* appears to be relatively stable, although with a slight increase over time (see Fig. 3.23). This is evident also from Fig. 3.20, where the core of the species presence does not change in time, and most of the variations in occupancy occur at the edge of this stable core.

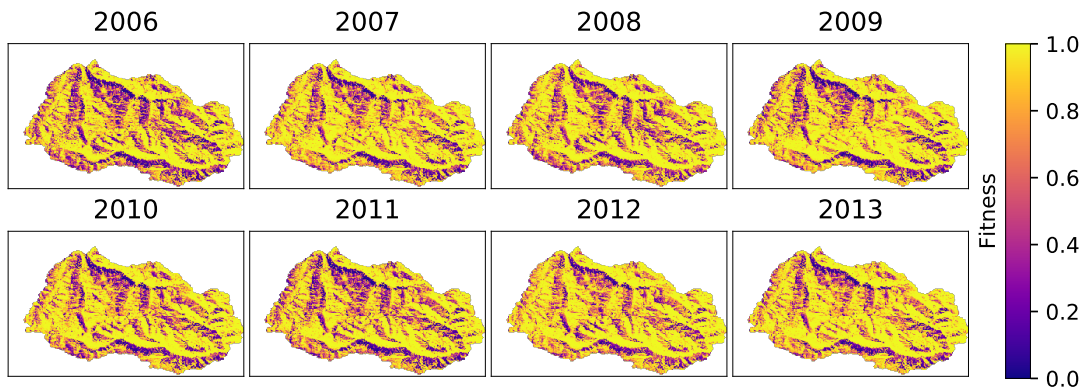


Figure 3.21 – Fitness of *Pterostichus flavofemoratus* in the GPNP. Computed from the calibrated parameters (equation 3.7, parameters shown in table 3.3) and the EO data for the simulated years.

To better understand the cause of the temporal changes in presence, Figs. 3.21 and 3.22 show

the fitness for *Pterostichus flavofemoratus* at each year and its temporal variations, which are only due to the changes in the co-factors. The variations in the *Pterostichus flavofemoratus* presence are, to a certain extent, related to the variations in fitness which are higher at the border of the occupied area (compare Figs. 3.22 and 3.20). Another important process that generates variations in presence is related to the changes in colonization pressure from surrounding occupied cells, which might lead to extinction if it does not counter the extinction process.

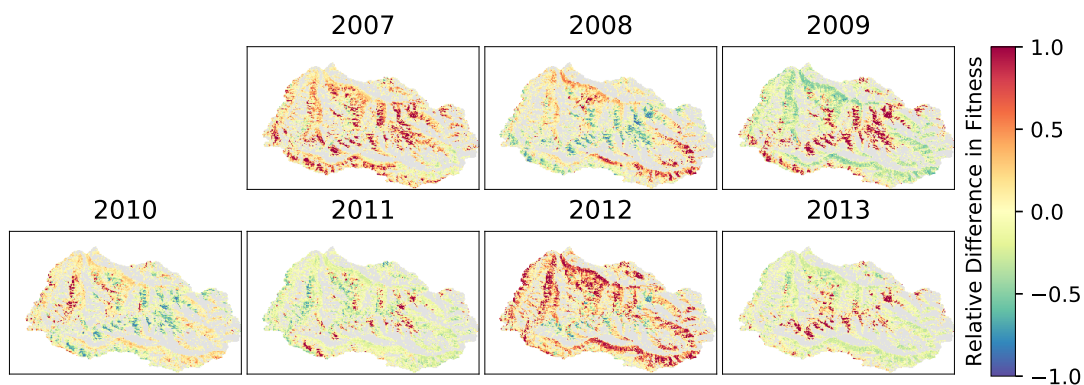


Figure 3.22 – Relative change in fitness value of *Pterostichus flavofemoratus* from one year to the other.

The fitness of the species appears to be generally high in large parts of the park (see Fig. 3.21). The logit-like fitness used here (equation 3.7), permits to understand the contribution of each parameter to the overall fitness (Hegel et al., 2010), where the change in the value of the parameter reflects the change in fitness. As all cofactors have been feature scaled (see section 3.2.1), a unit change in the parameter directly influences the change in the contribution of the covariate to the fitness relative to the other explanatory variables. For *Pterostichus flavofemoratus*, most of the variables contribute to the fitness, although brightness and greenness to a lesser extent. Temperature, wetness and forest presence contribute the most, but greenness eastness, northness and slope are not to be neglected. As eastness, northness, slope and forest presence do not vary in time, these factors, along with the intercept (α_0) represent the base fitness of the species, which is then modified in time by the time-dependent covariates. In time, a general increasing trend in the fitness can be observed, which could in part explain the trend in increasing number of occupied cells observed in Fig. 3.23. The variation of the fitness in time is to relate to the high positive values of the parameters multiplying temperature, brightness and greenness.

Fig. 3.24 shows a comparison between the modeled and in-situ number of times a species was observed in each plot (k) and year. The modeled k is derived by drawing 1'000 samples from the binomial distribution $P(k = K|m) = (m = 1)B(p_{TP}, n) + (m = 0)B(p_{FP}, n)$ for each particle,

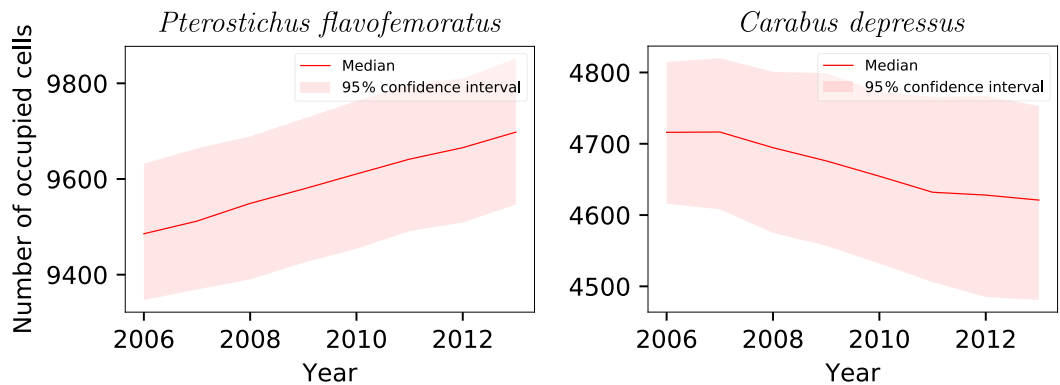


Figure 3.23 – Median occupancy of *Pterostichus flavofemoratus* and *Carabus depressus* in time. Time series of the median number of occupied cells with confidence interval for the two species of interest.

plot and year (with the values of p_{TP} and p_{FP} displayed in table 3.3). The displayed median k and the confidence interval are computed from the joint distribution. The modeled k of

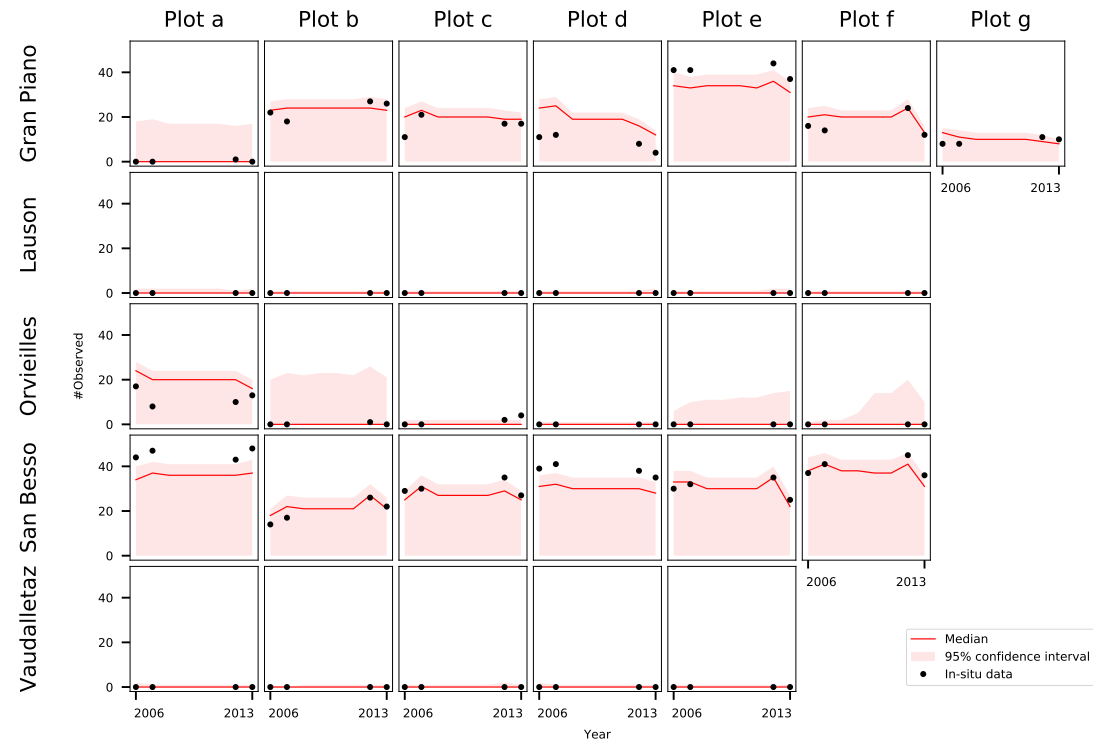


Figure 3.24 – Results at plot level for *Pterostichus flavofemoratus*. Modeled (red with confidence interval) and in-situ (black dots) number of times *Pterostichus flavofemoratus* was observed (k) in each plot and year. The modeled k is generated by sampling from a binomial distribution $P(k = K|m) = (m = 1)B(p_{TP}, n) + (m = 0)B(p_{FP}, n)$. For the years 2008 to 2011 the average n is taken.

Pterostichus flavofemoratus encapsulates the in-situ data k within its confidence interval in almost all of the plots. Plots b to g in the valley of Orvieilles (where little to no traps have been sampled positively) appear to have a large confidence interval overestimating the presence, but the median is close to the in-situ data. The median k in the plots in the valleys of Gran Piano and San Besso follows well the in-situ data, showing a good match in increasing and decreasing trends, although slightly underestimated in some plots.

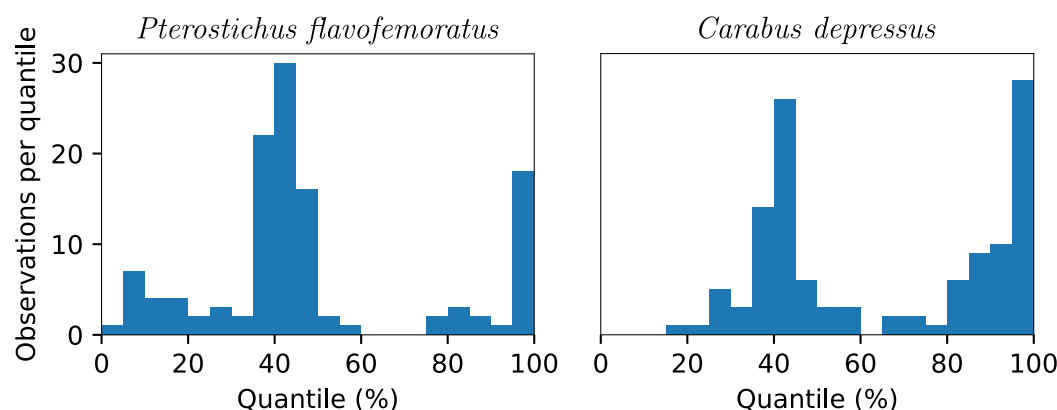


Figure 3.25 – Quantiles histogram. Histogram of the quantiles in which the in-situ data are located within the model result (see Figs. 3.24 and 3.30). Values on the right side of the 50% mark show where the model underestimates the occupancy, and on the left side where the model overestimates the chances of occupancy.

This is confirmed in Fig. 3.25, which shows the distribution of the data within the modeled confidence interval as displayed in Fig. 3.24. Most of the data are around the 50% quantile, with 88.3% of the observations within 95% of the model envelope. The highest source of deviation from the median is at quantile 100%, where the model underestimates the certainty of occupancy of the plot, which can for instance be observed in plot e of Gran Piano and plots a and d of San Besso. Overestimation of the presence (left hand side of the plot in Fig. 3.25), is less frequent, with plots d and f of Gran Piano being good examples.

3.3.2 *Carabus depressus*

As before, Fig. 3.26 show the simulated average occupancy of *Carabus depressus* computed from 480 repetitions, along the relative difference in average occupancy in each cell shown in Fig. 3.27.

The average occupancy of *Carabus depressus* well agrees with the in-situ data (Fig. 3.26). Overall, the average occupancy is more patchy, with clusters of high occupancy and surrounding lower occupancy maintained by the colonization process.

Similarly to *Pterostichus flavofemoratus*, the relative differences in occupancy of *Carabus*

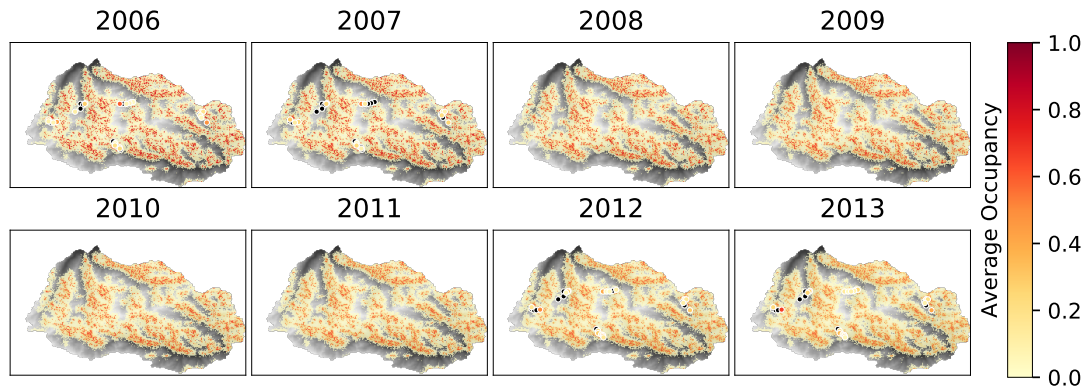


Figure 3.26 – Average occupancy of *Carabus depressus* in time. Output of the filtering algorithm for the calibrated parameters: average occupancy of *Carabus depressus* in time. For the sampling years (2006, 2007, 2012 and 2013) the ratio of number of times a species was observed vs the number of times it was sampled is displayed at the sampling location with a bullet colored using the displayed color scheme.

depressus (Fig. 3.27) are mostly within the borders of the high occupancy clusters, although a certain activity also happens within the clusters, to a higher extent than for *Pterostichus flavofemoratus*.

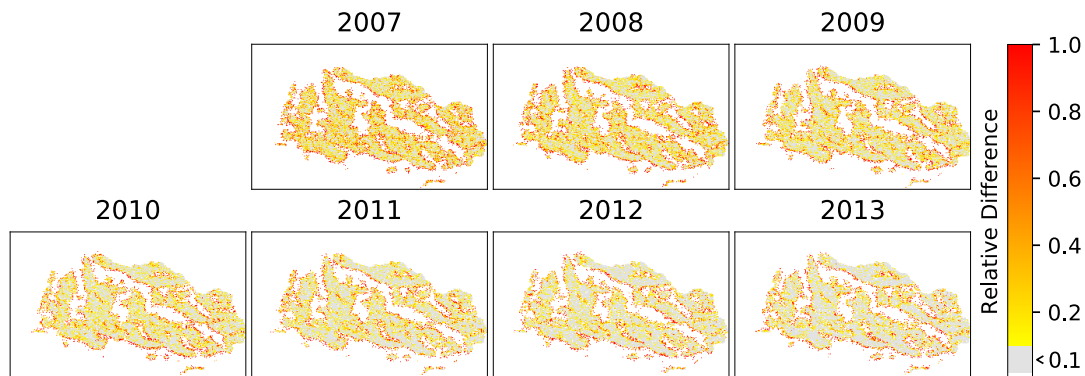


Figure 3.27 – Relative difference in average occupancy for *Carabus depressus*. The relative difference is computed from one year to the other as $|\hat{x}_y - \hat{x}_{y-1}| / \hat{x}_{y-1}$ which highlights large changes compared to the initial value. The color scale is shown in white where no change occur, grey where less than 10% of difference is observed, and a linear gradient capped at 100% for values above.

The fitness of *Carabus depressus* (see Fig. 3.28) is less general than the one of *Pterostichus flavofemoratus* in the sense that it highlights some distinct features on the valley sides. *Carabus depressus* appears to be more sensitive to the presence of vegetation (greenness, see table 3.3), with a base fitness consisting in the intercept, eastness, northness, and, to a lesser extent,

slope. The fitness parameters related to forest cover, temperature, wetness and brightness are not relevant for this species.

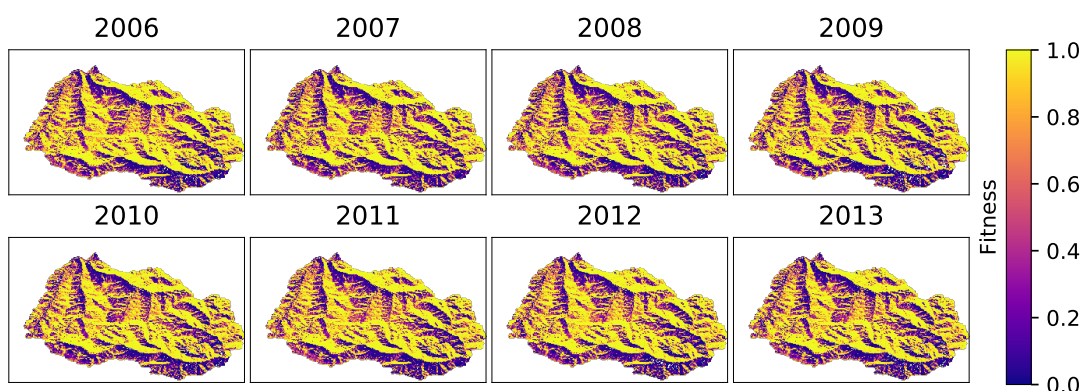


Figure 3.28 – Fitness of *Pterostichus flavofemoratus* in the GPNP. Computed from the calibrated parameters (equation 3.7, parameters shown in table 3.3) and the EO data for the simulated years.

In time, the fitness increases in certain part of the domain, and decreases in others, mostly driven by greenness in the southern valleys. The patterns in fitness differences shown in Fig. 3.29 are mostly in agreement with the trends in occupancy observed in Fig. 3.23.

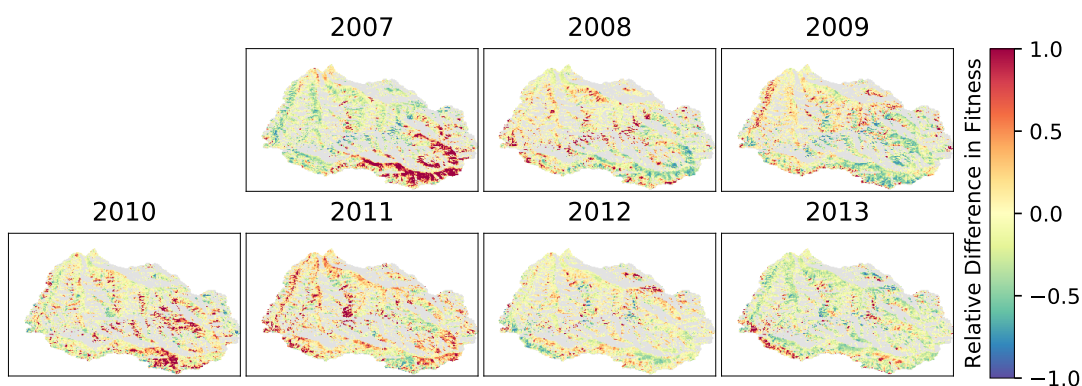


Figure 3.29 – Relative change in fitness value of *Carabus depressus* from one year to the other.

Fig. 3.30 shows a comparison between the in-situ and modeled k at the plot level, as done for *Pterostichus flavofemoratus*. Since the uncertainty on the false negative data ($1 - p_{TP}$, see table 3.3) is higher for the *Carabus depressus*, this translates in higher uncertainty above the median in the modeled k (Fig. 3.30). The modeled uncertainty captures most of the trends in the Gran Piano valley, and performs quite well in the Lauson and Vaudalletaz valley, but fails most of the times in Orvieilles. Plots a and f of Gran Piano, f of Lauson and a and e

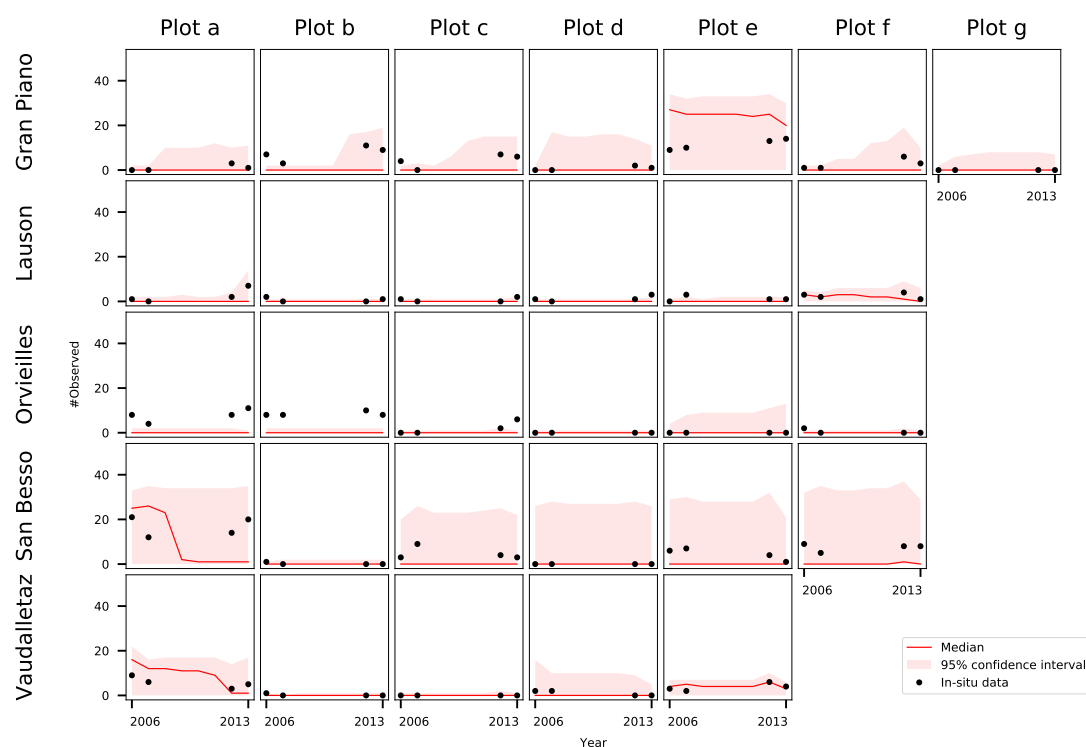


Figure 3.30 – Results at plot level for *Carabus depressus*. Modeled (red with confidence interval) and in-situ (black dots) number of times *Carabus depressus* was observed (k) in each plot and year.

of Vaudalletaz are particularly interesting. They show that the decreasing and successively increasing trends in the observations are well capture by the modeled through changes in the confidence interval and, in some cases, by strong variations in the median. The valley of San Besso is interesting as well, where the model is capable to predict the complete absence of observations in plot b, but encapsulates within the uncertainty all the observations in the other plots. This is confirmed as well in Fig. 3.25, where the distribution of observations in the model envelope is displayed. The modeled median (50% quantile) explains a good part of the data, with 85% of the observations within the 95% confidence interval, but there appears to be a strong underestimation of the occupancy (right hand side). This is for instance to be seen, as mentioned before, in the valley of Orvieilles.

From table 3.3 to some extend the importance of the explanatory variables can be understood. Both species appear to have a preferential orientation (south-east facing slopes). Temporally varying covariates appear to be important for both species, but *Carabus depressus* relies only on greenness.

3.3.3 Trends in presence and sensitivity to parameters

The two species appear to be very stable. The fluctuations happen around one or multiple stable cores, where the pressure of colonization lessens. The trends observed in the occupancy (Fig. 3.23) can mostly be related to the changes in fitness, but are only observed at the landscape level, with little to no trends observed at the pixel level. The average occupancy appears to be lower for *Carabus depressus* than for *Pterostichus flavofemoratus*, which is related to a more clustered fitness function along with a lower base fitness.

To further explore the link between occupancy and the model parameters, a sensitivity analysis of the mean final occupancy with respect to these parameters is performed. Each parameter is varied by 20% of itself (for the model parameters c , e and D) or its range (for the fitness parameters α_0 and β_j) in a positive and negative direction. The relative changes in the occupancy computed through this analysis are shown in Fig. 3.31.

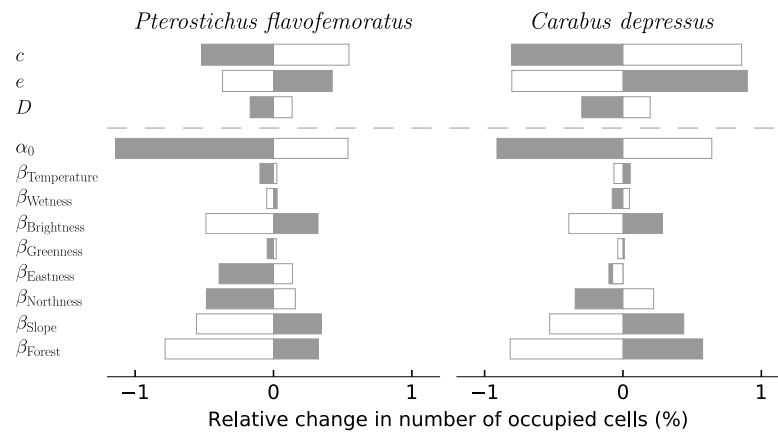


Figure 3.31 – Sensitivity analysis. Sensitivity of the calibrated model in terms of relative change in occupied cells to a 20% perturbation of the parameter values for the two species of interest. The white bars represent a positive change in the parameter value, and the grey bars a negative change. The dashed line separates the parameters intrinsic to the model (c , e and D) and the parameters employed by the fitness function (see equation 3.7).

Both species are fairly sensitive to changes in the intrinsic model parameters, c , e and D , which define how the buffer around the core of occupied cells behave. Of course, a larger value of e will lead to a lower average occupancy, and a higher value of c will increase the average occupancy. Interestingly, a change in the base fitness value (α_0) has a strong impact on the occupancy, and decreasing its value seems to have a much higher impact than increasing it. For both species, brightness is the most sensitive time-dependent covariate. Changes in occupancy are inversely proportional to the changes in the brightness value, displaying similar behaviors as the extinction coefficient. This is true as well for slope and the presence of forest. Eastness and northness both change proportionally to the change in parameter value,

but show a much stronger reaction for *Pterostichus flavofemoratus*, even though the initial parameter values are in the same order of magnitude for both species.

3.4 Discussion

The proposed framework shows how EO data can be used in conjunction with partially observed in-situ data to model the presence of a metapopulation in space and time. The resulting calibration process converges to parameter combinations that generate initial spatial occupancy comparable to the one proposed by the SDM (Fig. 3.17), and subsume the spatial dynamics of the metapopulation processes.

While static variables such as slope and aspect (northness and eastness) appear as essential to characterize the species' niche, temporally varying state variables emerge as key players in predicting temporal trends in species occupancy. Because the static variables do not change in time, the observed changes are stemming from two sources: i) colonization and extinction processes related to the metapopulation parameters (c , e and D), and ii) the time varying drivers. The metapopulation parameters explain most of the stochastic variations, with the spin-up period ensuring that the observed trends are not due to the model re-balancing the occupancy to match the parameter fluctuations. The observed general trends are therefore to be related to the variation of the time-dependent drivers. At the plot level, the simulated results show that the model is capable of reproducing, within a 95% confidence interval, the dynamics of the species (Figs. 3.24, 3.30 and 3.25). Similarly, the modeled envelope is produced by the SPOM stochastic structure, and the variations are induced by the variation in time of the covariates. An example is given in plot f of the valleys of Gran Piano and Lauson (Figs. 3.24 and 3.30) where the model envelope increases as the observed presence increases.

The results at plot level corroborate the assumption that the simulation reflects rather closely the observations, yielding a global interpretation of the species presence. As described in the results, the stochastic variations in occupancy occur around stable cores, which remind the classic metapopulation approach centered around patches, but highlight the importance of modeling the landscape-explicitly, as most of the changes occur at the edge of the stable cores or between them, and not within a patch of homogeneous quality. At a landscape level, changes are hardly observed considering the time frame and the domain's scale. In a period of eight years, perturbations of the environment in a protected area are hardly extreme and mostly observed in terms of variations in the number of individuals captured, but not in terms of major shifts in geographical space of the species' distribution. Indeed, alpine species are known to react slowly to changes in environmental conditions (Guisan and Zimmermann, 2000). This is precisely what is expected from near-term ecological predictions (Dietze et al., 2018).

The species' calibrated initial spatial presence is maintained throughout the simulation and so the occupancy in 2013 resembles the occupancy imposed in 2006. The trends, however weak, reflect the two species' long-term fate in the landscape and allow us to draw early warning of impending change. As mentioned above, *Pterostichus flavofemoratus* is mostly sensitive to temperature, wetness and to some extent greenness, while *Carabus depressus* almost exclusively reacts to changes in greenness (Table 3.3). The decreasing trend in *Carabus depressus* (Fig. 3.23) could therefore be explained by a parallel increase in the greenness values (see data analysis, and Fig. 3.14) as the relation proves of inverse proportionality. This could also explain, at least in part, the trend for *Pterostichus flavofemoratus* since greenness is the variable with the strongest increase over time. All parameters multiplying the time-variant covariates are positive, explaining the trend in occupancy observed in Fig. 3.23.

In terms of observation uncertainty, the model evaluates the probability of false negative *Carabus depressus* to be quite high (~37%) compared to the one of *Pterostichus flavofemoratus* (~21%). The model here reflects the sampling (Fig. 3.11), where *Carabus depressus* has been observed fewer times than *Pterostichus flavofemoratus*. Nevertheless, a question remains on whether the occurrences of species not observed reflect true absence or under-sampling. Because sampling reflects the species' activity-density, a species less active at certain times of the year will be less present in the observations. However, the model is meant to reflect the species average presence in the landscape during the year, regardless of its level of activity. Here, the model follows the assumption that in 37% of the cases *Carabus depressus* was indeed present but not observed, and accounts for this in the calibration. This problem is less evident the case of *Pterostichus flavofemoratus*, where over all plots the largest ratio of observed to sampled is higher.

The two species' fitness (Figs. 3.21 and 3.28) inform about the ecology of the focus species. With a comparably more homogeneous fitness and a higher average value in the whole domain, *Pterostichus flavofemoratus* appears to be – relatively – a generalist, whereas *Carabus depressus*, with its more refined fitness and patchy occupancy, can be classified more as a specialist species.

This study presents a number of limitations, which would have to be addressed to refine the modeling framework. Specifically:

1. Although the human effort involved in the collection of these data has been major, the time series of *in-situ* data is relatively short. The temporal dynamics of the species, especially the long-term landscape-wide trends, are difficult to detect from observed data. Relatively little change in the descriptors occurs, and the spatial distribution of the species does not drastically change in time. Further studies should perhaps be attempted on long-term ecological time series. The importance of long-term sampling of these habitats and the importance

of continuing the efforts as done in the context of the data provided for this study is hardly overestimated;

2. Obtaining consistently long time-series of EO data is uncommon. Landsat, for instance, is one the longest and most consistent time series of EO data, but even this data set suffers from failures, and matching the different data-sets of different Landsat missions is a demanding task. Other sources of errors or missing data arise when the weather corrupts images, e.g. when clouds obstruct the satellite image. Parts of the image therefore cannot be used and must be gap-filled, because the captured signal does not reflect the actual conditions on the ground. In mountainous regions this can be quite problematic as clouds are frequent. On given bad years, almost all images are clouded to some extent, and a reconstruction of the image is inevitable. Taking the median value over the year for each pixel as done here can mitigate this problem, at the cost of limiting the modeling to a yearly dynamic;

3. The spatial distribution of the sampling points, arranged in transects, is most suited for the studies of the species-elevation relationship, and identifying trends in altitudinal gradients, but inadequate for spatially-explicit modeling. In order to do so, a random distribution of the sampling points would be most useful (Woodcock, 2007). The sampling scheme chosen here informs on the species' presence on one side of the valley, but leaves out the presence on the other. The model then has to extrapolate from the climatic data in other valleys which have been sampled in similar conditions. Even though the data analysis suggests that the climatic data in the plots is representative of the whole domain, this might not be the case for the presence of the species, which not only depends on climatic data but on the dispersal and metapopulation dynamics as well. Specialist species, with small, patchy presence, or generalists with lower activity or limited in time, might especially be misrepresented by this sampling scheme. The impact of the sampling scheme on the results of this framework could constitute an interesting followup of the present analysis;

4. Although widely used in species distribution modeling and shown to be performing relatively well compared to other SDM techniques (Guisan and Zimmermann, 2000), the functional of the fitness function as proposed here, based on the same concept as generalized linear models, obviously has limitations. Here, the response curve of a species to an environmental driver is by definition monotonic and cannot be hump-shaped (Moilanen and Hanski, 1998; Bertuzzo et al., 2016) (c.f. chapter 2 for an example), or a smooth function as in generalized additive models (GAMs), Guisan et al. (2002) (but see Guisan and Zimmermann (2000) for a summary of response curves). This might not be a factor with SDMs where the parameters are calibrated once against a static presence. However, with dynamic models as presented here, the monotonicity would possibly be an issue if longer time series were to be considered. A choice would therefore have to be made based on the number of relevant drivers, and longer time series with possibly more sampling points would be needed.

3.5 Conclusion

The framework shown here must be seen a proof of concept of a dynamic landscape-explicit metapopulation model driven by Earth observations intended for mountain species epitomizing however complex landscapes (i.e. substrates for ecological interactions). The proposed framework allows the estimation of the initial distribution of the species in the landscape. In a first step the initial occupancy is obtained by means of an SDM, and, then, by calibrating the metapopulation model through the iterated filtering process, ensuring the occupancy in the landscape to be at equilibrium for the chosen fitness and metapopulation parameters. The calibration process identifies the parameters most suited for the species, which, in turn, permits the identification of trends in the spatial variability of the species. The framework permits the simulation of spatial occupancies of a calibrated species in years when the species was not sampled, thus filling the spatiotemporal gaps between in-situ observations. Here for instance, the metapopulation results are the only source of information for the occupancy from years 2008 to 2011, with the years 2006, 2007, 2012 and 2013 serving as reference for the calibration. Potentially, with only EO data available, or with projected simulated EO data, one could project the presence of these species into the future. Given the dynamical nature of the model, the presented spatial distribution serves as starting point for the simulation, which would then be driven by the EO data and the model dynamics.

4 An exact coarse-graining consistent metapopulation model

IN the present chapter¹, the consistency of the metapopulation model is investigated when considering different resolutions of the landscape matrix, i.e. different levels of coarse-graining, of paramount importance to understand how conclusions drawn from local studies can be made general and extrapolated to larger regions. A formulation of the metapopulation mode, taking into consideration a dispersal volume depending on the grid-cell area is proposed. This first derivation from the classical model is then extended in order to account for intra-cellular colonization (called self-colonization within the chapter), which permits an aggregation of cells, as typically done with coarse-graining. The consistency of the proposed model formulations is then investigated, first, in a flat homogeneous domain, where the results are independent of the landscape structure. In a second step, a complex landscape structure is introduced in the form of an elevation field, the Gran Paradiso National Park. The results suggest that the proposed formulations of the model are independent of coarse-graining in the flat domain. This appears to be the case in the park as well, up to a certain level of coarse-graining, where loss of information on the landscape matrix becomes too severe. In all considered levels of coarse-graining the proposed formulation of the model outperforms the previously proposed models in terms of convergence of the results.

4.1 Introduction

Spatially-explicit ecological models, such as species distribution and metapopulation models, are nowadays frequently adopted to investigate the relationship between habitat properties and species diversity and richness. In fact, the recently increased availability of high-resolution remote sensing maps is allowing to characterize in detail the habitat features that might determine the suitability of a species to a certain environment. The grain-size at which a

¹The content of this chapter is in preparation in order to be submitted to a peer reviewed journal.

species is meant to be modeled has to be carefully chosen, as the resulting species distribution may vary greatly (Kirchheimer et al., 2016). This is especially true for models calibrated at a certain grain and extrapolated to different grain sizes and extends (Keil et al., 2013).

Issues on how one should theoretically address the problem have long been considered. For example, whenever assessments of risk to biodiversity need to rely on spatial distributions of species and ecosystems, range-size metrics, quite sensitive to measurement scale, must be used extensively (Keith et al., 2018). One of the key measures in these assessments is the area of occupancy (AOO). Scale issues emerge therefore, prompting proposals to measure them at different scales based on the shape of the distribution or ecological characteristics of the biota. Despite their dominant role in the description of endangered species, decades, appropriate spatial scales of AOO for predicting risks of species' extinction or ecosystem collapse remain an active subject of research (Keith et al., 2018). By using stochastic simulation models to explore risks to ecosystems and species in complex landscapes, Keith et al. (2018) showed that area of occupancy proves an accurate predictor of risk in most cases only when measured with grid cells 0.1–1.0 times the largest plausible area threatened by an event. Estimates of AOO at relatively coarse scales thus prove better predictors of risk than finer-scale estimates. Because the optimal scale for modeling the relevant dynamics depend on the spatial scales of threats more than the shape or size of biotic distributions, appreciable potential for grid-measurement errors exist (Keith et al., 2018). Neutralizing geometric uncertainty embedding effective scaling procedures for assessing risks posed by landscape-scale threats to species and ecosystems is thus definitely relevant.

Hanski's metapopulation model (see chapter 1 and e.g. (Hanski and Gilpin, 1991)) lends itself to the study of the above issue. It is based on the interplay between colonization and extinction processes, where the colonization of an empty patch depends on the occupancy probability and distance of surrounding patches (see chapter 2 for a reasoned introduction to the topic). Such a model has been used in literature to simulate the distribution of different species, from butterflies to birds (e.g., Schnell et al. (2012)). The connectivity among patches is the main driver of the model and the landscape structure thus plays a fundamental role. Due to computational limitations, it is not always feasible to calibrate the model, say by comparing with data on habitat gathered by a digital terrain model over large-scales (see e.g. chapter 3), at the finest possible grid resolution. It is therefore important to understand how modeling results, such as species presence, vary depending on grain and, in particular, if these results are due to numerical errors introduced by the model or to the loss of information due to the upscale of the landscape structure.

While with different levels of coarse-graining certain quantities, such as the mean elevation, are preserved, Rodriguez-Iturbe and Rinaldo (2001) demonstrate that the connectivity properties of a landscape may drastically change under progressive coarse-graining. In particular,

drainage directions (i.e. the directions of topographic gradients) change dramatically with the level of coarsening, even if the mean elevation is preserved (Rodriguez-Iturbe and Rinaldo (2001), Chapter 4). This has to be considered because gravity effects affect decisively species dispersal, potentially creating barriers and/or limitations (Colwell and Hurtt, 1994; Colwell and Lees, 2000). Additionally, Palmer and White (1994) showed that “*species-richness patterns were neither self-similar nor hierarchical*”. In simpler terms, different regions might be connected or disconnected with different grid approximations of a given underlying landscape. Only scale-free distributions, epitomized by power laws, are invariant under coarse-graining (i.e. $p(bx) = g(b)p(x)$ where b is a scale factor), and it cannot be postulated that such characters are universal in species distributions – on the contrary, they almost never are. Patches with previously non-existing connections might be averaged into one larger region, allowing for interactions between populations that were not possible at a different scale. Small patches of habitat suitable for a focus species might simply vanish with scaling. Overall, connections between patches might be neglected, rendering population migration harder, and therefore changing the outcome of the simulation.

Here, we study how different levels of coarse-graining influence the spatial occupancy of a set of virtual species invading the Gran Paradiso National Park region when simulated by a gridded metapopulation model (Hanski, 1998; Fahrig and Nutton, 2005; Fahrig, 2007; Purves et al., 2007; Rybicki and Hanski, 2013). In particular, we propose a formulation of the metapopulation model where the numerical errors resulting from coarse-graining are to most parts limited to the spatial discretization of the dispersal process. This guarantees that the differences in the results are mostly due to the information on the landscape structure lost because of the coarse-graining, even though these are brought to a minimum as well.

Rybicki and Hanski (2013) and Giezendanner et al. (2019) have suggested that the landscape properties can be considered within the metapopulation model through a suitable fitness function, which re-scales the colonization and extinction parameters on the basis of how suitable a patch is for a given species. In this study, the elevation field is considered as the sole landscape feature relevant to highlight the scaling properties of the metapopulation model. This is also justified by the recent works of Bertuzzo et al. (2015, 2016), which show how terrain topology and elevation constitutes fundamental indicators of habitat suitability that can be considered as a proxy of other habitat properties. In fact, topology and elevation have an important contribution in shaping the habitat-connectivity and, thus, the population dynamics. By subdividing the landscape into cells, Bertuzzo et al. (2016) show that cells with low connectivity to cells with similar altitude - or available in a suitable range for given species - tend to be less populated, hence display a low species diversity. Connectivity is, in this case, defined as a function of the path between cells, specifically focusing on elevation gradients and distance. Peaks, as well as valleys, seem to prevent population movement, as species most

suited to inhabit these regions would have to cross through unfavorable terrain to propagate. Connectivity, as defined here, is strongly dependent on the underlying terrain, which needs to be sampled from the environment. In a raster-like approach, the size of the cells is thus a crucial variable to capture these connectivities (Palmer and White, 1994).

4.2 Materials and methods

4.2.1 Metapopulation model

The model considered in this study is based on Hanski's metapopulation model (Hanski and Gyllenberg, 1997), adapted by Purves et al. (2007) to a raster-like spatial structure ideal to incorporate Earth Observation data (EO data, see chapters 2 and 3 for a reasoned introduction to the subject). In the metapopulation model, given an initial spatial distribution of probabilities of occupancy $p_{i,0}$ ($i = 1, \dots, n$, with n number of cells), the variations in the occupancy are governed by the following system of ordinary differential equations (ODEs):

$$\begin{cases} \frac{dp_i(t)}{dt} = C_i(t)(1 - p_i(t)) - E_i p_i(t) \\ p_i(0) = p_{i,0} \end{cases} \quad (4.1)$$

where E_i and $C_i(t)$ are the extinction and colonization affecting the cell i . The colonization pressure of a species from cell j to cell i is expressed by the product of four quantities: i) the colonization rate c [T^{-1}]; ii) the probability of presence in cell j , $p_j(t)$; iii) a term representing the dispersal kernel, K_{ij} ; iv) and a term representing the quality of cell j , q_j^c [-]. The colonization term $C_i(t)$ in 4.1 is thus obtained by the sum of the colonization contributions from all cells:

$$C_i(t) = c \sum_{\substack{j=1 \\ j \neq i}}^n K_{ij} q_j^c p_j(t) \quad (4.2)$$

Similarly to the approach in Rybicki and Hanski (2013), the dispersal kernel is described using an exponential function:

$$K(d) = r \exp\left(-\frac{d}{D}\right) \quad (4.3)$$

where D [L] is the species dispersion, d [L] is the distance between two points, and r [L^2] is a normalization factor, typically computed imposing that the integral of the dispersal kernel is 1 on an infinite domain:

$$\int_{\mathbb{R}^2} K(d) = 1 \quad (4.4)$$

which results in $r = \frac{1}{2\pi D^2}$ (Rybicki and Hanski, 2013).

There exist several ways to discretize the dispersal kernel on the given domain (see, e.g., Keith

et al. (2018)). Given two cells i and j and a distance d_{ij} , a straightforward approach consists in assigning $K_{ij} = K(d_{ij})$. In this way, however, the sum of K_{ij} on the domain cells changes with the grid resolution, thus implying a different evaluation of the colonization pressure in each cell (because C_i in equation 4.2 depends upon the sum of K_{ij}). A different approach descends by imposing that the sum of the discretized kernel values approximate the integral of the kernel, thus satisfying the property in equation 4.4. A simple numerical approximation consists in setting $K_{ij} = A_j K(d_{ij})$. In the metapopulation model this means that the single contributions of cell j to the colonization of cell i depends on the area of the source cell j . Section 4.2.3 analyses more in detail the advantages of this choice.

The extinction term in equation 4.1 is represented by an extinction rate e [T^{-1}] scaled over a term q_i^e [-] representing the quality of cell i : $E_i = \frac{e}{q_i^e}$. In the original metapopulation model by Hanski (1998), q_i^c and q_i^e depend on the area A_i [L^2] of patch i :

$$q_i^c = A_i^{\alpha_c} \quad ; \quad q_i^e = A_i^{\alpha_e}, \quad (4.5)$$

where $\alpha_c \geq 0$ and $\alpha_e \geq 0$. In more complex formulations (see e.g., Rybicki and Hanski (2013); Bertuzzo et al. (2016); Giezendanner et al. (2019)) q_i^c and q_i^e are obtained through a fitness function $f(x)$ describing the suitability of the landscape features for the species: $q_i^c = q_i^e = f_i$, with f_i being an approximation of the fitness on cell i . For example, considering only the impact of elevation as a proxy of temperature (but see chapter 3 for a possible generalization), one may have:

$$f_i \propto \exp\left(\frac{z_{opt} - z_i}{\sigma}\right), \quad (4.6)$$

where z_i is the elevation of cell i (obtained, for example, from a DEM), and z_{opt} and σ are species-dependent parameters that represent the optimal elevation for the species and the niche width around the optimal elevation.

4.2.2 Graining problem

The described metapopulation model was designed to represent the species dynamics on an ensemble of disjointed patches of different sizes, representing the focus species' suitable areas. Changes in the model domain mainly consisted in different number of patches and in different spatial configurations.

The application of the metapopulation model on a regular grid is advantageous to well represent the landscape features in all the domain and to approximate the space-continuity of the dispersal process of the offsprings. In this framework, it is important to identify the suitable grain size at which modeling the extinction, colonization and dispersal processes of the species of interest. Intuitively, results obtained on more refined grid (i.e. the grains) should

yield a higher level of accuracy than those on coarse grids, because the dispersion process and the landscape features are better described when using finer discretization. However, this approach has two main limitations: i) the computational cost associated with the numerical solution of the model equation rapidly increases with the cell numbers, and ii) the data available to describe the landscape features have a fixed resolution (e.g., the resolution of remote sensing products), and using a finer grid in the metapopulation model without improving the resolution of the inputs might not add any improvement in the accuracy of the solution. For

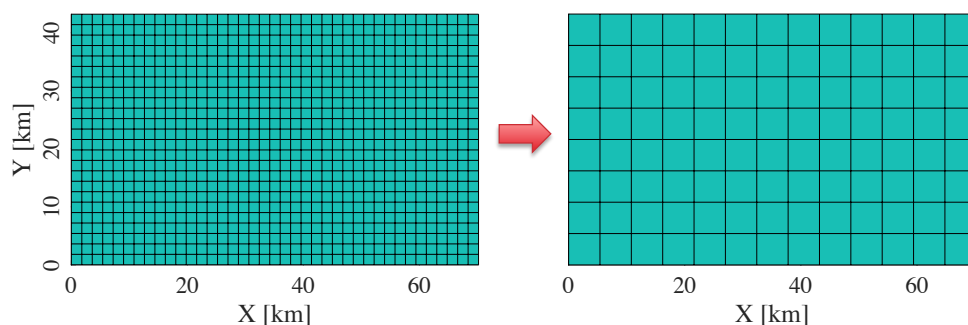


Figure 4.1 – Example of coarse-graining a landscape. In the coarse-graining problem, we are interested to assess the changes in the solution of the metapopulation model when changing the grain size in the domain, as depicted, for example, in this figure.

these reasons, coarser grains are frequently adopted in applications, seeking for a compromise between computational complexity and solution accuracy.

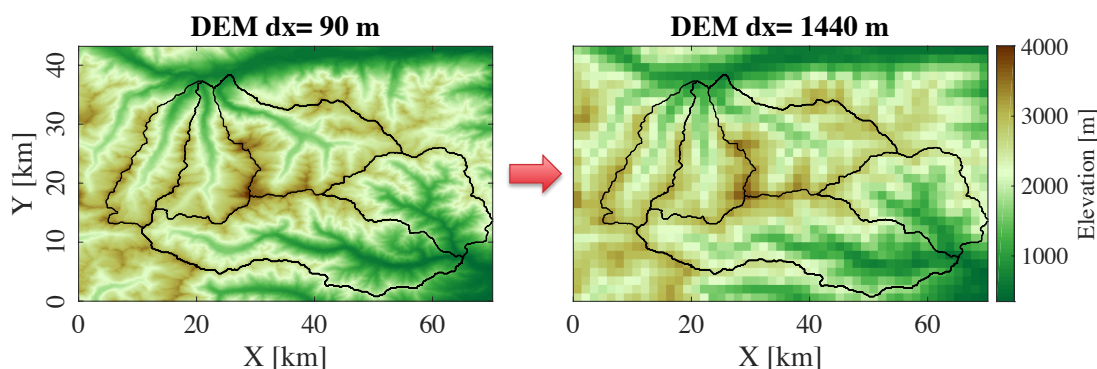


Figure 4.2 – Loss in information in landscape structure with coarse-graining: example on the GPNP. Changes in the metapopulation model solution after changing the grain size might be introduced by numerical errors and/or by the upscaling of the data describing the landscape features, as depicted in this example for the DEM of the GPNP passing from a grain size of 90 m to 1440 m.

However, it is fundamental to quantify the error in the metapopulation solution introduced by the process of coarse-graining. Here, we distinguish two type of errors introduced by

coarse-graining (see Fig. 4.1):

1. numerical errors due to the discretization of the dispersal process on coarser grids;
2. numerical errors due to the loss of information in the input data, in particular in those used for the characterization of the landscape (e.g., the DEM in the fitness function 4.6, as depicted in figure 4.2).

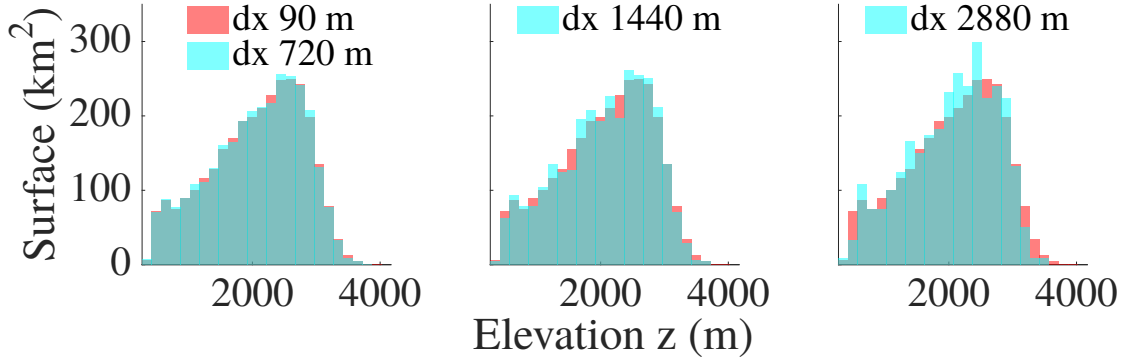


Figure 4.3 – Behavior of the hypsographic curves with coarse-graining. Hypsographic curve of three rescaled resolution and compared to the finest resolution ($dx = 90$ m). Note that the frequency of the quantity of area available at each elevation changes with coarse-graining, and that the average remains the same.

4.2.3 A metapopulation model consistent with coarse-graining

Before quantifying the impact of coarse-graining on the accuracy of the numerical solution, it is important to understand the properties of the model solution that should be preserved when using two different grain sizes.

For simplicity, we consider here the rectangular domain depicted in Fig. 4.4. We want to use the metapopulation model to describe the probabilities of occupancy in the finer cells,

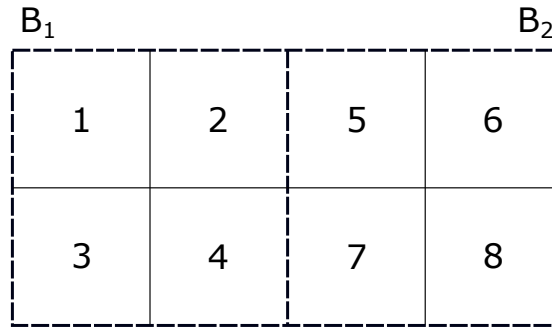


Figure 4.4 – Close up on coarse-graining. Example of a domain having eight squared cells (called cells $1, \dots, 8$) having area A_1 , upscaled to the two wider cells called B_1, B_2 , of area $A_2 = 4A_1$.

termed p_i , $i = 1, \dots, 8$, and those in the coarser cells, termed p_{B_1} and p_{B_2} . Intuitively, at every computational time the probabilities at the coarser grains, should correspond to the average of the probabilities at the finer grains:

$$p_{B_1}(t) = \frac{1}{4} \sum_{i=1}^4 p_i(t) \quad ; \quad p_{B_2}(t) = \frac{1}{4} \sum_{i=5}^8 p_i(t). \quad (4.7)$$

It is natural to question whether this property is satisfied by the solution of two metapopulation models that correspond to the two grain sizes.

Adapting equation 4.1 to the finer grid we have:

$$\frac{dp_i}{dt} = \left(c \sum_{j=1}^8 K_{ij}(A_1) q^c(A_1) p_j(t) \right) (1 - p_i(t)) - \frac{e}{q^e(A_1)} p_i(t) \quad , \quad i = 1, \dots, 8 \quad (4.8)$$

where we explicitly represented the possible dependence of q^c , q^e , and K_{ij} by the area. In an analogous way, adapting equation 4.1 to the coarser grid yields:

$$\begin{cases} \frac{dp_{B_1}}{dt} = (c K_{B_1 B_1}(A_2) q^c(A_2) p_{B_1}(t) + c K_{B_1 B_2}(A_2) q^c(A_2) p_{B_2}(t)) (1 - p_{B_1}(t)) - \frac{e}{q^e(A_2)} p_{B_1}(t) \\ \frac{dp_{B_2}}{dt} = (c K_{B_1 B_2}(A_2) q^c(A_2) p_{B_1}(t) + c K_{B_2 B_2}(A_2) q^c(A_2) p_{B_2}(t)) (1 - p_{B_2}(t)) - \frac{e}{q^e(A_2)} p_{B_2}(t) \end{cases} \quad (4.9)$$

Note that the parameters defining the species, i.e. the rates of extinction e , colonization c and the dispersal D have the same values in equations 4.8 and 4.9, since they do not depend on the particular grain size at which we discretize the problem. The same property holds true for the parameters in the fitness, such as z_{opt} and σ in equation 4.6.

In the following it is shown that, under these hypotheses, the terms q^c and q^e should be independent of the area of the cells in order to satisfy the scaling property in equation 4.7. Considering a species that persists in this domain (which exists for suitable parameters e , c and D), the stationary solution has a homogeneous probability of occupancy in each cell, due to the homogeneous area of the cells. We call \tilde{p} this probability of occupancy at steady state, $\tilde{p} \neq 0$, and, for (4.7), we have $\tilde{p} = p_A = p_B = p_i$, $i = 1, \dots, 8$.

We consider equation 4.8 at the stationary condition, which is constant in time, and thus the temporal derivatives in (4.8) are null. The sum of the first four equations results in:

$$c q^c(A_1) \left(\sum_{i=1}^4 \sum_{j=1}^4 K_{ij}(A_1) + \sum_{i=1}^4 \sum_{j=5}^8 K_{ij}(A_1) \right) (1 - \tilde{p}) = 4 \frac{e}{q^e(A_1)}, \quad (4.10)$$

which is strictly connected to the stationary condition of the first equation in 4.9:

$$cq^c(A_2)(K_{B_1B_1}(A_2) + K_{B_1B_2}(A_2))(1 - \bar{p}) = \frac{e}{q^e(A_2)}. \quad (4.11)$$

In particular the following equation must be verified:

$$q^c(A_1)q^e(A_1) \frac{\sum_{i=1}^4 \sum_{j=1}^4 K_{ij}(A_1) + \sum_{i=1}^4 \sum_{j=5}^8 K_{ij}(A_1)}{4} = q^c(A_2)q^e(A_2)(K_{B_1B_1}(A_2) + K_{B_1B_2}(A_2)). \quad (4.12)$$

The term $\frac{1}{4} \sum_{i=1}^4 \sum_{j=1}^4 K_{ij}(A_1)$ provides the mean dispersion within cells in B_1 , and thus should be an approximation of the term $K_{B_1B_1}(A_2)$. Similarly, the term $\frac{1}{4} \sum_{i=1}^4 \sum_{j=5}^8 K_{ij}(A_2)$ represents the dispersion from cells in B_1 to cells in B_2 , and should be an approximation of $K_{B_1B_2}(A_2)$. Note that these properties descend directly when considering $K_{ij}(A_1) = A_1 K(d_{ij})$ and $K_{B_1B_2}(A_2) = A_2 K(d_{B_1B_2})$.

Under this assumption we have that

$$q^c(A_1)q^e(A_1) = q^c(A_2)q^e(A_2)$$

which, under representation in equation 4.5, yields:

$$A_1^{\alpha_c} A_1^{\alpha_e} = (4A_1)^{\alpha_c} (4A_1)^{\alpha_e}, \implies (4)^{\alpha_c} (4)^{\alpha_e} = 1.$$

Since $\alpha_c \geq 0$ and $\alpha_e \geq 0$, this is possible only if q^c and q^e are area-independent ($\alpha_e = \alpha_c = 0$).

Note that in this example a self-colonization term is considered in the model equations, i.e., $cK_{ii}(A_1)q^c$ in equation 4.8 and $cK_{B_1B_1}(A_2)q^c$ in equation 4.9. The approach proposed here shows that this self-colonization term must be considered in metapopulation models when dealing with coarse-graining problems. In fact, this feature is essential because the intra-cellular dispersal mimics the dispersal between the corresponding internal cells at finer resolutions. The model obtained is thus made consistent. i.e. invariant under coarse-graining. Note that including the self-colonization term in the equation was proposed by some authors (e.g. Schnell et al. (2012)), but the role of area when changing the grain size was not considered.

The final model formulation thus reads:

$$\frac{dp}{dt} = C_i(t)(1 - p_i(t)) - E_i(t)p_i(t), \quad (4.13)$$

$$C_i(t) = c \sum_{j=1}^n K_{ij} q_j^c p_j(t), \quad (4.14)$$

$$K_{ij} = \frac{A_i}{2\pi D^2} \exp\left(-\frac{d_{ij}}{D}\right), \quad (4.15)$$

$$E_i(t) = e/q_j^e, \quad (4.16)$$

with the dispersal volume thus dependent on the area of the source pixel, the colonization of the focus pixel including self-colonization, and the extinction independent of the area.

4.2.4 Model comparison

In the following we want to highlight the importance of considering a model consistent with coarse-graining through numerical simulations. To achieve this goal, we compare the following three models:

- **Model M0.** This model corresponds to the original Hanski's model presented in equation 4.1, where we set:
 - the quality-properties of the cells equal to the area times a fitness function, $q_i^c = q_i^e = A_i f_i$;
 - the coefficients of the kernel discretization are set to be area-independent, $K_{ij} = K(d_{ij})$;
 - the self-colonization terms are not considered ($i \neq j$ in equation 4.2).
- **Model M1.** This model is a variation of the model presented in equation 4.13, where self-colonization is not considered. We set:
 - the quality-properties of the cells area-independent, $q_i^c = q_i^e = f_i$;
 - the coefficients of the kernel discretization are set to be area-dependent, $K_{ij} = A_j K(d_{ij})$;
 - the self-colonization terms are not considered ($i \neq j$ in equation 4.2).
- **Model M2.** This corresponds to the model in equation 4.13. Differently from **M1**, self-colonization is considered.

4.2.5 Simulations

To test the consistency of the model under coarse-graining, we simulate the occupancy dynamics of an invading species within an area of about $70 \times 43 \text{ km}^2$ in two landscapes (Figs. 4.1 and 4.2):

- **Landscape L1.** A flat domain meant to investigate the consistency of the model with graining when not affected by the heterogeneous landscape matrix ($f_i = 1$). In this landscape we compare results for the three considered models: **M0**, **M1**, and **M2**.
- **Landscape L2.** A domain consisting of a rectangular area surrounding the Gran Paradiso National Park. In this case the quality of the cell expressed in terms of the cell-elevation (used as a proxy of temperature), i.e. f_i is computed using equation 4.6. Elevation is based on a digital elevation model (DEM) extracted from the Copernicus EU-DEM v1.1 (25 m resolution). In this landscape we compare results for models **M1**, and **M2**.

Both landscapes are considered with grain-sizes of 90 m, 180 m, 360 m, 720 m, 1440 m and

2880.

In landscape **L2**, the original DEM of 90 m resolution is upsampled to the coarser grains by bilinear interpolation, which preserves the mean elevations (Fig. 4.3). Fig. 4.2 shows the DEMs at resolutions of 90 m and 1440 m. We can see that the main landscape features are preserved in the coarser grid, however, the available surface at elevations between 1800–2300 m is slightly overestimated (Fig. 4.3).

The model comparison in the homogeneous domain (landscape **L1**) is meant to investigate the consistency of the dispersal approach with coarse-graining.

In landscape **L2**, the complex GPNP domain, we investigate how the added heterogeneity influences the consistency of the model with scaling. In this case, the process of coarse-graining causes loss of information in the habitat of the virtual species (the quality), which is set dependent on the elevation. This deterioration in the input data, might be more or less relevant in the model results depending on the particular properties characterizing the species, e.g. the dispersion D and the niche width σ .

Table 4.1 – Metapopulation parameters of the species considered in the study

Species	S1	S2	S3	S4	S5	S6
c [y^{-1}]	1					
e [y^{-1}]	0.1					
z_{opt} [m]	150					
σ [m]	150			300		
D [m]	100	500	1000	100	500	1000

The invasion of six virtual species (called S1, ..., S6) is simulated in both landscapes for a period of 100 years. The species are characterized by different values of the five parameters (c, e, D, z_{opt}, σ) described in Table 4.1 (note that σ has no influence of the species in the flat landscape which means only three species are considered there).

4.3 Results

4.3.1 Homogeneous landscape (L1)

Fig. 4.5 depicts the average occupancy over time for three invading species characterized by different values of dispersal. Occupancy results are computed using the three variations of the model and for the six different grain sizes, thus highlighting the different impacts of coarse-graining in the solutions. Differences in the occupancy results are also represented by relative errors with respect the reference solution ($dx = 90$ m). The occupancy results depicted in Fig. 4.5 highlight that, for the three species considered in this landscape, the original formulation

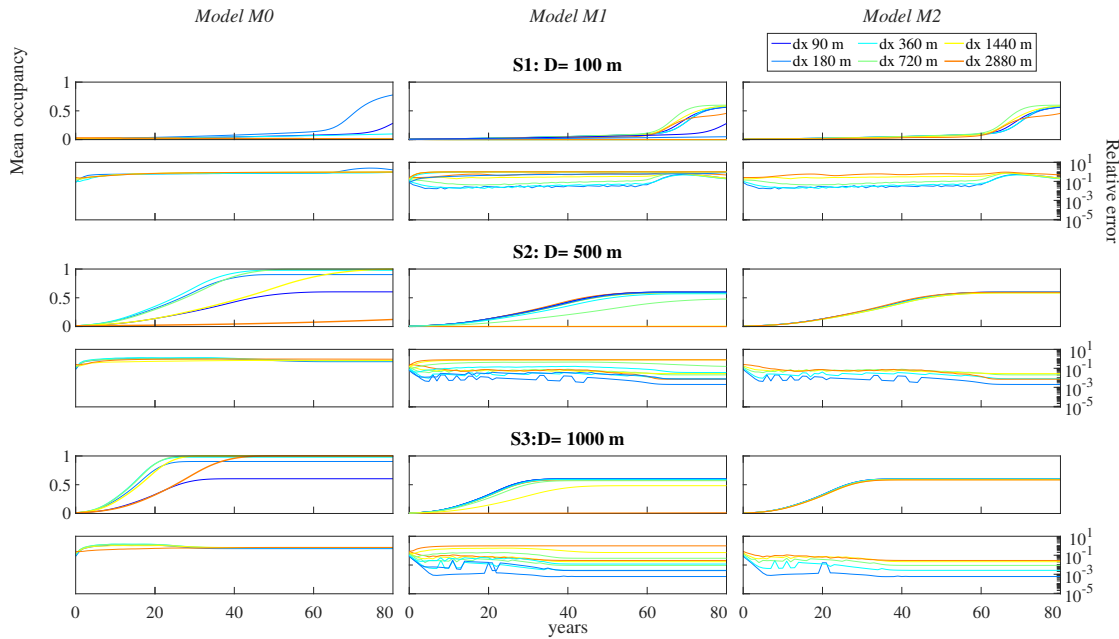


Figure 4.5 – Behavior of the different model formulations under coarse-graining in a flat domain. Landscape **L1**, homogeneous domain. Temporal evolution of the probability of occupancy (averaged over the entire domain) and relative root mean squared error between an occupancy map and the corresponding reference solution obtained at the finest grain size ($dx = 90$ m, dark blue line). Results are depicted for the three different dispersal distances of the species and the six grain sizes. The three columns show the results for the three different models (c.f. section 4.2.4): (Left) model **M0**; (Center) model **M1**; (Right) model **M2**.

of the model (model **M0**) converges to different steady states depending on the grain size. Instead, the proposed new formulation but without self-colonization (model **M1**) leads to results more stable with coarse-graining, especially for species with large dispersal (species **S2** and **S3**) and small differences in grains.

The self-colonization term considered in model **M2** has a strong positive impact when dealing with large grains. In fact, when $dx = 1440$ m or 2880 m, **M1** is not able to obtain the same occupancy value that is reached with finer grains. This problem, instead, is not present in the results from **M2**, thanks to the added colonization pressure provided by the self-colonization term. This claim is corroborated by the lower relative error associate to **M2** results

M2 results for species **S1** also show that very fine grains are necessary to well simulate the dynamics of the colonization process when dealing with species having short dispersal values. In fact, only for this species, **M1** occupancies associated to different grains show different patterns when the colonization process become faster (e.g. due to a larger part of the domain occupied). The relative errors between the occupancy maps also increase during this phase of

fast occupancy of the domain.

These results suggest that, in a homogeneous landscape, the proposed metapopulation model **M2** is the most consistent with respect coarse-graining. However, there might still be numerical errors arising for species having short dispersal values (e.g., species S1). For these short dispersal values, fine graining is necessary in order to correctly approximate the transient states. The main reason for the presence of these errors is related to the technique used for the discretization of the dispersal kernel. When the dispersal length is significantly smaller than the cell size, the discrete kernel used in any simulation does not adequately approximate the dispersal process and more accurate discretization techniques should be employed, as discussed for example by Keith et al. (2018).

4.3.2 Complex GPNP landscape (L2)

Fig. 4.6 shows the time evolution of occupancy (and its associated error) of model **M1** and **M2** for the six invading species (c.f. table 4.1) in the GPNP region (**landscape L2**). The difference between **M1** and **M2** clearly shows the effect of considering self-colonization. Considering for instance species S1 or S4, without self-colonization (**M1**), only the most detailed landscape ($dx = 90$ m) converges to the intended steady state, whereas almost all grain sizes converge to the same steady state for model **M2**. Model **M1** still struggles to reach the same average occupancy for very coarse grains (orange line in Fig. 4.6, **M2**, S1), but the error is not comparable to what is experienced in model **M1**.

To a certain extent, the observed differences in occupancy in model **M2** can still be related to the errors observed above in the flat landscape (error in discretizing the dispersal kernel), but another part is explained by the loss of information on the landscape when coarse-graining it. This is especially visible when comparing species with the same dispersal but different niche width. Considering for instance species S3 and S6: although the dispersal distance is the same for both species, S6 converges to the same value for all considered grains. The difference between the two species is that S6 has a larger niche than S3, and loss in complexity with graining affects it less. Indeed, given the larger niche, species S6 is less sensitive to small losses in suitable area induced by the rescaling, i.e. the averaging of the cell. As such, the impact of graining is highest for species S1, where both dispersal distance and niche width are small, inducing the largest errors in numerical approximation of the dispersal volume and habitat suitability.

Fig. 4.7 shows an example of the occupancy of an invading species in space and time, and the associated difference.

It is interesting to see that the errors in occupancy all seem to stem from overly complex areas,

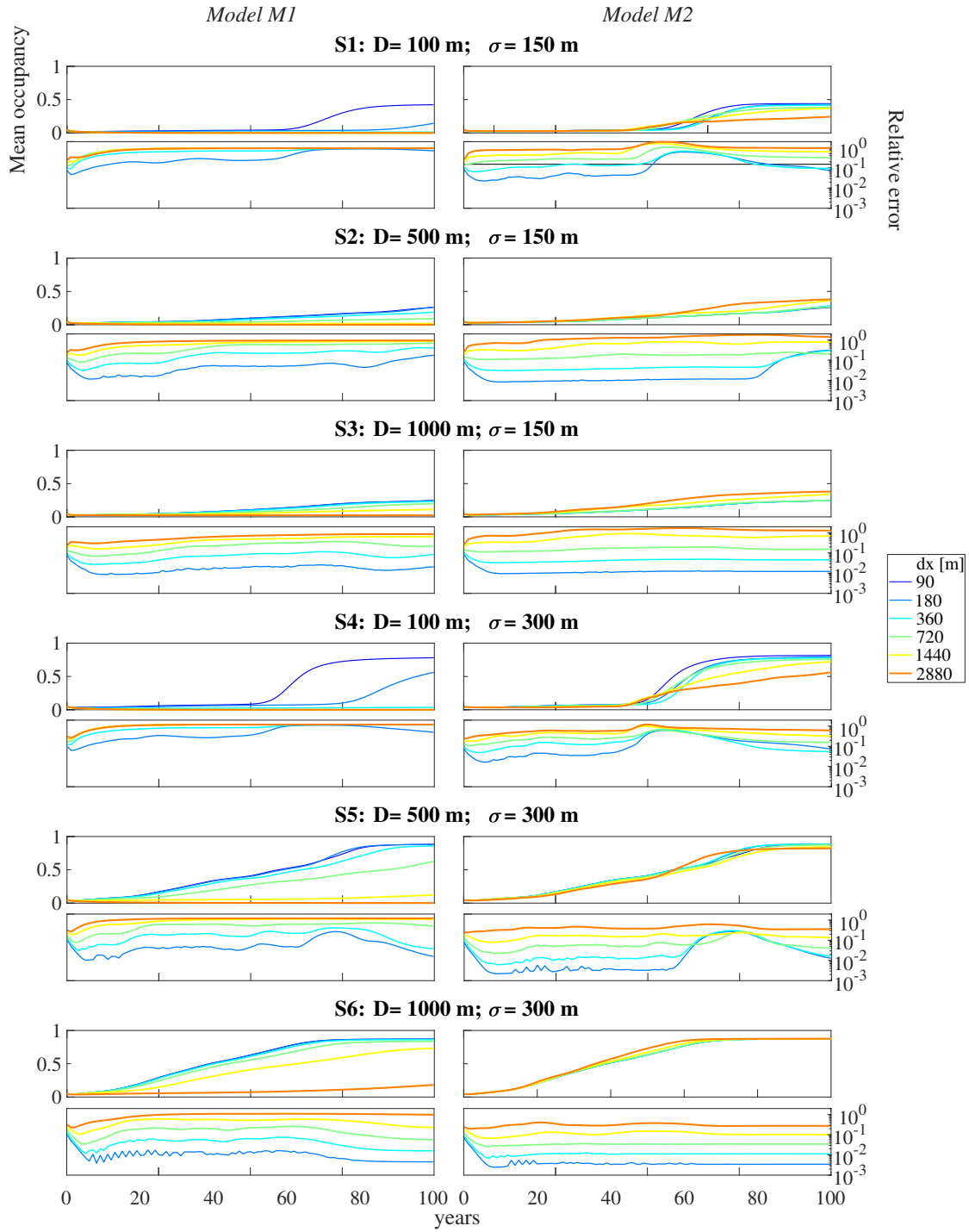


Figure 4.6 – Behavior of the different model formulations under coarse-graining in a the GPNP domain. Landscape L2, GPNP domain. Temporal evolution of the probability of occupancy (averaged over the entire domain) and relative root mean squared error between an occupancy map and the corresponding reference solution obtained at the finest grain size ($dx = 90$ m, dark blue line). Results are depicted for the six species and the six grain sizes considered. The two columns show the results for model **M1** (left), and model **M2** (right) (c.f. section 4.2.4).

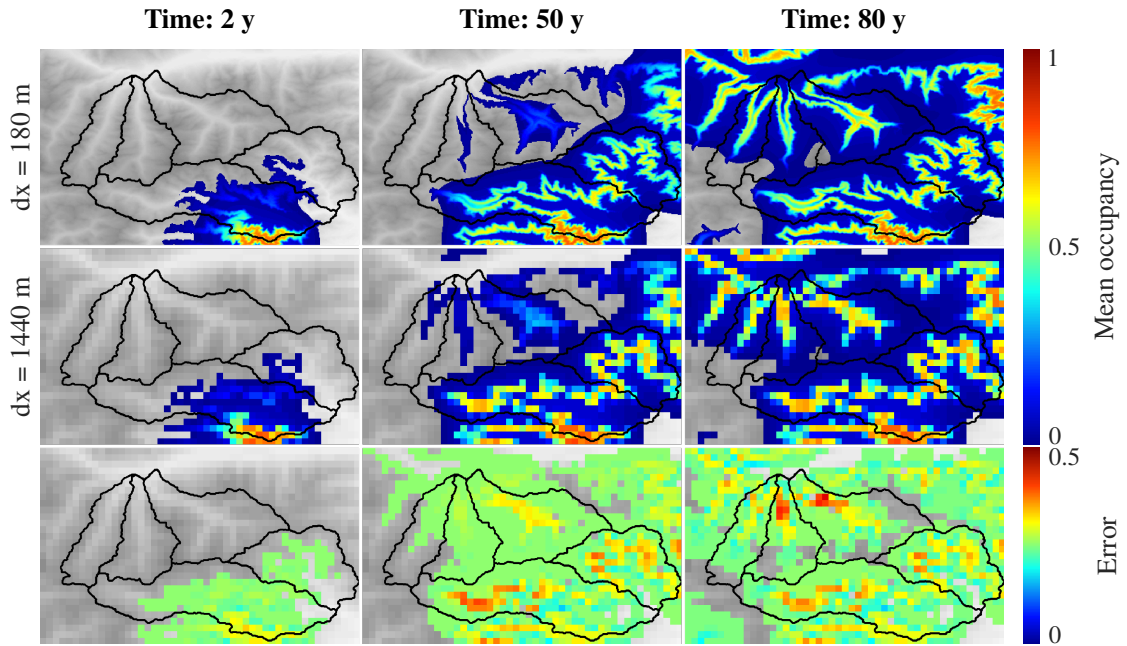


Figure 4.7 – Spatial comparison of probability of occupancy in time. Probability of occupancy for the invading species S2 at three times (2 y, 50 y, 80 y) and for two grains (180 m and 1440 m). The last row shows the error computed when upscaling the occupancy from the 180 m resolution to the coarser resolution.

and mostly from an overestimation of the occupancy of the coarser grid, which is not always the case (c.f. Fig. 4.6 S4 for instance, where the coarser grid underestimates the occupancy). This overestimation could be due to the fact that the heterogeneous cells are averaged to a value closer to the optimal elevation of the focus species, and the inverse effect could mean that the averaging removes favorable area, although the underestimation of the coarse grid observed in species S1 and S4 could also be linked to the small dispersal value.

4.4 Discussion

In this work we propose an innovative formulation of the continuous metapopulation model for the simulation of the probability of presence of a focus species in a landscape represented by a regular raster of cells. The proposed model (indicated with **M2** differs from the traditional metapopulation formulation (indicated with **M0**) in three points:

1. The extinction and colonization rates of the species on a cell are independent from the area of the cell, but might depend on the habitat quality of the cell (e.g. elevation).
2. The coefficients of the discretized dispersal kernel are proportional to the cell areas, in order to preserve the integral of the kernel on the domain.
3. A term of self-colonization is introduced in the model equations in order to consider

the dispersal processes that occur within the cell.

We showed that these properties naturally descend by asking that the model is consistent with coarse-graining, i.e. that the probability of occupancy of a coarse cell is equal to the average of the probabilities computed on the finer-level cells occupying the same surface.

Additionally, the model corresponding to **M2**, but without self-colonization was indicated as **M1**.

To show the benefits of the new metapopulation formulation when dealing with coarse-graining, Models **M0** and **M2** have been compared using numerical simulations on two landscapes, one depicting a flat domain and one depicting the DEM of the Gran Paradiso National Park.

The results described here show that:

- The proposed model **M2** strongly mitigates the numerical errors introduced in metapopulation models **M0** and **M1** when considering different grain sizes.
- Also when using model **M2**, there exists a threshold on the grid resolution which should not be exceeded. In fact, the discretization of the dispersal kernel on large cells might alter the colonization pressure thus affecting the simulation outcome. This is especially relevant for species having a short dispersal, as observed in Fig. 4.5 for species S1.
- Self-colonization appears to be an essential tool in reducing the loss in information occurring from coarse-graining, as evidently shown when comparing models **M1** and **M2** in Fig. 4.6.
- When using coarse grains ($dx = 1440$ or $dx = 2880$) in heterogeneous landscapes, the loss of information in the data describing the cell quality introduces an additional source of error for the metapopulation solution. This error, added to the poor numerical approximation of the colonization pressure, is particularly relevant when species are characterized by short dispersals and small niche widths (see 4.6, species S1, and S2).

4.5 Conclusion

Depending on the species of interest, metapopulation models have been applied in the literature at different scales, considering both local and regional domains. However, when dealing with large domain sizes, only a coarse resolution might be adopted for computational limitations, which might corrupt the model results due to the loss of information on the landscape structure and the introduction of numerical errors. This study shows that, by using a metapopulation model with a graining-consistent formulation, it is possible to identify the grain sizes at which the loss on information becomes critical when simulating the species occupancy.

Conclusions and perspectives

UNDERSTANDING the dynamics of mountain species has, given the current threat to biodiversity with climate change, become increasingly important. In mountainous landscapes, the complexity of the environmental conditions driving the presence of species presents a fundamental challenge for modeling. The goal of this thesis has been to further explore how these complex landscape matrices and changing environmental conditions drive the spatial dynamics of mountain species. The tools developed in the thesis to achieve this goal are based on the metapopulation modeling approach (Hanski, 1998; Hanski and Ovaskainen, 2000; Ovaskainen and Saastamoinen, 2018), which provides a suitable framework for the analyses of dynamical patterns of species distribution. Metapopulation models are particularly attractive for studies on complex landscapes due to their minimalist assumptions in the modeled process, which permits to single out specific effects of the landscape matrix (Fahrig, 2007). Throughout the thesis, Earth observations (EOs) are utilized in order to characterize the habitat, one of the main driver of species presence, and determine its possible temporal changes. The proposed inclusion of EOs within a fitness function describing the cells qualities permits to explicitly consider the landscape features in the model equations, thus adopting a landscape-explicit approach to metapopulation modeling (Purves et al., 2007; Rybicki and Hanski, 2013; García-Valdés et al., 2013).

Metapopulation models integrating EOs have been the main instrument of analysis to address the following research questions: 1) how geomorphology, here considered as one of the main habitat feature, impacts the persistence of a species under a climate change scenario (chapter 2); 2) how to extrapolate scarce spatial and temporal sampling (in this case referring to real data of carabids species in the GPNP) to capture temporal variations of species occupancies on a large area (chapter 3); and 3) how the low resolution in the description of the landscape matrix due to coarse-graining might impact connectivity and, thus, the modeled description of species occupancy (chapter 4).

To answer these questions, three independent, but evidently connected, research studies constituted the core chapters of the thesis. The main results obtained per chapter are summarized here.

- Chapter 2 was dedicated to the relation between geomorphological complex landscapes and the fate of species under climate change, investigating the integration of long-term climate forcing into metapopulation modeling. The chapter showed that the landscape structure, which defines the distribution and connectivity between areas, strongly influence whether a species can persist in a given landscape, and its fate under climate change. The landscape-explicit metapopulation model permitted to successfully distinguish between the different fates that a focus species might face: extinction during climate warming, linked to reduction of habitat or lag of the species (i.e. would the species survive in the post-climate change landscape if ported there), extinction debt, and finally species survival, with increased and decreased presence. These different fates have been linked to hypsographic curves and landscape attributes.
- Chapter 3 presented a novel framework for the application of a metapopulation model to the simulation of carabids dynamics by combining EO-based products and spatially-and temporally-scarce *in-situ* data. The developed modeling strategy permitted to integrate short-term regionally-correlated environmental drivers into the fitness function representing the temporal-varying quality a cell in the metapopulation model.

The challenge of identifying the model parameters in the context of discrete and spatiotemporal scarce sampling, has been tackled by developing a consistent parameter calibration approach. The strategy adopted, which combines species distribution models and iterative particle filters, allowed to address typical difficulties intrinsically-linked to dynamical models, such as spin-up periods, estimation of initial presence, and limited spatial anchor points for likelihood computation. In particular, an innovative observability operator considering imperfect detectability of species is introduced to link the model results to the available *in-situ* data. The proposed approach provided a consistent method to integrate *in-situ* and EO-based data in a dynamic population model.

- Chapter 4 investigated the consistency of the metapopulation model with graining, and proposed a formulation of the model which accounted for grain size in the landscape-explicit gridded approach. This feature is fundamental when one requires to change the domain resolution, but avoiding the difficult and computational expensive process of re-calibration. In this chapter, algebraic considerations and numerical simulations were used to deduce the assumptions of the metapopulation formulation that reduce the impact of coarse-graining, which are: (i) the coefficient approximating the dispersal should be dependent on the cell areas, (ii) the extinction and colonization rates should not change during the process of coarse-graining, and, (iii) the model should include a term of self-colonization. Even under these assumptions, the modeling results highlighted the presence of relevant errors in the solution when the focus species has a dispersal distance much shorter than the grain dimension. These errors are due to a combination of two factors: (i) numerical errors in the discretization of the dispersal processes, and (ii) changes in the spatial connectivity of the landscape representation due the loss of

accuracy in the environmental features with coarse-graining.

From the conclusions of these individual studies, the following final remarks can be stressed.

The present thesis suggests, through a number of theoretical results and evidence from case studies, that landscape-explicit approaches are fundamental tools in metapopulation modeling in order to incorporate the spatial heterogeneity of a complex mountainous landscape into long- and short-term predictive models of species distribution. Through the relatively low complexity of the model itself, the simulation results clearly highlight the impact and interactions of the intricate underlying governing processes of extinction and colonization with the landscape matrix. Indeed, the modeling framework considered in the thesis, the metapopulation model in its continuous and stochastic formulations, is based on a minimalist approach in terms of ecological processes represented, i.e. species extinction, dispersion, and colonization. Although certain assumptions on the focus species are required for the direct application of the model (Hanski, 1998; Moilanen, 2004; Ebenhard, 1991; Ovaskainen and Saastamoinen, 2018), the simplicity in the processes is fundamental to understand the importance of landscape features in the species spatial distribution. This result is not achievable when adopting more complex ecological models (Moilanen, 1999; Etienne et al., 2004), where the convoluted relations between model processes and estimated parameters often prevent one to depict a clear picture of the ongoing dynamics. A clear advantage of this approach with respect more complex ecological models is that the relative small number of parameters permit an easier calibration process. In a context such as this one, where the availability of *in-situ* data describing the species presence is often limited, reducing the number of parameters permits a general and realistic understanding of the regional trends and dynamics of the focus species, which would not be possible with more complex models. The thesis further shows that the inclusion of spatially-correlated fluctuations in the environmental features results in the explicit representation of the stochasticity of species presence, and positively contributes to the explanatory power of short- and long-term predictions of species presence. These main results of the thesis are achieved thanks to the integration of two factors in the model equations: (i) the use of a fitness function to explicitly relate the patches quality to the features of the heterogeneous landscape matrix (here represented by elevation, slope, and aspect), and (ii) the introduction of temporal-dependent drivers, which explicitly represent the changing in the environmental conditions (e.g. temperature, wetness, greenness and brightness). Incorporating these two features in metapopulation models leads to a landscape-explicit approach that offers a reasonable and reliable compromise between generality, precision and realism of the results. The developed landscape-explicit metapopulation model is the key to this analyses, and, constitutes a solid basis for future modeling work of metapopulation dynamics.

From the bulk of this work, certain perspectives and outlooks can be formulated.

1. It is important to underline that further environmental features can be included in the

description of the species' fitness and habitat quality. Two of such features are land use and land cover. Although these factors are typically adopted in ecological models, they were not considered in this thesis since less relevant in the area of interest (the protected area of the Gran Paradiso National Park) and for the focus species (carabids). Incorporating these two factors into the definition of habitat quality would permit, for instance, to analyze the human pressure on the focus species. As possible strategy to incorporate human pressure in the model, one can compute an index representing the degree to which a certain area is dominated by human activity. This index should then be inserted in the fitness function and suitably weighted with respect to the other environmental factors thanks to calibration on *in-situ* data. Finally, the model simulations would evaluate the impact of changing this index on the species' presence. It can be said with confidence that significant work will be soon surfacing in the literature regarding this topic.

2. A second possible improvement to the model concerns the use of more complex dispersal kernels that better describe of the connectivity of the landscape. Due to computational restrictions, the dispersal kernel adopted in this thesis is only dependent on the two-dimensional Euclidean distance among patches, which, for certain species, might not be a realistic representation of the dispersion path. A more suitable approach, however computationally expensive, would be to explicitly consider the heterogeneity of the landscape in the dispersal process, by incorporating the quality of the landscape directly into the distances used in dispersal matrix, and thus effectively reshaping the dispersal kernel (Graves et al., 2014; Bertuzzo et al., 2016). Species movement could be favored when moving through patches having suitable qualities, and on the contrary, more difficult when moving through unfavorable terrains (Ewers and Didham, 2006). In the model adopted here, this quality-dependent dispersal is implicitly present, given that the extinction is driven by the quality of the target patch, effectively limiting the possibility of a species to further disperse from this patch. Nevertheless, including the quality of the patch in the dispersal kernel would lower the probability of the species to arrive at the given patch in the first place, forcing it to move through more favorable terrain, movement corridors (Ricketts, 2001). Note that graph-base approaches have proposed to incorporate such movement corridors in the definition of the network by changing the weight of link between patches (Urban and Keitt, 2001; With, 2004; Albert et al., 2013). Including this process in a landscape-explicit metapopulation model would permit to more accurately model the movement of a species through the landscape in time.
3. A third modeling aspect that might improve the results for certain species concerns the adoption of a more realistic description of the colonization process. Given that local populations in newly colonized areas are more prone to extinction, the extinction rate can decrease in time once an empty patch has been occupied (Ebenhard, 1991). In

the extreme case, this would lead to age-structured metapopulations, where the age of the different individuals or groups of individuals is considered, as done in Akçakaya et al. (1995); Akçakaya (2000); Anderson et al. (2009). Combining these approaches with landscape-explicit metapopulation models might provide greater insights in the persistence of a species at the local level, but calibrating such complex models might prove difficult.

4. A whole field where in perspective the work presented in this thesis may be extended concerns the relation between spatial relevant network structures and metapopulation persistence. Recalling classic work on this subject (Gilaranz and Bascompte, 2012; Gilaranz et al., 2017) where the relationship between network structure and metapopulation persistence stemming from the embedded ecological dynamics was investigated, it is reasonable to assume that an approach akin to the metapopulation model extensions of the type pursued in chapters 2 and 3 apply to other complex substrates for ecological interactions. In particular, one wonders whether river networks seen as ecological corridors (Rinaldo et al., 2020) may be looked up closely in the light of a *ad hoc* landscape matrix including hierarchical habitat capacity. This, of course, would be predictable on the basis of geomorphological analyses (Rodriguez-Iturbe and Rinaldo, 2001) whose relevance was shown by contrasting fish biodiversity data and neutral models in the Mississippi river basin (Muneepeerakul et al., 2008; Rodriguez-Iturbe et al., 2009) and experimentally in the laboratory study of networked communities of protists (Carrara et al., 2012, 2014).

Integrating and modeling all these processes and added complexity is of course possible, and highly interesting. Nevertheless, one has to consider that this is only possible either in simulations, or when complex data sets are available, given that adding processes results in a larger number of parameters to be calibrated. For instance, the inclusion in the model of population demography, which specifically describes the exchange of individual between age groups of different local populations, requires mark-recapture data, which are highly expensive to gather, both in term of money and human effort.

The availability of species data is, of course, one of the most relevant issues when considering long-term predictions, as in the case of modeling the impact of climate change. In this case, long-time series of observations of species presence are required to make meaningful predictions, given that the uncertainty of ecological models explode quickly in time. Predicting the presence of a species for the next century based on, for example, four years of data seems rather difficult. This advocates for long-term monitoring efforts as undertaken in the Gran Paradiso National Park, which are greatly needed for advances in theoretical and applied ecology.

One of the main tenets of this thesis lies in the iterative process of gaining feedback from field

Conclusions & perspectives

evidence and Earth observations, thus building on expert knowledge to correct models and methods. This loop centered on models and their assimilation of data is deemed critical for improving ecological forecasts, whether near- or long-term. It certainly has been advocated that iterative, near-term forecasting will accelerate ecological research and, in the process, making it more relevant to society in relation to informed and sustainable decision-making. However, long-term predictions need the scenarios that only modeling may provide. In this sense a metapopulation dynamics framework, as the one developed in this thesis, may represent a good starting point for several variations on the same theme.

Although ecologists have made considerable progress in applying computational and statistical tools, plenty of opportunities exist for improving forecast-specific theory, methods, and infrastructure in the process, prompting change in scientific training and cultural habits, in particular towards the power and flexibility of computational environmental sciences.

A Appendix of chapter 2

Simulation and additional results

As described in Figs. 1 and 5 of the main text, the experiment is done in several steps, the details of these steps are presented here. The initial stage is designed to identify the species supposed to exist in the landscape, the ‘native’ species. To this intend the experiment is run from a fully occupied landscape until reaching a steady state (step 0). For each species, this first step is repeated a 100 times, and species with at least 50% of the runs leading to at least one cell in the landscape being occupied are considered to be native species. The results of this step are shown in Figs. A.1, A.5, A.9, A.13, A.17, A.21, A.25, A.29 and A.33, left the count of the species with at least one occupied cell at steady state, and center the initial average fraction of occupied cells.

The spatial occupancy generated after the initial step (state 1) is then used for step 2. For species with less than 100 runs leading to occupied landscapes, the remaining initial configurations are generated by bootstrapping from the other occupied configurations. Climate change is then applied, following the reasoning described in the methods (step 2). The fraction of occupied cells after this step (state 2) is depicted in Figs. A.1, A.5, A.9, A.13, A.17, A.21, A.25, A.29 and A.33 (right). Here, a first classification is done: the species being able to track climate change, vs the species unable to track climate change (going extinct). For the species going extinct, an additional simulation is done (step 4 and 5), the landscape is again fully occupied and run to steady state, but with the species’ optimal elevation after climate change. This allows to differentiate between species going extinct because they are unsuited, and species going extinct because they are unable to track the change but would have been able to survive in the new conditions. The number of runs leading to these outcomes are displayed in Figs. A.3, A.7, A.11, A.15, A.19, A.23, A.27, A.31 and A.35 (left and center).

The last step (step 3) is run to see which species were able to follow climate change, but are

actually not suited to the new conditions, the extinction debt, and, once at steady state, to see which species increase or decrease their presence.

Finally, taking into account the fates towards which the different steps of the simulation lead, a classification can be made for each species, which can be seen in Figs. A.4, A.8, A.12, A.16, A.20, A.24, A.28, A.32 and A.36 (center).

Figs. A.1 to A.36 present the results and the intermediate steps of the simulation of the experiment for the different landscapes of interest: Roof, Pyramid, Cone in a square, OCN (0,1,2,3), Gran Paradiso National Park (IT) and Alpes Vaudoises (CH).

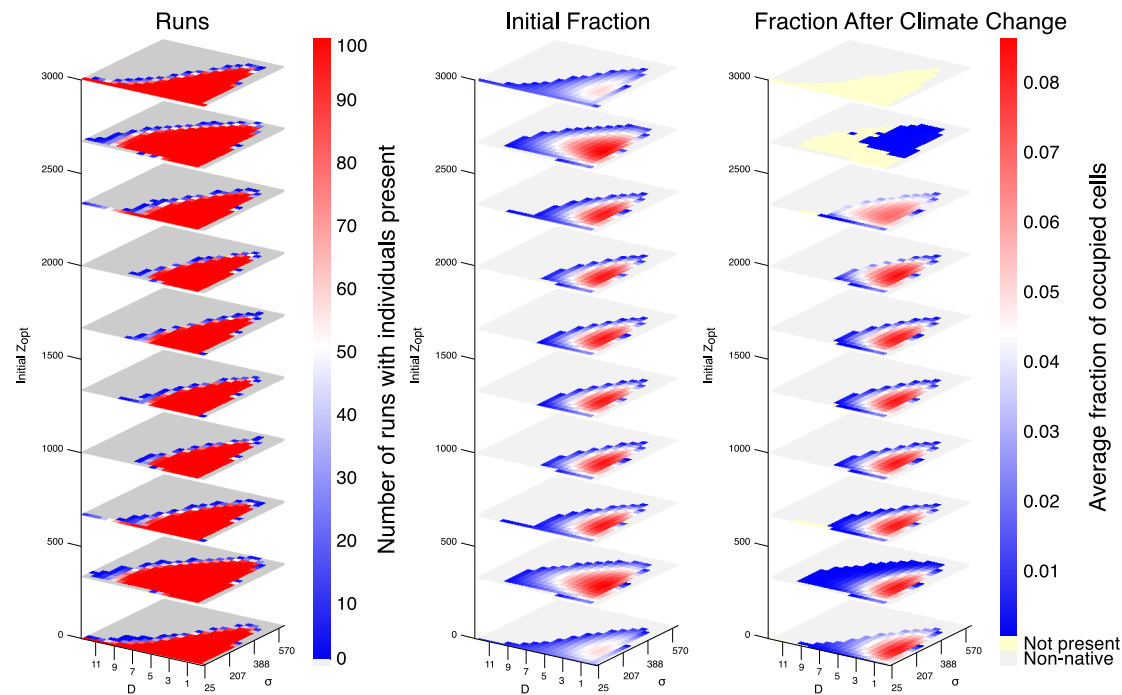


Figure A.1 – Intermediate results for the ‘Roof’ landscape. Number of runs leading to at least one occupied cell after the initial phase (left). Average fraction of occupied cell in the 100x100 grid-system over 100 runs, after the initial phase (center), and after climate change (right).

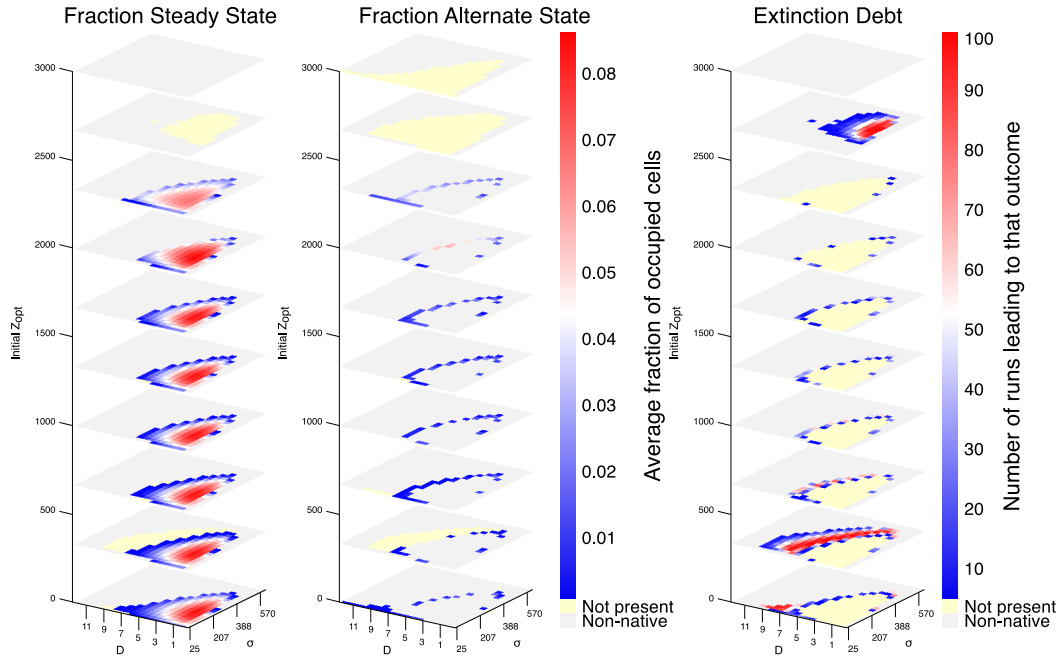


Figure A.2 – Intermediate results for the ‘Roof’ landscape. Average fraction of occupied cell in the 100x100 grid-system over 100 runs, at steady state after climate change (left), and at the alternate state for the species going extinct during the climate change phase (see methods) (center). Number of runs leading to the fate ‘Extinction debt’ for each species (right).

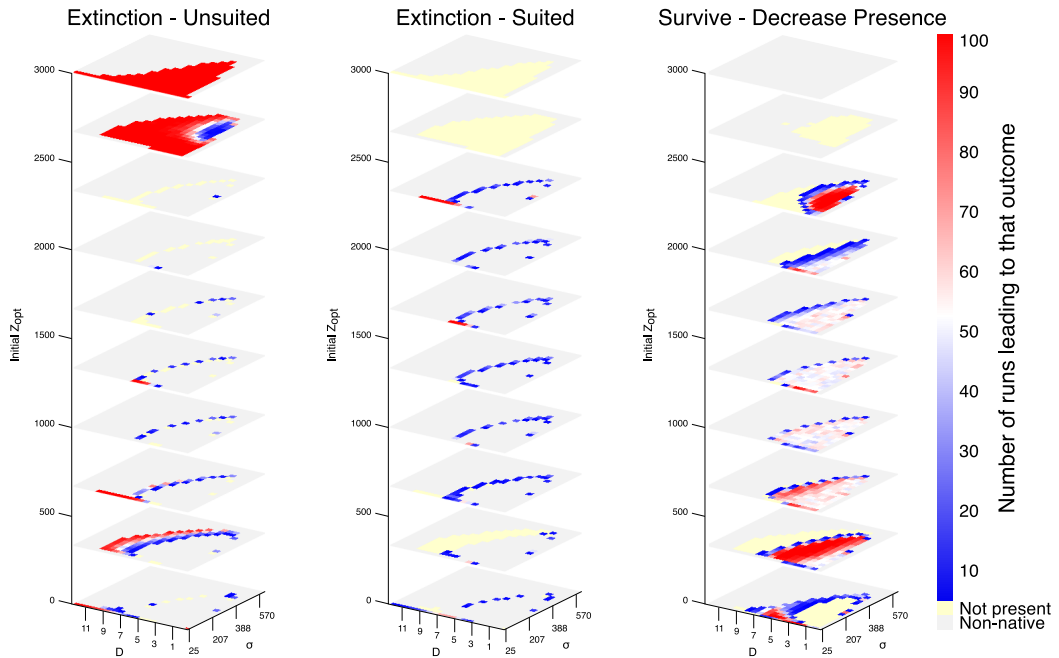


Figure A.3 – Intermediate results for the ‘Roof’ landscape. Number of runs leading to the fate ‘Extinction unsited’ for each species (left), ‘Extinction sited’ (center) and ‘Survive - Decrease Presence’ (right).

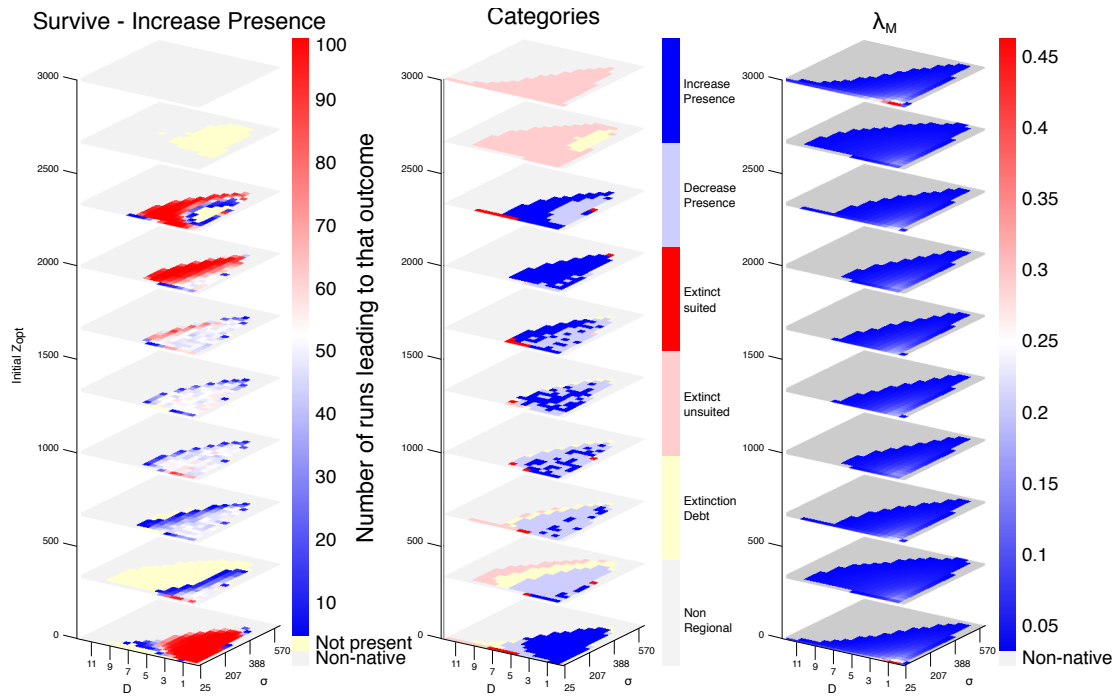


Figure A.4 – Intermediate results for the 'Roof' landscape. Number of runs leading to the fate 'Survive - Increase Presence' for each species (left). Classification of the most probable outcome for each species based on the previous figures (center). λ_M -value for each species, defining the threshold value of e/c for species survivability in the landscape (right).

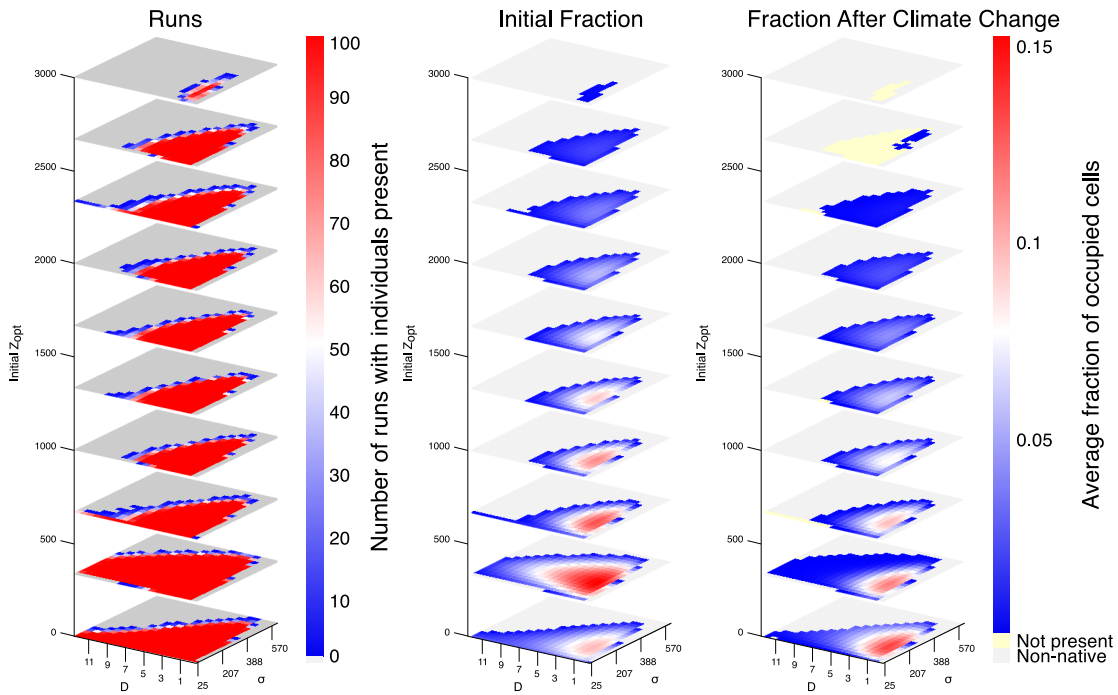


Figure A.5 – Same as Fig. A.1 but for the Pyramid

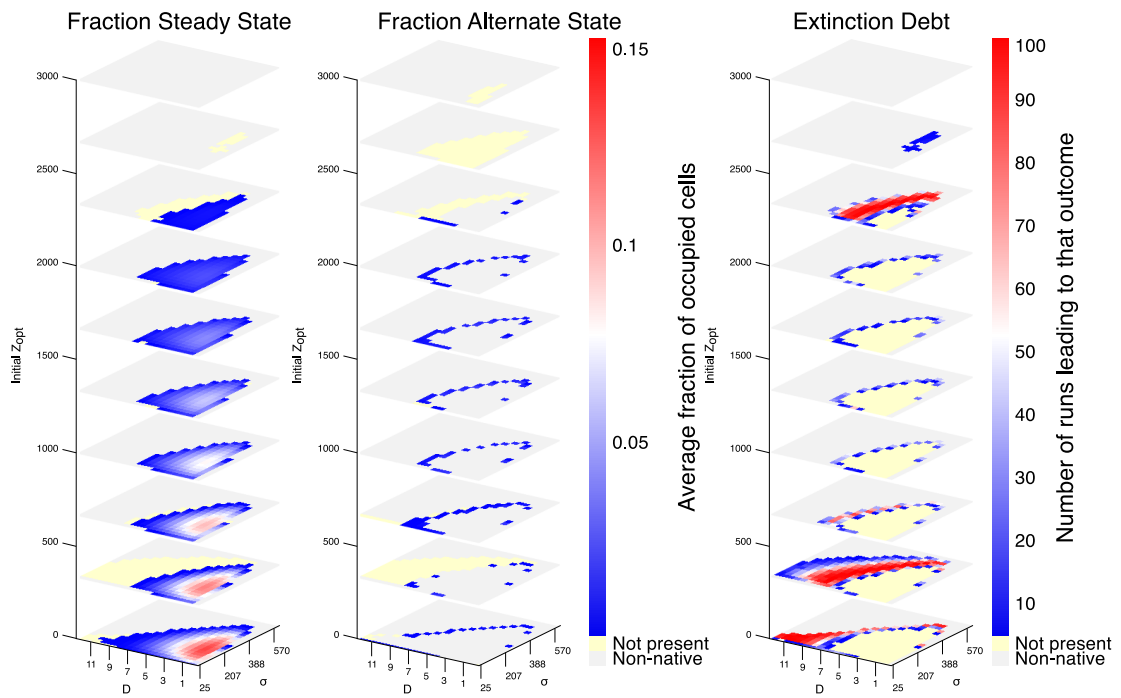


Figure A.6 – Same as Fig. A.2 but for the Pyramid

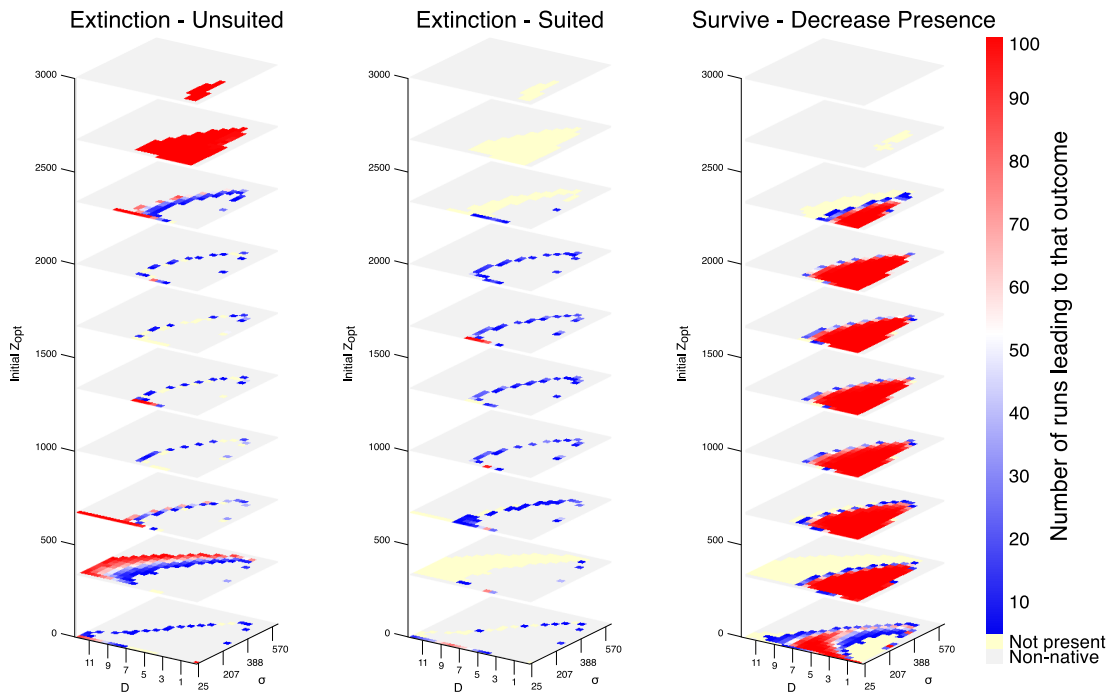


Figure A.7 – Same as Fig. A.3 but for the Pyramid

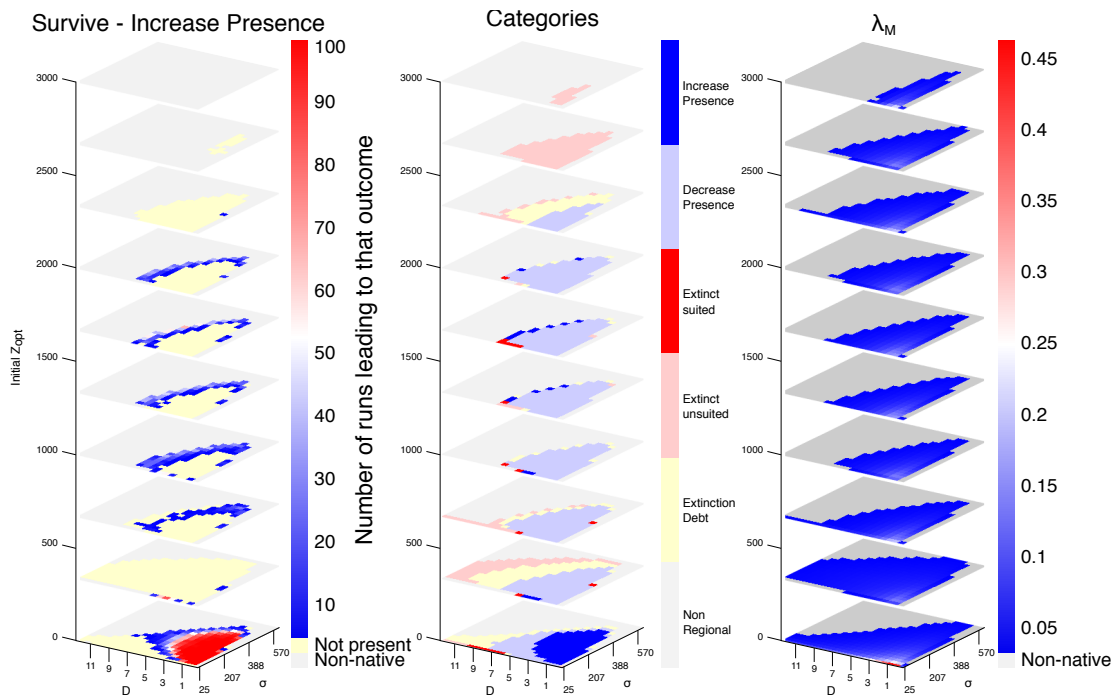


Figure A.8 – Same as Fig. A.4 but for the Pyramid

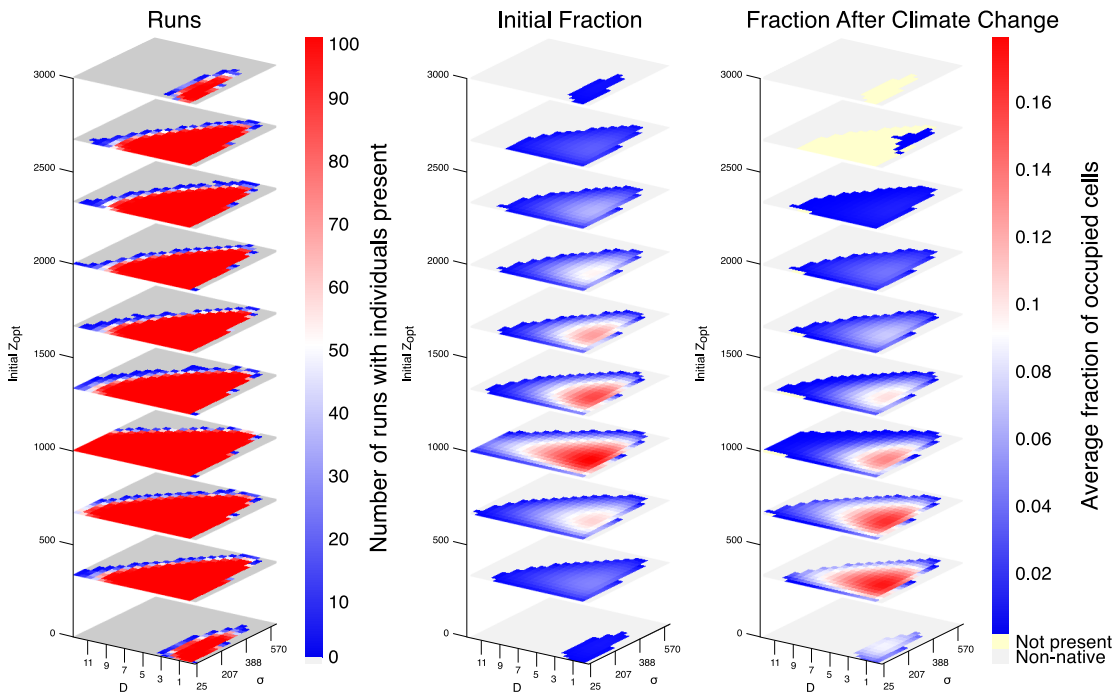


Figure A.9 – Same as Fig. A.1 but for the Cone in a square

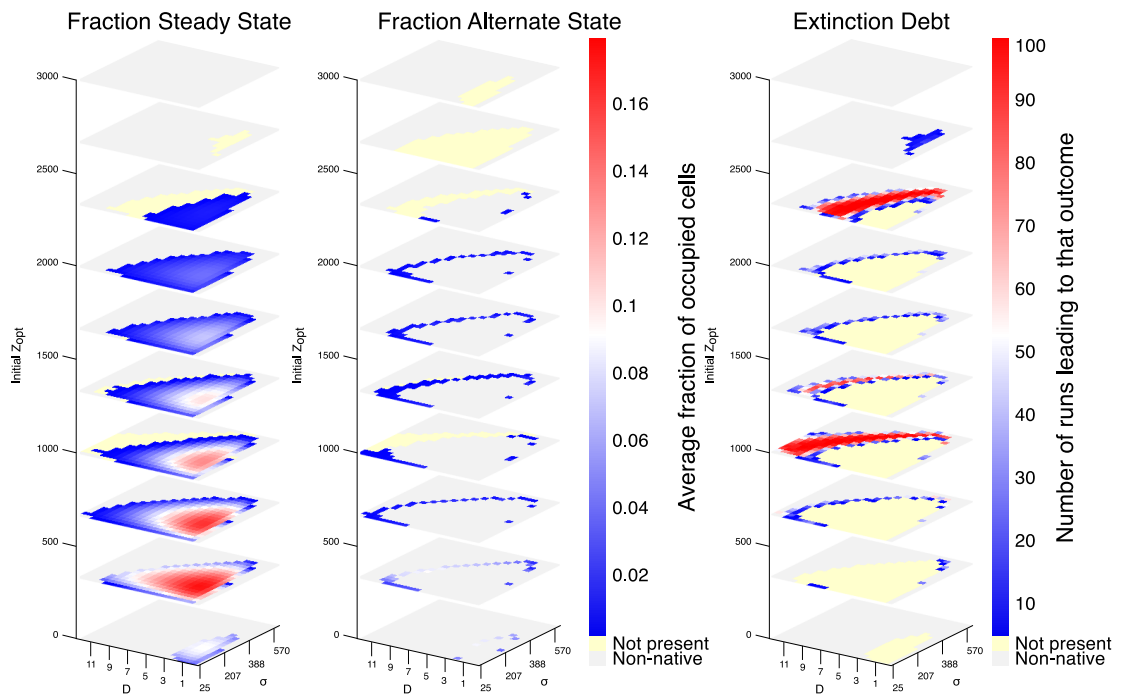


Figure A.10 – Same as Fig. A.2 but for the Cone in a square

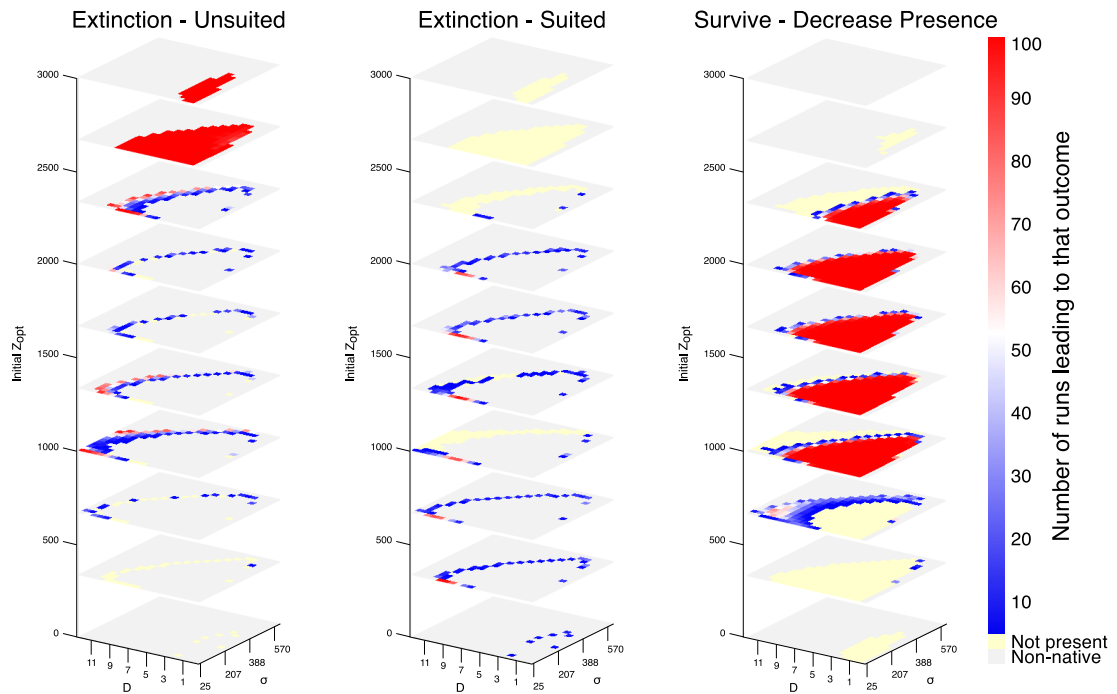


Figure A.11 – Same as Fig. A.3 but for the Cone in a square

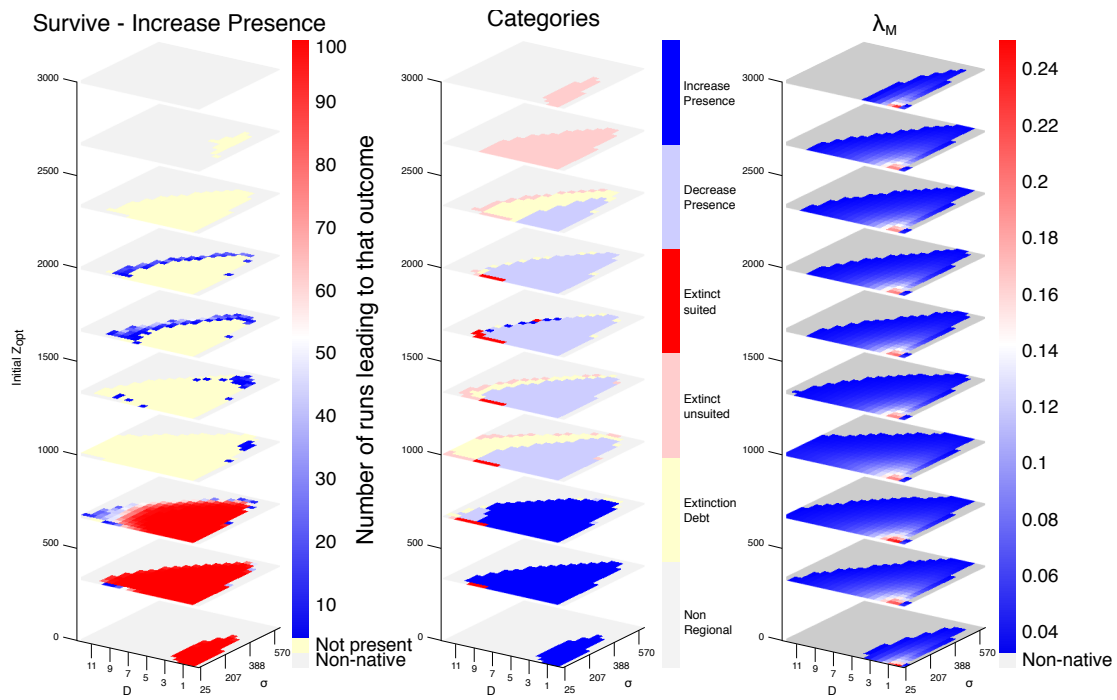


Figure A.12 – Same as Fig. A.4 but for the Cone in a square

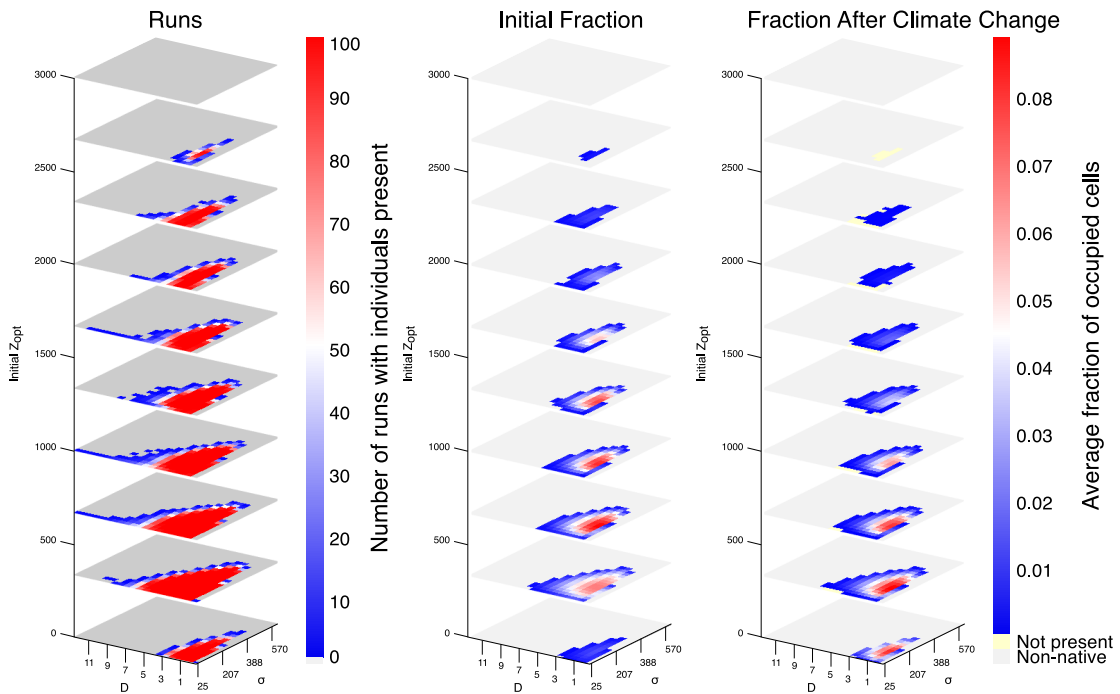


Figure A.13 – Same as Fig. A.1 but for the OCN

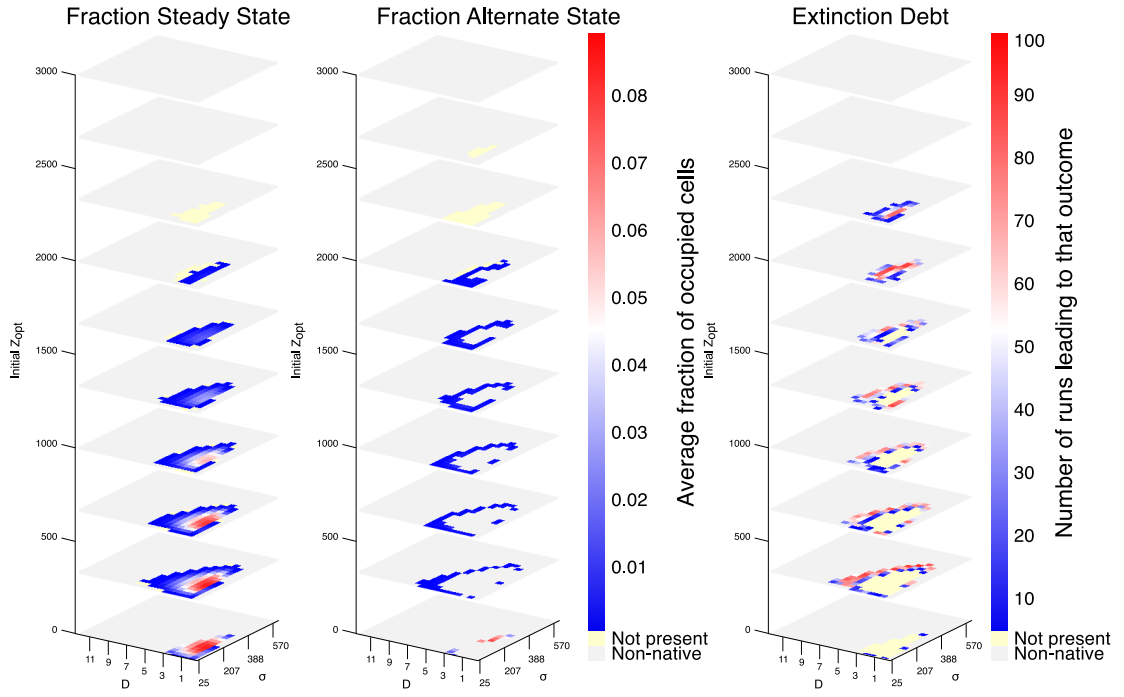


Figure A.14 – Same as Fig. A.2 but for the OCN

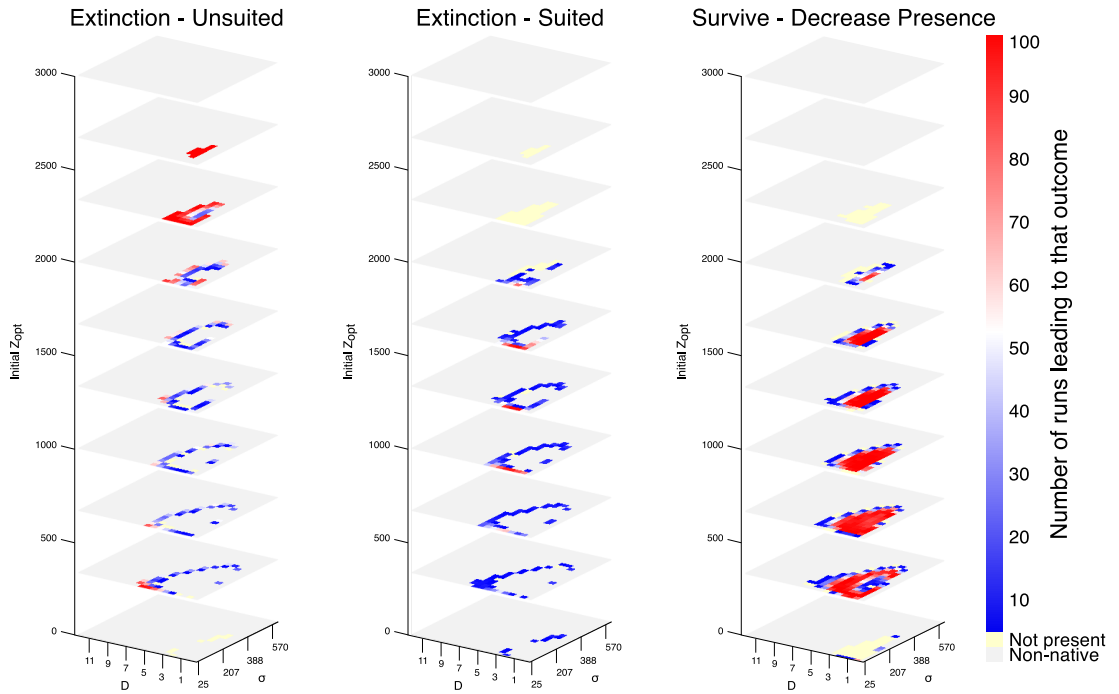


Figure A.15 – Same as Fig. A.3 but for the OCN

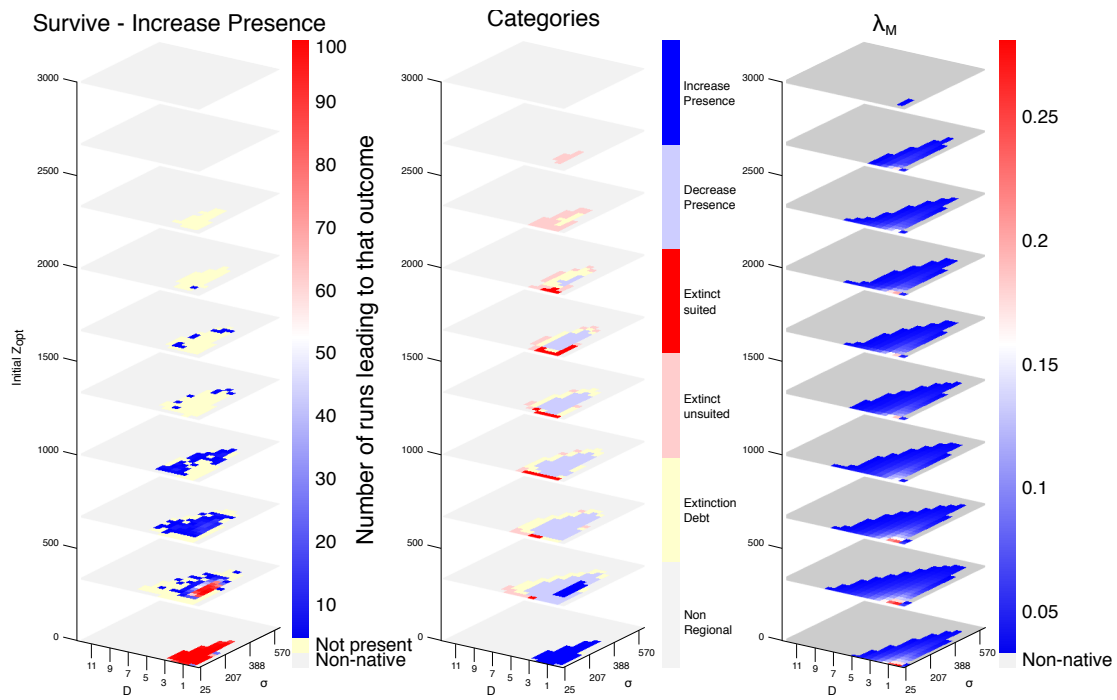


Figure A.16 – Same as Fig. A.4 but for the OCN

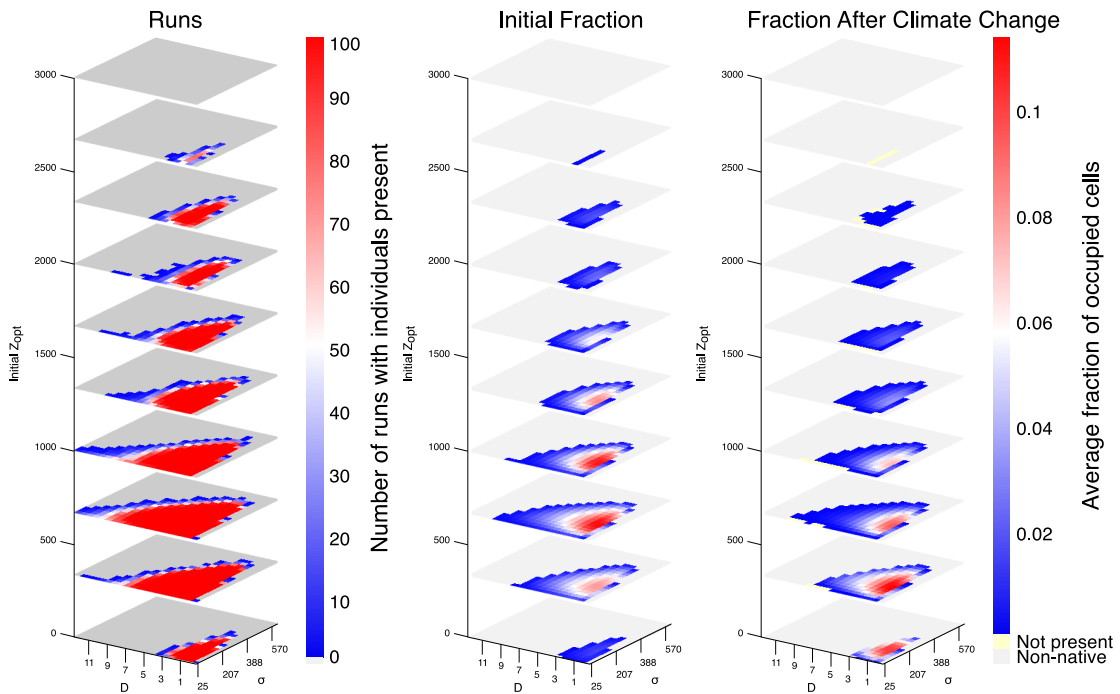


Figure A.17 – Same as Fig. A.1 but for the OCN1

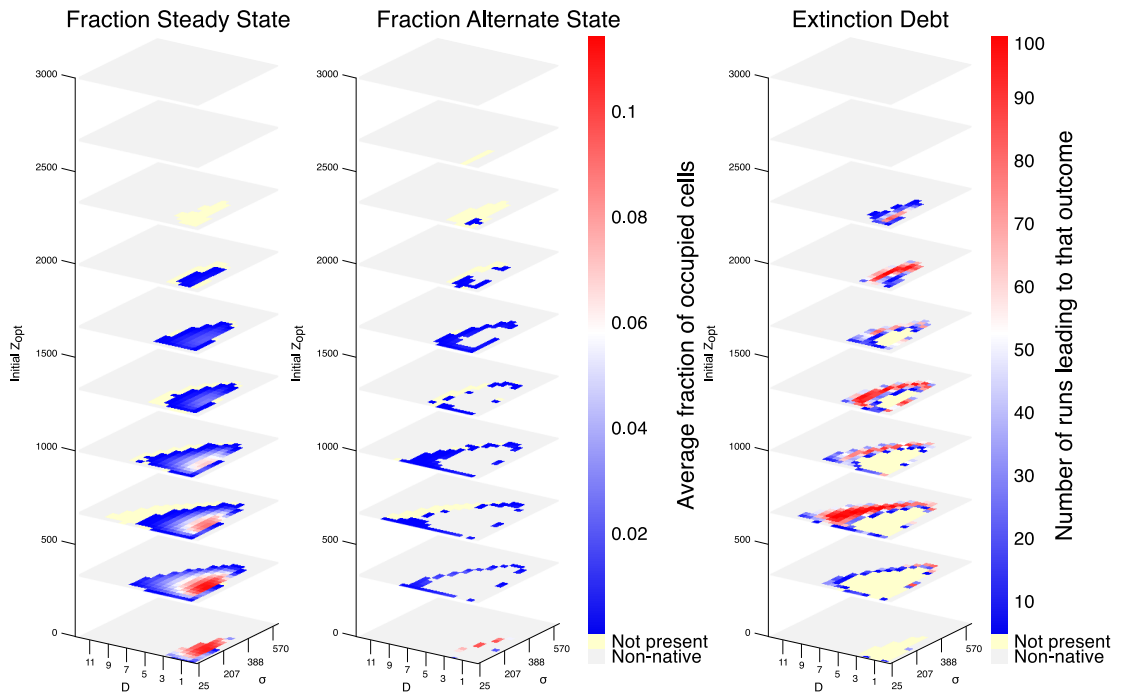


Figure A.18 – Same as Fig. A.2 but for the OCN1

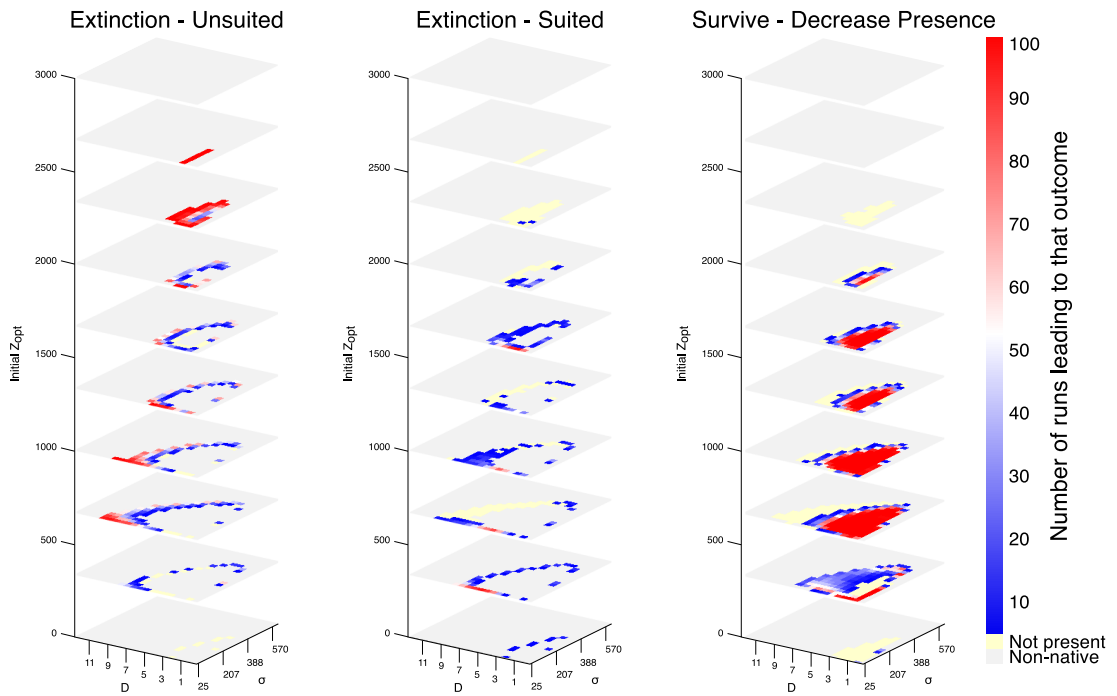


Figure A.19 – Same as Fig. A.2 but for the OCN1

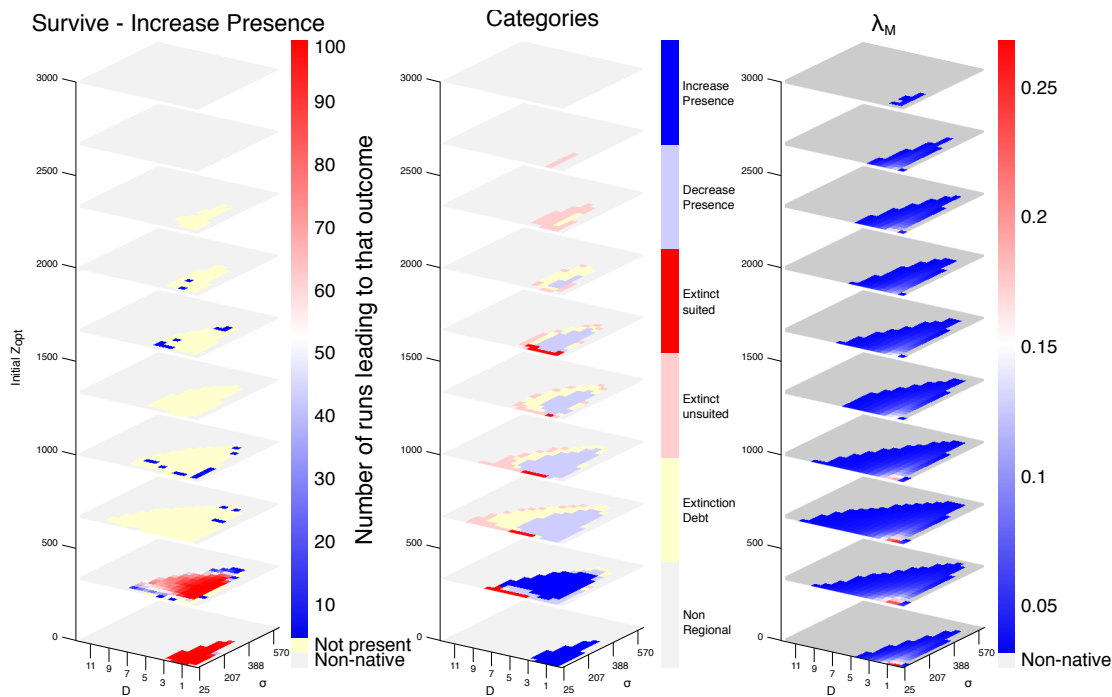


Figure A.20 – Same as Fig. A.2 but for the OCN1

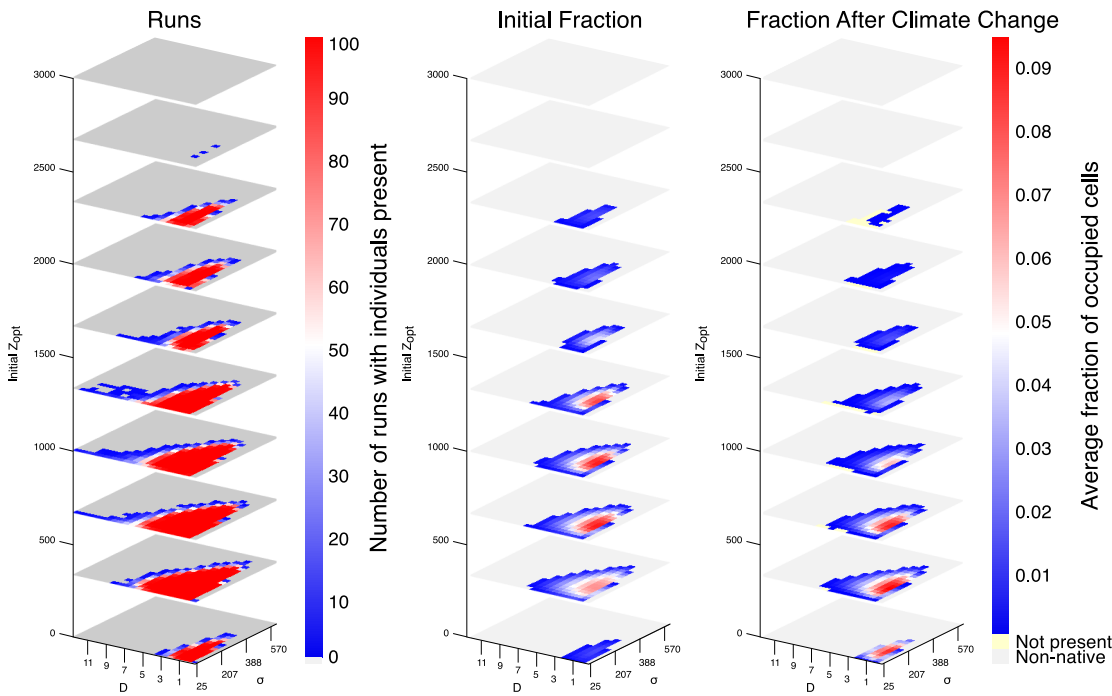


Figure A.21 – Same as Fig. A.1 but for the OCN2

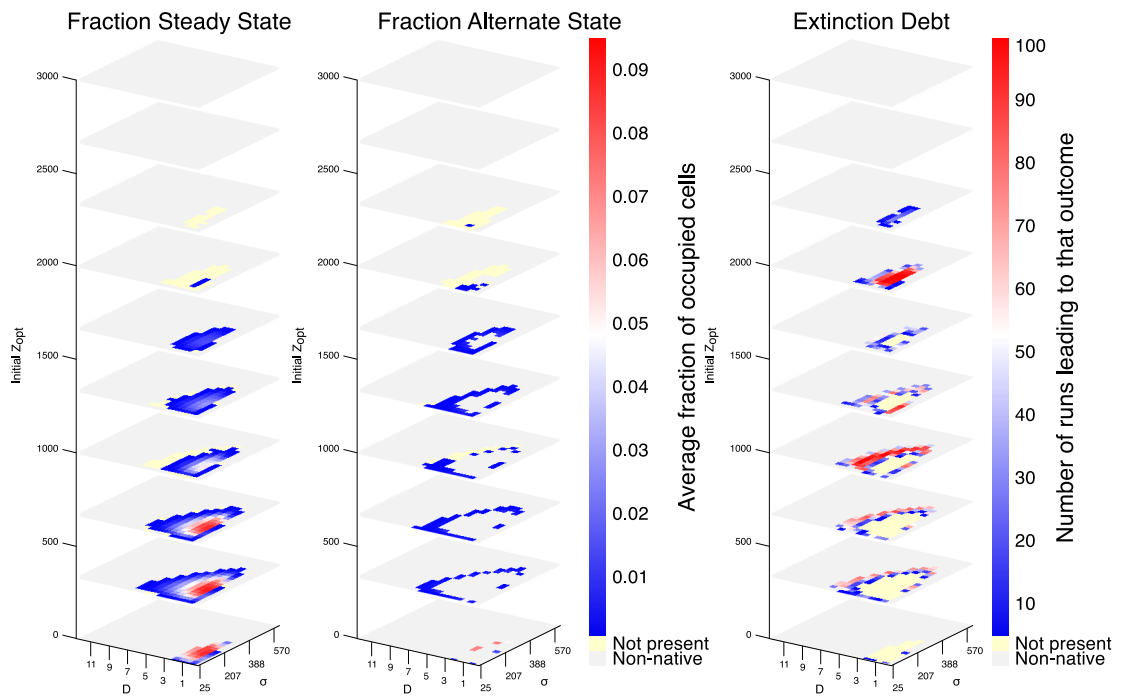


Figure A.22 – Same as Fig. A.2 but for the OCN2

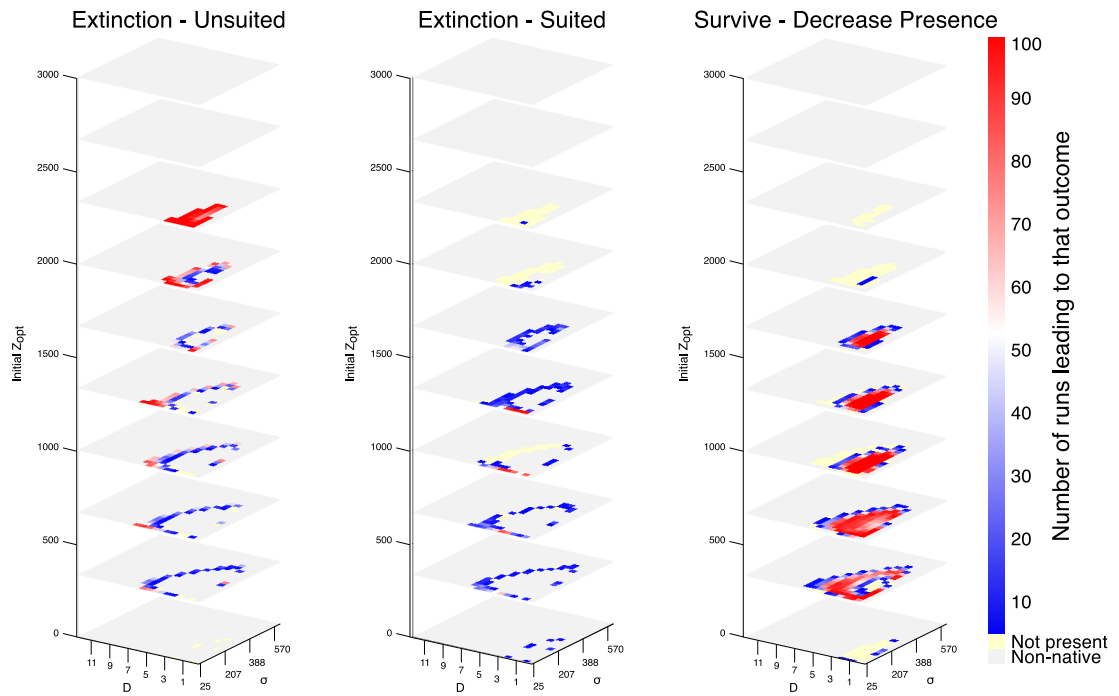


Figure A.23 – Same as Fig. A.3 but for the OCN2

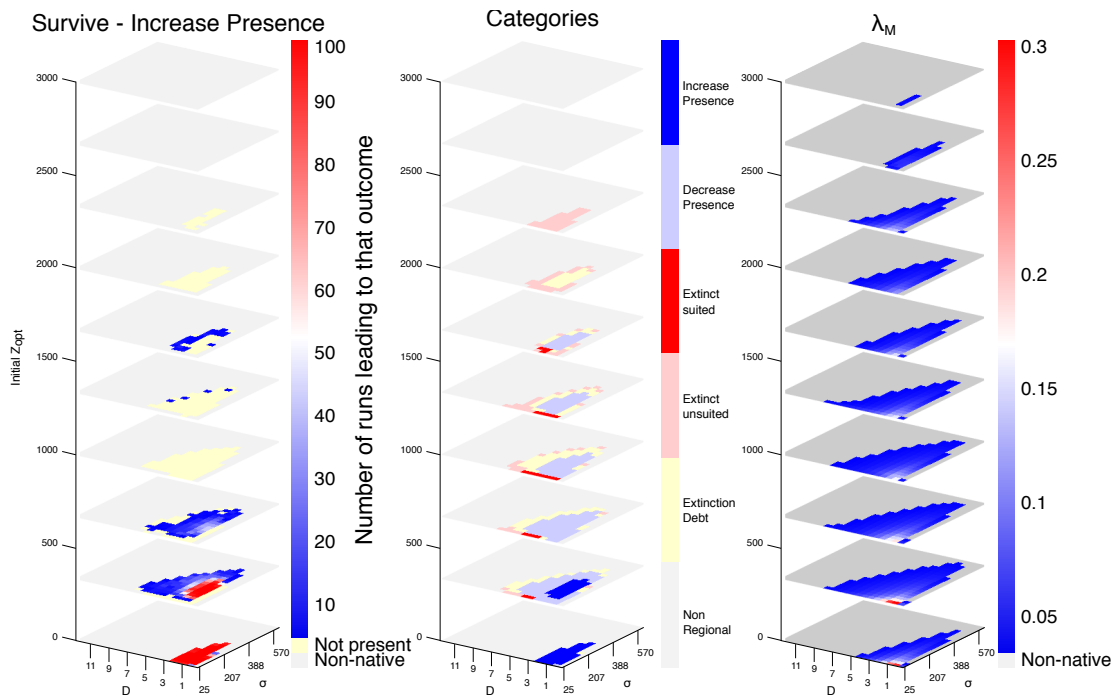


Figure A.24 – Same as Fig. A.4 but for the OCN2

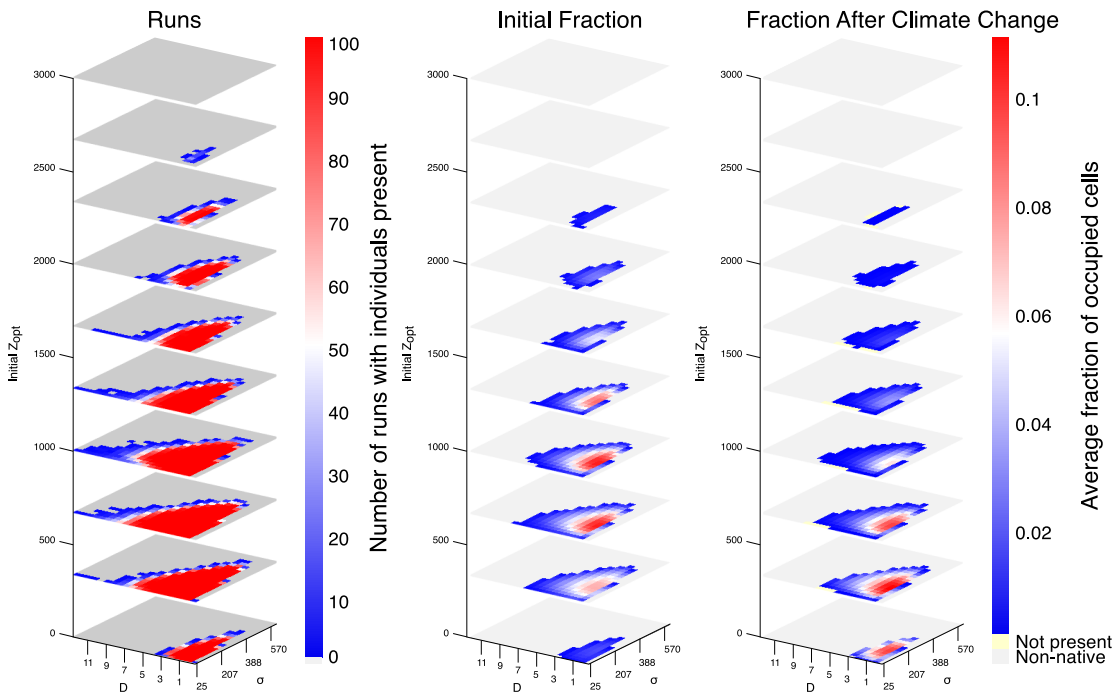


Figure A.25 – Same as Fig. A.1 but for the OCN3

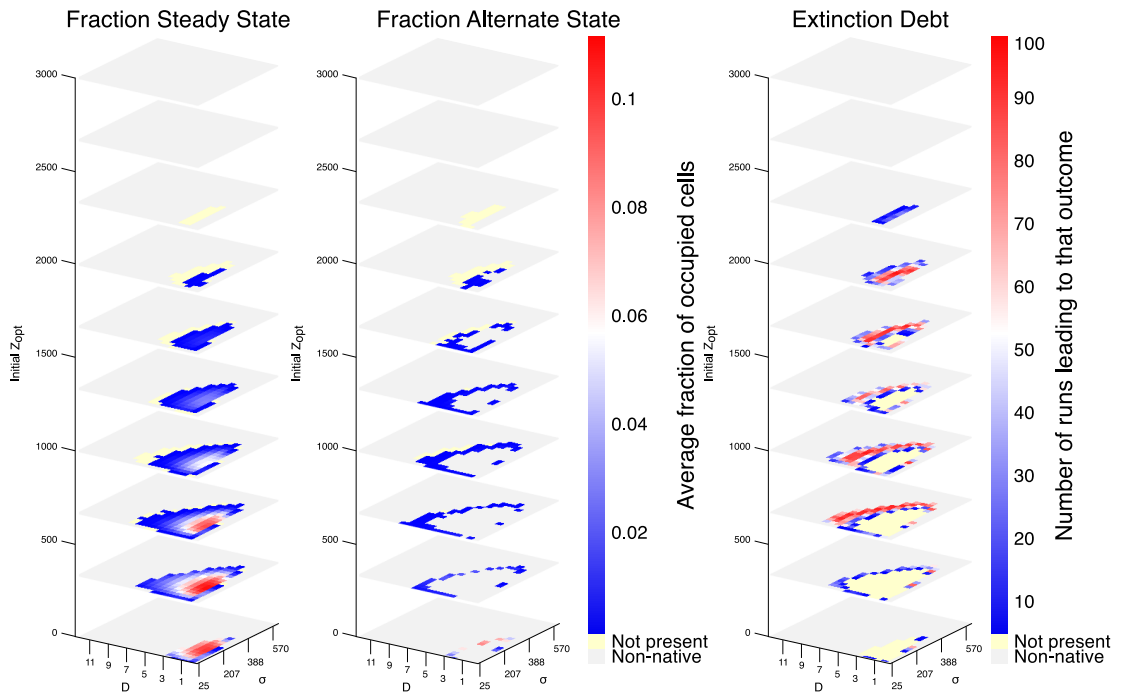


Figure A.26 – Same as Fig. A.2 but for the OCN3

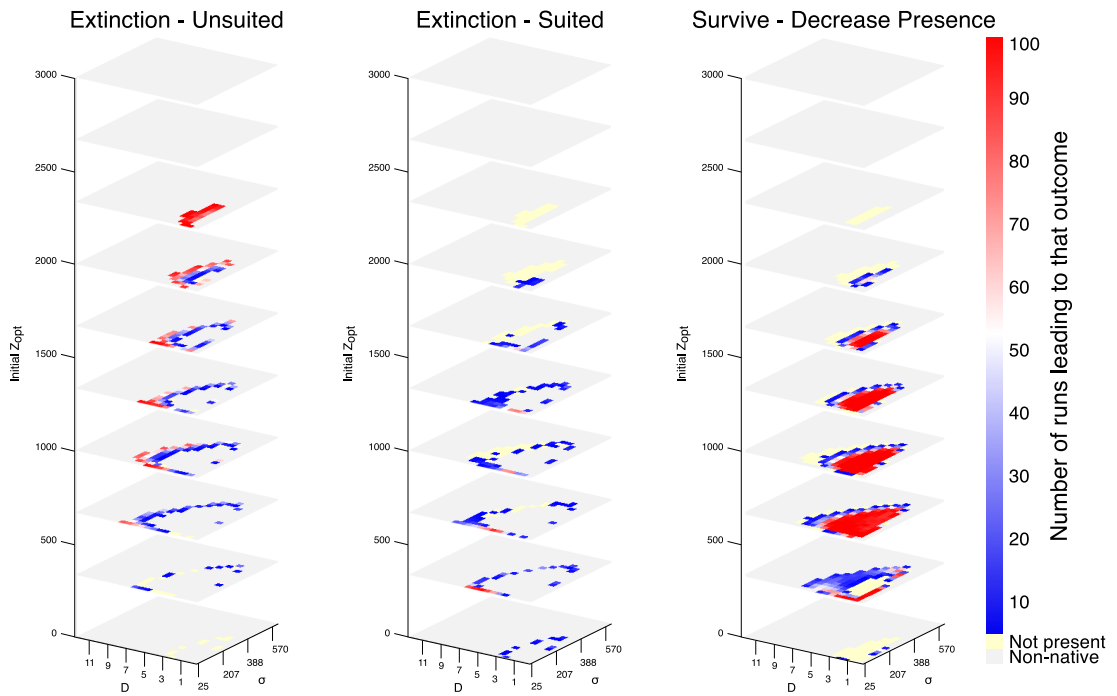


Figure A.27 – Same as Fig. A.3 but for the OCN3

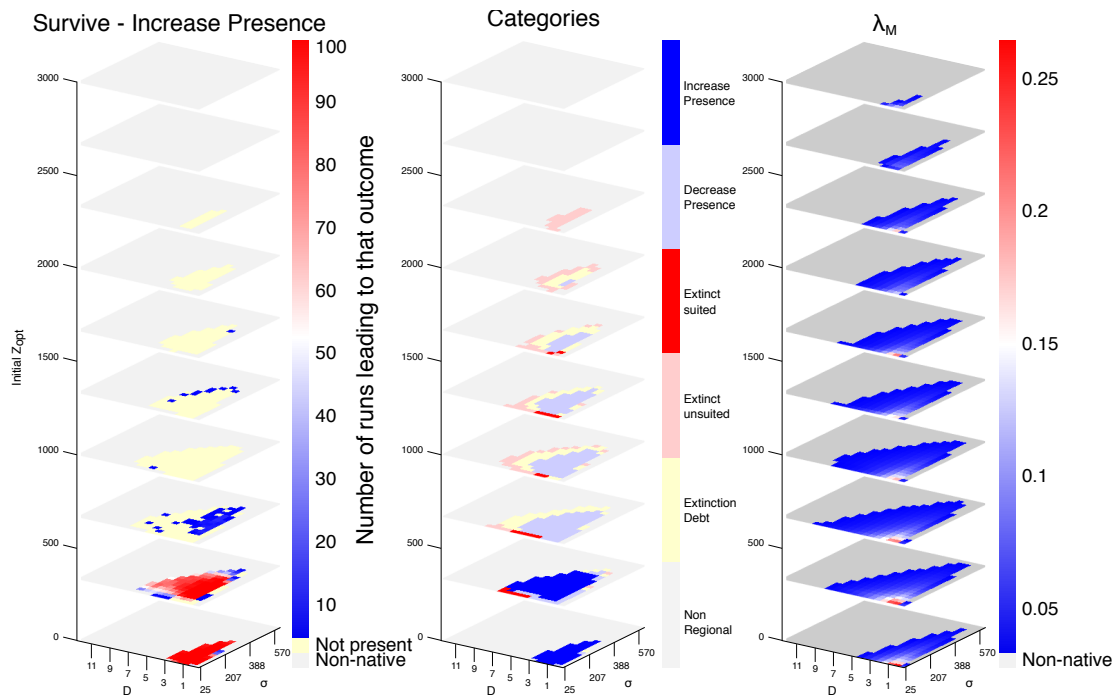


Figure A.28 – Same as Fig. A.4 but for the OCN3

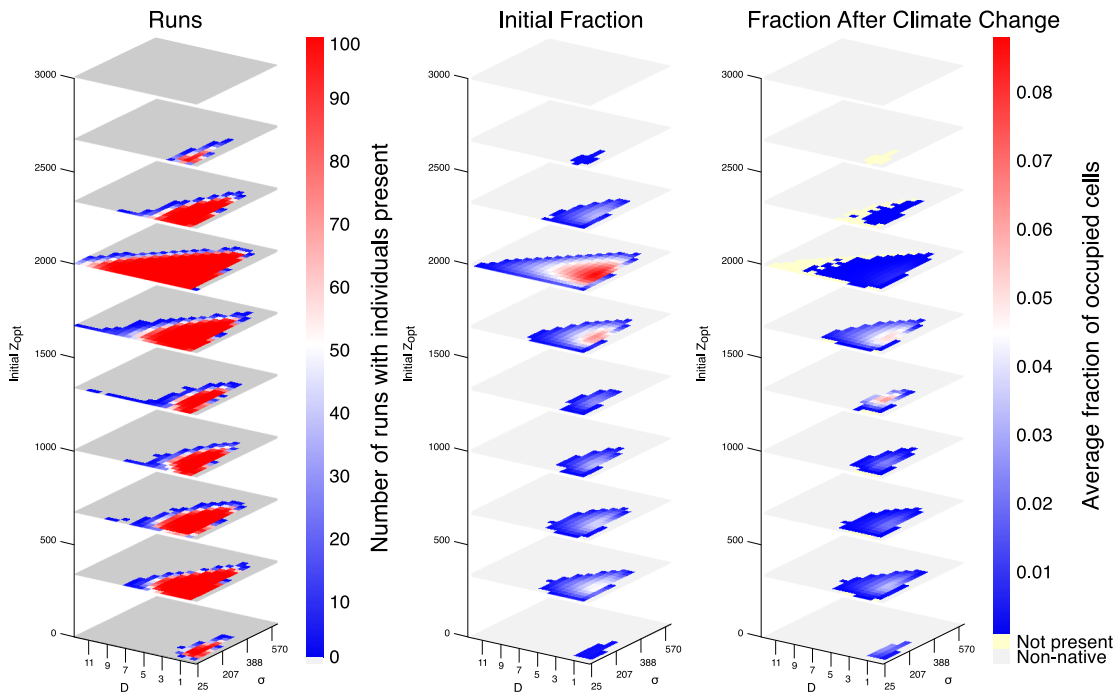


Figure A.29 – Same as Fig. A.1 but for the GPNP

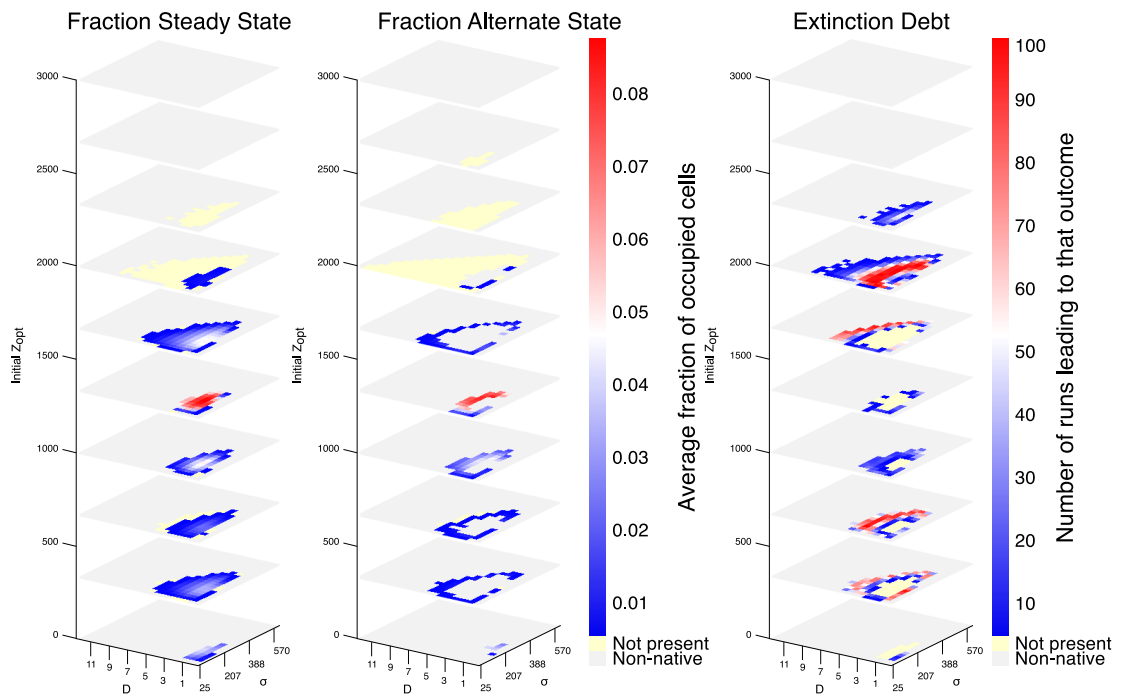


Figure A.30 – Same as Fig. A.2 but for the GPNP

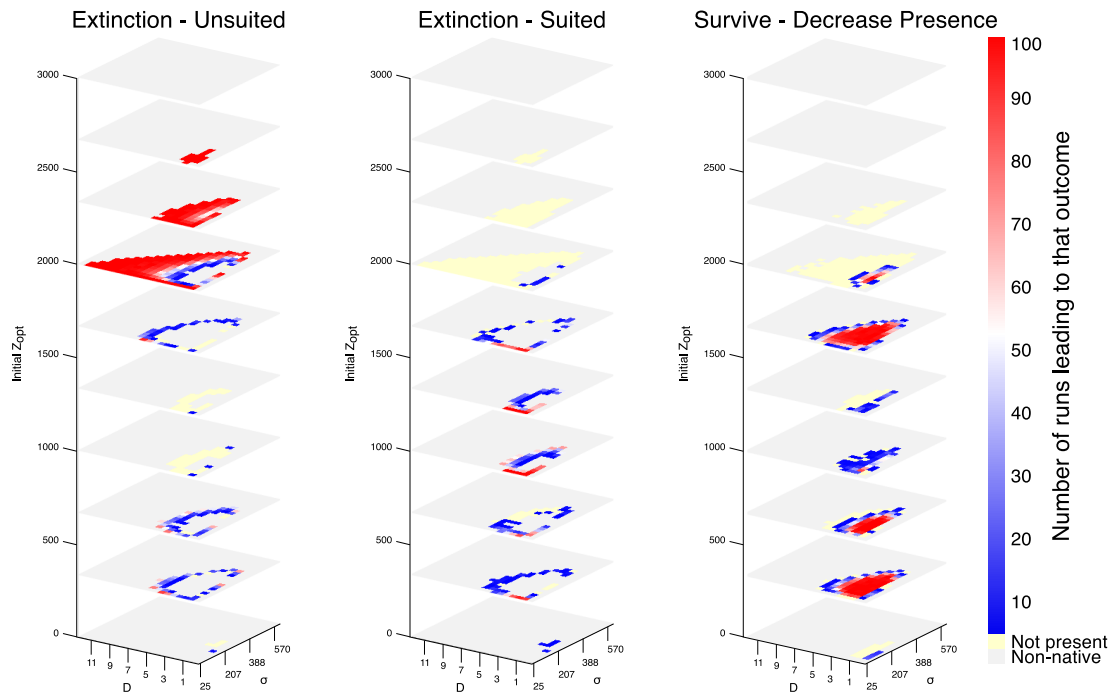


Figure A.31 – Same as Fig. A.3 but for the GPNP

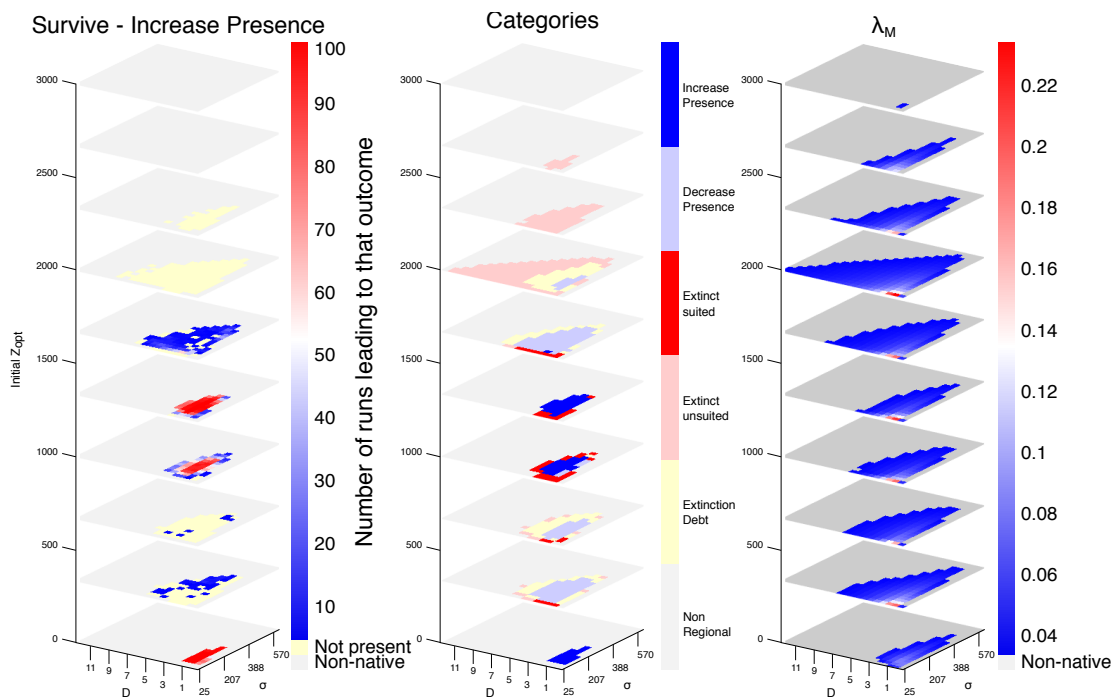


Figure A.32 – Same as Fig. A.4 but for the GPNP

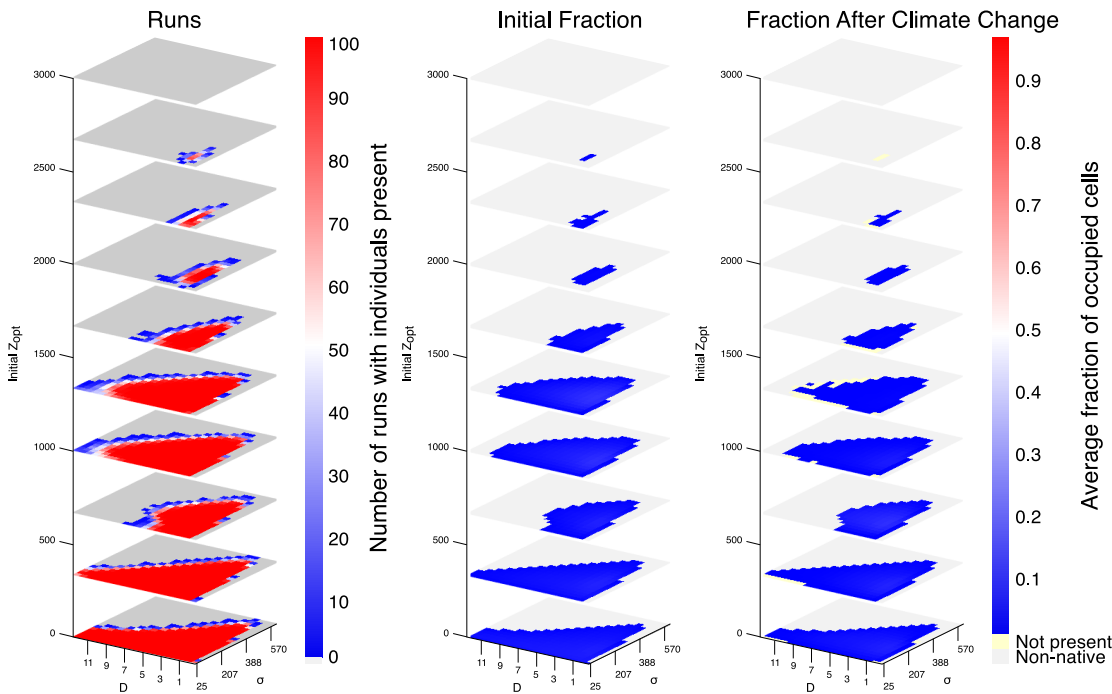


Figure A.33 – Same as Fig. A.1 but for the Alpes Vaudoises

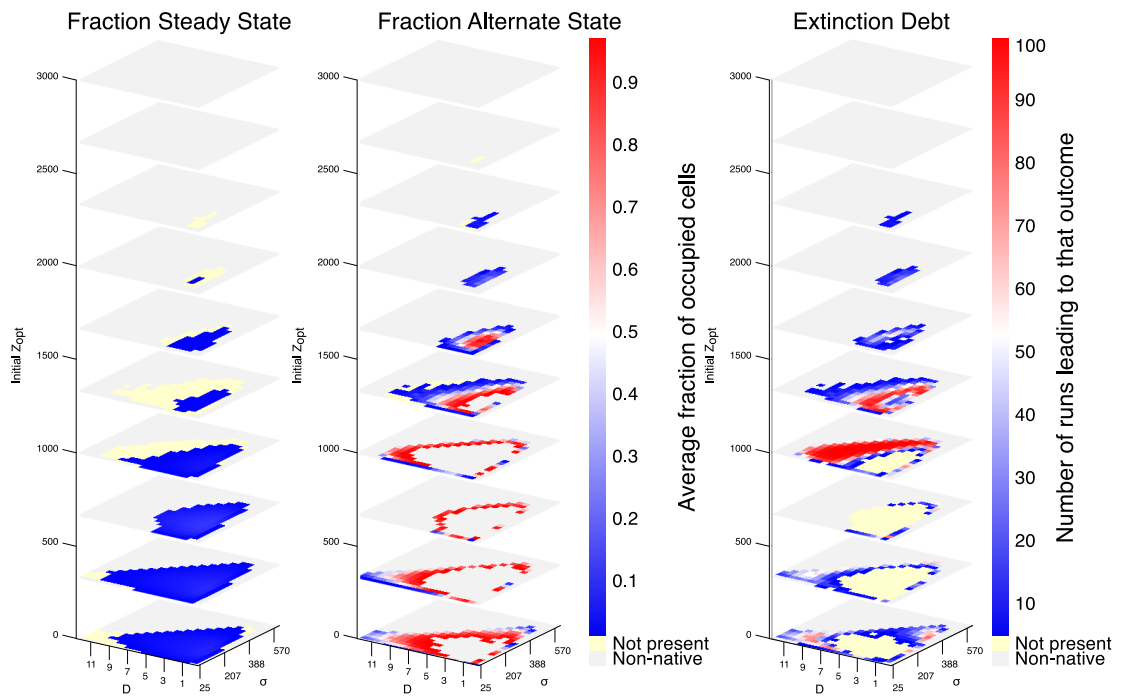


Figure A.34 – Same as Fig. A.2 but for the Alpes Vaudoises

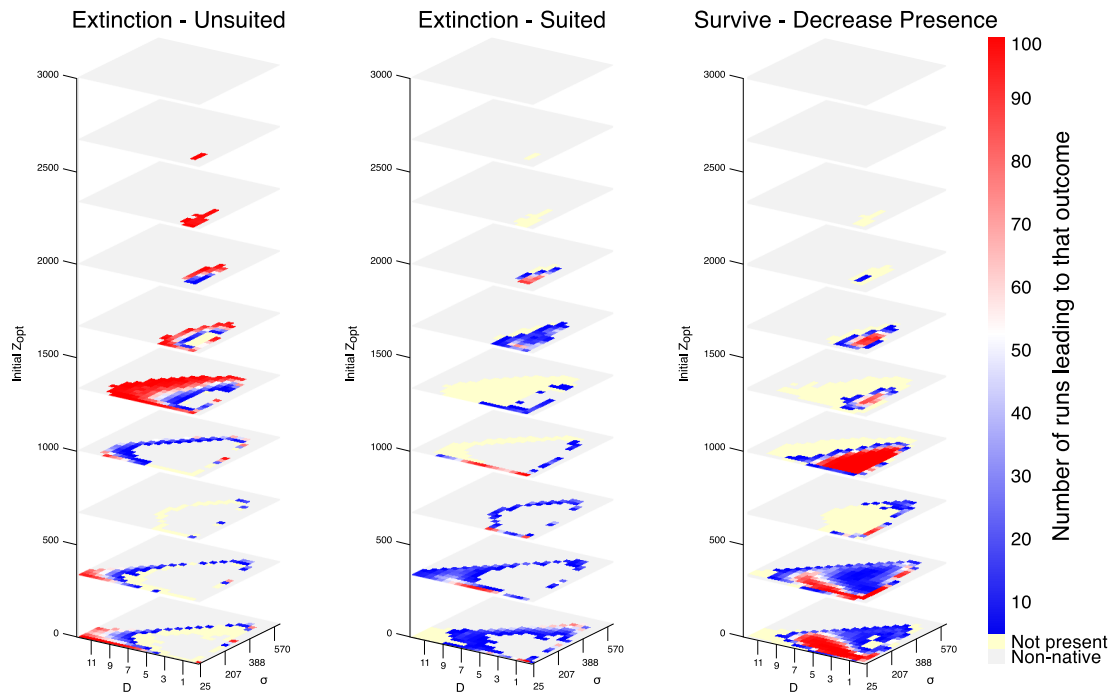


Figure A.35 – Same as Fig. A.3 but for the Alpes Vaudoises

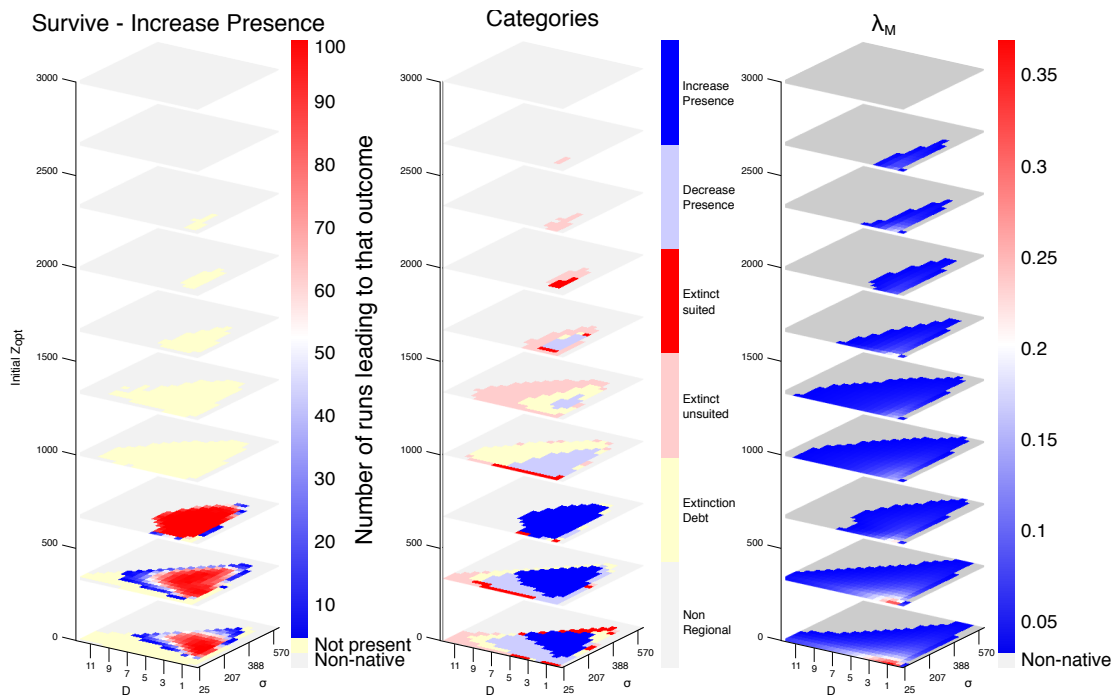


Figure A.36 – Same as Fig. A.4 but for the Alpes Vaudoises

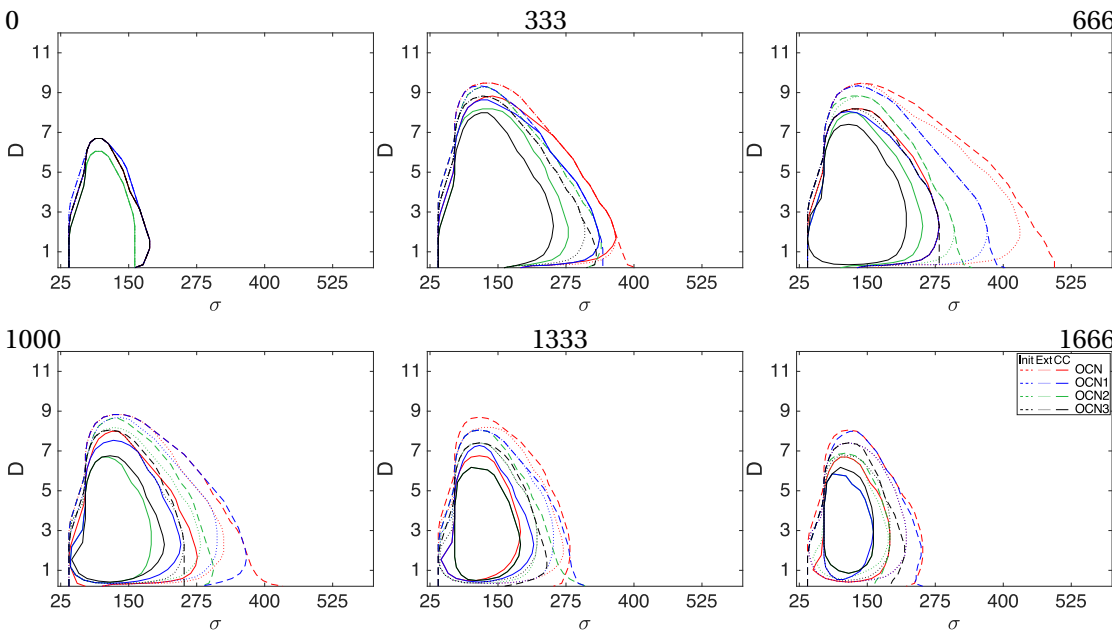


Figure A.37 – As Fig. 2.9 for additional landscapes and elevations

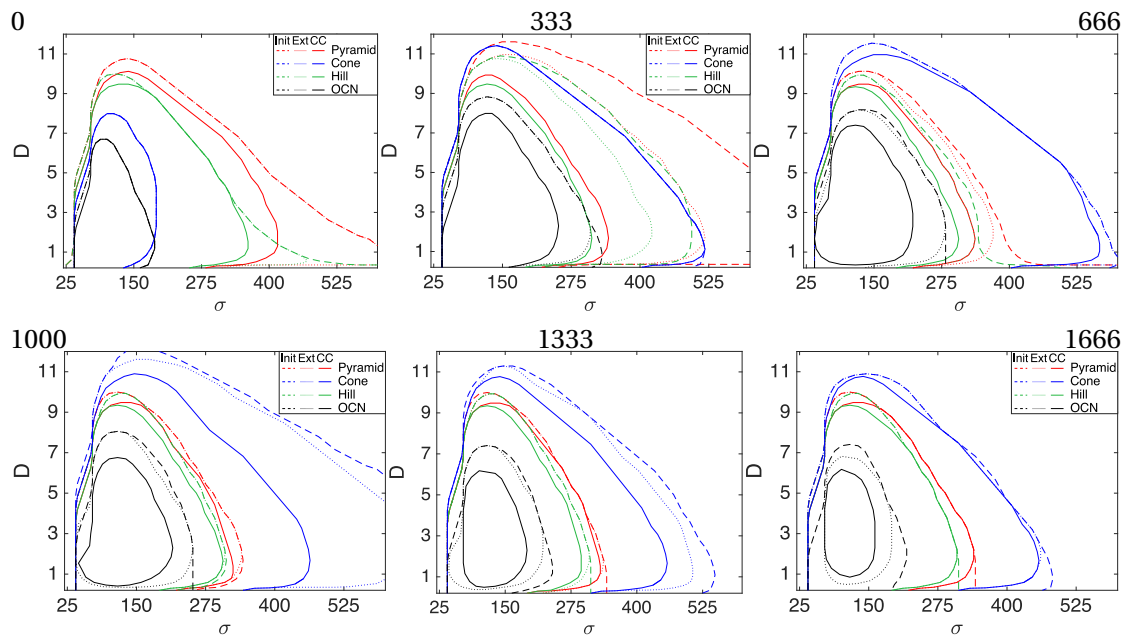


Figure A.38 – As Fig. 2.9 for additional landscapes and elevations

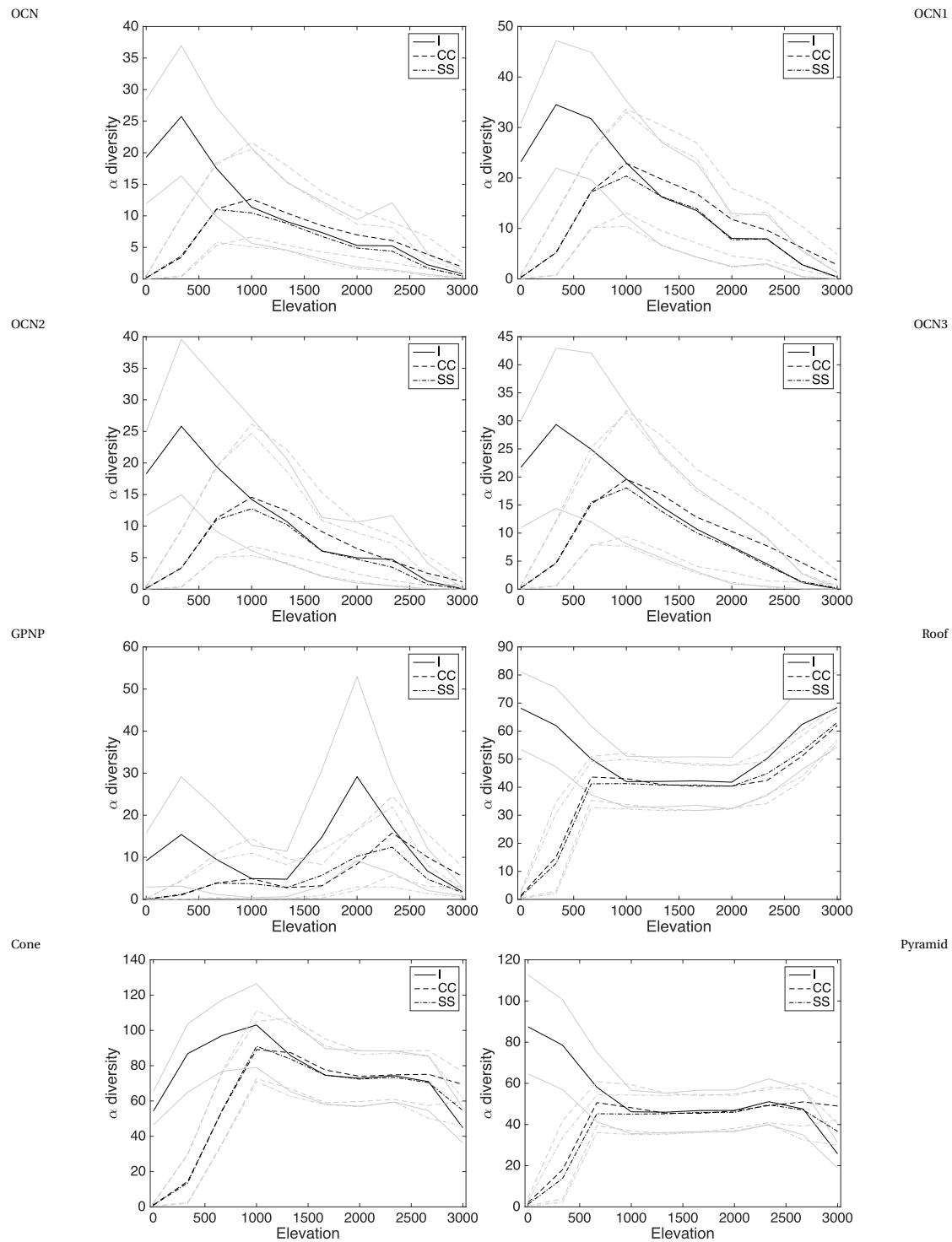


Figure A.39 – Evolution of the α -diversity for the different shapes and the different states - initial (I), after climate change (CC) and at steady state after climate change (SS)

Bibliography

- Acevedo, P., Ferreres, J., Escudero, M. A., Jimenez, J., Boadella, M., and Marco, J. (2017). Population dynamics affect the capacity of species distribution models to predict species abundance on a local scale. *Diversity and Distributions*, 23(9):1008–1017.
- Akçakaya, H. R. (2000). Viability analyses with habitat-based metapopulation models. *Researches on Population Ecology*, 42(1):0045.
- Akçakaya, H. R., McCarthy, M. A., and Pearce, J. L. (1995). Linking landscape data with population viability analysis: management options for the helmeted honeyeater. *Biological Conservation*, 9(4):169–176.
- Albert, E. M., Fortuna, M. A., Godoy, J. A., and Bascompte, J. (2013). Assessing the robustness of networks of spatial genetic variation. *Ecology Letters*, 16:86–93.
- Alexander, J. M., Diez, J. M., Hart, S. P., and Levine, J. M. (2016). When Climate Reshuffles Competitors: A Call for Experimental Macroecology. *Trends in Ecology and Evolution*, 31(11):831–841.
- Anderson, B. J., Akçakaya, H. R., Araújo, M. B., Fordham, D. A., Martinez-Meyer, E., Thuiller, W., and Brook, B. W. (2009). Dynamics of range margins for metapopulations under climate change. *Proceedings of the Royal Society B: Biological Sciences*, 276(1661):1415–1420.
- Anderson, M. J., Crist, T. O., Chase, J. M., Vellend, M., Inouye, B. D., Freestone, A. L., Sanders, N. J., Cornell, H. V., Comita, L. S., Davies, K. F., Harrison, S. P., Kraft, N. J. B., Stegen, J. C., and Swenson, N. G. (2011). Navigating the multiple meanings of beta diversity: A roadmap for the practicing ecologist. *Ecology Letters*, 14(1):19–28.
- Araújo, M. B. and Guisan, A. (2006). Five (or so) challenges for species distribution modelling. *Journal of Biogeography*, 33(10):1677–1688.
- Arrhenius, O. (1921). Species and area. *Journal of Ecology*, 9:95–99.

Bibliography

- Arulampalam, M. S., Maskell, S., Gordon, N., and Clapp, T. (2002). A tutorial on particle filters for online nonlinear/non-Gaussian Bayesian tracking. *IEEE Transactions on Signal Processing*, 50(2):174–188.
- Balister, P., Balogh, J., Bertuzzo, E., Bollobás, B., Caldarelli, G., Maritan, A., Mastrandrea, R., Morris, R., and Rinaldo, A. (2018). River landscapes and optimal channel networks. *Proceedings of the National Academy of Sciences of the United States of America*, 115(26):6548–6553.
- Banavar, J. R., Colaiori, F., Flammini, A., Maritan, A., and Rinaldo, A. (2000). Topology of the fittest transportation network. *Physical Review Letters*, 84:4745–4748.
- Banavar, J. R., Colaiori, F., Flammini, A., Maritan, A., and Rinaldo, A. (2001). Scaling, optimality and landscape evolution. *Journal of Statistical Physics*, 104:1–33.
- Banavar, J. R., Damuth, J., Maritan, A., and Rinaldo, A. (2007). Scaling in ecosystems and the linkage of macroecological laws. *Physical Review Letters*, 98(1):68104.
- Barry, R. G. (2008). *Mountain Weather and Climate*. Cambridge University Press, 3 edition.
- Barry, R. G. and Chorley, R. J. (2009). *Atmosphere, weather and climate*. Routledge, London.
- Bascompte, J. (2009). Mutualistic networks. *Frontiers in Ecology and the Environment*, 7(8):429–436.
- Bascompte, J. and Jordano, P. (2014). *Mutualistic Networks*. Princeton University Press.
- Bascompte, J. and Solé, R. V. (1996). Habitat fragmentation and extinction thresholds in spatially explicit models. *Journal of Animal Ecology*, 65:465–473.
- Bascompte, J. and Solé, R. V. (1998). Effects of habitat destruction in a prey-predator metapopulation model. *Journal of Theoretical Biology*, 195(3):383–393.
- Becker, A., Körner, C., Brun, J.-j., Guisan, A., and Tappeiner, U. (2007). Ecological and land use studies along elevational gradients. *Mountain Research and Development*, 27(1):58–65.
- Bellin, A. and Rubin, Y. (1996). HYDRO_GEN: A spatially distributed random field generator for correlated properties. *Stochastic Hydrology and Hydraulics*, 10(4):253–278.
- Benda, L. and et al. (2004). The network dynamics hypothesis: How channel networks structure riverine habitats. *BioScience*, 54:384–398.
- Benjamin, R., Cédric, G., and Pablo, I. (2008). Modeling spatially explicit population dynamics of *Pterostichus melanarius* I11. (Coleoptera: Carabidae) in response to changes in the composition and configuration of agricultural landscapes. *Landscape and Urban Planning*, 84(3-4):191–199.

- Bertrand, R., Lenoir, J., Piedallu, C., Dillon, G. R., De Ruffray, P., Vidal, C., Pierrat, J. C., and Gégout, J. C. (2011). Changes in plant community composition lag behind climate warming in lowland forests. *Nature*, 479(7374):517–520.
- Bertuzzo, E., Carrara, F., Mari, L., Altermatt, F., Rodriguez-Iturbe, I., and Rinaldo, A. (2016). Geomorphic controls on elevational gradients of species richness. *Proceedings of the National Academy of Sciences*, 113(7):1737–1742.
- Bertuzzo, E., Rodriguez-Iturbe, I., and Rinaldo, A. (2015). Metapopulation capacity of evolving fluvial landscapes. *Water Resources Research*, 51(4):2696–2706.
- Bertuzzo, E., Suweis, S., Mari, L., Maritan, A., Rodriguez-Iturbe, I., and Rinaldo, A. (2011). Spatial effects on species persistence and implications for biodiversity. *Proceedings of the National Academy of Sciences of the United States of America*, 108(11):4346–4351.
- Blackburn, T. M. and Gaston, K. J. (2003). *Macroecology: Concepts and Consequences*. Blackwell Scientific Publications, Oxford.
- Booth, T. H., Nix, H. A., Busby, J. R., and Hutchinson, M. F. (2014). Bioclim: The first species distribution modelling package, its early applications and relevance to most current MaxEnt studies. *Diversity and Distributions*, 20(1):1–9.
- Borile, C., Maritan, A., and Munoz, M. (2013). The effect of quenched disorder in neutral theories. *Journal of Statistical Mechanics: Theory and Experiment*, 4:p04032.
- Brooks, T. and Balmford, A. (1995). Atlantic forest extinctions. *Nature*, 380:115–116.
- Brooks, T. e. a. (2002). Habitat loss and extinction in the hotspots of biodiversity. *Conservation Biology*, 16:909–923.
- Brown, J. H. (1995). *Macroecology*. The University of Chicago Press.
- Brown, J. H. (2001). Mammals on mountainsides: Elevational patterns of diversity. *Global Ecology and Biogeography*, 10(1):101–109.
- Brown, J. H., Gillooly, J. F., Allen, A. P., Savage, V. M., and West, G. B. (2004). Toward a metabolic theory of ecology. *Ecology*, 85(7):1771–1789.
- Burel, F., Butet, A., Delettre, Y. R., and Millàn De La Peña, N. (2004). Differential response of selected taxa to landscape context and agricultural intensification. *Landscape and Urban Planning*, 67:195–204.
- Busby, J. R. (1988). Potential impacts of climate change on Australia's flora and fauna. In Pearman, G. I., editor, *Greenhouse: Planning for Climate Change*, chapter 30, pages 387–398. CSIRO Publishing.

Bibliography

- Carrara, F., Altermatt, F., Rodriguez-Iturbe, I., and Rinaldo, A. (2012). Dendritic connectivity controls biodiversity patterns in experimental metacommunities. *Proceedings of the National Academy of Sciences of the United States of America*, 109(15):5761–5766.
- Carrara, F., Rinaldo, A., Giometto, A., and Altermatt, F. (2014). Complex interaction of dendritic connectivity and hierarchical patch size on biodiversity in river-like landscapes. *American Naturalist*, 183(1):13–25.
- Carraro, L., Mari, L., Gatto, M., Rinaldo, A., and Bertuzzo, E. (2018). Spread of proliferative kidney disease in fish along stream networks: A spatial metacommunity framework. *Freshwater Biology*, 63(1):114–127.
- Colwell, R. K., Gotelli, N., and Rahbek, C. (2004). The Mid-Domain Effect and Species Richness Patterns: What Have We Learned So Far? *The American Naturalist*, 163(3):E1–E23.
- Colwell, R. K. and Hurtt, G. C. (1994). Nonbiological Gradients in Species Richness and a Spurious Rapoport Effect. *The American Naturalist*, 144(4):570–595.
- Colwell, R. K. and Lees, D. C. (2000). The mid-domain effect: Geometric constraints on the geography of species richness. *Trends in Ecology and Evolution*, 15(2):70–76.
- Cornes, R. C., van der Schrier, G., van den Besselaar, E. J., and Jones, P. D. (2018). An Ensemble Version of the E-OBS Temperature and Precipitation Data Sets. *Journal of Geophysical Research: Atmospheres*, 123(17):9391–9409.
- Davies, K. F. and Margules, C. R. (1998). Effects of Habitat Fragmentation on Carabid Beetles: Experimental Evidence. *Journal of Animal Ecology*, 67(3):460–471.
- Davies, R. G., Orme, C. D. L., Storch, D., Olson, V. A., Thomas, G. H., Ross, S. G., Ding, T. S., Rasmussen, P. C., Bennett, P. M., Owens, I. P., Blackburn, T. M., and Gaston, K. J. (2007). Topography, energy and the global distribution of bird species richness. *Proceedings of the Royal Society B: Biological Sciences*, 274(1614):1189–1197.
- den Boer, P. J. (1990). The Survival Value of Dispersal in Terrestrial Arthropods *. *Biological Conservation*, 54(356):175–192.
- Devictor, V., Van Swaay, C., Brereton, T., Brotons, L., Chamberlain, D., Heliölä, J., Herrando, S., Julliard, R., Kuussaari, M., Lindström, Å., Reif, J., Roy, D. B., Schweiger, O., Settele, J., Stefanescu, C., Van Strien, A., Van Turnhout, C., Vermouzek, Z., WallisDeVries, M., Wynhoff, I., and Jiguet, F. (2012). Differences in the climatic debts of birds and butterflies at a continental scale. *Nature Climate Change*, 2(2):121–124.
- Dietze, M. C., Fox, A., Beck-Johnson, L. M., Betancourt, J. L., Hooten, M. B., Jarnevich, C. S., Keitt, T. H., Kenney, M. A., Laney, C. M., Larsen, L. G., Loescher, H. W., Lunch, C. K., Pijanowski, B. C., Randerson, J. T., Read, E. K., Tredennick, A. T., Vargas, R., Weathers, K. C.,

- and White, E. P. (2018). Iterative near-term ecological forecasting: Needs, opportunities, and challenges. *Proceedings of the National Academy of Sciences of the United States of America*, 115(7):1424–1432.
- Dodson, R. and Marks, D. (1997). Daily air temperature interpolated at high spatial resolution over a large mountainous region. *Climate Research*, 8(1):1–20.
- Dufour, A., Gadallah, F., Wagner, H. H., Guisan, A., and Buttler, A. (2006). Plant species richness and environmental heterogeneity in a mountain landscape: Effects of variability and spatial configuration. *Ecography*, 29(4):573–584.
- Dullinger, S., Gattringer, A., Thuiller, W., Moser, D., Zimmermann, N. E., Guisan, A., Willner, W., Plutzer, C., Leitner, M., Mang, T., Caccianiga, M., Dirnböck, T., Ertl, S., Fischer, A., Lenoir, J., Svenning, J.-C., Psomas, A., Schmatz, D. R., Silc, U., Vittoz, P., and Hülber, K. (2012). Extinction debt of high-mountain plants under twenty-first-century climate change. *Nature Climate Change*, 2(8):619–622.
- Durrett, R. and Levin, S. A. (1996). Spatial models for species-area curves. *Journal of Theoretical Biology*, 179(2):119–127.
- D'Onofrio, D., Palazzi, E., von Hardenberg, J., Provenzale, A., and Calmanti, S. (2014). Stochastic Rainfall Downscaling of Climate Models. *Journal of Hydrometeorology*, 15(2):830–843.
- Ebenhard, T. (1991). Metapopulations: a Review of Theory and Observations. *Biological Journal of the Linnean Society*, 42:105–121.
- Economo, E. P. and Keitt, T. H. (2008). Species diversity in neutral metacommunities: A network approach. *Ecology Letters*, 11(1):52–62.
- Economo, E. P. and Keitt, T. H. (2010). Network isolation and local diversity in neutral metacommunities. *Oikos*, 119(8):1355–1363.
- Elsen, P. R. and Tingley, M. W. (2015). Global mountain topography and the fate of montane species under climate change. *Nature Climate Change*, 5:5–10.
- Engler, R., Randin, C. F., Vittoz, P., Czaka, T., Beniston, M., Zimmermann, N. E., and Guisan, A. (2009). Predicting future distributions of mountain plants under climate change: does dispersal capacity matter? *Ecography*, 32(1):34–45.
- Etienne, R. S., Braak, C. J. F., and Vos, C. C. (2004). Application of Stochastic Patch Occupancy Models To Real Metapopulations. In Hanski, I. and Gaggiotti, O. E., editors, *Ecology, Genetics and Evolution of Metapopulations*, chapter 5, pages 105–132. Academic Press.
- Eversham, B. C., Roy, D. B., and Telfer, M. G. (1996). Urban, industrial and other manmade sites as analogues of natural habitats for Carabidae. *Annales Zoologici Fennici*, 33(c):149–156.

Bibliography

- Ewers, R. M. and Didham, R. K. (2006). Confounding factors in the detection of species responses to habitat fragmentation. *Biological Reviews of the Cambridge Philosophical Society*, 81(1):117–142.
- Fagan, W. F. (2002). Connectivity, fragmentation, and extinction risk in dendritic metapopulations. *Ecology*, 83(12):3243–3249.
- Fahrig, L. (2007). Landscape heterogeneity and metapopulation dynamics. In Wu, J. and Hobbs, R. J., editors, *Key topics and perspectives in landscape ecology*, chapter 5, pages 78–89. Cambridge University Press.
- Fahrig, L. and Nutton, W. K. (2005). Population Ecology in heterogeneous environments. In *Ecosystem function in heterogeneous landscapes*, chapter 6, pages 95–118. Springer.
- Fernandes, R. F., Scherrer, D., and Guisan, A. (2018a). Effects of simulated observation errors on the performance of species distribution models. *Diversity and Distributions*, 25(April):1–14.
- Fernandes, R. F., Scherrer, D., and Guisan, A. (2018b). How much should one sample to accurately predict the distribution of species assemblages? A virtual community approach. *Ecological Informatics*, 48(June):125–134.
- Fleishman, E., Ray, C., Sjögren-Gulve, P., Boggs, C. L., and Murphy, D. D. (2002). Assessing the roles of patch quality, area, and isolation in predicting metapopulation dynamics. *Conservation Biology*, 16(3):706–716.
- Fortuna, M. A., Gómez-Rodríguez, C., and Bascompte, J. (2006). Spatial network structure and amphibian persistence in stochastic environments. *Proceedings of the Royal Society B: Biological Sciences*, 273(1592):1429–1434.
- Fox, J. (2015). Generalized Linear Models. In *Applied Regression Analysis and Generalized Linear Models*, chapter 15, pages 379–424. SAGE Publications, Inc, third edition.
- Frey, S. J., Strong, A. M., and McFarland, K. P. (2012). The relative contribution of local habitat and landscape context to metapopulation processes: A dynamic occupancy modeling approach. *Ecography*, 35(7):581–589.
- García-Valdés, R., Zavala, M. A., Araújo, M. B., and Purves, D. W. (2013). Chasing a moving target: projecting climate change-induced shifts in non-equilibrium tree species distributions. *Journal of Ecology*, 101(2):441–453.
- Gavish, Y., Marsh, C. J., Kuemmerlen, M., Stoll, S., Haase, P., and Kunin, W. E. (2017). Accounting for biotic interactions through alpha-diversity constraints in stacked species distribution models. *Methods in Ecology and Evolution*, 8(9):1092–1102.

- Giezendanner, J., Bertuzzo, E., Pasetto, D., Guisan, A., and Rinaldo, A. (2019). A minimalist model of extinction and range dynamics of virtual mountain species driven by warming temperatures. *PLoS ONE*, 14(3):1–19.
- Gilarranz, L. J. and Bascompte, J. (2012). Spatial network structure and metapopulation persistence. *Journal of Theoretical Biology*, 297:11–16.
- Gilarranz, L. J., Rayfield, B., Liñán-Cembrano, G., Bascompte, J., and Gonzalez, A. (2017). Effects of network modularity on the spread of perturbation impact in experimental metapopulations. *Science*, 357(6347):199–201.
- Gilpin, M. and Hanski, I. (1991). *Metapopulation dynamics: empirical and theoretical investigations*. Academic Press.
- Gleason, H. A. (1922). On the relation between species and area. *Ecology*, 3:156–162.
- Gobbi, M., Rossaro, B., Vater, A., De Bernardi, F., Pelfini, M., and Brandmayr, P. (2007). Environmental features influencing Carabid beetle (Coleoptera) assemblages along a recently deglaciated area in the Alpine region. *Ecological Entomology*, 32(6):682–689.
- González-Ferreras, A. M., Bertuzzo, E., Barquín, J., Carraro, L., Alonso, C., and Rinaldo, A. (2019). Effects of altered river network connectivity on the distribution of *Salmo trutta* : Insights from a metapopulation model. *Freshwater Biology*, 0(June):1–19.
- Gotelli, N. J. . (1991). Metapopulation Models : The Rescue Effect , the Propagule Rain , and the Core-Satellite Hypothesis. *The American Naturalist*, 138(3):768–776.
- Graae, B. J., Vandvik, V., Armbruster, W. S., Eiserhardt, W. L., Svenning, J. C., Hylander, K., Ehrlén, J., Speed, J. D., Klanderud, K., Bråthen, K. A., Milbau, A., Opedal, Ø. H., Alsos, I. G., Ejrnæs, R., Bruun, H. H., Birks, H. J. B., Westergaard, K. B., Birks, H. H., and Lenoir, J. (2017). Stay or go - how topographic complexity influences alpine plant population and community responses to climate change. *Perspectives in Plant Ecology, Evolution and Systematics*, 30(September 2017):41–50.
- Graves, T., Chandler, R. B., Royle, J. A., Beier, P., and Kendall, K. C. (2014). Estimating landscape resistance to dispersal. *Landscape Ecology*, 29(7):1201–1211.
- Griffith, D. M. and Brown, J. S. (1992). A Null Model of Patch Assessment with an Application to a Carabid Cave Beetle. *Oikos*, 64(3):523.
- Grilli, J., Barabas, G., and Allesina, S. (2015). Metapopulation persistence in random fragmented landscapes. *PLoS Computational Biology*, 11(5):e100251.

Bibliography

- Grytnes, J. A. and Vetaas, O. R. (2002). Species richness and altitude: a comparison between null models and interpolated plant species richness along the Himalayan altitudinal gradient, Nepal. *The American Naturalist*, 159(3):294–304.
- Gu, W., Heikkilä, R., and Hanski, I. (2002). Estimating the consequences of habitat fragmentation on extinction risk in dynamic landscapes. *Landscape Ecology*, 17:699 – 710.
- Gudowska, A., Schramm, B. W., Czarnoleski, M., Antoń, A., Bauchinger, U., and Kozłowski, J. (2017). Mass scaling of metabolic rates in carabid beetles (Carabidae) – the importance of phylogeny, regression models and gas exchange patterns. *The Journal of Experimental Biology*, 220(18):3363–3371.
- Guisan, A., Edwards, T. C., and Hastie, T. (2002). Generalized linear and generalized additive models in studies of species distributions: Setting the scene. *Ecological Modelling*, 157(2-3):89–100.
- Guisan, A., Petitpierre, B., Broennimann, O., Daehler, C., and Kueffer, C. (2014). Unifying niche shift studies: Insights from biological invasions.
- Guisan, A. and Theurillat, J.-P. J.-P. (2001). Assessing alpine plant vulnerability to climate change: a modeling perspective. *Integrated Assessment*, 1(1):307–320.
- Guisan, A. and Thuiller, W. (2005). Predicting species distribution: Offering more than simple habitat models. *Ecology Letters*, 8(9):993–1009.
- Guisan, A., Thuiller, W., and Zimmermann, N. E. (2017). *Habitat Suitability and Distribution Models With Applications in R*. Cambridge University Press.
- Guisan, A. and Zimmermann, N. E. (2000). Predictive habitat distribution models in ecology. *Ecological Modelling*, 135(2-3):147–186.
- Gyllenberg, M. and Hanski, I. (1997). Habitat Deterioration, Habitat Destruction, and Metapopulation Persistence in a Heterogenous Landscape. *Theoretical Population Biology*, 52.
- Gyllenberg, M., Hastings, A., and Hanski, I. (1997). Structured Metapopulation Models. In Hanski, I. and Gilpin, M. E., editors, *Metapopulation Biology*, pages 93–122. Academic Press, San Diego.
- Hanski, I. (1994). A Practical Model of Metapopulation Dynamics. *The Journal of Animal Ecology*, 63(1):151.
- Hanski, I. (1997). Metapopulation Dynamics: From Concepts and Observations to Predictive Models. In Hanski, I. and Gilpin, M. E., editors, *Metapopulation Biology*, pages 69–91. Academic Press, San Diego.

- Hanski, I. (1998). Metapopulation dynamics. *Nature*, 396(6706):41–49.
- Hanski, I. (1999a). Habitat Connectivity, Habitat Continuity, and Metapopulations in Dynamic Landscapes. *Oikos*, 87(2):209.
- Hanski, I. (1999b). *Metapopulation ecology*. Oxford University Press.
- Hanski, I. (2001). Spatially realistic theory of metapopulation ecology. *Naturwissenschaften*, 88(9):372–381.
- Hanski, I. (2016). *Messages from Islands. A Global Biodiversity Tour*. University of Chicago Press.
- Hanski, I. and Gilpin, M. (1991). Metapopulation dynamics: brief history and conceptual domain. *Biological Journal of the Linnean Society*, 42(1-2):3–16.
- Hanski, I. and Gyllenberg, M. (1997). Uniting Two General Patterns in the Distribution of Species. *American Association for the Advancement of Science*, 275(5298):397–400.
- Hanski, I. and Ovaskainen, O. (2000). The metapopulation capacity of a fragmented landscape. *Nature*, 404(6779):755–758.
- Hanski, I. and Ovaskainen, O. (2003). Metapopulation theory for fragmented landscapes. *Theoretical Population Biology*, 64(1):119–127.
- Hanski, I., Zurita, G. A., Bellocq, M. I., and Rybicki, J. (2013). Species–fragmented area relationship. *Proceedings of the National Academy of Sciences of the United States of America*, 110(31):12715–20.
- Harrison, S. and Taylor, A. D. (1997). Empirical Evidence for Metapopulation Dynamics. In Hanski, I. and Gilpin, M. E., editors, *Metapopulation Biology*, pages 27–42. Academic Press, San Diego.
- Harte, J., Smith, A. B., and Storch, D. (2009). Biodiversity scales from plots to biomes with a universal species–area curve. *Ecology Letters*, 12:789–797.
- Hawkins, B. A., Field, R., Cornell, H. V., Currie, D. J., Guegan, J.-F. E., Kaufman, D. M., Kerr, J. T., Mittelbach, G. G., Oberdorff, T., O'Brien, E. M., Porter, E. E., and Turner, J. R. G. (2003). Energy, water, and broad-scale geographic patterns of species richness. *Ecological Society of America*, 84(12):3105–3117.
- Haylock, M. R., Hofstra, N., Klein Tank, A. M., Klok, E. J., Jones, P. D., and New, M. (2008). A European daily high-resolution gridded data set of surface temperature and precipitation for 1950–2006. *Journal of Geophysical Research: Atmospheres*, 113(20).

Bibliography

- Hegel, T. M., Cushman, S. A., Evans, J., and Huettmann, F. (2010). Current State of the Art for Statistical Modelling of Species Distributions. In Cushman, S. A. and Huettmann, F., editors, *Spatial Complexity, Informatics, and Wildlife Conservation*, volume 9784431877, chapter Current St, pages 1–458. Springer.
- Huang, C., Wylie, B., Yang, L., Homer, C., and Zylstra, G. (2002). Derivation of a tasseled cap transformation based on Landsat 8 at- Derivation of a tasseled cap transformation based on Landsat 8 at- satellite reflectance. *International Journal of Remote Sensing*, 23(April):1741–1748.
- Hutchinson, G. E. (1957). Concluding remarks: The demographic symposium as a heterogeneous unstable population. *Foundations of Ecology: Classic Papers with Commentaries*, 22(0):415–427.
- Ionides, E. L., Nguyen, D., Atchadé, Y., Stoev, S., and King, A. A. (2015). Inference for dynamic and latent variable models via iterated, perturbed Bayes maps. *Proceedings of the National Academy of Sciences of the United States of America*, 112(3):719–724.
- IPBES (2019). Summary for policymakers. In Díaz, S., Settele, J., E.S., E. S. B., Ngo, H. T., Guèze, M., Agard, J., Arneth, A., Balvanera, P., Brauman, K. A., Butchart, S. H. M., Chan, K. M. A., Garibaldi, L. A., Ichii, K., Liu, J., Subramanian, S. M., Midgley, G. F., Miloslavich, P., Molnár, Z., Obura, D., Pfaff, A., Polasky, S., Purvis, A., Razzaque, J., Reyers, B., Chowdhury, R. R., Shin, Y. J., Visseren-Hamakers, I. J., Willis, K. J., and Zaya, C. N., editors, *Global assessment report on biodiversity and ecosystem services of the Intergovernmental Science-Policy Platform on Biodiversity and Ecosystem Services*, volume 45, pages 1–44. IPBES secretariat, Bonn, Germany.
- IPCC (2013). Summary for Policymakers. In Stocker, T., Qin, D., Plattner, G.-K., Tignor, M., Allen, S., Boschung, J., Nauels, A., Xia, Y., Bex, V., and Midgley, P., editors, *Climate Change 2013: The Physical Science Basis. Contribution of Working Group I to the Fifth Assessment Report of the Intergovernmental Panel on Climate Change*, chapter SPM, page 1–30. Cambridge University Press.
- IPCC (2014). Impacts, Adaptation and Vulnerability. In Field, C. B., Barros, V. R., Mastrandrea, M., Mach, K. J., Abdrabo, M., Adger, W., Anokhin, Y. A., Anisimov, O., Arent, D., Barnett, J., Burkett, V. R., Cai, R., Chatterjee, M., Cohen, S., Cramer, W., Dasgupta, P., Davidson, D., Denton, F., Doell, P., and Yohe, G., editors, *Climate Change 2014*. Cambridge University Press.
- Jackson, S. T. and Sax, D. F. (2010). Balancing biodiversity in a changing environment: extinction debt, immigration credit and species turnover. *Trends in Ecology and Evolution*, 25(3):153–160.

- Jacob, S., Laurent, E., Haegeman, B., Bertrand, R., Prunier, J. G., Legrand, D., Cote, J., Chaine, A. S., Loreau, M., Clobert, J., and Schtickzelle, N. (2018). Habitat choice meets thermal specialization: competition with specialists may drive suboptimal habitat preferences in generalists. *Proceedings of the National Academy of Sciences of the United States of America*, 115(47):1–33.
- Janžekovič, F. and Novak, T. (2012). PCA – A Powerful Method for Analyze Ecological Niches. In Sanguansat, P., editor, *Principal Component Analysis - Multidisciplinary Applications*, chapter 8, pages 127–142. IntechOpen, intech edition.
- Jopp, F. and Reuter, H. (2005). Dispersal of carabid beetles - Emergence of distribution patterns. *Ecological Modelling*, 186(4):389–405.
- Jordán, E., Magura, T., Tóthmérész, B., Vasas, V., and Ködöböcz, V. (2007). Carabids (Coleoptera: Carabidae) in a forest patchwork: A connectivity analysis of the Bereg Plain landscape graph. *Landscape Ecology*, 22(10):1527–1539.
- Kadmon, R. and Allouche, O. (2007). Integrating the effects of area, isolation, and habitat heterogeneity on species diversity: a unification of island biogeography and niche theory. *Proceedings of the National Academy of Sciences of the United States of America*, 170:10941–10946.
- Kauth, R. J. and Thomas, G. S. (1976). Tasselled Cap - a Graphic Description of the Spectral-Temporal Development of Agricultural Crops as seen by Landsat. In *Proceedings of the Symposium on Machine Processing of Remotely Sensed Data, Perdue University, West Lafayette*, volume Paper 59, pages 41–51.
- Kearney, M. and Porter, W. (2009). Mechanistic niche modelling: combining physiological and spatial data to predict species' ranges. *Ecology letters*, 12(4):334–50.
- Keil, P., Belmaker, J., Wilson, A. M., Unitt, P., and Jetz, W. (2013). Downscaling of species distribution models: A hierarchical approach. *Methods in Ecology and Evolution*, 4(1):82–94.
- Keith, D. A., Akçakaya, H. R., and Murray, N. J. (2018). Scaling range sizes to threats for robust predictions of risks to biodiversity. *Conservation Biology*, 32(2):322–332.
- Keith, D. A., Akçakaya, H. R., Thuiller, W., Midgley, G. F., Pearson, R. G., Phillips, S. J., Regan, H. M., Araújo, M. B., and Rebelo, T. G. (2008). Predicting extinction risks under climate change: Coupling stochastic population models with dynamic bioclimatic habitat models. *Biology Letters*, 4(5):560–563.

Bibliography

- Kempeneers, P., Sedano, F., Seebach, L., Strobl, P., and San-Miguel-Ayanz, J. (2011). Data Fusion of Different Spatial Resolution Remote Sensing Images Applied to Forest-Type Mapping. *IEEE Transactions on Geoscience and Remote Sensing*, 49(12):4977–4986.
- Kéry, M., Guillera-Aroita, G., and Lahoz-Monfort, J. J. (2013). Analysing and mapping species range dynamics using occupancy models. *Journal of Biogeography*, 40(8):1463–1474.
- Kessler, M. (2000). Elevational gradients in species richness and endemism of selected plant groups in the central Bolivian Andes. *Plant Ecology*, 149:181–193.
- Kessler, M., Kluge, J., Hemp, A., and Ohlemüller, R. (2011). A global comparative analysis of elevational species richness patterns of ferns. *Global Ecology and Biogeography*, 20(6):868–880.
- Keymer, J. E., Marquet, P. A., and Johnson, A. R. (1998). Pattern formation in a patch occupancy metapopulation model: A cellular automata approach. *Journal of Theoretical Biology*, 194(1):79–90.
- Kirchheimer, B., Schinkel, C. C. F., Dellinger, A. S., Klatt, S., Moser, D., Winkler, M., Lenoir, J., Caccianiga, M., Guisan, A., Nieto-Lugilde, D., Svenning, J.-C., Thuiller, W., Vittoz, P., Willner, W., Zimmermann, N. E., Hörandl, E., and Dullinger, S. (2016). A matter of scale: apparent niche differentiation of diploid and tetraploid plants may depend on extent and grain of analysis. *Journal of Biogeography*, 43(4):716–726.
- Kleinwächter, M. and Rickfelder, T. (2007). Habitat models for a riparian carabid beetle: Their validity and applicability in the evaluation of river bank management. *Biodiversity and Conservation*, 16(11):3067–3081.
- Körner, C. (2000). Why are there global gradients in species richness? Mountains might hold the answer. *Trends in Ecology and Evolution*, 15(12):513–514.
- Körner, C. (2007). The use of 'altitude' in ecological research. *Trends in Ecology and Evolution*, 22(11):569–574.
- Kotze, D. J., Brandmayr, P., Casale, A., Dauffy-Richard, E., Dekoninck, W., Koivula, M. J., Lövei, G. L., Mossakowski, D., Noordijk, J., Paarmann, W., Pizzolotto, R., Saska, P., Schwerk, A., Serrano, J., Szyszko, J., Taboada, A., Turin, H., Venn, S., Vermeulen, R., and Zetto, T. (2011). Forty years of carabid beetle research in Europe - from taxonomy, biology, ecology and population studies to bioindication, habitat assessment and conservation. *ZooKeys*, 100(SPEC. ISSUE):55–148.
- Kromp, B. (1999). Carabid beetles in sustainable agriculture: a review on pest control efficacy, cultivation impacts and enhancement A2 - Paoletti, M.G. BT - Invertebrate Biodiversity

- as Bioindicators of Sustainable Landscapes. *Agriculture, Ecosystems and Environment*, 74:187–228.
- Lande, R. (1987). Extinction Thresholds in Demographic Models of Territorial Populations. *The American Naturalist*, 130(4):624–635.
- Lee, C.-B., Chun, J.-H., Song, H.-K., and Cho, H.-J. (2012). Altitudinal patterns of plant species richness on the Baekdudaegan Mountains, South Korea: mid-domain effect, area, climate, and Rapoport's rule. *The Ecological Society of Japan*, 28:67–79.
- Leibold, M. A. and Miller, T. E. (2004). From Metapopulations to Metacommunities. In Hanski, I. and Gaggiotti, O. E., editors, *Ecology, Genetics and Evolution of Metapopulations*, chapter 6, pages 133–150. Academic Press.
- Lenoir, J., Gégout, J. C., Guisan, A., Vittoz, P., Wohlgemuth, T., Zimmermann, N. E., Dullinger, S., Pauli, H., Willner, W., and Svenning, J.-C. (2010). Going against the flow: Potential mechanisms for unexpected downslope range shifts in a warming climate. *Ecography*, 33(2):295–303.
- Lenoir, J., Gégout, J. C., Marquet, P. A., de Ruffray, P., and Brisse, H. (2008). A significant upward shift in plant species optimum elevation during the 20th century. *Science*, 320(5884):1768–71.
- Lenoir, J. and Svenning, J. C. (2015). Climate-related range shifts - a global multidimensional synthesis and new research directions. *Ecography*, 38(1):15–28.
- Levin, S. A. (1992). The problem of pattern and scale in ecology. *Ecology*, 76:1943–1963.
- Levine, J. M., Bascompte, J., Adler, P. B., and Allesina, S. (2017). Beyond pairwise mechanisms of species coexistence in complex communities. *Nature*, 546(7656):56–64.
- Levins, R. (1966). The strategy of model building in population biology. *American Scientist*, 54(4):421–431.
- Levins, R. (1969). Some Demographic and Genetic Consequences of Environmental Heterogeneity for Biological Control'. *Bulletin of the Entomological society of America*, 15(3):237–240.
- Lomolino, M. V. (2000). Ecology's most general, yet protean pattern: the species–area relationship. *Journal of Biogeography*, 27(12):17–26.
- Lomolino, M. V. (2001). Elevation gradients of species-density: Historical and prospective views. *Global Ecology and Biogeography*, 10(1):3–13.

Bibliography

- Lövei, G. L. and Sunderland, K. D. (1996). Ecology and Behavior of Ground Beetles. *Annual review of Entomology*, 41(1 12):231 – 256.
- MacArthur, R. H. (1972). *Geographical Ecology*. Harper and Rowe Publishers, New York.
- MacArthur, R. H. and Wilson, E. O. (1967). *The Theory of Island Biogeography*. Princeton University Press, Princeton, USA.
- MacKenzie, D. I., Nichols, J. D., Hines, J. E., Knutson, M. G., and Franklin, A. B. (2003). Estimating site occupancy , colonization , and local extinction when a species is detected imperfectly. *Ecology*, 84(8):2200–2207.
- Mandelbrot, B. B. (1983). *The Fractal Geometry of Nature*. Henry Holt and Company, New York, USA.
- Mari, L., Casagrandi, R., Bertuzzo, E., Rinaldo, A., and Gatto, M. (2014). Metapopulation persistence and species spread in river networks. *Ecology Letters*, 17(4):426–434.
- Marquet, P. A. (2017). Integrating macroecology through a statistical mechanics of adaptive matter. *Proceedings of the National Academy of Sciences of the United States of America*, 114(40):10523–10525.
- Marquet, P. A., Allen, A. P., Brown, J. H., Dunne, J. A., Enquist, B. J., Gillooly, J. F., Gowaty, P. A., Green, J. L., Harte, J., Hubbell, S. P., O'Dwyer, J., Okie, J. G., Ostling, A., Ritchie, M., Storch, D., and West, G. B. (2014). On theory in ecology. *BioScience*, 64(8):701–710.
- Marquet, P. A., Quiñones, R. A., Abades, S., Labra, F., Tognelli, M., Arim, M., and Rivadeneira, M. (2005). Scaling and power-laws in ecological systems. *Journal of Experimental Biology*, 208:1749–1769.
- Matern, A., Drees, C., Meyer, H., and Assmann, T. (2008). Population ecology of the rare carabid beetle *Carabus variolosus* (Coleoptera: Carabidae) in north-west Germany. *Journal of Insect Conservation*, 12(6):591–601.
- May, R. M., Lawton, J. H., and Stork, N. E. (1995). Assessing extinction rates. In *Extinction Rates*, pages 1–24. Oxford University Press, Oxford.
- McCain, C. M. (2007). Area and mammalian elevational diversity. *Ecology*, 88(1):76–86.
- McCain, C. M. and Colwell, R. K. (2007). Assessing montane biodiversity from discordant shifts in temperature and precipitation in a changing climate. *Ecology Letters*, 14:1236–1245.
- McCain, C. M. and Grytnes, J.-A. (2010). Elevational Gradients in Species Richness. *Encyclopedia of Life Sciences*, 15:1–10.

- Mckay, M. D., Beckman, R. J., and Conover, W. J. (1977). A Comparison of Three Methods for Selecting Values of Input Variables in the Analysis of Output from a Computer Code. *Technometrics*, 21(2):239–245.
- McVinish, R. and Pollett, P. K. (2013). The limiting behaviour of a stochastic patch occupancy model. *Journal of Mathematical Biology*, 67(3):693–716.
- Moilanen, A. (1999). Patch Occupancy Models of Metapopulation Dynamics : Efficient Parameter Estimation Using Implicit Statistical Inference. *Ecology*, 80(3):1031–1043.
- Moilanen, A. (2000). The equilibrium assumption in estimating the parameters of metapopulation models. *Journal of Animal Ecology*, 69(1):143–153.
- Moilanen, A. (2004). SPOMSIM: Software for stochastic patch occupancy models of metapopulation dynamics. *Ecological Modelling*, 179(4):533–550.
- Moilanen, A. and Hanski, I. (1998). Metapopulation dynamics: Effects of habitat quality and landscape structure. *Ecology*, 79(7):2503–2515.
- Muneepeerakul, R., Bertuzzo, E., Lynch, H. J., Fagan, W. F., Rinaldo, A., and Rodriguez-Iturbe, I. (2008). Neutral metacommunity models predict fish diversity patterns in Mississippi–Missouri basin. *Nature*, 453(May):220–223.
- Murphy, D. D., Freas, K. E., and Weiss, S. B. (1990). An Environment-Metapopulation Approach to Population Viability Analysis for a Threatened Invertebrate. *Conservation Biology*, 4(1):41–51.
- Nee, S. and May, R. M. (1992). Dynamics of Metapopulations : Habitat Destruction and Competitive Coexistence. *Journal of Animal Ecology*, 61(1):37–40.
- Neukom, R., Barboza, L. A., Erb, M. P., Shi, F., Emile-Geay, J., Evans, M. N., Franke, J., Kaufman, D. S., Lücke, L., Rehfeld, K., Schurer, A., Zhu, F., Brönnimann, S., Hakim, G. J., Henley, B. J., Ljungqvist, F. C., McKay, N., Valler, V., and Gunten, L. v. (2019a). Consistent multidecadal variability in global temperature reconstructions and simulations over the Common Era. *Nature Geoscience*, 12(8):643–649.
- Neukom, R., Steiger, N., Gómez-Navarro, J. J., Wang, J., and Werner, J. P. (2019b). No evidence for globally coherent warm and cold periods over the preindustrial Common Era. *Nature*, 571(7766):550–554.
- Newell, S. C. (1986). *Dispersal in carabids*. PhD thesis, University of Plymouth.
- Ney-Nifle, M. and Mangel, M. (2000). Habitat loss and changes in the species-area relationship. *Conservation Biology*, 14:893–898.

Bibliography

- Niemelä, J. (2001). Carabid beetles (Coleóptera : Carabidae) and habitat fragmentation : a review. *European Journal of Entomology*, 98:127–132.
- Nogues-Bravo, D., Araujo, M. B., Romdal, T., and Rahbek, C. (2008). Scale effects and human impact on the elevational species richness gradients. *Nature*, 453:216–219.
- O'Brien, E. M. (2006). Biological relativity to water-energy dynamics. *Journal of Biogeography*, 33(11):1868–1888.
- Opdam, P. (1991). Metapopulation theory and habitat fragmentation: a review of holarctic breeding bird studies. *Landscape Ecology*, 5(2):93–106.
- Ovaskainen, O. and Hanski, I. (2001). Spatially Structured Metapopulation Models: Global and Local Assessment of Metapopulation Capacity. *Theoretical Population Biology*, 60:281–302.
- Ovaskainen, O. and Hanski, I. (2003). Extinction threshold in metapopulation models. *Annales Zoologici Fennici*, 40(40):81–97.
- Ovaskainen, O. and Hanski, I. (2004). Metapopulation Dynamics in Highly Fragmented Landscapes. In Hanski, I. and Gaggiotti, O. E., editors, *Ecology, Genetics and Evolution of Metapopulations*, chapter 4, pages 73–103. Academic Press.
- Ovaskainen, O. and Saastamoinen, M. (2018). Frontiers in Metapopulation Biology: The Legacy of Ilkka Hanski. *Annual Review of Ecology, Evolution, and Systematics*, 49(1):231–252.
- Ovaskainen, O., Sato, K., Bascompte, J., and Hanski, I. (2002). Metapopulation models for extinction threshold in spatially correlated landscapes. *Journal of Theoretical Biology*, 215(1):95–108.
- Pacifici, M., Foden, W., Visconti, P., Watson, J., Butchart, H. M. S., Kovacs, K., Scheffers, B., Hole, D., Martin, T., Akcakaya, H. R., Corlett, R., Huntley, B., Bickford, D., Carr, A. J., Hoffmann, A. A., Midgley, G., Pearce-Kelly, P., Pearson, G. R., Williams, S., and Rondinini, C. (2015). Assessing species vulnerability to climate change. *Nature Climate Change*, 5:215–224.
- Palmer, M. W. (1992). The Coexistence of Species in Fractal Landscapes. *The American Naturalist*, 139(2):375–397.
- Palmer, M. W. and White, P. S. (1994). Scale Dependence and the Species-Area Relationship. *The American Naturalist*, 144(5):717–740.
- Papaïx, J., David, O., Lannou, C., and Monod, H. (2013). Dynamics of Adaptation in Spatially Heterogeneous Metapopulations. *PLoS ONE*, 8(2).
- Parkinson, L. and Marshall, E. J. P. (1998). Isolating the components of activity-density for the carabid beetle *Pterostichus melanarius* in farmland. *Oecologia*, 116(1):103–112.

- Parmesan, C. (2006). Ecological and Evolutionary Responses to Recent Climate Change. *Annual Review of Ecology, Evolution, and Systematics*, 37(1):637–669.
- Parmesan, C. and Yohe, G. (2003). A globally coherent fingerprint of climate change impacts across natural systems. *Nature*, 421:37–42.
- Pasetto, D., Arenas-Castro, S., Bustamante, J., Casagrandi, R., Chrysoulakis, N., Cord, A. F., Dittrich, A., Domingo-Marimon, C., El Serafy, G., Karnieli, A., Kordelas, G. A., Manakos, I., Mari, L., Monteiro, A., Palazzi, E., Poursanidis, D., Rinaldo, A., Terzago, S., Ziemba, A., and Ziv, G. (2018). Integration of satellite remote sensing data in ecosystem modelling at local scales: Practices and trends. *Methods in Ecology and Evolution*, 9(8):1810–1821.
- Pauchard, A., Kueffer, C., Dietz, H., Daehler, C. C., Alexander, J., Edwards, P. J., Arévalo, J. R., Cavieres, L. A., Guisan, A., Haider, S., Jakobs, G., McDougall, K., Millar, C. I., Naylor, B. J., Parks, C. G., Rew, L. J., and Seipel, T. (2009). Ain't no mountain high enough: Plant invasions reaching new elevations. *Frontiers in Ecology and the Environment*, 7(9):479–486.
- Pearman, P. B., Guisan, A., Broennimann, O., and Randin, C. F. (2008). Niche dynamics in space and time. *Trends in Ecology and Evolution*, 23(3):149–158.
- Petit, S. and Burel, F. (1998). Effects of landscape dynamics on the metapopulation of a ground beetle (Coleoptera, Carabidae) in a hedgerow network. *Agriculture, Ecosystems & Environment*, 69(3):243–252.
- Pichancourt, J. B., Burel, F., and Auger, P. (2006). Assessing the effect of habitat fragmentation on population dynamics: An implicit modelling approach. *Ecological Modelling*, 192(3–4):543–556.
- Pimm, S. L. and Askins, R. A. (1995). Forest losses predict bird extinctions in eastern North America. *Proceedings of the National Academy of Sciences of the United States of America*, 92:9343–9347.
- Pradervand, J.-N., Dubuis, A., Pellissier, L., Guisan, A., and Randin, C. (2014). Very high resolution environmental predictors in species distribution models: Moving beyond topography? *Progress in Physical Geography*, 38(1):79–96.
- Pulliam, H. R. (2000). On the relationship between niche and distribution. *Ecology Letters*, 3:349–361.
- Purves, D. W., Zavala, M. A., Ogle, K., Prieto, F., and Benayas, J. M. R. (2007). Environmental Heterogeneity, Bird-mediated Directed Dispersal, and Oak Woodland Dynamics in Mediterranean Spain. *Ecological Monographs*, 77(1):77–97.

Bibliography

- Rahbek, C. (1997). The Relationship among Area, Elevation, and Regional Species Richness in Neotropical Birds. *The American Naturalist*, 149(5):875–902.
- Rahbek, C. and Museum, Z. (1995). The elevational gradient of species richness: a uniform pattern? *Ecography*, 2:200–205.
- Rainio, J. and Niemelä, J. K. (2003). Ground beetles (Coleoptera : Carabidae) as bioindicators. *Biodiversity and Conservation*, 12(McGeoch 1998):487–506.
- Räsänen, A., Kuitunen, M., Hjort, J., Vaso, A., Kuitunen, T., and Lensu, A. (2016). The role of landscape, topography, and geodiversity in explaining vascular plant species richness in a fragmented landscape. *Boreal Environment Research*, 21:53–70.
- Reuter, H., Hölker, F., Middelhoff, U., Jopp, F., Eschenbach, C., and Breckling, B. (2005). The concepts of emergent and collective properties in individual-based models - Summary and outlook of the Bornhöved case studies. *Ecological Modelling*, 186(4):489–501.
- Richerson, P. J. and Lum, K.-L. (1980). Patterns of Plant Species Diversity in California: Relation to Weather and Topography. *The American Naturalist*, 116(4):504–536.
- Ricketts, T. H. (2001). The matrix matters: Effective isolation in fragmented landscapes. *The American Naturalist*, 158(1):87–99.
- Rinaldo, A., Gatto, M., and Rodriguez-Iturbe, I. (2020). *River networks as ecological corridors. Species, populations, pathogens*. Cambridge Univ. Press, New York.
- Rinaldo, A., Rigon, R., Banavar, J. R., Maritan, A., and Rodriguez-Iturbe, I. (2014). Evolution and selection of river networks: Statics, dynamics, and complexity. *Proceedings of the National Academy of Sciences of the United States of America*, 111(7):2417–2424.
- Rinaldo, A., Rodriguez-Iturbe, I., and Rigon, R. (1998). Channel Networks. *Annual Review of Earth and Planetary Sciences*, 26:289–327.
- Rinaldo, A., Rodriguez-Iturbe, I., Rigon, R., Bras, R. L., Ijjasz-Vasquez, E., and Marani, A. (1992). Minimum energy and fractal structures of drainage networks. *Water Resources Research*, 28:2183–2195.
- Rodriguez-Iturbe, I., Muneeppeerakul, R., Bertuzzo, E., Levin, S. A., and Rinaldo, A. (2009). River networks as ecological corridors: A complex systems perspective for integrating hydrologic, geomorphologic, and ecologic dynamics. *Water Resources Research*, 45.
- Rodriguez-Iturbe, I. and Rinaldo, A. (2001). *Fractal River Basins: Chance and Self-Organization*. Cambridge University Press.

- Rodriguez-Iturbe, I., Rinaldo, A., Rigon, R., Bras, R. L., and Ijjasz-Vasquez, E. (1992a). Energy dissipation, runoff production and the three dimensional structure of channel networks. *Water Resources Research*, 28(4):1095–1103.
- Rodriguez-Iturbe, I., Rinaldo, A., Rigon, R., Bras, R. L., Ijjasz-Vasquez, E., and Marani, A. (1992b). Fractal structures as least energy patterns: The case of river networks. *Geophysical Research Letters*, 19(9):889–892.
- Rolland, C. (2003). Spatial and seasonal variations of air temperature lapse rates in Alpine regions. *Journal of Climate*, 16(7):1032–1046.
- Romdal, T. S. and Grytnes, J. A. (2007). An indirect area effect on elevational species richness patterns. *Ecography*, 30(3):440–448.
- Rosenzweig, M. L. (1995). *Species Diversity in Space and Time*. Cambridge Univ. Press, New York.
- Rumpf, S. B., Hülber, K., Klonner, G., Moser, D., Schütz, M., Wessely, J., Willner, W., Zimmermann, N. E., and Dullinger, S. (2018). Range dynamics of mountain plants decrease with elevation. *Proceedings of the National Academy of Sciences of the United States of America*, 115(8):1848–1853.
- Rumpf, S. B., Hülber, K., Wessely, J., Willner, W., Moser, D., Gattringer, A., Klonner, G., Zimmermann, N. E., and Dullinger, S. (2019). Extinction debts and colonization credits of non-forest plants in the European Alps. *Nature Communications*, 10(2019):1–9.
- Rushton, S., Sanderson, R., Luff, M., and Fuller, R. (1996). Modelling the spatial dynamics of ground beetles (Carabidae) within landscapes. *Annales Zoologici Fennici*, 33(1):233–241.
- Rybicki, J. and Hanski, I. (2013). Species-area relationships and extinctions caused by habitat loss and fragmentation. *Ecology Letters*, 16:27–38.
- Saari, L., Åberg, J., and Swenson, J. E. (1998). Factors influencing the dynamics of occurrence of the hazel grouse in a fine-grained managed landscape. *Conservation Biology*, 12(3):586–592.
- Salles, T. and Rey, P. (2019). bioLEC: A Python package to measure Landscape Elevational Connectivity. *Journal of Open Source Software*, 4(39):1530.
- Salles, T., Rey, P., and Bertuzzo, E. (2019). Mapping landscape connectivity under tectonic and climatic forcing. *Earth Surface Dynamics*, 7(2019):895–910.
- Sanders, N. J. (2002). Elevational gradients in ant species richness: area, geometry, and Rapoport's rule. *Ecography*, 25(1):25–32.

Bibliography

- Schnell, J. K., Harris, G. M., Pimm, S. L., and Russell, G. J. (2012). Estimating extinction risk with metapopulation models of large-scale fragmentation. *Conservation Biology*, 27(3):520–530.
- Schröder, B. (2008). Challenges of species distribution modeling belowground. *Journal of Plant Nutrition and Soil Science*, 171(3):325–337.
- Seebens, H., Blackburn, T. M., Dyer, E. E., Genovesi, P., Hulme, P. E., Jeschke, J. M., Pagad, S., Pyšek, P., van Kleunen, M., Winter, M., Ansong, M., Arianoutsou, M., Bacher, S., Blasius, B., Brockhoff, E. G., Brundu, G., Capinha, C., Causton, C. E., Celesti-Grapow, L., Dawson, W., Dullinger, S., Economo, E. P., Fuentes, N., Guénard, B., Jäger, H., Kartesz, J., Kenis, M., Kühn, I., Lenzner, B., Liebhold, A. M., Mosena, A., Moser, D., Nentwig, W., Nishino, M., Pearman, D., Pergl, J., Rabitsch, W., Rojas-Sandoval, J., Roques, A., Rorke, S., Rossinelli, S., Roy, H. E., Scalera, R., Schindler, S., Štajerová, K., Tokarska-Guzik, B., Walker, K., Ward, D. E., Yamanaka, T., and Essl, F. (2018). Global rise in emerging alien species results from increased accessibility of new source pools. *Proceedings of the National Academy of Sciences of the United States of America*, 115(10):201719429.
- Skłodowski, J. (2009). Interpreting the condition of the forest environment with use of the SCP/MIB model of carabid communities (Coleoptera: Carabidae). *Baltic Journal of Coleopterology*, 9(2):89–100.
- Soberón, J. and Peterson, A. T. (2005). Interpretation of models of fundamental ecological niches and species' distributional areas. *Biodiversity Informatics*, 2:1–10.
- Southwood, T. R. E., May, R. M., and Sugihara, G. (2006). Observations on related ecological exponents. *Proceedings of the National Academy of Sciences of the United States of America*, 103(18):6931–6933.
- Stanton, J. C., Pearson, R. G., Horning, N., Ersts, P., and Akçakaya, H. R. (2012). Combining static and dynamic variables in species distribution models under climate change. *Methods in Ecology and Evolution*, 3(2):349–357.
- Steinbauer, M. J., Grytnes, J.-A., Jurasinski, G., Kulonen, A., Lenoir, J., Pauli, H., Rixen, C., Winkler, M., Bardy-Durchhalter, M., Barni, E., Bjorkman, A. D., Delimat, A., Dullinger, S., Erschbamer, B., Felde, V. A., Fernández-Arberas, O., Fossheim, K. F., Gómez-García, D., Georges, D., Lamprecht, A., Matteodo, M., Morra, U., Cella, D., Normand, S., Odland, A., Olsen, S. L., Palacio, S., Petey, M., Piscová, V., Sedlakova, B., Steinbauer, K., Stöckli, V., Svenning, J.-C., Teppa, G., Theurillat, J.-P., Vittoz, P., Woodin, S. J., Zimmermann, N. E., and Wipf, S. (2018). Accelerated increase in plant species richness on mountain summits is linked to warming. *Nature*.
- Stevens, G. C. (1992). The Elevational Gradient in Altitudinal Range: An Extension of Rapoport's Latitudinal Rule to Altitude. *American Society of Naturalists*, 140(6):893–911.

- Sutherland, C. S., Elston, D. A., and Lambin, X. (2014). A demographic, spatially explicit patch occupancy model of metapopulation dynamics and persistence. *Ecology*, 95(11):3149–3160.
- Tenan, S., Maffioletti, C., Caccianiga, M., Compostella, C., Seppi, R., and Gobbi, M. (2016). Hierarchical models for describing space-for-time variations in insect population size and sexratio along a primary succession. *Ecological Modelling*, 329:18–28.
- Theurillat, J.-P. and Guisan, A. (2001). Potential impact of climate change on vegetation in the European Alps: a review. *Climatic Change*, 50:77–109.
- Thibaud, E., Petitpierre, B., Broennimann, O., Davison, A. C., and Guisan, A. (2014). Measuring the relative effect of factors affecting species distribution model predictions. *Methods in Ecology and Evolution*, 5(9):947–955.
- Thiele, H.-U. (1977). *Carabid Beetles in Their Environments - A Study on Habitat Selection by Adaptations in Physiology and Behaviour*. Springer, Berlin, Heidelberg.
- Thomas, C. D., Cameron, A., Green, R. E., Bakkenes, M., Beaumont, L. J., and Collingham, Y. C. e. a. (2004). Extinction risk from climate change. *Nature*, 427:145–148.
- Thomas, C. D. and Hanski, I. (2004). Metapopulation dynamics in changing environments: butterfly responses to habitat and climate change. In Hanski, I. and Gaggiotti, O. E., editors, *Ecology, Genetics and Evolution of Metapopulations*, chapter 20, pages 489–514. Academic Press.
- Thomas, C. F., Green, F., and Marshall, E. J. (1997). Distribution, Dispersal and Population Size of the Ground Beetles, *Pterostichus melanarius* (Illiger) and *Harpalus rufipes* (Degeer) (Coleoptera, Carabidae), in Field Margin Habitats. *Biological Agriculture and Horticulture*, 15(1-4):337–352.
- Thuiller, W., Münkemüller, T., Schiffrers, K. H., Georges, D., Dullinger, S., Eckhart, V. M., Edwards, T. C., Gravel, D., Kunstler, G., Merow, C., Moore, K., Piedallu, C., Vissault, S., Zimmermann, N. E., Zurell, D., and Schurr, F. M. (2014). Does probability of occurrence relate to population dynamics? *Ecography*, 37(12):1155–1166.
- Tilman, D. and Kareiva, P. M. (1997). *Spatial ecology: the role of space in population dynamics and interspecific interactions*, volume 30. Princeton University Press.
- Tilman, D., May, R. M., Lehman, C. L., and Nowak, M. a. (1994). Habitat destruction and the extinction debt. *Nature*, 371(6492):65–66.
- Tingley, M. W., Koo, M. S., Moritz, C., Rush, A. C., and Beissinger, S. R. (2012). The push and pull of climate change causes heterogeneous shifts in avian elevational ranges. *Global Change Biology*, 18:3279–3290.

Bibliography

- Turner, M. G. (1989). Landscape ecology: the effect of pattern on process. *Annual Review of Ecology and Systematics*, 20:171–197.
- Turner, M. G. (2005). Landscape ecology: What is the state of the science?
- Urban, D. and Keitt, T. (2001). Landscape Connectivity: a graph-theory perspective. *Ecology*, 82(5):1205–1218.
- van Nouhuys, S. (2016). Metapopulation Ecology. In *eLS*, pages 1–9. John Wiley & Sons, Ltd.
- Vetaas, O. R. (2015). Biological relativity to water-energy dynamics: A potential unifying theory? *Journal of Biogeography*, 33:1866–1867.
- Vetaas, O. R. and Grytnes, J.-A. (2002). Distribution of vascular plant species richness and endemic richness along the Himalayan elevation gradient in Nepal. *Global Ecology and Biogeography*, 11(4):291–301.
- Viterbi, R., Cerrato, C., Bassano, B., Bionda, R., Hardenberg, A., Provenzale, A., and Bogliani, G. (2013). Patterns of biodiversity in the northwestern Italian Alps: a multi-taxa approach. *Community Ecology*, 14(1):18–30.
- Wachmann, E., Platen, R., and Barndt, D. (1995). *Laufk{ä}fer, Beobachtung, Lebensweise*. Augsburg : Naturbuch-Verlag.
- Whitmore, T. C. and Sayer, J. E. (1992). *Tropical Deforestation and Species Extinction*. Chapman & Hall, London UK.
- Whittaker, R. H. (1972). Evolution and Measurement of Species Diversity. *Taxon*, 21(2):213–251.
- Wiens, J. A. (1997). Metapopulation Dynamics and Landscape Ecology. In Hanski, I. and Gilpin, M. E., editors, *Metapopulation Biology*, pages 43–62. Academic Press, San Diego.
- With, K. A. (2004). Metapopulation dynamics: perspectives from landscape ecology. In Hanski, I. and Gaggiotti, O. E., editors, *Ecology, Genetics and Evolution of Metapopulations*, chapter 2, pages 23–44. Academic Press.
- Woodcock, B. A. (2007). Pitfall Trapping in Ecological Studies. In Leather, S. R., editor, *Insect Sampling in Forest Ecosystems*, chapter 3, pages 37–57. John Wiley & Sons, Ltd.
- Wu, J. and Hobbs, R. (2002). Key issues and research priorities in landscape ecology. *Landscape Ecology*, 17(4):355–365.
- Yee, T. W. (2013). *Vector Generalized Linear and Additive Models with Implementation in R*. Springer.

- Zaoli, S., Giometto, A., Giezendanner, J., Maritan, A., and Rinaldo, A. (2019). On the probabilistic nature of the species-area relation. *Journal of Theoretical Biology*, 462:391–407.
- Zaoli, S., Giometto, A., Maritan, A., and Rinaldo, A. (2017). Covariations in ecological scaling laws fostered by community \mbox{dynamics}. *Proceedings of the National Academy of Sciences of the United States of America*, 114:10672–10677.
- Zuur, A. F., Ieno, E. N., and Smith, G. M. (2007). *Analyzing Ecological Data*. Springer.



Jonathan Giezendanner

Environmental and Computational Engineer

- 5 September 1989
- Rue de la madelaine 21C
1800 Vevey, Switzerland
- +41 79 423 53 76
- jonathan.giezendanner@gmail.com
- j-giezendanner

Languages

French: Mother Tongue
German: Father Tongue
English: Fluent
Italian: Basic Knowledge

Skills

Mathematical Modeling, Data Analysis and Sciences, Programming, Optimisation, Calibration

Computer Skills

Languages: Python, Matlab, R, C#, C++, C, Java, SQL
WebDev: HTML, CSS, JS
GIS: QGIS, ArcGis, PostGIS (Postgres)
Others: GIT, Unity3D, Latex, Linux, Windows

Interests

Cycling, ski-touring, mountaineering, cooking, game development, music, films, books, concerts, coffee, beers

Experience

- since 2016 Ph.D. researcher in Civil and Environmental Engineering EPFL
Specialised in theoretical ecology, with a focus on metapopulation dynamics of mountain species, at the laboratory of ecohydrology ECHO led by Prof. A. Rinaldo
Teaching duties: main teaching assistant for Water Resources Engineering, teaching assistant in probability and statistics
- 2015 Research Assistant (Civil Service) Insel
Assistance in the development of a tool for automated tumor detection using spectral imaging and machine learning, at SCAN - "Support Center for Advanced Neuroimaging", University Hospital Bern (Insel)
- 2012-2015 Teaching Assistant EPFL
Classes: Signals, Instruments and Systems, Numerical Analysis, Geomatics, Analysis II
- 2013 Ingeneering Intern Emch+Berger
Internship at the Engineering Office Emch+Berger in Bern, in the Environmental Section. Involved in projects regarding water flow management in urban environment
- 2011 Research Assistant (Civil Service) SHL
Assistance in the development of BioChar, at the "Schweizerische Hochschule für Landwirtschaft (SHL)"
- 2009 Caregiver Intern Regional Hospital of Moutier
Internship as caregiver at the Regional Hospital of Moutier (Be)
- 2008-2009 Military service Swiss Armed Forces
Military service in Airolo, as Paramedic. Graduated with the rank of Sergeant (Group Leader)
- 2005 Farming assistant Gstaad
Landdienst in Gstaad

Education

- 2013-2015 Master of Science EPFL
Major in Environmental Sciences and Engineering
Minor in Computational Sciences and Engineering
- 2009-2013 Bachelor of Science EPFL
Major in Environmental Sciences and Engineering
- 2005-2008 Bilingual high school (D/F) Alpenstrassen Gymnasium Biel
Specializing in Economics and Law

Extracurricular

- since 2014 Founder and Developer at Sharped Stone Studios, a swiss independent game creation collective
- 2014-2017 Organisation of the Balélec Festival (15'000 People) on EPFL campus
Chief Financial Officer (2016), Internal Catering Manager (2015), Electricity- and Water-supply Manager (2014)
- 2013-2015 Class representative
- 2012-2014 Founder and vice-President of the association TREE (Table Ronde des Étudiants en Environnement)

Publications

- 2019 A minimalist model of extinction and range dynamics of virtual mountain species driven by warming temperatures PLoS ONE
<https://doi.org/10.1371/journal.pone.0213775>
- 2019 On the probabilistic nature of the species-area relation JTB
<https://doi.org/10.1016/j.jtbi.2018.11.032>
- 2016 Towards 3-D Distributed Odor Source Localization : An Extended Graph-Based Formation Control Algorithm for Plume Tracking.IROS
<https://doi.org/10.1109/IROS.2016.7759277>